Remaining Capacity of Corrosion Damaged Steel Structures

By

Velautham Sarveswaran

A thesis submitted to the University of Bristol in accordance with the requirements for the degree of Doctor of Philosophy in the Faculty of Engineering, Department of Civil Engineering.

September 1996

Abstract

The number of exposed steelwork structures used in various industries is steadily increasing as a result of building new structures and extending the life of older structures. Many of the existing structures are more than 50 years old. Corrosion damage is a serious problem for these structures. Current assessment methods of corrosion damaged steelwork involve visual inspection which tends to be used very conservatively. This often results in premature plant closures. There is a need for more accurate assessment methods which can be used to make reliable decisions affecting the cost and safety.

Current methods of evaluation of corrosion damaged steel beams are reviewed, and improved evaluation methods are provided for two cases (coped beams and beams with web holes). Corrosion decay models are developed based on the information on the locations where corrosion occurs. The effects of corrosion on steel beams are analysed by evaluating the remaining capacity with regard to bending stresses, shear failure, lateral torsional buckling, and bearing failure. Results show that the governing failure mode may change with time and corrosion penetration. Four samples of corrosion damaged beams, which were removed from a chemical works, were subjected to load test for their ultimate capacities. The failure loads of the beams are compared with the calculated capacities of various corrosion damage models. It was found that even the most severely corrosion damaged beam possessed substantial residual capacity.

In order to estimate the percentage remaining capacity of corrosion damaged I-beams, assessment methods are developed that can be used in conjunction with the information on the thickness loss of the beams. They are developed for various failure modes of I-beams of all manufactured sizes in the UK. Lower bound estimates are also proposed for the remaining capacity. Experimental failure loads of the samples of corrosion damaged beams are compared with these methods. The comparison shows that the proposed methods give slightly conservative estimates for the remaining capacity. These methods can easily be used by practising engineers or inspectors to make rapid and realistic estimates of the remaining capacity of corrosion damaged beams following

visual inspection. Improved condition categories called the Strength Categories, which are based on both the capacity loss and the condition of the beams, are introduced using the lower bound estimates.

Structural reliability theory is reviewed and existing methods for the computation of component and system reliability are discussed. For system reliability, a recently developed theory called interval probability theory is introduced. Methods are proposed to compute the component reliability of corrosion damaged steel members. The application of interval probability theory for system reliability is illustrated using the data obtained from the actual samples of corrosion damaged beams.

Acknowledgements

I am indebted to Dr J W Smith for his guidance, advice and support throughout the course of this research. I would like to thank Professor D I Blockley and Dr N J Woodman for their advice and assistance. I would also like to thank Mr Peter Whereat, Mr Alun Young and Mr Roy Sansom for their assistance in conducting the experiments.

The assistance of ICI Technology, and in particular Mr M J Gallon, who contributed to this research project in various forms, and the financial support of EPSRC are greatly acknowledged.

Finally, I would like to thank my wife, Ananthi, for her encouragement and unconditional support throughout my undergraduate and postgraduate courses of studies during the past six years. Without her support, it would have been very difficult to complete this work. I would also like to thank my relatives and friends especially Dr. Nishan Canagarajah and Adiththan for their support.

Declaration

This thesis entitled "Remaining Capacity of Corrosion Damaged Steel Structures" is submitted for the degree of Doctor of Philosophy in the Faculty of Engineering, Department of Civil Engineering at the University of Bristol.

The research on which this thesis is based was carried out under the supervision of Dr J W Smith from October 1993 to September 1996. It is entirely due to the author except where otherwise acknowledged in the text and has not formed the basis for a submission for any other degree.

The following papers are based on the work described in this thesis:

1. Gallon M J, Sarveswaran V, and Smith J W [1995]
   Structural assessment of corrosion damaged steelwork. Extending the Life Span of Structures, IABSE Symposium, San Francisco, Volume 73/1, pp 699-704.

2. Sarveswaran V, and Smith J W
   Development of "Minimum Curves" for the assessment of remaining capacity of corrosion damaged steel beams. To be submitted to Structural Engineer, the Journal of Institution of Structural Engineers (in preparation).

3. Sarveswaran V, and Smith J W
   Assessment of corrosion damaged steelwork using Minimum Capacity Curves. Abstract was submitted for the ICOSSAR'97 conference in Japan.

Signed.....

Date.....27-09-96.....

To my wife Ananthi and to my parents, the late Mr K Velautham, and Mrs E Velautham

CONTENTS

List of figures

List of tables

Notation

Chapters 1 - 6

Symbol	Meaning
A	area
A_e	effective area
A_f	area of flange
A_v	shear area
A_w	area of web
a	Robertson constant
a_s	spacing of transverse stiffeners
B	width of flange
b	width of outstand element of flange
b_1	stiff bearing length
D	depth of beam section
d	depth between fillets of beam section
d_c	cope depth
E	Modulus of elasticity of steel
E_{st}	strain hardening modulus of steel
F_v	shear force
f_v	shear stress
G	shear modulus of steel
G_{st}	strain hardening modulus in shear of steel
H	warping constant of section
h_s	distance between the shear centres of flanges
h_w	depth of web
I_x	second moment of area about the major axis
I_y	second moment of area about the minor axis

J	torsion constant
k	buckling coefficient
L	Length of span
L_C	cope length
L_E	effective length
L_{ECrit}	critical effective length
LFT	loss of flange thickness
LWT	loss of web thickness
M	bending moment
M_b	buckling resistance moment (lateral torsional)
M_c	moment capacity
M_E	elastic critical moment
M_P	plastic moment capacity
n	slenderness correction factor
P_v	shear capacity of a section
P_w	buckling resistance of an unstiffened web
P_{wbg}	web bearing strength
P_x	buckling resistance of load carrying stiffener
p_b	bending strength
p_c	compressive strength
p_{cr}	elastic critical compressive strength
p_E	Euler strength
p_y	design strength
p_{yw}	design strength of web
q_b	basic strength of a web
q_{cr}	critical shear strength of a web panel
q_e	elastic critical shear strength of web panel
q_f	flange dependent shear strength factor
r	root radius
r_x	radius of gyration of a member about its major axis
r_y	radius of gyration of a member about its minor axis
RBRW	remaining buckling resistance of webs

RLTBC	remaining lateral torsional buckling capacity
RMC	remaining moment capacity
RSC	remaining shear capacity
RWBC	remaining web bearing capacity
S_x	plastic modulus of a section about its major axis
S_y	plastic modulus of a section about its minor axis
T	thickness of flange
T_B	thickness of bottom flange
T_C	average thickness of flange of a corroded section
T_N	thickness of flange of an as-new section
T_T	thickness of top flange
t	thickness of web
t_C	average thickness of web of a corroded section
t_L	thickness of lower part of web ($0.25h_w$)
t_N	thickness of web of an as-new section
t_U	thickness of upper part of web ($0.75h_w$)
u	buckling parameter of the section
V	average shear force in a section
V_b	shear buckling resistance of stiffened web using tension field action
v	slenderness factor for beam
x	torsional index of section
Y_b	basic tension field strength
Z_x	elastic modulus of a section about its major axis
Z_y	elastic modulus of a section about its major axis
ε	factor $(275/p_y)^{1/2}$
Φ_B	a term in lateral torsional buckling equation
η	Perry factor
η_{LT}	Perry coefficient
λ	slenderness
λ_{LO}	limiting equivalent slenderness
λ_{LT}	equivalent slenderness
λ_0	limiting slenderness

λ_w	equivalent web slenderness factor
ν	Poisson's ratio
τ_{cr}	elastic critical shear stress
τ_s	elastic shear stress
ξ	thickness loss factor = %LFT / 100
ϵ_{st}	strain at which strain hardening begins

Chapters 7 - 8

Symbol	**Meaning**
E [A]	expected value or mean of A
$F_A(x)$	cumulative probability distribution function of A
$f_A(x)$	probability density function of A
G ( ) = 0	limit state function
M	safety margin or failure indicator
P(A)	probability of A
P_f	probability of failure
R	resistance
S	load or load effect
V	coefficient of variation
Var	variance
β	reliability index
Φ	standard normal distribution function
γ	correlation coefficient
μ	mean value
ρ	degree of dependence
σ	standard deviation
$\cup$	union of events
$\cap$	intersection of events

Chapter 1

Introduction

1.1 Introduction

Energy is required to extract iron from iron ore, and to process it further to produce steel. If left unprotected steel will tend to revert to its natural ore by the process of corrosion. The loss of material due to corrosion and the cost of the consequences of corrosion are very high in any industrial country. Both in the UK and in the USA, for example, the cost of corrosion has been estimated to be around 3% of the gross national product, if all the costs are included [Scully 1990].

In the UK, the petro-chemical industry uses steel extensively as the primary structural material for pipe bridges, frame supports for vessels and process equipment. The most common problem for all of these steel structures is deterioration due to corrosion, which is more rapid in aggressive environments encountered in chemical plants. In addition, the exposed coastal locations in which chemical plants are often located tend to exacerbate the problem. Many of these structures have exceeded 50 years of service life (more than 25% for ICI Ltd) and are often in a severely deteriorated condition [Gallon 1993].

Inspection, maintenance and repair are becoming increasingly costly because of the growing number of structures reaching the latter end of their useful lives. Repair is generally complex because of the need to keep important manufacturing processes in continuous operation. The cost of closing down plants and consequent loss of production of a continuous process may be very high. This cost should, if possible, be compared with costs arising from structural failure. The latter may also be very high depending on the nature of the materials being processed, whether they are toxic, explosive, inflammable or alternatively, relatively less hazardous.

Corrosion of steel structures is a serious problem throughout the world. In the USA, 40% of the bridges are built of steel. Many of these bridges are deteriorating due to corrosion caused by aggressive environments and inadequate maintenance [Kayser et al 1987]. The necessity to determine the capacity of existing bridges has been spurred by catastrophic failures such as the collapses in the USA of Silver bridge in 1967 and the Mianus bridge in 1983. Guidelines have been established to evaluate existing bridges. However, much of the methodology is left to the experience of the engineer.

The simplest consequence of corrosion is reduction in material strength [Smith 1993] and section size due to loss of material. This in turn leads to a reduction in the carrying capacity of the structure, and in its member stiffness thus causing excessive distortions in the members. The accumulation of rust may also cause problems such as frozen pin connections [Bellenoit et al 1985]. The analysis of corrosion damaged structures may differ from the analysis of a structure under design. For example, the thinner webs and flanges may affect the critical failure mode.

It was found during a study carried out by Gallon [1993] that a number of examples of heavily loaded structures with quite severe corrosion were behaving satisfactorily and yet were notionally unsafe. It therefore seemed that those structures had reserves of strength that could be used if quantified. Whilst current procedures for inspection [ICI Engineering 1990a] provide confidence in the remaining capacity of old structures, it is considered that benefits are possible from more realistic appraisals. At present there is a lack of accurate but simple analytical tools for the assessment of remaining capacity of corrosion damaged steel structures. More effective assessment techniques will allow better informed decisions to be made on future action, thus ensuring consistent levels of safety and effective maintenance expenditure.

Recently, a formal procedure for inspection of deteriorated structures (both steel and concrete structures) was introduced throughout the UK by ICI Engineering [1990a]. The procedure laid down requirements for filing data on each structure including design calculations, drawings and inspection history. The deteriorated structures are visually inspected and categorised into four condition categories according to their level of

deterioration. The categories with most severe condition are then subjected to design checks using appropriate codes and standards and using section properties based on the measured section sizes. Although these practices appear to be reasonably safe, on the one hand they may be conservative whilst on the other hand there may be critical details which receive insufficient attention.

However, as yet there is no simple relationship between the magnitude of structural defects due to corrosion (e.g. loss of thickness) and the corresponding reduction in carrying capacity. There is an urgent need for this information to avoid the financial penalty of plant closure when the capacity of the supporting steelwork may be adequate, and to identify the weaker members whose capacities are reaching the service load levels, thus avoiding structural failures. Therefore, a more accurate method of assessment of remaining capacity of deteriorated steel structures will be beneficial in terms of cost and safety. As a consequence, the study of remaining capacity of corrosion damaged steel structures has now become an important issue.

1.2 Objectives of this thesis

The overall aim of this thesis is to enhance understanding of the structural behaviour of corrosion damaged steel structures, to search for improved methods of assessment for their remaining capacity, and to present an approach for quantifying the reduction in safety of these structures.

The specific objectives are:

1. To understand the nature of corrosion and to study the effects of corrosion on steel structures (Chapter 2).
2. To review the current evaluation methods for various failure modes of I-beams and to propose improved evaluation methods for certain failure modes (Chapter 3).
3. To develop corrosion decay models for steel beams, to test samples of corrosion damaged I-beams in the laboratory, and to analyse the failure modes of these beams (Chapter 4).

4. To develop assessment methods to estimate the remaining capacity of corrosion damaged I-beams and to compare these methods with the experimental failure loads of samples of corrosion damaged I-beams (Chapter 5).
5. To recommend improved condition categories to be used in the visual assessment procedure for corrosion damaged steel beams (Chapter 6).
6. To consider the application of structural reliability analysis to the assessment of corrosion damaged steelwork (Chapter 7).
7. To propose a method for the computation of component reliability of corrosion damaged steel members, and to consider the application of interval probability theory for assessing the system reliability of corrosion damaged steel structures (Chapter 8).
8. To summarise the outcomes of this research project (Chapter 9).

1.3 Review of relevant research

The two main causes of deterioration of steel structures are fatigue and corrosion. Fatigue cracking is relevant to structures subjected to many repeated applications of loading. This is the case for bridges which are subjected to loading by millions of heavy goods vehicles per year, and for offshore structures which are subjected to wave loading. Fatigue is not normally relevant to buildings or industrial structures, except where there are crane movements. Fatigue problems of welded structures and bridges have been extensively reviewed by Gurney [1979] and Fisher [1984].

The combination of fatigue and corrosion is very important for offshore structures [Ramachandra Murthy et al 1994] and is also important for bridges where corrosion pits act as stress raisers for fatigue damage [Zurasski 1986, and Albrecht and Naeemi 1984]. There is a voluminous literature in the field of corrosion fatigue but this is not relevant to the current study. Corrosion damage of reinforced and pre-stressed concrete structures is another large and important area of research [Eyre and Nokhasteh 1992], but in general it is not relevant to this investigation.

Previous research works that are more specific to the current study of remaining capacity of corrosion damaged steel structures are given below. They include corrosion damaged industrial steel structures and steel girder-bridges.

An investigation was carried out by Smith [1993] on the mechanical properties of samples of structural steel (nearly 50 years old) affected severely by corrosion. It was concluded that the presence of corrosion pitting of steel surfaces reduces the yield strength slightly compared with smooth steel, and also results in a small reduction in the ductility of the material. Otherwise the material properties were similar to those of modern mild steel.

A study on managing structural corrosion in chemical plants was conducted by Gallon [1993]. The work mainly concentrated on the experiences of ICI Ltd at the Billingham works in Cleveland. Reconstruction of a pipe bridge (EA1), which was built in 1929, was carried out between 1981 and 1986. The project was valued at £25 million. The paper pointed out that the expenditure of such large sums of money on structural refurbishment has promoted the need to carry out regular inspection. The early identification of structural deterioration and maintenance requirements allows action to be taken in a planned fashion making full use of routine plant shutdowns. The current practice of inspection and maintenance of ICI Ltd, which includes classification of structures based on visual inspection, is already mentioned in this chapter. The paper also pointed out that a number of examples of heavily loaded structures which were severely corroded were behaving satisfactorily. Therefore, there is a need to quantify these reserves of strength in order to use them effectively.

A theoretical study on the structural effects of corrosion damage to a pipe bridge was carried out by Smith and Woodman [1992] for ICI Ltd. The purpose of the study was to carry out an analysis of the vulnerability of pipe bridges to loss of structural strength due to corrosion damage. The main findings of the study were that close attention should be paid to the condition of diagonal members which are thin and susceptible to corrosion. Severe corrosion damage to these members could result in structural failure of the frame.

It also concluded that the lower boom members close to the columns are also critical and may tend to trap dirt and moisture.

An investigation into the capacity loss due to corrosion in steel girder-bridges [Kayser and Nowak 1989a] concentrated on developing a corrosion damage model and determining the load carrying capacity with regard to bending, shear and bearing. The evaluation was demonstrated on two typical steel girder-bridges in an aggressive environment. The investigation concluded that the deteriorated capacity of steel girder-bridges can be modelled by combining information about the location and rate of corrosion with structural analysis methods. The modes of resistance that govern the design of a new bridge may not be the same as those which govern when the bridge is old. It was pointed out that the presence of stiffeners will increase the capacity of the corrosion damaged steel bridges.

Another study on the reliability of corrosion damaged steel girder-bridges [Kayser and Nowak 1989b] focused on developing a corrosion damage model which evaluates the reliability of a steel girder-bridge over time. The model was used to evaluate the effects of bridge design and environment on safety. A sensitivity analysis was carried out to identify the most important parameters in corroded bridge safety. The study concluded that the safety of corroding steel girder-bridges can be evaluated using models based on the probable rate and location of corrosion. These corrosion predictions can be combined with structural analysis methods to determine the statistics of resistance. Reliability methods can then be applied to determine the reliability of a corrosion damaged steel bridge over a given length of time.

An investigation into the possibility of using Bayesian updating for improving capacity estimates of corrosion damaged structures [Kayser and Nowak 1987] revealed that the Bayesian approach can be used to update the capacity estimates when new information becomes available. It also suggested a framework in which probabilistic methods can be used to evaluate bridges.

Work has yet to be done on determining the performance and behaviour of beams with holes in the web created by corrosion. A similar problem exists in steel floor framing comprising solid web beams that require the frequent use of large web openings for the passage of service ducts. This led to the investigation of the behaviour of steel and composite beams with web holes [Redwood and Cho 1987]. A general method of prediction of ultimate strength for design use was presented and related to a number of previous studies. Comparisons were made with the results of experimental research. The applicability of this method to the problems with web holes due to corrosion has to verified.

Chapter 2

Corrosion of steel structures

2.1 Introduction

Steel has been used extensively throughout the world for the construction of bridges, buildings, factories, etc. In order to produce steel, iron ores must be processed. During the process of metal extraction, it consumes a large amount of energy to separate the metal from the ore. In the natural environment, it has a tendency to oxidise to a form similar to its natural state under the influence of air and water. This deterioration process is known as corrosion. In a more precise sense, it is an electro-chemical reaction in which water with various pollutants in solution acts as the electrolyte. The aim of this chapter is to consider the main aspects of corrosion of steel structures.

The specific objectives of this chapter are:

1. To consider the deterioration process of steel.
2. To study the different forms and rates of penetration of corrosion of steelwork.
3. To consider the effects of corrosion on steel structures.

2.2 Deterioration process of steel

Corrosion of steel is an electro-chemical process in which iron, Fe, reacts with oxygen to form iron oxides. The familiar iron compounds are: $Fe(OH)_2$, ferrous hydroxide; $Fe(OH)_3$, ferric hydroxide; Fe_2O_3, iron oxide; and Fe_3O_4, magnetite. When steel is attacked under humid conditions in a clean rural atmosphere, the first oxidation product is ferrous ion in the lowest oxidation state, namely, Fe^{+2}. Because of the presence of air dissolved in moisture, the ferrous ion can react with it and precipitate ferrous hydroxide,

$Fe(OH)_2$, which can be quickly oxidised further to the ferric state, Fe^{+3}, to give the gelatinous precipitate of ferric hydroxide. This series of reactions can be expressed as follows [Albrecht and Naeemi 1984]:

The anodic iron dissolves in the condensed moisture film as:

$$Fe \xrightarrow{\text{Humidity}} Fe^{+2} + 2e^- \qquad (2.1)$$

To counter balance this reaction, the cathode accepts the electrons and these electrons react with oxygen as follows:

$$O_2 + 2\,H_2O + 4e^- \longrightarrow 4\,OH^- \qquad (2.2)$$

With free ferrous ions and free hydroxyl ions in solution, the following reaction occurs,

$$Fe^{+2} + 2\,OH^- \longrightarrow Fe(OH)_2 \qquad (2.3)$$

If sufficient oxygen is present, the fresh ferrous hydroxide is then oxidised to produce hydrated ferric oxide, a corrosion product commonly known as yellow rust which contains entrained water.

$$2\,Fe(OH)_2 + O_2 \longrightarrow \underset{\text{Rust}}{2\,FeO.OH} + 2\,OH^- \qquad (2.4)$$

Where FeO.OH is sometimes written as $Fe_2O_3.H_2O$.

When the supply of oxygen is not sufficient, the following reaction takes place to produce another corrosion product which consists of black anhydrous magnetite,

$$6\,Fe(OH)_2 + O_2 \longrightarrow \underset{\text{corrosion product}}{2\,Fe_3O_4} + 6\,H_2O \qquad (2.5)$$

The above mentioned reactions are rather slow. Moist air produces little rusting of iron in the absence of dust and pollutants [Evans 1972]. Rural environments are usually free from aggressive pollutants. They contain relatively small amounts of sulphur oxides and carbon dioxide from combustion products. In such a clean air, the rate at which steel corrodes increases only when the relative humidity exceeds about 70 percent [Albrecht and Naeemi 1984]. Rural environments are generally not aggressive towards steel.

Rapid corrosion of steel observed in service is caused by the more active stimulants such as the pollutants in an industrial environment. The most common pollutants in an industrial environment are the sulphur oxides (SO_x) and carbon dioxide (CO_2) produced during the combustion of fossil fuels, such as oil and coal, each sulphur oxide containing several percent of sulphur. Upon oxidation, sulphur dioxide is the predominant gas with the reminder being sulphur trioxide. The conversion of these gases to mixed sulphurous and sulphuric acids becomes a source of corrosive pollutant. Atmospheric corrosion is most severe where the sulphur oxide levels are high and temperature drops are sufficiently low at night to result in condensation. Urban environments contain sulphur oxides and nitrogen oxides from the combustion of fossil fuels and from automobile exhaust gases. Both contaminants promote the corrosion of steel.

In marine environments airborne salt spray droplets, salt fog, and low temperature at night can keep the steel damp for long periods of time. On drying, salt crystals attract moisture at low relative humidities. The aggressiveness of a marine environment is dependent on the nature of wave action at the surf line, prevailing wind direction, shoreline topography, and relative humidity. Corrosivity from marine salts decreases rapidly with increasing distance from the shore [La Que 1951].

While rural atmospheres are less corrosive than industrial and much less than marine atmospheres, this broad classification by macro-environment is not necessarily a reliable description of the aggressiveness of an atmosphere towards steel. The corrosiveness of an exposure site depends mainly on: (a) the time of wetness, determined largely by the length of time during which the relative humidity exceeds a critical value, (b) degree of airborne sulphur oxide pollution, and (c) chloride contamination. The severity of these

factors are greatly influenced by differences in the micro-environments of the exposure sites even though the macro-environments may be the same [Albrecht and Naeemi 1984].

The corrosion resistance of unprotected steel is dependent on its chemical composition, the degree of pollution in the atmosphere, and the frequency of wetting and drying. Low strength carbon steels are inexpensive but are particularly susceptible to atmospheric corrosion which is often greatest in industrial or coastal environments. High strength low alloy steels (weathering steels) have several times the corrosion resistance of carbon steels, as the rust that forms on the surface of weathering steels becomes a protective coating against further deterioration [Martin and Purkiss 1992].

2.3 Forms of corrosion

2.3.1 General Corrosion

General or uniform corrosion is the formation of oxide, distributed uniformly over an exposed surface. This is the most common form of the corrosion, which will lead to the gradual thinning of members, accounting for the greatest destruction of metals [Fontana 1986]. General corrosion is the most serious form of corrosion observed on steel bridges [Kayser 1988]. This can be a serious problem when it occurs in compression members such as beam webs because the critical mode of failure may change. The rate of uniform loss is highly variable, depending on conditions such as temperature, time of wetness, and chemistry [Guttman and Sereda 1968]. These conditions themselves depend on the local environment such as industrial or marine, as described in Section 2.3.

2.3.2 Pitting corrosion

If the corrosion is concentrated in a small area it may form a pit at the metal surface. This form of corrosion can be serious in high-stress regions because it can penetrate into the metal showing little evidence of its existence. Pits will form imperfections on the metal surface and these imperfections will act as stress concentrations, reducing the fatigue capacity of the metal and increasing the metal's sensitivity to cracking. Pitting is

random in nature and occurs quickly. Pitting may be initiated by external factors, e.g. where external deposits such as debris and de-icing salts have settled on a metal surface. Pitting corrosion is prone to occur in certain environments, particularly in the presence of salt.

2.3.3 Galvanic Corrosion

Galvanic corrosion occurs when two different metals are in contact in a moist or immersed environment. In such instances, one metal will serve as the cathode, and the other will serve as the anode, and a current will flow through the electrolyte from anode to the cathode and back through the metallic contact. Such a galvanic couple causes the anodic metal to corrode more than it would when exposed alone in the same environment, and the cathodic metal to corrode less than when exposed alone. This kind of corrosion may occur in bolted or welded connections. For example, galvanic corrosion can be promoted by the chemical differences between a base metal and adjacent weld material. Galvanic corrosion can be local, leading to pit formation. The rate of galvanic corrosion is difficult to predict but the location where galvanic corrosion could occur can be predicted if material variations are known.

2.3.4 Crevice corrosion

Crevice corrosion is a form of localised attack of a metal surface at or immediately adjacent to an area shielded from exposure to the environment. This condition may be found in a lap splice, beneath peeling paint or any place where two metal surfaces are in close proximity. The mechanism of crevice corrosion involves electro-chemical reactions that take place between the surfaces within the crevice or between the surfaces of the crevice and those freely exposed to the environment outside the crevice [Ellis and La Que 1951]. It is usually caused by a low concentration of dissolved oxygen in the moisture held within a crevice. Material accumulated on a flat surface can also serve as a location for crevice corrosion [Kayser 1988]. If rust or dirt is not cleaned from the surface of beams, girders, etc., crevice corrosion can be initiated in the moist environment beneath the debris.

2.3.5 Stress corrosion

This form of corrosion occurs when a metal is subjected to tensile stress in a corrosive environment. For mild carbon steel in an ordinary environment, stress concentration is not a particular problem. However, high strength low alloy steel is susceptible to stress corrosion in a chloride environment. In general, the lower the fracture toughness of a metal the higher its susceptibility to stress corrosion. Steels used in many structures such as bridges are normally ductile and hence are not subjected to stress corrosion.

2.4 Corrosion pattern

Corrosion of steel occurs when the electrolytes are present on the surface, particularly in places where water and contaminants can accumulate. In members like I- beams, the top surface of the bottom flange is the most vulnerable part for accumulation of the electrolytes. Therefore the top surface of the bottom flange and the bottom part of the web are the places where severe corrosion may take place as shown in Figure 2.1 [Kayser 1988].

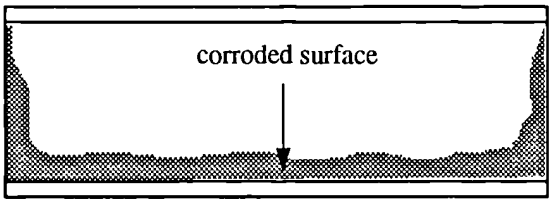

Figure 2.1 Typical beam locations which are susceptible to severe corrosion

The top surface of the top flange can also accumulate contaminants due to spillage from tanks especially in chemical industries. This would cause the corrosion of the top surface of the top flange as well, but may not be to the extent of the bottom flange. Loss of material in the web near the supports may also occur because of the leakage from the top. Visual examination and measurement of the thickness of four samples of severely corroded I-beams obtained from a chemical works also indicated that the corrosion pattern is similar to what is described above (see Chapter 4).

2.5 Rate of corrosion

The rate of corrosion of steel is highly variable, depending on the local environment such as industrial, marine, or rural. The rate of corrosion in different environments has been evaluated using a large amount of data that has been collected on the loss of material of metal specimens in several ongoing studies. It has been observed that the curve that best fits the time-corrosion penetration data is a power law [Townsend and Zoccola 1982] which is given by the following equation:

$$C = At^B \tag{2.6}$$

where

C is the average corrosion penetration, in μm,

t is the exposure time in number of years and

A and B are parameters determined from the regression analysis of experimental data.

The values of A and B depend on the environment in which the structure is located. The parameters A and B for carbon and weathering steels obtained from tests data from different environments in the UK and USA were given by Albrecht and Naeemi [1984]. The average values of A and B for mild and Cor-Ten B steels exposed in the rural, industrial and marine environments in the UK are given in Table 2.1.

Table 2.1 Average values of corrosion parameters A and B for steel

Environment	Mild steel		Cor-Ten B steel	
	A	B	A	B
Rural	43.17	0.577	39.20	0.490
Industrial	90.74	0.621	58.96	0.632
Marine	61.95	0.646	46.10	0.548

The conclusion of a joint study by the British Steel Corporation and the British Transport and Road Research Laboratory [Kilcullen and McKenzie 1979] is worth mentioning here. In this study, specimens of mild, Cor-Ten A and Cor-Ten B steels were exposed in different environments (e.g. Battersea - an industrial site, Teesside - a severe industrial site, Rye - a marine site) to collect data on the rate of penetration of corrosion. The study concluded that it is difficult to predict the long term performance of these steels even on the basis of tests carried out over a number of years. The study found that the corrosion rates of Cor-Ten steels are always significantly lower than that of mild steel, but corrosion rates of Cor-Ten steels in the UK are higher than the results reported from USA.

The rate of penetration of corrosion of steel is highly variable depending upon the local environment. Equation 2.6 is useful for predicting the corrosion loss but it will be very approximate when applied to a real situation, as the equation was obtained using experimental data from small tests coupons. The assessment of remaining capacity of existing structures requires only the information of the magnitude of the loss of material at the time of the assessment. Therefore, in this work, the analysis of corrosion effects will be carried out using percentage loss of thickness of elements.

2.6 The effects of corrosion on steel structures

Steel structures can be affected by corrosion in many ways. The main effects can be loss of material from the surface, which leads to thinner sections, loss of material strength and accumulation of corrosion products (rust) on the surface. Several types of corrosion lead to loss of material. Section loss may take place over a large area (uniform corrosion) or within a small area (pitting corrosion). The loss of material due to uniform corrosion results in the reduction of section properties of a member, such as second moment of area, area, radius of gyration, etc., thus causing a reduction in the carrying capacity of the structure. The stiffness of members may also be reduced due to loss of material. At severe levels of corrosion, the ultimate capacity of a steel member may fall below the service loads. At loading levels still within the ultimate range, reduced member stiffness may cause excessive deflection in the members.

Modes of failure of the structure can also be changed due to the fact that the class of section can be altered due to loss of material. For example, a plastic section may become semi-compact section due to loss of material (thickness) and local buckling may prevent the development of full plastic moment. Pitting corrosion will increase the sensitivity of a member to cracking due to local stress concentrations in the region around the pit. The fatigue resistance of the member will also be reduced due to pitting.

The accumulation of corrosion products (rust) on the surface can affect the behaviour of a steel structure. Rust formation may exert pressure on adjacent elements. Brockenbrough [1983] found that the resulting stress can exceed 8 MPa. Such accumulation of rust inside a bolted or welded connection will cause prying action on the connectors. The formation of tightly packed rust around a bearing or pin connection will freeze the connection. The change in boundary conditions will create unintended stresses in the structure. Components such as hanger plates in suspended steel girder bridges are particularly sensitive to frozen pin connections [Bellenoit et al 1985].

2.7 Summary and conclusions

The main aspects that are associated with corrosion of steel have been discussed in this chapter. The discussion of deterioration process of steel helped to identify the major factors that influence the corrosion of steel. It showed that the local environment is a critical factor in corrosion of steel. The occurrence of various forms of corrosion and their effect on steel structures have also been discussed in this chapter. The discussion showed that this is another important aspect of corrosion.

We have seen that the corrosion of steel occurs on the surface where water and contaminants can accumulate. The corrosion pattern of an I-beam has been outlined in this chapter. In order to help to model the corrosion damage to be used in this study, the following assumptions are made with regard to the corrosion pattern of an I-beam:

1. Top surface of the bottom flange and the bottom part of the web are the places where the most severe corrosion takes place.

2. Corrosion takes place on the top surface of the top flange but not to the same extent as on the bottom flange.
3. Corrosion also takes place in the top part of the web but the loss is very much less compared to that of the bottom part of the web.
4. At the initial stages of corrosion, corrosion penetration may be taken as uniform everywhere.

These assumptions may be used as the basis for the development of corrosion decay models which will be discussed in Chapter 4.

The discussion on the rate of penetration of corrosion of steel showed that the prediction of corrosion loss is very difficult since it is highly variable depending on the local environment. There are two main effects of corrosion on steel structures and they are loss of material from the surface, and accumulation of corrosion products. Loss of material reduces the capacity of a structure and may also change the failure mode of the structure. Accumulation of rust may cause prying action on the connectors and also cause frozen pin connections.

Chapter 3

Review of assessment methods

3.1 Introduction

The corrosion of steel structures is a serious problem throughout the world. The most significant consequence of corrosion is reduction of section size. This in turn leads to reduction in the carrying capacity and structural safety. The corrosion also causes a small reduction in the ductility of the material and the presence of steel surfaces with corrosion pitting reduces the yield strength by about 3% [Smith 1993]. The analysis of existing structures may differ from the analysis of structures under design, especially if there is damage by corrosion. Some of the assumptions made in design may no longer be true and other failure mechanisms may become significant.

Currently, for deteriorated structures, structural design checks are carried out to appropriate codes and standards using re-assessed section properties based on measured section sizes and simple analytical models [Gallon 1993]. In the case of structural steelwork, BS 5950: Part 1 [1985] can be used to assess the capacity of corroded members with regard to various failure modes. There are, however, a few cases which are not adequately covered in the present codes.

Common examples of corrosion that have been found in the petro-chemical industry include loss of section in flanges and holes in the web. The existence of holes in the web is likely to reduce the shear capacity significantly. In steel construction, beam flanges must often be coped or notched to provide enough clearance for the supports when the framing beams are at the same elevation as the main beams or when the bottom flanges of intersecting beams are held at the same elevation for architectural purposes. These beams are called "coped beams" and the lateral end restraint is considerably reduced

because rotation of the flange in plan is not resisted at the coped end. As there is no clear provision of recommendations for such cases in the present codes, there is a need for simple assessment methods to deal with them effectively.

The main objectives of this chapter are therefore:

1. To review the current evaluation methods for various failure mechanisms of beams.
2. To provide assessment methods based on the works of other researchers for lateral torsional buckling capacity of coped beams and shear capacity of beams which have holes in the web.

3.2 Moment capacity

3.2.1 Local buckling of flanges

Structural steel members such as I-beams, columns, channels, etc. are composed of connected elements (e.g. web, flanges, etc.) which, for the purpose of analysis and design, can be treated as flat plates. When compression forces are applied to opposite edges of a flange as shown in Figure 3.1, a theoretical critical stress can be evaluated indicating that the flange may buckle locally before the member as a whole becomes unstable or before the yield stress of the material is reached. Such a critical stress may be in either the elastic or inelastic range.

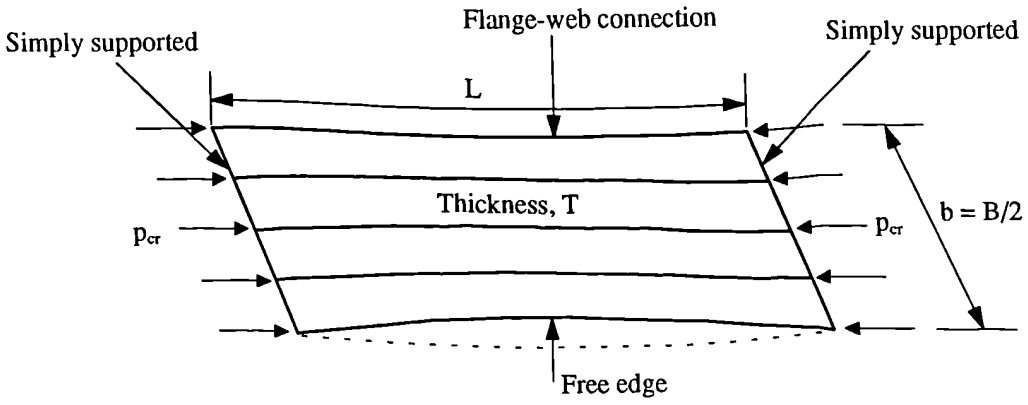

Figure 3.1 Buckled shape of a plate free along one side

The resistance of an element to plate buckling depends on its geometry, its material properties and its external restraint conditions along the boundaries. For the case of flange buckling, the critical factor is found to be the ratio of the width of the outstand element of compression flange, b(= B / 2), to the flange thickness, T [Lay 1965].

3.2.2 Elastic buckling of flanges

The thin plate shown in Figure 3.1 is simply supported along both transverse edges and one longitudinal edge and is free along the other and is subjected to compression forces as shown. When the applied forces are equal to the critical value, the plate can buckle by deflecting laterally out of its original plane as shown in Figure 3.1. The magnitude of this elastic critical compressive stress, p_{cr}, at which the plate buckles is given by Timoshenko [1961] as:

$$p_{cr} = k\frac{\pi^2 E}{12(1-\nu^2)(b/T)^2} \qquad (3.1)$$

where k is a buckling coefficient determined by a theoretical critical load analysis [Timoshenko 1961, and Stowell et al 1952]. It is a function of plate geometry and restraint conditions.

This elastic critical compressive stress was obtained by assuming that the buckled shape of the plate is in the form of a sinusoidal half-wave over the full length of the flange as shown in Figure 3.1. When a member cross section is composed of various connected elements, a lower bound of the critical stress can be determined by assuming, for each plate element, a simple support condition for each edge attached to another plate element, or a free condition for any edge not so attached [Johnston 1976]. In the case of a flange (by treating it as a plate), the restraint condition can be taken as simple support along the connection with the web and free at the other.

In this case, the buckling coefficient, k, is approximated by Trahair [1977] as:

$$k = 0.425 + \left(\frac{b}{L}\right)^2 \qquad (3.2)$$

For long plate elements, which are used in most structural steel members, the length of the plate, L, can be taken as large or infinity and the buckling coefficient, k, can be taken as the minimum value of 0.425. In this case, the elastic critical stress is equal to the yield stress, p_y, of a steel for which E = 205 kN/mm^2 and $\nu = 0.3$ when the limiting b/T ratio is as follows:

$$b/T = 16.9\varepsilon \qquad (3.3)$$

where $\varepsilon = \sqrt{275/p_y}$

If this b/T ratio is exceeded, elastic buckling of the outstanding element is predicted. However this b/T ratio is not necessarily a conservative basis for design, since residual stresses and initial imperfections will have their greatest strength reducing influence precisely at the b/T ratio found in this manner [Johnston 1976]. BS 5950 [1985] predicts elastic buckling of outstanding elements of rolled sections when the ratio, $b/T > 9.5\varepsilon$. BS 5950 [1985] recommends a reduced design strength, p_y, when the ratio, $b/T > 15\varepsilon$, i.e. for slender cross sections.

3.2.3 Plastic buckling of flanges

For plastic buckling of flanges of I beams, two solutions have been proposed: an orthotropic-plate solution and a torsional buckling solution for a restrained rectangular plate. In both cases it is assumed that the material is strained uniformly to ϵ_{st}, the strain at which the strain hardening begins and that the material will then strain harden with a strain hardening modulus, E_{st} (see Figure 3.2).

For both solutions, the limiting ratio of the width of the outstand element of compression flange, b, to the flange thickness, T, to avoid local buckling in the flange has been determined as described below.

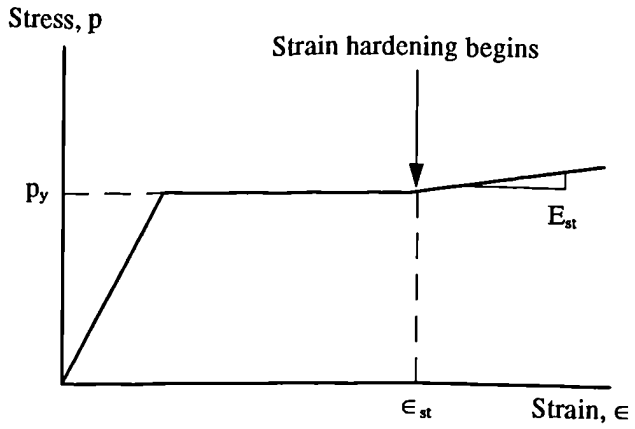

Figure 3.2 Idealised Stress-Strain relationship of steel

a) Assuming that the flange is unrestrained from buckling by the web (i.e. the flange-web connection edge is hinged), and the buckled shape of the flange is in the form of a sinusoidal half-wave over the full length of the flange as in Figure 3.1, the orthotropic-plate solution gives [Haaijer 1957],

$$\frac{b}{T} = \sqrt{\frac{G_{st}}{p_y}} \tag{3.4}$$

b) Assuming that the flange is restrained against buckling by the web, and the flange buckles in 'n' sinusoidal half-waves where 'n' is found as the 'n' that gives the lowest value of compressive stress, p_{cr}, and is given by Equation 3.6b, the torsional buckling solution gives [Lay 1965],

$$\frac{b}{T} = \sqrt{\frac{G_{st}}{p_y} + 0.381\left(\frac{E_{st}}{p_y}\right)\left(\frac{t}{T}\right)^2\left(\frac{BT}{th_w}\right)^{1/2}} \tag{3.5}$$

where G_{st} is the strain hardening modulus in shear and is given by [Lay 1965]:

$$G_{st} = \frac{2G}{1+(E/4E_{st}(1+\nu))} \tag{3.6a}$$

n is the number of sinusoidal half-wave lengths and is given by Lay [1965] as:

$$n = 1.40\frac{L}{b}\frac{t}{T}\left(\frac{BT}{th_w}\right)^{1/4} \qquad (3.6b)$$

and E_{st} is the strain hardening modulus.

The first term under the square root of Equation 3.5 is the basic equation (Equation 3.4) whereas the second term represents the contribution of web restraint in the plastic range. For most sections, the increase in allowable b/T ratio resulting from web restraint is about 3% [Lay 1965]. For rolled sections, Haaijer [1957] assumed 9% increase in allowable b/T ratio resulting from web restraint.

$$\text{i.e. } \frac{b}{T} = 1.09\sqrt{\frac{G_{st}}{p_y}} \qquad (3.7)$$

For example, when using, E = 205 kN/mm^2, ν = 0.3, and E_{st} = 5.65 kN/mm^2;

Equation 3.4 gives,

$$b/T \leq 8.5\varepsilon \qquad (3.8)$$

Equation 3.7 gives,

$$b/T \leq 9.25\varepsilon \qquad (3.9)$$

where

$$\varepsilon = \sqrt{275/p_y}$$

It should be noted that the limiting b/T ratios recommended by BS 5950 [1985] for plastic buckling of welded and rolled sections are 8.5ε and 9.5ε respectively.

3.2.4 Effect of shear force on moment capacity

The effect of shear force (F_v) on moment capacity is to reduce the plastic moment of resistance but the reduction for an I-section is small for $F_v < 0.6P_v$, where P_v (Shear capacity) = $0.6A_vP_y$. BS 5950 [1985] recommends that, for low shear loads, where $F_v < 0.6P_v$, there is no reduction in the plastic moment of resistance for plastic or compact sections. This recommendation was based on the work of Morris and Randall [1979] who stated that shear can be ignored unless the average shear stress in the web exceeds $p_y/3$ or $p_y/4$ when the ratio of D/B exceeds 2.5. For high shear loads, where $F_v > 0.6P_v$, reduced plastic moment of resistance for plastic and compact sections is recommended by BS 5950 [1985].

3.3 Shear capacity

3.3.1 Shear capacity without tension field action

The web panel shown in Figure 3.3 is loaded by shear stresses, τ, along its edges. It is assumed that all four edges of the web panel are simply supported. When these stresses are equal to the elastic critical shear stress, the web panel can buckle. This elastic critical shear stress, τ_{cr}, at which the web buckles can be predicted from plate buckling theory and is given by Timoshenko [1961] as:

$$\tau_{cr} = k\frac{\pi^2 E}{12(1-\nu^2)(d/t)^2} \qquad (3.10)$$

where k is a buckling coefficient determined by a theoretical critical load analysis [Timoshenko 1961, and Stowell et al 1952]. It is a function of plate geometry and boundary conditions and is given by Johnston [1976] as:

$$k = 4.00 + \frac{5.34}{(a_s/d)^2} \quad \text{for } a_s/d \le 1 \qquad (3.11a)$$

$$k = 5.34 + \frac{4.00}{(a_s/d)^2} \quad \text{for } a_s/d > 1 \qquad (3.11b)$$

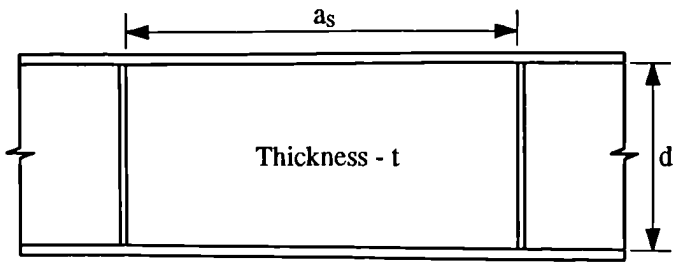

(a) Geometry of web panel

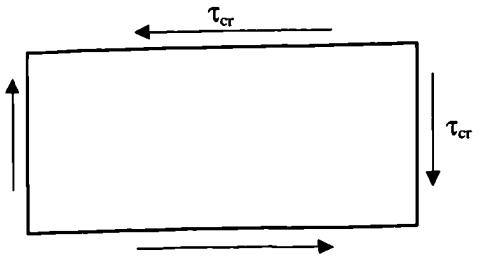

(b) Buckled shape

Figure 3.3 Web buckling due to pure shear

If the numerical values for $\nu = 0.3$ and $E = 205\ kN/mm^2$ are substituted in to Equation 3.10, and Equations 3.11a and 3.11b are combined with Equation 3.10, then,

$$\tau_{cr} = \left(0.75 + \frac{1}{(a_s/d)^2}\right)\left(\frac{995}{d/t}\right)^2 \qquad \text{for } a_s/d \le 1 \qquad (3.12a)$$

$$\tau_{cr} = \left(1 + \frac{0.75}{(a_s/d)^2}\right)\left(\frac{995}{d/t}\right)^2 \qquad \text{for } a_s/d > 1 \qquad (3.12b)$$

The shear stresses in many structural members are transmitted by unstiffened webs, for which the aspect ratio, a_s/d, can be taken as large or infinity. Therefore, for unstiffened webs, using Equation 3.12b, τ_{cr} can be given by:

$$\tau_{cr} = \left(\frac{995}{d/t}\right)^2 \qquad (3.13)$$

If a factor of safety of 1.5 against web buckling with no stiffener is needed, then

$$1.5\tau_{cr} = \left(\frac{995}{d/t}\right)^2 \qquad (3.14)$$

Using maximum distortion strain energy theory (Von-Mises yield criterion), it can be shown that the yield stress in shear, τ_y, is equal to $p_{yw}/\sqrt{3}$ ($\approx 0.6p_{yw}$), where p_{yw} is the design strength of the web [Trahair 1977]. Stocky unstiffened webs in steel beams yield in shear before they buckle elastically. When a web panel yields, the critical shear stress is equal to yield stress in shear.

$$\text{i.e. } \tau_{cr} = \frac{p_{yw}}{\sqrt{3}} \qquad (3.15)$$

Using Equations 3.14 and 3.15, the limiting ratio of d/t for web yielding in shear can be given by:

$$d/t = 65\varepsilon \qquad (3.16)$$

where

$$\varepsilon = \sqrt{275/p_{yw}}$$

BS 5950 recommends that when d/t exceeds 63ε the web should be checked for shear buckling. This limiting value of d/t is based on the experimental work by Longbottom and Heyman [1956] and later work by Horne [1958]. The code uses the notation q_e instead of τ_{cr} for the elastic critical shear stress. It also identifies three modes of behaviour of webs which is shown in Figure 3.4. The first is where the web strength is governed by its ultimate yield strength, i.e. $p_{yw}/\sqrt{3}$, the third is where the capacity is solely governed by the elastic critical shear stress, q_e, and the intermediate stage is where an interaction occurs between the first and third behaviours. The divisions between the three modes are quantified by equivalent web slenderness factor, λ_w, which is given by:

$$\lambda_w = \left(\frac{0.6p_{yw}}{q_e}\right)^{1/2} \qquad (3.17)$$

The code gives the critical shear strength, q_{cr}, of a web panel as follows:

for $\lambda_w \leq 0.8$, $q_{cr} = 0.6p_{yw}$ (3.18a)

for $0.8 < \lambda_w < 1.25$, $q_{cr} = 0.6p_{yw}[1 - 0.8(\lambda_w - 0.8)]$ (3.18b)

for $\lambda_w \geq 1.25$, $q_{cr} = q_e$ (3.18c)

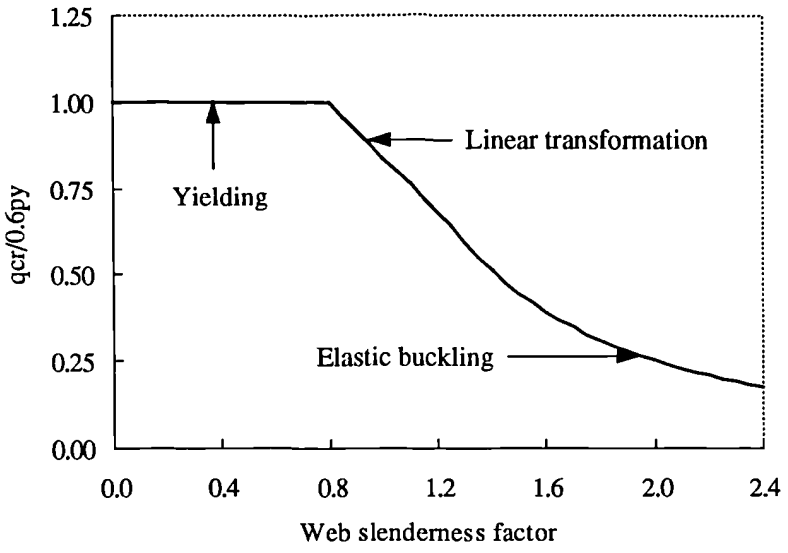

Figure 3.4 Ultimate strength of unstiffened webs in shear

When no stiffener is provided, using Equations 3.13 and 3.17 it can be shown that,

if $\lambda_w = 0.8$, then $d/t = 63\varepsilon$

and if $\lambda_w = 1.25$, then $d/t = 98\varepsilon$

When an I-beam is subjected to bending most of the shear force is resisted by the web. The web thickness of a corroded beam can be uniform at the initial stages of corrosion. In sections, where web thickness does not vary significantly due to corrosion, the

average web thickness may be used for evaluating the shear capacity. Under these circumstances the shear capacity can be evaluated in accordance with cl 4.2.3 of BS 5950 [1985]. When the depth to thickness ratio, d/t, exceeds 63ε the web should be checked for shear buckling in accordance with cl 4.4.5 of BS 5950 [1985].

3.3.2 Shear capacity with tension field action

As the shear load increases on a stiffened web panel no undue deformation occurs until the web panel buckles in shear. The load at this point is not the maximum load capacity as the load can still be increased with the effect of the web that has buckled taking load in tension. This tension member acts obliquely across the web panel although it is not coincident with the diagonal of the web panel. This additional reserve of strength is known as tension field action.

There are three components to the predicted shear strength of a web using tension field action [Porter et al 1975]: first is the buckling strength, the second due to the tension action of the web and the third due to the contribution of the flanges. The code gives the shear capacity of a web using tension field action as follows:

$$\frac{V_b}{dt} = q_b + q_f\sqrt{K_f} \leq 0.6p_{yw} \qquad (3.19)$$

where

V_b is the shear capacity,

q_b is the basic web capacity and

$q_f\sqrt{K_f}$ is the flange component.

The basic web capacity, q_b, of a web panel is given as:

$$q_b = q_{cr} + \frac{Y_b}{2\left[(a_s/d)+\left(1+(a_s/d)^2\right)^{1/2}\right]} \qquad (3.20)$$

where Y_b is the basic tension field strength given by:

$$Y_b = \left(P_{yw}^2 - 3q_{cr}^2 + \phi_t^2\right)^{1/2} - \phi_t \quad \text{and} \tag{3.21}$$

$$\phi_t = \frac{1.5q_{cr}}{\left(1+(a_s/d)^2\right)^{1/2}} \tag{3.22}$$

The contribution of the flanges is given by:

$$q_f = \left(4\sqrt{3}\,\mathrm{Sin}(\theta/2)\left(\frac{Y_b}{P_{yw}}\right)^{1/2}\right)0.6p_{yw} \tag{3.23a}$$

where

$$\theta = \tan^{-1}(d/a_s) \tag{3.23b}$$

It is evident from Equations 3.20 and 3.22 that the aspect ratio, a_s/d, is the major factor that governs the basic web capacity and tension field strength.

3.3.3 Shear capacity of beams with varying web thickness

The web thickness of corrosion damaged beams are not normally uniform. The bottom part of the web loses more material than the upper part as shown in Figure 3.5. In such cases, BS 5950 [1985] recommends that the shear stress should be calculated from first principles assuming elastic behaviour. The maximum shear stress, f_v, should not exceed $0.7p_y$. The elastic shear stress, τ_C, at a point C in the web is given by:

$$\tau_C = \frac{VA_Cy_C}{It_C} \tag{3.24}$$

where

V is the shear force in the section,

A_C is the area of the hatched section (area between the point C and the extreme fibres), y_C is the distance between the centroid of the area A_C and the neutral axis of the section, I is the second moment of area of the whole section about its neutral axis, and t_C is the web thickness at point C.

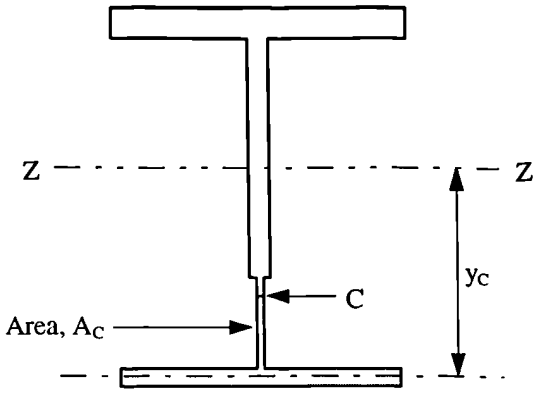

Figure 3.5 Corrosion damaged I-section with varying web thickness

By taking the maximum allowable shear stress as $0.7p_y$, the shear capacity of the section can be given as:

$$V = 0.7p_y \frac{It_C}{A_C y_C} \tag{3.25}$$

The critical shear force, V_{cr}, for the maximum shear stress will be given by V_{min} of Equation 3.25. As the area of hatched section, A_C, reduces the magnitude of y_C increases, but the variation in y_C is very small. It is evident from Equation 3.25 that the magnitude of shear force, V, will be minimum when the magnitudes of A_C and y_C are maximum and t_C is minimum. Therefore, by neglecting the variation in y_C, the critical shear force can be obtained by identifying the combination of critical minimum web thickness and the corresponding area of the hatched section, A_C.

3.3.4 Shear capacity of beams with holes in the web

A single opening (hole) in a beam web and its dimensions are shown in Figure 3.6. Tests have shown that under the action of bending moment and shearing force, a stocky webbed beam fails at the opening due to plastic deformation which occurs near each corner of the opening and in the webs above or below the opening [Redwood and Cho 1987]. Well defined plastic hinges near the hole corners lead to large relative deflection between its ends. A typical failure mode is shown in Figure 3.7. This deformation which is called 'Vierendeel' deformation occurs at openings placed at any height within the web, when a shearing force is present. This deformation is found to occur under all combinations of moment and shearing force except for pure bending.

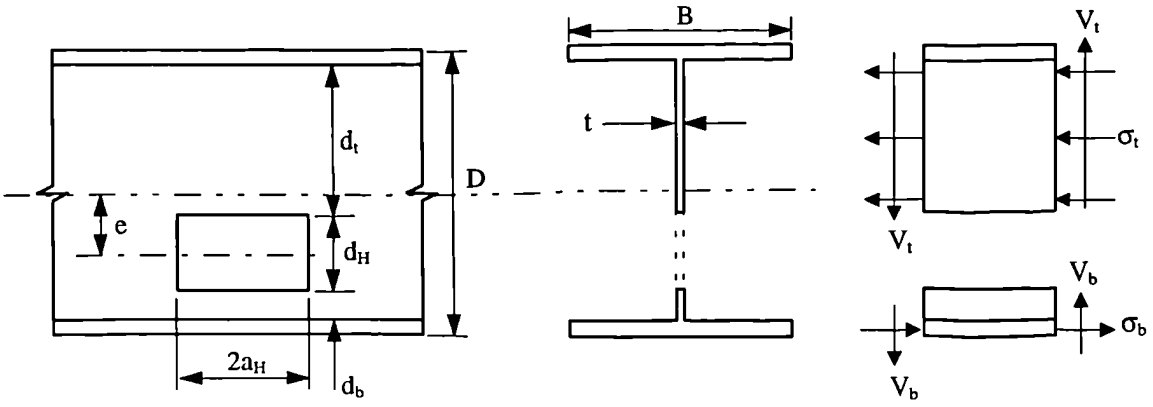

Figure 3.6 Dimensions of a web hole in a non-composite steel beam

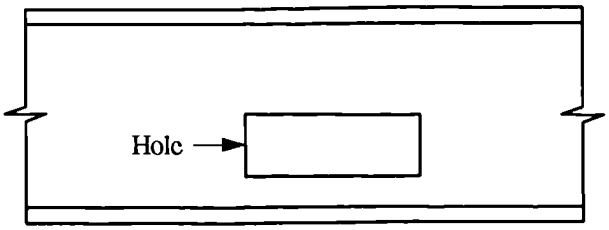

Figure 3.7 Mode of failure of a web which has a hole

The analysis was based on the assumption of stresses at the four sections near the opening corners which are in equilibrium with the applied loads and which satisfy the

Von Mises yield criterion, thus leading to a lower bound solution [Redwood and Cho 1987]. Redwood and Cho, and others have directed their attention to identify two or three points from which a moment-shear interaction diagram can be constructed as shown in Figure 3.8. For a given case, when the applied loads produce a bending moment, M, and shear force, V, the section is not analysed under these actual loads, but rather the interaction diagram is constructed, and the particular load combination is examined to see if it lies within the bounds of the diagram. Therefore, the beam resistance is directly compared with the applied loading.

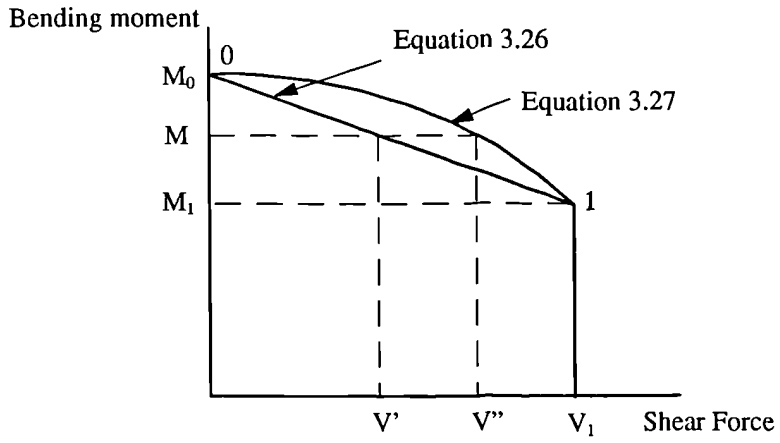

Figure 3.8 Moment-shear interaction diagram

Several different equations for the interaction diagram have been suggested and in particular Redwood and Cho [1987] proposed the following:

$$\left(\frac{M-M_1}{M_0-M_1}\right)+\left(\frac{V}{V_1}\right)=1 \quad \text{where } V = V' \tag{3.26}$$

or

$$\left(\frac{M-M_1}{M_0-M_1}\right)^2+\left(\frac{V}{V_1}\right)^2=1 \quad \text{where } V = V'' \tag{3.27}$$

If the loading on the beam at the opening, represented by M_f and V_f, is to be less than the beam resistance given by the interaction diagram (Equation 3.26), then,

$$V_f \leq V_1 \tag{3.28}$$

$$M_f \leq M_0 - \frac{(M_0 - M_1)V_f}{V_1} \tag{3.29}$$

It has been shown by Wang et al [1975] that in the case where there is no reinforcement at the opening (see Figure 3.6), the salient points, M_0, M_1 and V_1, of the interaction diagram are given by:

$$\frac{M_0}{M_p} = \frac{1 + \frac{A_w}{A_f}\left[\frac{1}{4} - \frac{(d_H/2)^2 + 2(d_H/2)e}{D^2}\right]}{1 + \frac{A_w}{4A_f}} \tag{3.30}$$

$$\frac{M_1}{M_p} = \frac{1 - \frac{A_w}{2A_f}\left[\left(1 - \frac{2(d_H/2) + 2e}{D}\right)^2\left(\frac{1}{1+\beta_b}\right)\right]^{1/2}}{1 + \frac{A_w}{4A_f}} \tag{3.31a}$$

or

$$\frac{M_1}{M_p} = \frac{1 - \frac{2}{\sqrt{3}}\frac{A_w}{A_f}\frac{a_H}{D}\left(\frac{\beta_b}{1+\beta_b}\right)^{1/2}}{1 + \frac{A_w}{4A_f}} \tag{3.31b}$$

$$\frac{V_1}{V_p} = \frac{2}{\sqrt{3}}\frac{a_H}{D}\left[\frac{\beta_t}{\sqrt{1+\beta_t}} + \frac{\beta_b}{\sqrt{1+\beta_b}}\right] \tag{3.32}$$

where

a_H, d_H, and D are as shown in Figure 3.6,

e is the distance between the centroids of the beam and hole,

A_f and A_w are the area of the flange and web respectively,

M_p is the plastic moment capacity of the section = $p_y S_x$,

V_p is the shearing capacity of the section = $0.6 p_y A_w$,

$$\beta_b = 3\left(\frac{d_b}{2a_H}\right)^2 \text{ and} \tag{3.33}$$

$$\beta_t = 3\left(\frac{d_t}{2a_H}\right)^2 \tag{3.34}$$

where d_b and d_t are as shown in Figure 3.6.

These equations are only applicable for low shear load cases, as full plastic moment capacity (no reduction for shear force effect) was used by Wang et al [1975] for the derivation of these equations. Therefore, approximate equations were derived by the writer for high shear load cases using maximum shear load ($V = V_p$) and are given by:

$$\frac{M_0}{M_p^1} = 1 + \frac{A_w}{A_f}\left[\frac{1}{4} - \frac{(d_H/2)^2 + 2(d_H/2)e}{D^2}\right] \tag{3.35}$$

$$\frac{M_1}{M_p^1} = 1 - \frac{2}{\sqrt{3}}\frac{A_w}{A_f}\frac{a_H}{D}\left(\frac{\beta_b}{1+\beta_b}\right)^{1/2} \tag{3.36}$$

where $M_p^1 = p_y(S_x - S_v\rho)$ [BS5950 1985]

This method is illustrated by an example of a beam with a corrosion hole as shown in Figure 3.9. The beam is taken as simply supported at the ends and loaded at the midspan with high shear load.

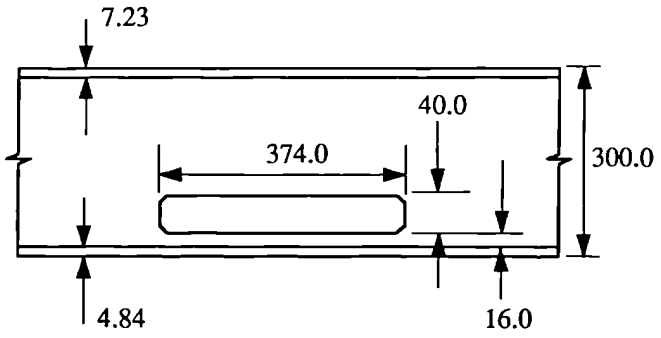

L = 1114.0
B = 160.9
t = 4.88

All dimensions are in millimetres

Figure 3.9 Beam with a corrosion hole

Using Equations 3.35 and 3.36, the salient points, M_0, M_1 and V_1, of the interaction diagram were obtained and the interaction diagram was constructed as shown in Figure 3.10.

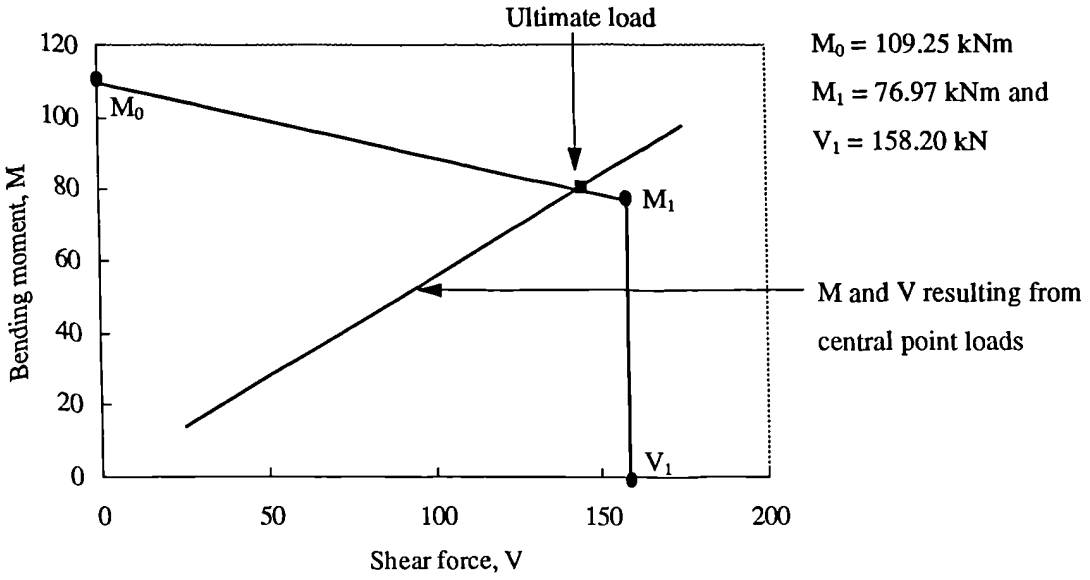

Figure 3.10 Moment-shear interaction diagram for the beam given in Figure 3.9.

3.4 Lateral torsional buckling capacity

3.4.1 Lateral torsional buckling capacity of I-beams

The compression flange of an I-beam acts like a column and will buckle sideways if the beam is not sufficiently stiff or the flange is not restrained laterally. The load at which the beam buckles can be much less than that causing the full moment capacity to develop. For an idealised perfectly straight beam, there are no deformations out of the plane of the loading until the applied moment reaches a critical value M_E, less than the moment capacity, where it buckles by deflecting laterally and twists as shown in Figure 3.11. These two deformations are interdependent: when the beam deflects laterally, the applied moment exerts a component torque about the deflected longitudinal axis which causes the beam to twist. This behaviour, which is important for long unrestrained I-beams, is called lateral torsional buckling.

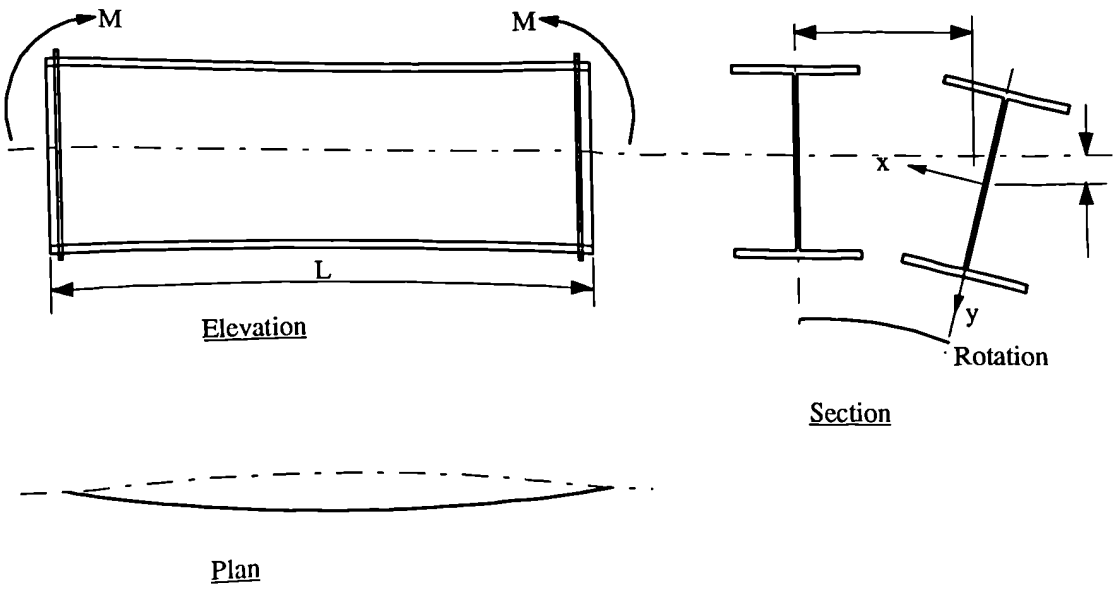

Figure 3.11 Lateral torsional buckling of I-beams

A perfectly straight beam which is loaded by equal and opposite end moments is shown in Figure 3.11. The beam is simply supported at its ends so that lateral deflection and twist are prevented, while the flange ends are free to rotate in plan. Elastic theory is used to set up equilibrium equations to equate the disturbing effect to the lateral bending and torsional resistance of the beam. The solution of these equations for the elastic critical moment was given by Timoshenko [1961] as:

$$M_E = \frac{\pi}{L}\left(EI_y GJ\right)^{1/2}\left(1+\frac{\pi^2 EH}{L^2 GJ}\right)^{1/2} \qquad (3.37)$$

The magnitude of the critical moment given by Equation 3.37 does not depend on the major axis flexural rigidity EI_x of the beam in the vertical plane. This conclusion is obtained as a result of the assumption that the deflections in the vertical plane are small (see Figure 3.11), which is justifiable when the flexural rigidity EI_x is very much greater than the rigidity EI_y. If the rigidities are of the same order of magnitude, the effect of bending in the vertical plane may be of importance and should be considered [Timoshenko 1961]. The equation for the elastic critical buckling moment, which includes the effect of major axis bending, is given by Martin and Purkiss [1992] as:

$$M_E = \frac{\pi}{L}\left(\frac{EI_yGJ}{\gamma}\right)^{1/2}\left(1+\frac{\pi^2 EH}{L^2GJ}\right)^{1/2} \qquad (3.38)$$

where γ is the correction factor, which is just less than unity for most beam sections, and is given by,

$$\gamma = 1 - \frac{I_y}{I_x} \qquad (3.39)$$

In the theoretical analysis, the beam was assumed to be geometrically perfect, i.e. had no imperfections due to lack of straightness, and had no residual stresses due to the manufacturing process. In reality, beams have initial curvature, twist, residual stresses, and the loads are applied eccentrically. The theory set out above requires modification to account for actual behaviour. Theoretical studies and tests [Nethercot 1974] show that at low slenderness ratios the beam achieves its full plastic moment capacity, whereas at high slenderness ratios the behaviour closely approximates to that predicted by Equation 3.38. At intermediate slenderness ratios the behaviour is dependent on the buckling moment and the plastic moment of resistance. This lateral torsional buckling behaviour of a beam as a function of slenderness is shown in Figure 3.12.

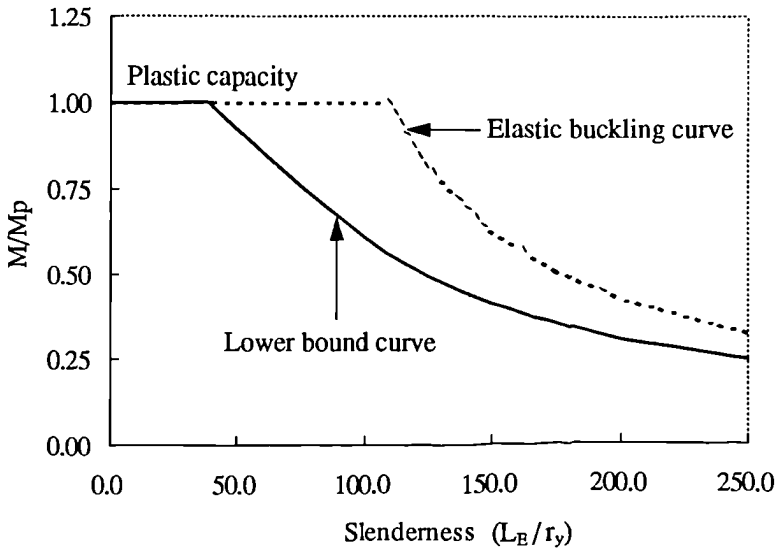

Figure 3.12 Lateral torsional buckling behaviour of a beam

The equivalent slenderness ratio for beam buckling, λ_{LT}, is defined as:

$$\lambda_{LT} = \left(\frac{\pi^2 E}{p_y}\right)^{1/2}\left(\frac{M_P}{M_E}\right)^{1/2} \qquad (3.40)$$

The equation for λ_{LT} is not convenient for design purposes as the calculation of M_E is cumbersome. To simplify the problem, two further section properties are required and are defined by either of the following Equations, 3.41 or 3.42, for sections symmetric about both axes (e.g. I-beams).

For sections symmetric about the major axis:

$$u = \left(\frac{I_y S_x^2 \gamma}{AH}\right)^{1/4} \qquad (3.41a)$$

$$x = 1.132\left(\frac{AH}{I_y J}\right)^{1/2} \qquad (3.41b)$$

For sections symmetric about the minor axis:

$$u = \left(\frac{4S_x^2 \gamma}{A^2 h_s^2}\right)^{1/4} \qquad (3.42a)$$

$$x = 0.566 h_s\left(\frac{A}{J}\right)^{1/2} \qquad (3.42b)$$

where h_s is the distance between the shear centres of the flanges.

Using,

$$r_y^2 = I_y/A \qquad (3.43)$$

$$G = \frac{E}{2(1+\nu)} = \frac{E}{2.6} \qquad (\nu = 0.3 \text{ for steel}) \qquad (3.44)$$

and defining $\lambda = L_E/r_y$, (3.45)

Equation 3.38 for elastic critical moment can be given as:

$$M_E = \frac{\pi^2 ES_x}{(\lambda uv)^2} \tag{3.46}$$

where

$$v = \text{slenderness factor for I sections} = \left(1+\frac{1}{20}\left(\frac{\lambda}{x}\right)^2\right)^{-1/4} \tag{3.47}$$

Now using Equations 3.40 and 3.46 it can be shown that,

$$\lambda_{LT} = uv\lambda \tag{3.48}$$

To deal with the intermediate slenderness cases between elastic buckling (M_E) and full plastic moment (M_P), a 'Perry-Robertson' approach is used in BS 5950 [1985] and the buckling resistance moment, M_b, is given as the least root of

$$(M_P - M_b)(M_E - M_b) = \eta_{LT} M_E M_b \tag{3.49}$$

where η_{LT} is a coefficient to allow for initial imperfections and residual stresses.

The least root of Equation 3.49, M_b, is given by:

$$M_b = \frac{M_E M_P}{\Phi_B + (\Phi_B^2 - M_E M_P)^{1/2}} \tag{3.50}$$

$$\Phi_B = \frac{M_P + (\eta_{LT}+1)M_E}{2} \tag{3.51}$$

It was noticed from tests that buckling does not occur at values of $(M_P/M_E)^{1/2}$ of less than 0.4, thus a limiting slenderness ratio, λ_{LO}, is defined by:

$$\lambda_{LO} = 0.4\left(\frac{\pi^2 E}{p_y}\right)^{1/2} \qquad (3.52)$$

The imperfection coefficient, called the Perry coefficient is defined by:

a) $\eta_{LT} = 0.007(\lambda_{LT} - \lambda_{LO})$ for rolled sections (3.53)

b) $\eta_{LT} = 2\alpha_b\lambda_{LO}$ for welded sections (3.54)

where α_b is a constant.

The theoretical solution applies to a beam subjected to a uniform moment. In other cases where the moment varies, the tendency to buckling is reduced. If the load is applied to the top flange and can move sideways it is destabilising, and buckling occurs at lower loads than if the load were applied at the centroid or to the bottom flange. It is therefore necessary to modify the above approach to allow for loading along the span of the beam either in the form of distributed loading or in the form of point loading and to allow for the effects of support conditions where for example twisting may occur. The problems of non-uniform moments and varying end conditions can be solved using cl 4.3 of BS 5950 [1985].

In summary, the lateral torsional buckling capacity of I-beams depends on several geometric parameters such as the beam length, end (support) conditions, Plastic modulus, lateral stiffness, torsional properties and the warping resistance of its section. The application of the loads and shape of the bending moment diagram between restraints also influences lateral torsional buckling capacity.

3.4.2 Lateral torsional buckling capacity of coped I-beams

In steel construction, beam flanges must often be coped or notched to provide enough clearance for the supports when the framing beams are at the same elevation as the main beams or when the bottom flanges of intersecting beams are held at the same elevation for architectural purposes, as shown in the Figure 3.13. Such a cut-out is called a cope

or notch. Simply supported end conditions are usually assumed in the design of coped beams connections.

The basic theoretical formulas for lateral torsional buckling of pinned end beams derived by Timoshenko [1961], upon which current design recommendations are based, assume that the flanges at the ends of the beams are restrained against lateral movement. However, when a laterally unsupported beam has copes at the connections, the lateral end restraint will be reduced, because movement at the end flange is not resisted. The lateral torsional buckling capacity of the coped beams will be significantly less than that predicted by the formulae in Section 3.4.1.

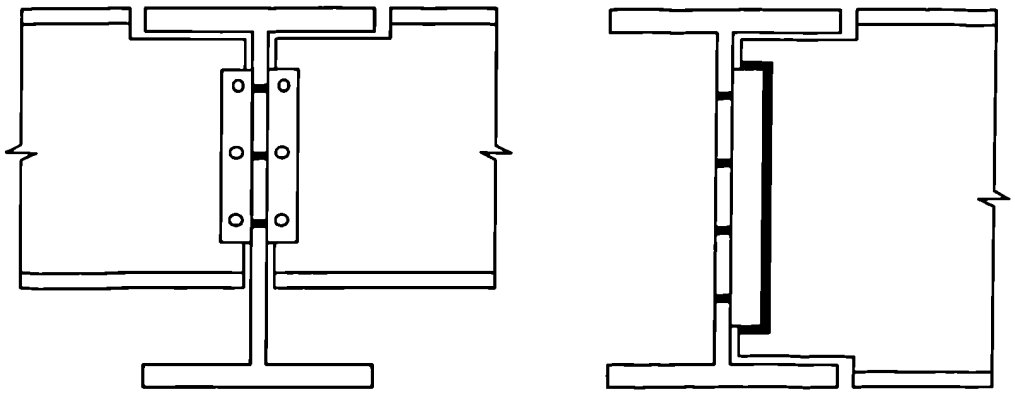

Figure 3.13 Types of coped beam connections

Four laterally unsupported coped beams were tested by Du Plessis [1977] and it was found that the beams failed in lateral torsional buckling. The results showed the importance of the coping details, connection restraint and loading conditions on lateral torsional buckling capacity of a coped beam. An approximate energy method for evaluating the lateral torsional buckling capacity of top flange coped beams subjected to a concentrated load at midspan was presented by Gupta [1984]. Gupta showed that copes in beams with short unbraced length had a greater effect on lateral torsional buckling capacity than long beams with similar copes.

Cheng et al [1988a] proposed a method for evaluating the lateral torsional buckling capacity of top flange coped beams by treating the problem as an interaction between the

buckling capacities of the Tee cross section in the coped region and the I-section of the uncoped region. They also found that the cope length, L_C, cope depth, d_C, h_w/t and the number of copes within the unbraced length (one or two copes) influence the buckling capacity significantly.

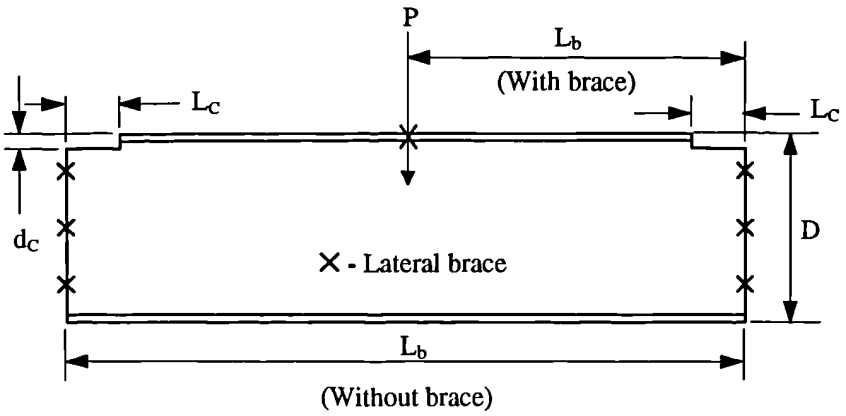

Figure 3.14 Buckling of a beam coped at the ends of the top flange

The method proposed by Cheng et al [1988a] is chosen for the assessment of lateral torsional buckling capacity of coped beams. The lateral torsional buckling model is shown in Figure 3.14. The proposed interactive design formulas [Cheng et al 1988a] to evaluate the lateral torsional buckling capacity are given below:

a) Coped at both ends of the unbraced length:

$$\frac{1}{M_{cr}} = \frac{1}{M_I} + \frac{1}{\left(\frac{L_b M_T}{2L_C}\right)} \tag{3.55}$$

b) Coped at one end of the unbraced length:

$$\frac{1}{M_{cr}^2} = \frac{1}{M_I^2} + \frac{1}{\left(\frac{L_b M_T}{L_C}\right)^2} \tag{3.56}$$

where

L_b is the unbraced length,

M_I is the lateral torsional Buckling moment of uncoped region (I-section),

M_T is the lateral torsional Buckling moment of coped region

(Tee-section), and

M_{cr} is the critical Lateral torsional buckling moment of the coped beam.

Note: The above interactive design formulas are valid for cases with $d_C < 0.1D$.

For the lateral torsional buckling moment of I-sections the theory given in Section 3.4.1 can be used. The lateral torsional buckling moment of Tee-section (M_T) may be evaluated using the method proposed by Hogan and Thomas [1980] and is given by:

$$M_T = \frac{\pi}{2L_C}\sqrt{EI_yGJ}\left[\sqrt{1+\left(\frac{\pi\gamma_m}{2}\right)^2} + \frac{\pi\gamma_m}{2}\right] \qquad (3.57a)$$

where

$$\gamma_m = \frac{\beta_x}{2L_C}\sqrt{\frac{EI_y}{GJ}} \qquad (3.57b)$$

$$\beta_x = -\left\{\frac{1}{I_x}\left[\frac{t}{4}\left((h_0-\bar{y})^4-(\bar{y}-T)^4\right) - \left(\bar{y}-\frac{T}{2}\right)\left(\frac{B^3T}{12}+BT\left(\bar{y}-\frac{T}{2}\right)^2\right)\right]\right\} - 2\bar{y} + T \qquad (3.57c)$$

$h_0 = D - d_C$

and $\bar{y}$ is the distance between the neutral axis of the coped (Tee) section and the extreme fibre of the remaining flange. Equation 3.57a was derived from the critical moment for a monosymmetric section given by Trahair [1977].

It was found that the buckling capacity of short coped beams is controlled mainly by the coped (Tee) section [Cheng et al 1988a]. The uncoped region (I-section) simply deflects by rigid body motion and severe cross-section distortion occurs in the coped region. The buckling capacity of long coped beams was found to be controlled mainly by the uncoped section although coping does decrease the buckling capacity.

3.5 Web bearing and buckling capacities

3.5.1 Web bearing Capacity

Plate elements (e.g. webs) are subjected to bearing stresses by concentrated loads or locally distributed edge loads (reactions from supports or other members) as shown in Figure 3.15. For example, a concentrated load applied to the top flange of a beam induces local bearing stresses in the web immediately beneath the load. When the load reaches its critical value, the web crushes (cripples) by combined compression and folding directly under the load.

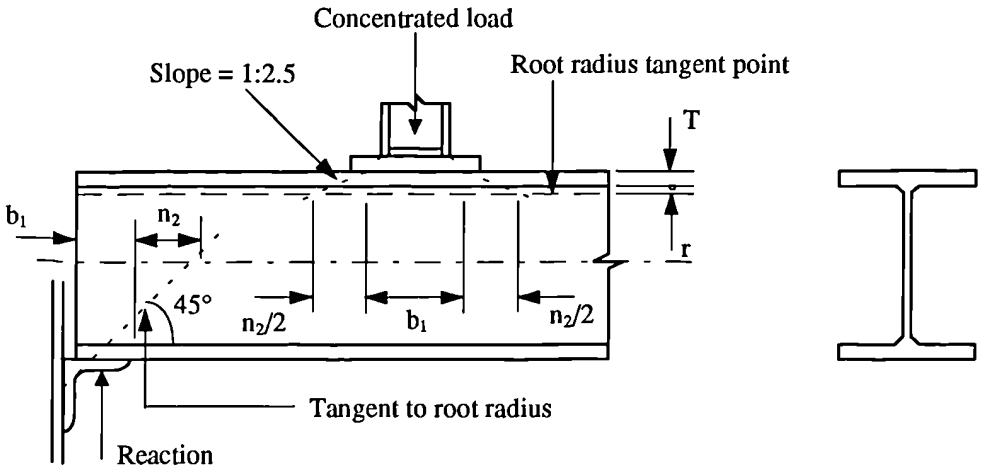

Figure 3.15 Effective web bearing length to resist crushing

The ultimate bearing strength of a thick web depends on its design strength, p_y. Although yielding first occurs under the centre of the bearing plate, general yielding does not takes place until the applied load is large enough to cause yielding of a web area defined by a dispersion of the applied stress through the flange. Even at this load the web does not collapse catastrophically, and some further yielding and redistribution is possible [Trahair 1977].

Where point loads or reactions from supports or other members are applied to a beam as shown in Figure 3.15 then the web should be checked for bearing stresses. The web

bearing capacity can be evaluated using cls 4.5.1.3 and 4.5.3 of BS 5950 [1985]. The web bearing strength, P_{wbg}, is given by:

$$P_{wbg} = (b_1 + n_2)tp_{yw} \quad (3.58)$$

where

b_1 is the stiff bearing length,

n_2 is the length obtained by the slope 1:2.5 dispersion through the flange (Figure 3.15) and can be taken as follows:

$n_2 = 2\times2.5(T + r)$ for forces applied through a flange by loads or reactions in the length between the ends and

$n_2 = 2.5(T + r)$ for forces applied through a flange by loads or reactions at the ends,

t is the thickness of the web and,

p_{yw} is the design strength of the web.

The code recommends that if the forces applied through a flange by loads or reactions exceeds the local capacity of the web at its connection to the flange, then bearing stiffeners should be provided.

3.5.1 Buckling resistance of webs

The webs of beams and girders are subjected to compressive stresses by concentrated loads or reactions from supports or other members as shown in Figure 3.16. When the applied load reaches its critical value, it causes web buckling. The various types of web buckling modes are illustrated in Figure 3.17. The web buckles at the centre if the flanges are restrained against rotation relative to the web and lateral movement relative to the other flange. Otherwise sideways movement (sway between flanges) or rotation of one flange relative to the other occurs.

Where point loads or reactions from supports or other members are applied to a beam as shown in Figure 3.16 then the web should be checked for buckling as a strut. The

buckling resistance of unstiffened webs can be evaluated using cl 4.5.1.3 and cl 4.5.2.1 of BS 5950 [1985]. The code recommends that if compressive forces applied through a flange by loads or reactions exceeds the buckling resistance, P_w, of unstiffened webs, load carrying web stiffeners should be provided. The effective width of web (acting as a strut) to resist buckling is determined by assuming a 45° dispersion angle from the edge of the load as shown in the Figure 3.16.

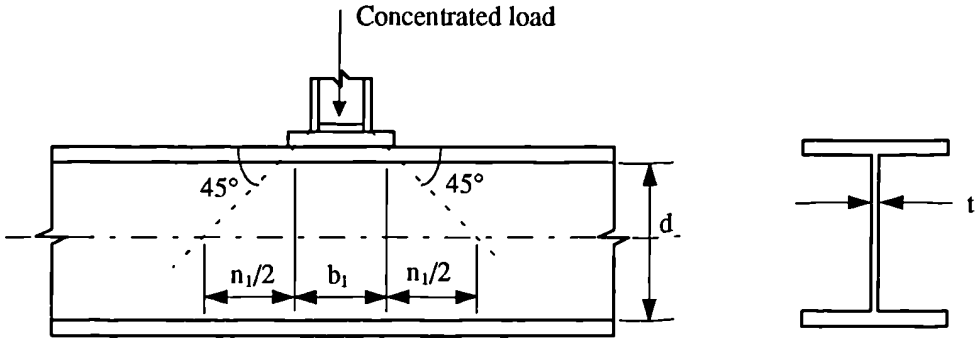

Figure 3.16 Effective width of a strut for buckling

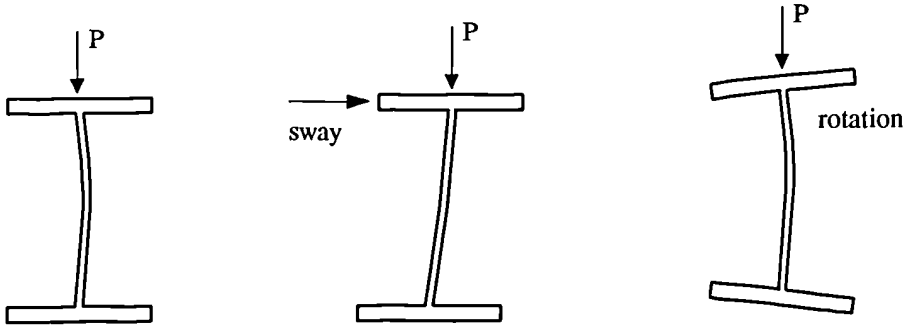

Figure 3.17 Various types of buckling modes of a web due to compressive forces applied through a flange by loads or reactions.

The buckling resistance, P_w, of an unstiffened web is given in BS 5950 [1985] as:

$$P_w = (b_1 + n_1)tp_c \qquad (3.59)$$

where

b_1 is the stiff bearing length,

n_1 is the length obtained by assuming that the load is dispersed at 45° through one half the depth of the beam and,

p_c is the compressive strength obtained from table 27(c) of BS 5950 [1985] with a slenderness, $\lambda = 2.5d/t$.

The slenderness of an unstiffened web is obtained by considering the buckling of the web about an axis parallel to the web. The radius of gyration can be calculated as:

$$r_y = (I_y/A)^{1/2}$$

By making substitutions for I_y and A, the radius of gyration can be given as:

$$r_y = t/2\sqrt{3} \tag{3.60}$$

If the effective length of the web is taken as 0.72d, the slenderness ($\lambda = L/r_y$) of the web can be given as:

$$\lambda = 2.5d/t \tag{3.61}$$

A Perry-Robertson approach is used in BS 5950: Part 1 [1985] to calculate the compressive strength, p_c, of a strut and is given as the least root of

$$(p_E - p_c)(p_y - p_c) = \eta p_E p_c \tag{3.62}$$

and the least root of Equation 3.62, p_c, is given by:

$$p_c = \frac{p_E p_y}{\Phi + (\Phi^2 - p_E p_y)^{1/2}} \tag{3.63}$$

$$\Phi = \frac{p_y + (\eta+1)p_E}{2} \tag{3.64}$$

where

p_E is the Euler strength $= \dfrac{\pi^2 E}{\lambda^2}$ and, (3.65)

η is Perry factor $= 0.001a(\lambda - \lambda_o)$.

where

a is the Robertson constant which depends on the shape of the section = 5.5 for table 27(c),

λ is the slenderness of unstiffened web $= 2.5d/t$, and

λ_0 is the limiting slenderness $= 0.2\left(\dfrac{\pi^2 E}{p_y}\right)^{1/2}$ (3.66)

The value of the effective length of 0.72d is empirical but it gives reasonable accuracy in tests where the flanges are effectively fixed ended [Astill et al 1980]. This is the minimum practical effective length of the equivalent strut and if lateral movement or rotation of the ends is possible the effective length must be increased. Alternatively stiffeners can be introduced to prevent these movements and resist part of the load.

3.5.3 Buckling resistance of stiffeners

Various types of stiffeners are used in practice to strengthen webs. Three main types of stiffeners are: (a) Load carrying web stiffeners which are required where compressive forces applied through a flange by loads or reactions exceeds the buckling resistance, P_w, of an unstiffened web, (b) Load bearing stiffeners which are used to prevent local crushing of the web due to compressive forces applied through a flange by loads or reactions and, (c) Intermediate stiffeners which are used to prevent buckling of slender webs. The load carrying stiffeners may also function as intermediate stiffeners. The buckling resistance of all types of stiffener can be evaluated using BS 5950 [1985]. Only the case of load carrying web stiffener will be discussed in detail in this work.

The buckling resistance of a load carrying web stiffener is calculated on a section which includes part of the web, as it was observed by Rockey et al [1981] that part of the web

also acted with the stiffener to resist the effects of stiffener buckling. The code allows a section of web to be equal to twenty times the web thickness on each side of the centre line of the stiffeners to be taken into account when calculating the section properties of the load carrying stiffeners, i.e. effective cross sectional area, A_e, (Figure 3.18), second moment of area, I_e, about the centre line of the web and the corresponding radius of gyration, r_y.

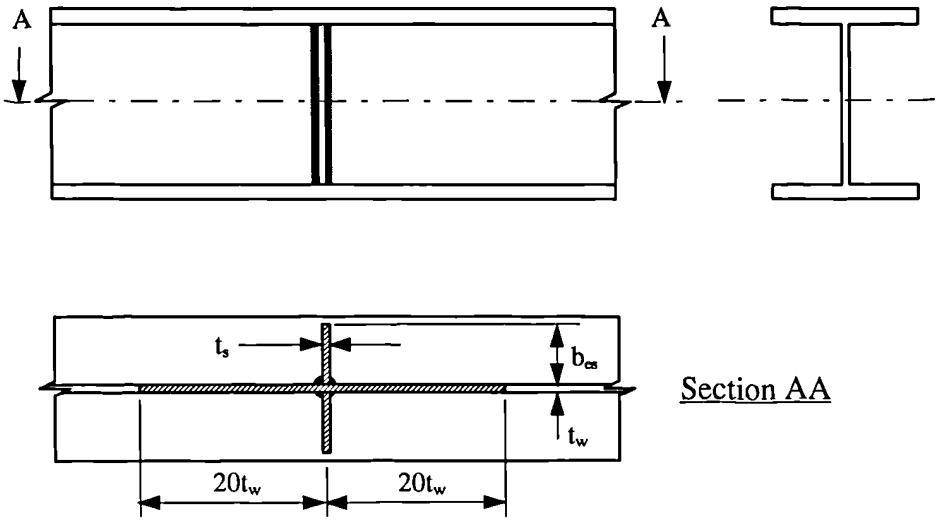

Figure 3.18 Effective cross sectional area of load carrying web stiffeners

The section properties of load carrying web stiffeners can be calculated as:

$$A_e = t_s(2b_{es} + t_w) + 40t_w^2 \tag{3.67}$$

$$I_e = \frac{t_s(2b_{es} + t_w)^3}{12} + \frac{40t_w^4}{12} \tag{3.68}$$

$$r_y = \left(\frac{I_e}{A_e}\right)^{0.5} \tag{3.69}$$

The buckling resistance, P_x, should be based on the compressive strength, p_c, using table 27(c) of BS 5950 [1985], with an effective design strength, p_y', taken as $20N/mm^2$ less than the actual design strength of the stiffener, p_y. The reason for this reduction is an attempt to make a simple allowance for the higher residual stresses in welded sections

than those in rolled sections. In determining the compressive strength, p_c, the slenderness, λ, is taken as:

$$\lambda = L_E / r_y \qquad (3.70)$$

where L_E is the effective length of the load carrying web stiffener and is taken as follows:

a) Flange restrained against rotation in the plane of the stiffener (by other structural elements):

$$L_E = 0.7L$$

b) Flange not so restrained:

$$L_E = L$$

where L is the stiffener length.

The buckling resistance, P_x, of the load carrying web stiffener is as follows:

$$P_x = p_c A_e \qquad (3.71)$$

3.6 Summary and conclusions

Assessment of existing structures involves the use of appropriate codes and standards for carrying out structural design checks using re-assessed section properties based on measured section sizes and simple analytical models. In the case of corroded steel structures, the BS 5950 [1985] recommendations are widely used for the assessment of the remaining capacity. In this chapter, we discussed the existing methods that can be used for the assessment of corroded steel structures. We also discussed two cases of failure mode which are not adequately covered in the present codes.

The existence of holes in web, created by corrosion, is likely to reduce the capacity significantly. We have also seen that the lateral torsional buckling capacity of coped beams will be significantly less than that predicted by the current codes. In this chapter, simple assessment methods are provided, based on works by various researchers, in order to deal effectively with the cases described. It will be shown in the next chapter that there is good agreement between the failure loads obtained using the methods provided and the experimental failure loads of four samples of corrosion damaged beams obtained from a chemical plant.

Chapter 4

Analytical and experimental study of corrosion damaged steel beams

4.1 Introduction

The most important effect of corrosion on steel members is the loss of material, which will cause smaller net sections. The reduction in section area will decrease the geometrical properties, such as second moment of area, radius of gyration, etc., of the member. This will in turn lead to the reduction in carrying capacity of the member. This change may occur in a non-linear manner because the geometrical properties are related to the square or cube of the dimensions. It is also possible that the critical failure mode of a member may be changed depending on the location affected by corrosion. To evaluate these effects of corrosion on structural performance of steel members, the various regions where corrosion will occur must be evaluated in terms of remaining area.

There have been examples of heavily loaded structures, which are in a severe corrosion damaged condition and have been behaving satisfactorily and yet were notionally unsafe [Gallon 1993]. The service life of these structures may be increased if the reserves of strength are quantified. The behaviour and strength of corrosion damaged steel structures have not been well established yet. Improved knowledge of structural behaviour will allow more informed decisions to be made on future action thus ensuring consistent levels of safety and effective maintenance expenditure.

In order to obtain these benefits, clear understanding of the corrosion effects on the behaviour of corrosion damaged members is essential. The main aim of this chapter is to study the behaviour of corrosion damaged beams analytically and experimentally.

The main objectives of this chapter are:

1. To develop corrosion decay models by analysing the effects of corrosion damage of beams.
2. To load test samples of corrosion damaged beams obtained from a chemical plant for their ultimate failure loads in the laboratory.
3. To analyse the failure modes of these beams.

4.2 Analysis of the effect of corrosion damage of steel beams

4.2.1 Corrosion decay models

The development of corrosion decay models mainly requires the information on the locations where corrosion normally occurs and the types of corrosion damage of steel members. The most common form of corrosion damage of steel is general surface corrosion. The locations where corrosion occurs was discussed in Chapter 2. From these discussions, basic conclusions were made concerning the location of corrosion. Using this information, two corrosion decay models were considered by reducing the thickness of the sections. The two models which are shown in Figure 4.1 are as follows:

1. Uniform thickness loss in both flanges and web (Model 1).
2. Varying thickness loss in both flanges and web (Model 2).

In the case of Model 2, the thickness loss of flanges and web were in similar proportion to the thickness loss of the samples of corrosion damaged beams obtained from a chemical plant. The measured thicknesses of these beams are given in Table 4.1. It can be established from Table 4.1 that the thickness loss of the bottom flange of three sample beams is approximately twice as that of the loss of the top flange. The thickness loss of the lower part of the web ($0.25h_w$) is nearly five times as that of the loss of the upper part of the web ($0.75h_w$). For two sample beams, the average thickness loss of the web is approximately half of that of the average loss of the flanges. These ratios were used for the development of Model 2 (varying thickness loss model) as shown in Figure 4.1b.

The thickness loss of the stiffeners of all the sample beams is very minimal, i.e. only about 10% of its original thickness. It is also observed that the percentage thickness loss of the stiffeners is nearly the same as that of the upper part of the web. Therefore, for developing the corrosion decay models, it was assumed that the loss of material in the stiffeners was in similar proportion to the thickness loss of the upper part of the web.

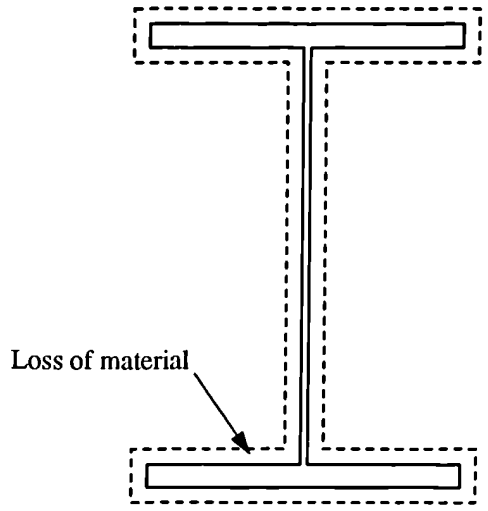

Loss of Material

Flanges	ξT_N
web	ξt_N

where T_N and t_N are the thicknesses of the flanges and web of as-new section,

ξ = %LFT / 100 = %LWT / 100,

%LFT = Percentage loss of flange thickness, and

%LWT = Percentage loss of web thickness

(a) Uniform thickness loss (Model 1)

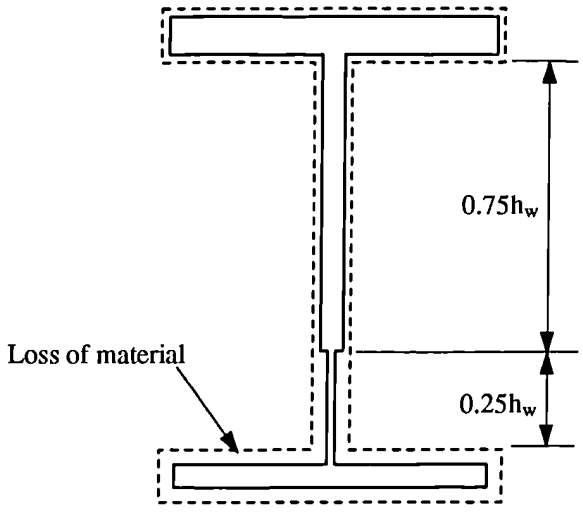

Loss of Material

Top Flange	$0.7\xi T_N$
Upper part of the web ($0.75h_w$)	$0.25\xi t_N$
Lower part of the web ($0.25h_w$)	$1.25\xi t_N$
Bottom flange	$1.3\xi T_N$

where ξ = %LFT / 100

(b) Varying thickness loss (Model 2)

Figure 4.1 Corrosion decay models simulated by reducing the thickness of elements

4.2.2 Analysis of corrosion effects

A steel member subjected to bending can fail in different ways depending on its dimensions and loading. The main modes of failure are:

1. Yielding of flanges under normal bending stresses.
2. Lateral torsional buckling.
3. Shear failure of web.
4. Bearing failure of the web near the support or under the loads.

While loss of material due to corrosion reduces the section properties and hence the carrying capacity of a member, it can also change the mode of failure from one to another depending on the rate and place of corrosion. In order to verify these effects of corrosion, an analysis was carried out using the two corrosion decay models above. A universal rolled I-section (457×191 UB 67 kg) of arbitrary dimensions was used to illustrate this phenomenon.

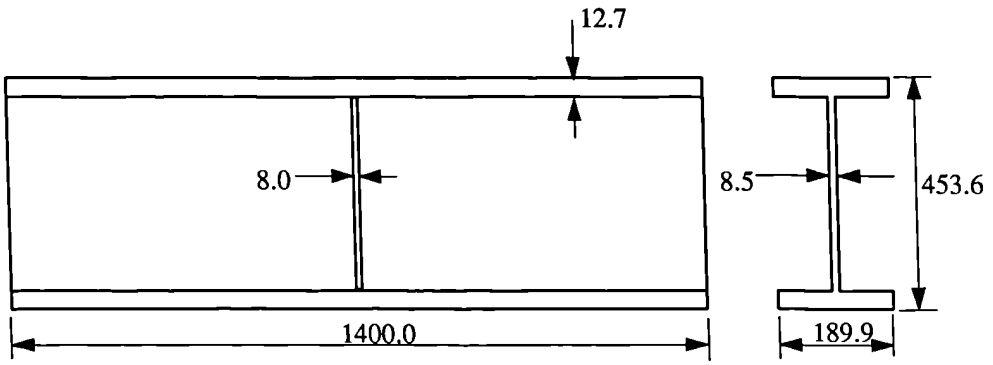

All dimensions are in millimetres

Figure 4.2 Dimensions of universal beam 457×191 UB 67 kg

It was assumed that the beam is 1400 mm long and simply supported at the ends. It was also assumed that the beam, which carries a central point load, is provided with a load carrying stiffener at the mid span. The dimensions of the beam are shown in Figure 4.2. Assuming that the yield strength of steel is 300 N/mm^2, it was found that the class of the compression flange is plastic and the d/t ratio of the web is less than 63ε in its as-new

condition. The theories given in Chapter 3 were used for the assessment of the capacities with regard to the failure mechanisms mentioned above. The results, obtained from the above analysis, are plotted in Figure 4.3.

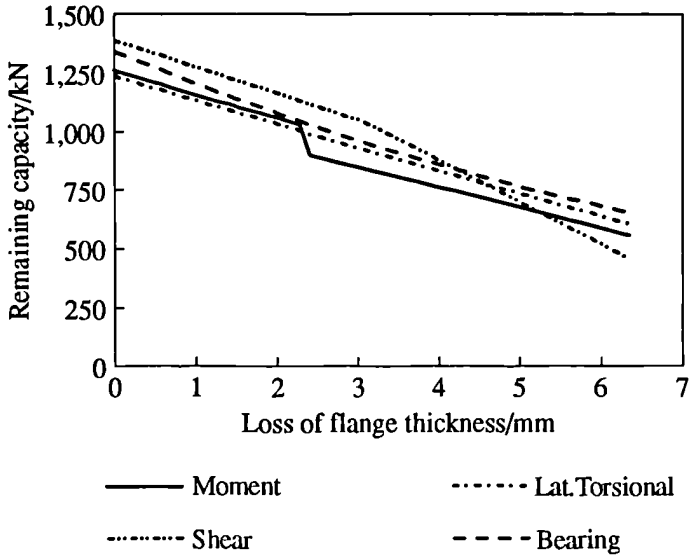

(a) Uniform thickness loss (Model 1)

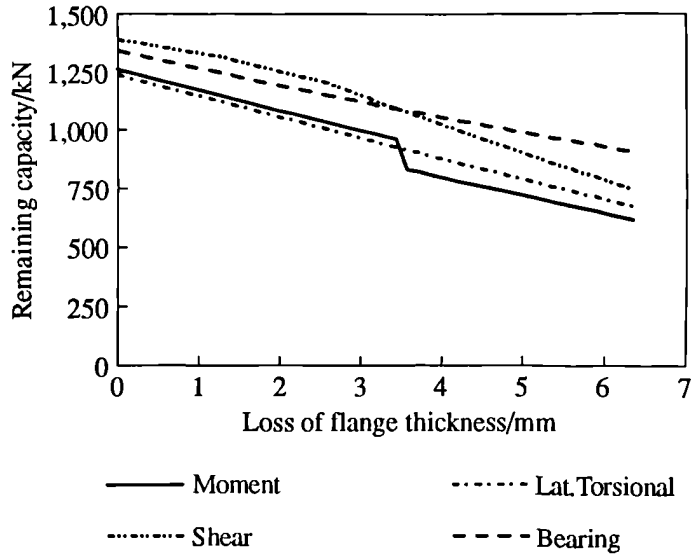

(b) Varying thickness loss (Model 2)

Figure 4.3 Remaining capacities of a corrosion damaged I-beam

4.2.3 Discussion

4.2.3.1 Moment capacity

The reduction in moment capacity is linearly proportional to the flange thickness loss but at a certain point there is a sudden drop in the moment capacity as it can be seen from Figures 4.2a and 4.2b. This happens when the class of the compression flange is changed from one to another due to loss of thickness. In our example (Section 4.2.2), the compression flange of the section was plastic in its as-new condition and became semi-compact at the corroded states due to loss of thickness. When this happens local buckling may prevent the development of full plastic moment and elastic properties are used to calculate the moment capacity in such cases.

4.2.3.2. Lateral torsional buckling capacity

Figures 4.2a and 4.2b show how the remaining lateral torsional buckling capacity of a member is reduced with the loss of thickness. The lateral torsional buckling capacity declines at a considerable rate with the loss of flange thickness. The reduction in lateral torsional buckling capacity of the beam is almost linearly proportional to the section loss in this case. The lateral torsional buckling is the critical failure mode at the early stages of corrosion for both corrosion decay model beams.

4.2.3.3 Shear capacity

The shear failure mechanism depends on the buckling strength of the web, which is reduced in thickness by corrosion. The most interesting point, observed from these graphs, is the rate of reduction of the shear capacity with the loss of thickness in the web. It can be seen from Figure 4.2a that severe loss of thickness in the web may lead to a considerable reduction in its shear capacity. The slope of the remaining shear capacity curve, which is a straight line in this case, is increased considerably at an intermediate stage of corrosion. This change of slope occurs when the web behaviour changes from plastic yielding to elastic buckling, i.e. when $d/t > 63\varepsilon$. After the buckling stage is

reached, shear capacity diminishes rapidly. It is observed from these analyses that the rate of reduction of shear capacity is greater than of the bending capacities.

4.2.3.4 Bearing capacity

The corrosion can also affect the bearing capacity of a member as can be seen from Figures 4.2a and 4.2b. Bearing forces are mainly resisted by the web, immediately above the supports and at the loads. Generally stiffeners are provided to increase the bearing capacity of the web. The presence of the stiffeners was taken into account when evaluating the bearing capacity. If load carrying web stiffeners are provided, then the bearing failure mode becomes less significant as can be seen from Figure 4.2. This is due to the fact that the stiffeners are less susceptible to corrosion as they are normally vertical. The detailed measurements of the thicknessess of the stiffeners of the samples of corrosion damaged beam confirm that the loss of material in the stiffeners is small compared to the loss in other elements (see Table 4.1).

4.2.3.5 Failure mechanisms

It can be seen from Figure 4.2a that when the loss of thickness of the section is uniform in both flanges and web, the critical failure mode changes from lateral torsional buckling to local buckling of flanges and then to shear. The lateral torsional buckling failure mode governs the member in its early stages. Then, after few years of corrosion, the local buckling of flanges becomes the critical failure mode. Then, after several years of corrosion, the shear failure mechanism becomes critical. The shear mode also becomes critical when there is significant loss of thickness in the web and holes are present in the web.

When the loss of thickness in the flanges is greater than in the web (variable thickness loss model), the bending failure modes govern the member, as it can be seen from Figure 4.2b. The lateral torsional buckling failure mode governs the member in its early stages. Then, after several years of corrosion, the local buckling of flanges becomes the critical failure mode.

4.3 Load test on samples of corrosion damaged beams

4.3.1 Sample beams

Four identical universal beams (305×165 UB 40 kg) were recovered from the site of a chemical plant undergoing demolition. The beams formed corner supports for a steel tank as shown in Figure 4.4 and were all in severely corroded condition (nearly 30 years old). Photos of the four sample beams are shown in Figure 4.5. Holes were found in the webs and flanges of two of the beams, one of which is shown in Figure 4.6.

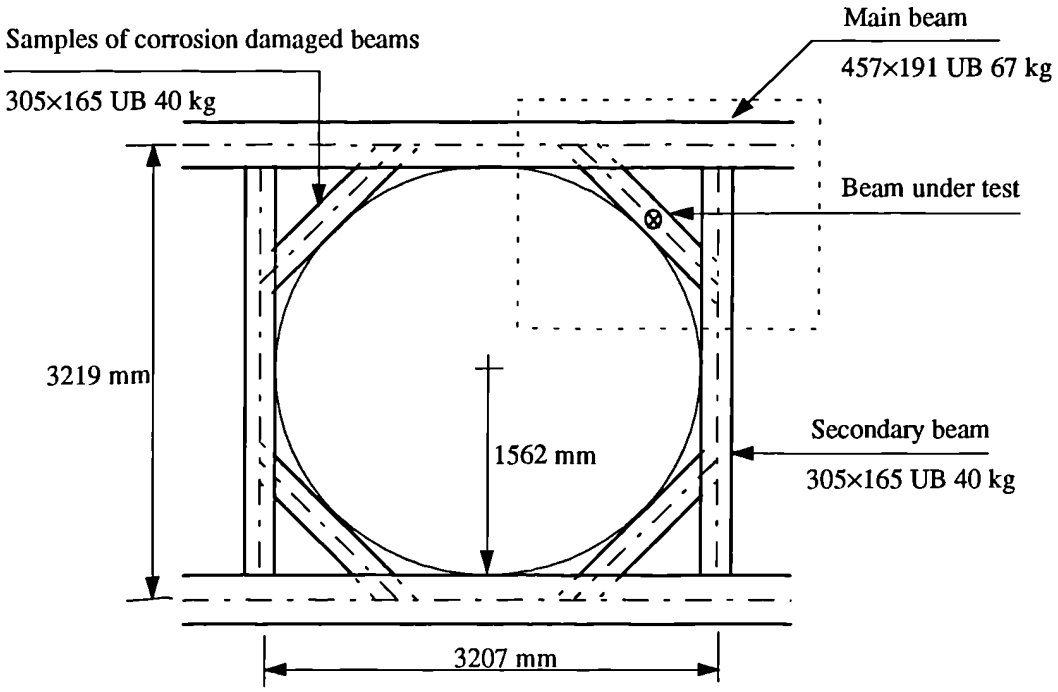

Figure 4.4 Plan of general arrangement of sample beams as in service

The thicknessess of these beams were measured by an instrument, which was designed specially for this purpose. The instrument, which was used together with a depth gauge, is shown in Figure 4.7. The measured thicknessess of the elements are given in Table 4.1. As many readings as possible (up to 150 readings for each element) were taken in order to increase the accuracy of the measurements. It will be noted in Table 4.1 that the loss of thickness on average was more significant in the flanges than the webs.

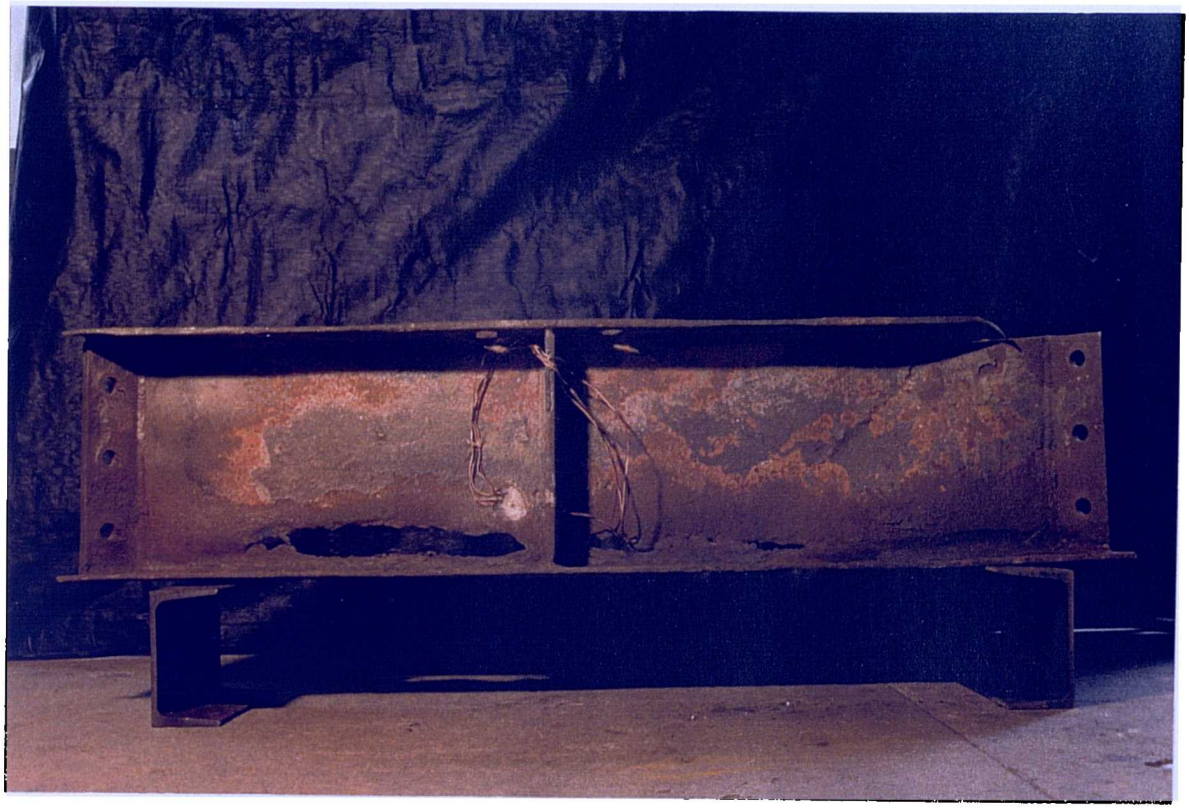

(a) Beam 1

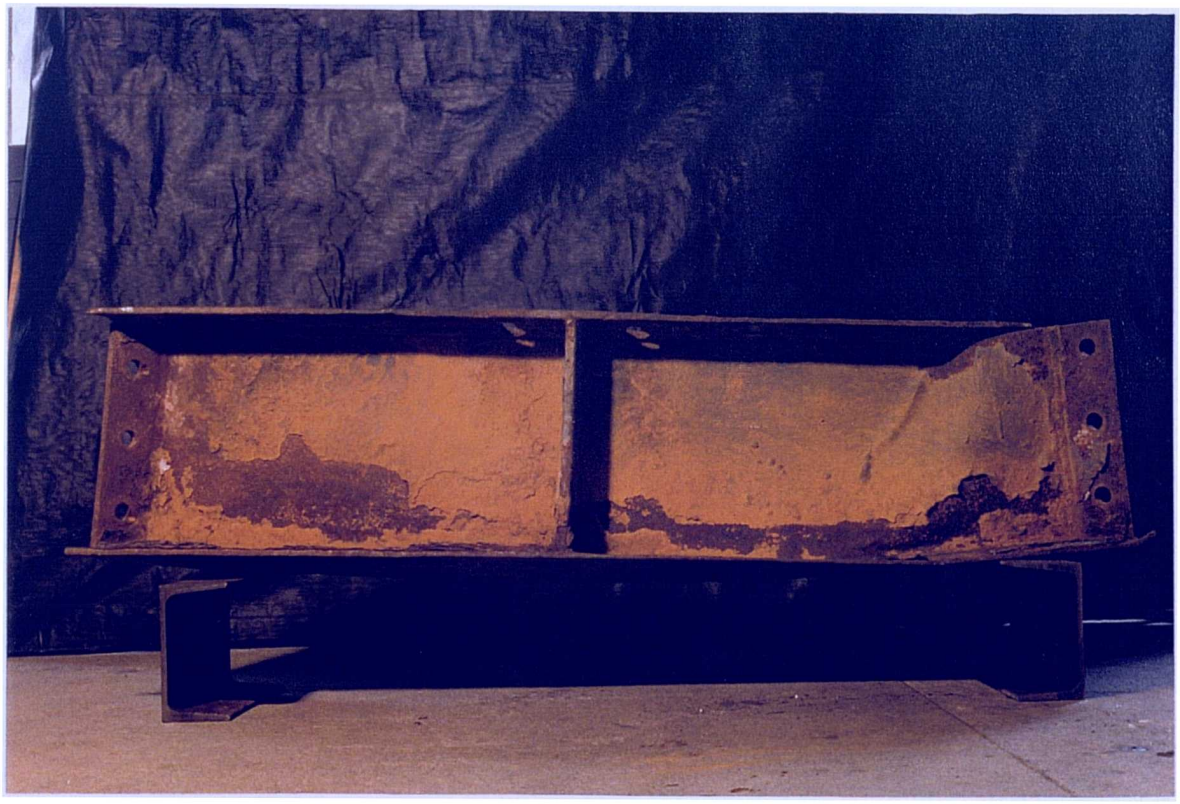

(b) Beam 2

Figure 4.5 Samples of corrosion damaged beams

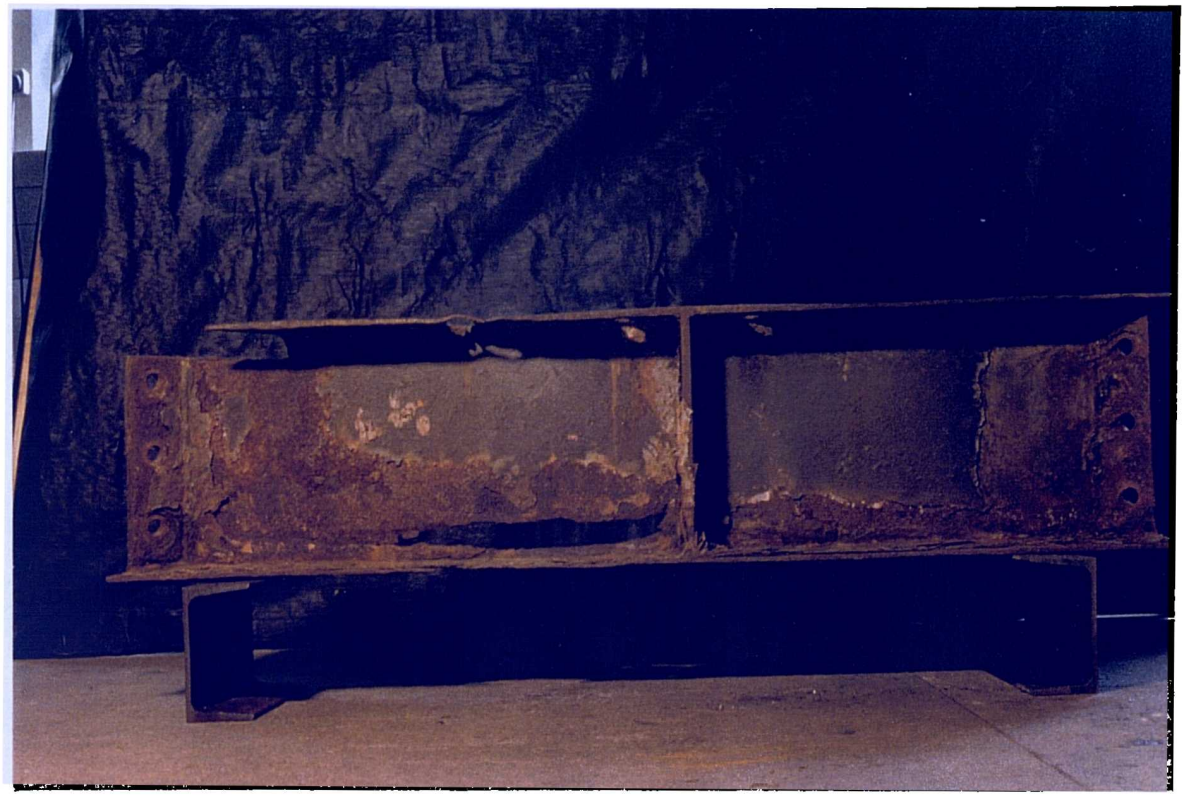

(c) Beam 3

(d) Beam 4

Figure 4.5 (Continued) Samples of corrosion damaged beams

Table 4.1 Average measured thickness of samples of corrosion damaged beams

Element	As-new	Beam 1	Beam 2	Beam 3	Beam 4
Top flange - T_T	10.20	7.45	7.81	7.23	7.83
Bottom flange - T_B	10.20	5.62	5.85	4.84	7.61
Average flange thickness - T	10.20	6.54	6.83	6.04	7.72
Average thickness loss of T	0.00	3.66	3.37	4.16	2.48
% Average thickness loss of T	0.00	35.9	33.0	40.8	24.3
Upper part of web ($0.75h_w$) - t_U	6.10	5.63	5.74	5.45	5.84
Lower part of web ($0.25h_w$) - t_L	6.10	3.16	4.32	3.18	4.74
Average web thickness - t	6.10	5.01	5.39	4.88	5.57
Average thickness loss of t	0.00	1.09	0.71	1.22	0.53
% Average thickness loss of t	0.00	17.8	11.7	20.0	8.77
Average stiffener thickness - t_S	9.53	8.55	8.66	8.63	8.71
Average thickness loss of t_S	0.00	0.98	0.87	0.90	0.82
% Average thickness loss of t_S	0.00	10.3	9.13	9.44	8.60

All measurements are in millimetres

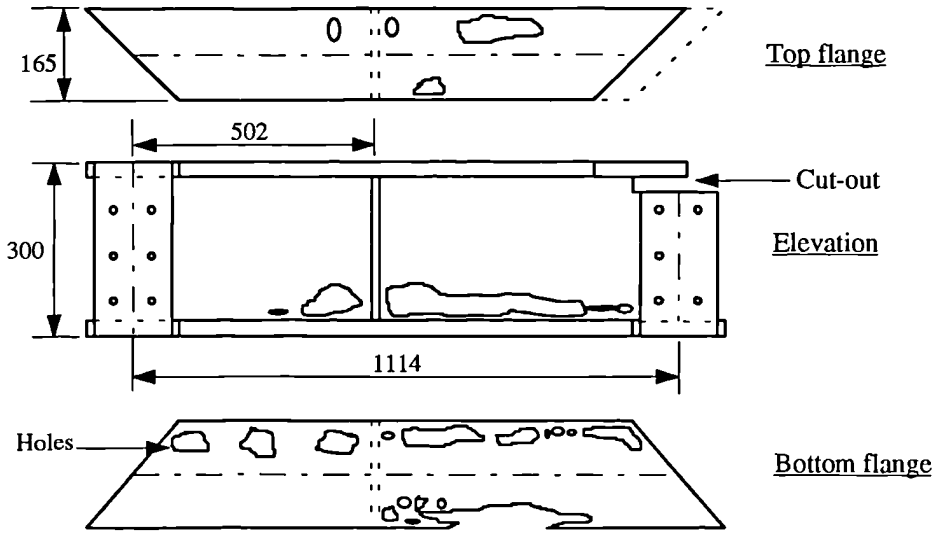

Figure 4.6 Detail of holes in Beam 3

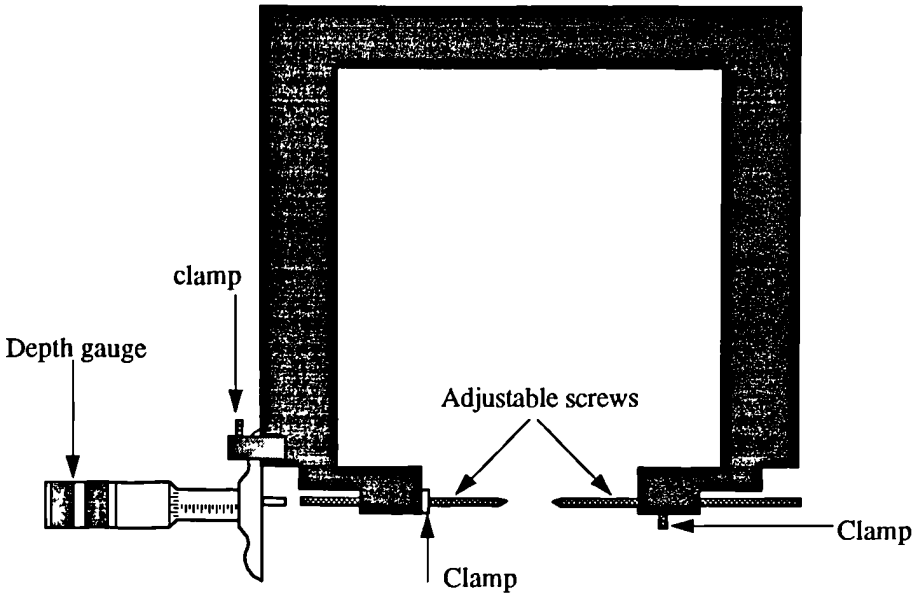

Figure 4.7 Instrument used for thickness measurements of sample beams

4.3.2 Load test to failure

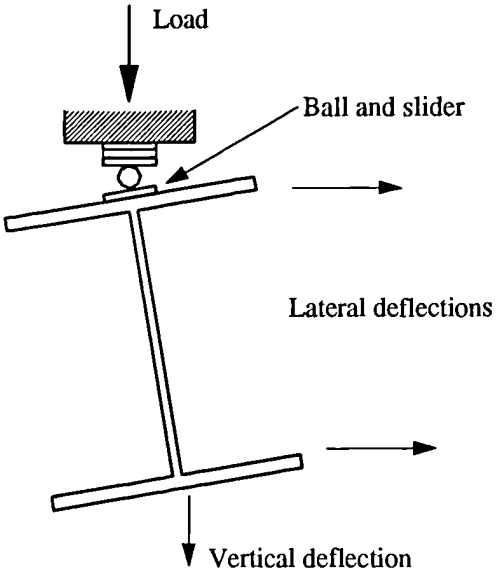

Figure 4.8 Loading and deflection measurements

Each of the four beams were installed in turn in a testing reaction frame designed to simulate the support conditions for the steel tank as in service (see Figure 4.4). Strain gauges were mounted at critical places in beams 3 and 4. A 300 ton hydraulic testing machine was used to apply a vertical point load directly over the stiffener, which is

located at a distance of 55.0 mm away from the mid-span, until failure. The load was applied through a ball and slider seating to permit rotation of the cross section of the test beam, as would be the case in service. The sample beams were not restrained between the ends against sideways movement of the compression flange or movement of one flange relative to the other in service. The vertical deflection of the loaded point was also recorded, together with the lateral deflections of the beams at the top and bottom of the stiffener. This provided information on the onset of lateral torsional buckling and is shown in Figure 4.8. A photograph of the test frame is shown in Figure 4.9.

4.3.3 Results

The failure loads obtained from the above tests for the four beams are given in Table 4.2. It may be seen that there is a correlation between the condition of each beam and its failure load. The failure of the beams took place in the web that buckled at a corner where there was a cut-out in the top flange (see Figure 4.6). This failure was caused by lateral torsional buckling originating from the cut-out portion of the top flange. The buckled shape of a beam is shown in Figure 4.10. The vertical and lateral deflections for beams 3 and 4 are plotted in Figures 4.11 and 4.12 respectively.

Table 4.2 Ultimate failure loads obtained from the load test

Beam No.	Ultimate load / kN	Description of the beam (see Figure 4.5)
Beam 1	277.0	Severe material loss and holes in the flanges and lower part of the web. Upper part of the web in good condition.
Beam 2	318.0	Severe material loss in the flanges and lower part of the web but no holes. Upper part of the web in good condition.
Beam 3	287.0	Severe material loss all over and holes in the flanges and lower part of the web.
Beam 4	440.0	Fairly good condition, loss of material all over but no holes. Material loss greater in the lower part of the web and upper part of the web in good condition.

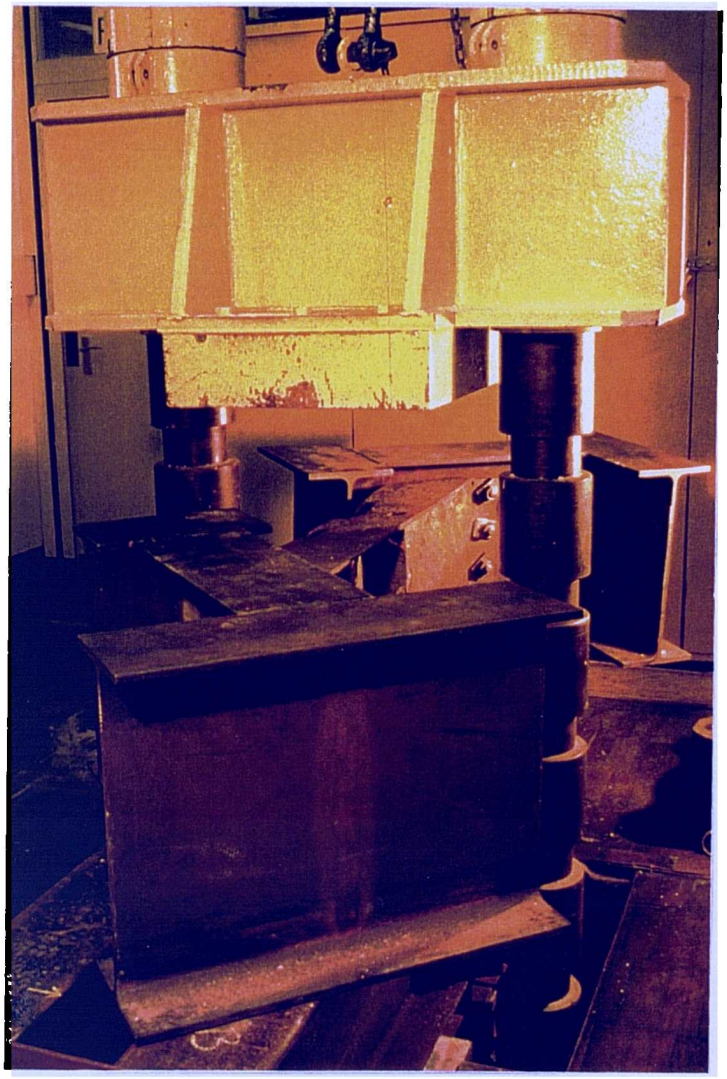

Figure 4.9 Test frame

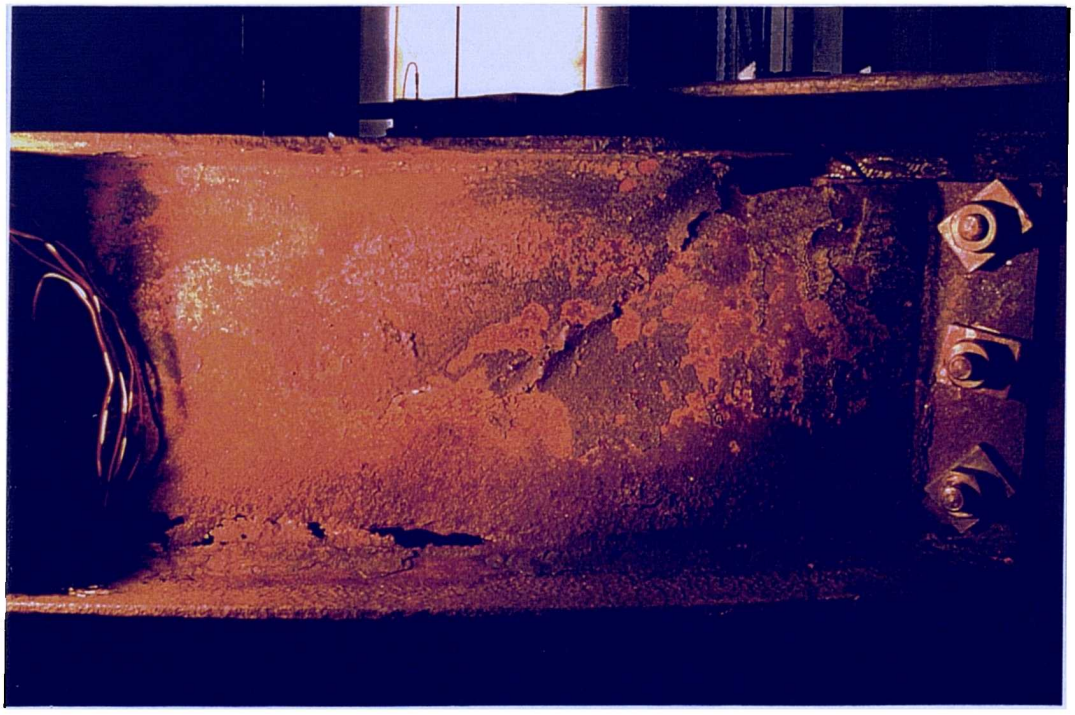

Figure 4.10 Buckled shape of a beam

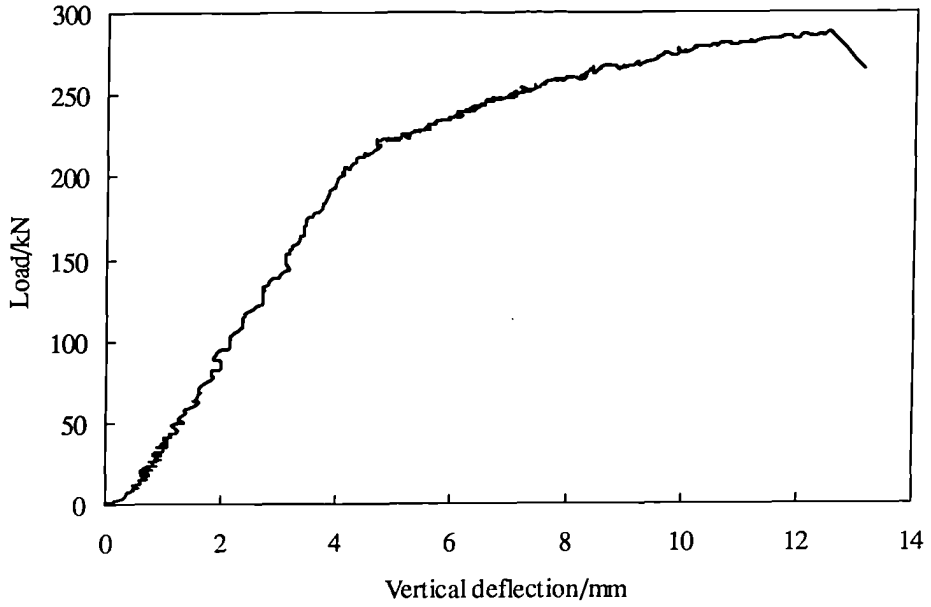

Figure 4.11a Vertical deflection of the loaded point of Beam 3

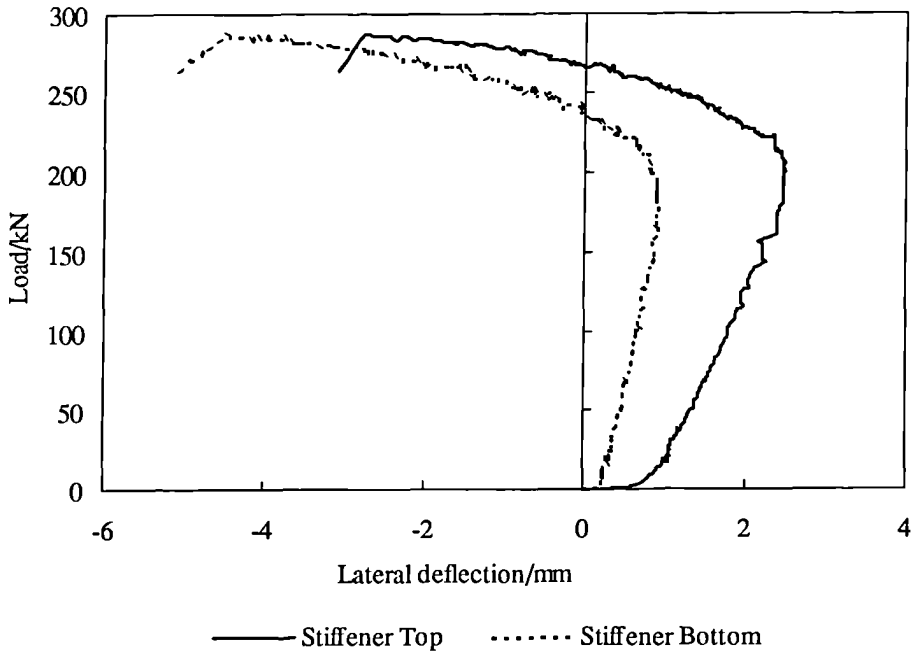

Figure 4.11b Lateral deflections of top and bottom of the stiffener of Beam 3

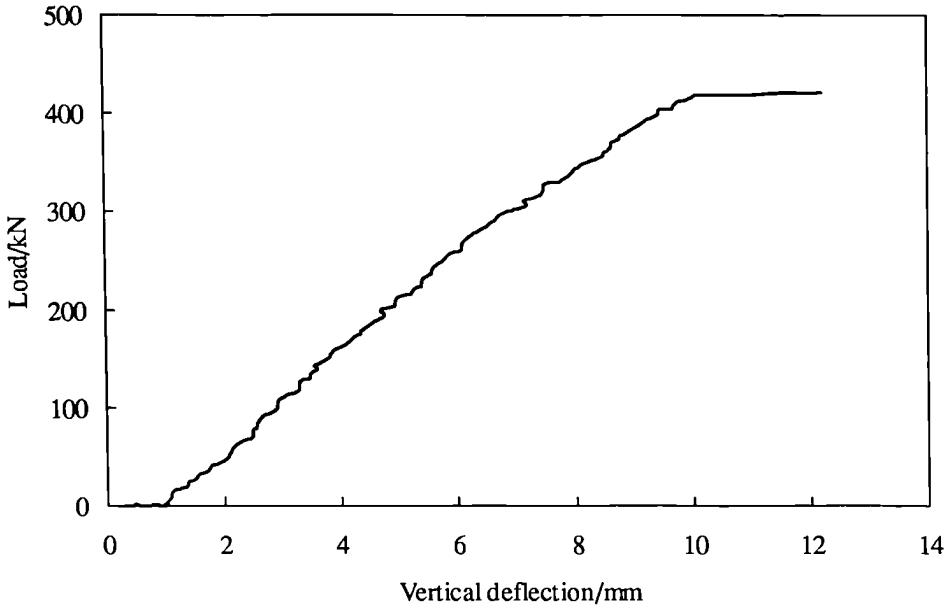

Figure 4.12a Vertical deflection of the loaded point of Beam 4

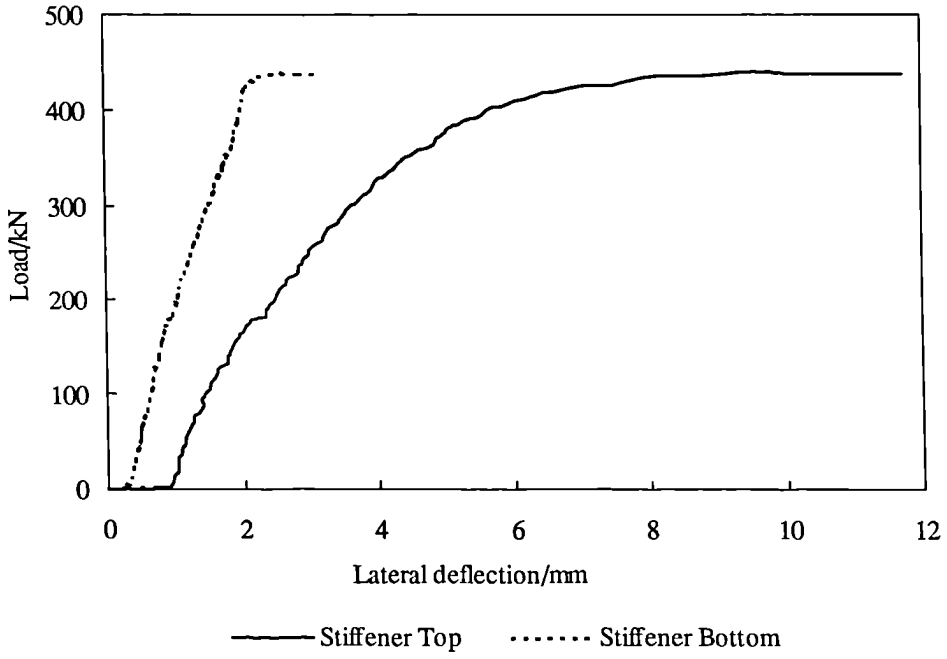

Figure 4.12b Lateral deflections of top and bottom of the stiffener of Beam 4

4.4 Theoretical analysis of samples of corrosion damaged beams

4.4.1 Analysis of samples of corrosion damaged beams

The four samples of corrosion damaged beams together with a beam in its undamaged state were analysed to determine their failure mode and ultimate failure load. The thickness measurements of these beams, which are given in Table 4.1, were used to re-assess the section properties of these beams. These beams, which have a length of 1.114 m, were designed to carry a point load near the mid-span and were provided with load carrying web stiffeners at the loaded point (see Figure 4.6).

The theory given in Section 3.2 was used for the assessment of the moment capacity, which is mainly dependent on the yield strength and the flange area of the beam. These beams have a cut-out at one end of the top flange. For these coped beams, the lateral end restraint is considerably reduced because rotation of the flange in plan is not resisted at the coped end. It was found during the load tests that lateral torsional buckling was the most important failure mechanism for these beams. The method of assessment proposed by Cheng et al [1988a], which is given in Section 3.4.2, was used in this case. In this method, the problem is treated as an interaction between the buckling capacities of the coped region (T-section) and the uncoped region (I-section).

Failure of the web due to shear buckling was the next most significant failure mechanism. The shear capacity of a web mainly depends on its slenderness ratio. The effects of varying web thickness and uniform thickness loss were calculated based on the theory given in Section 3.3. The effect of web holes due to corrosion was assessed by the method proposed by Wang et al [1975], which is given in Section 3.3.4. This assumes that plastic deformation occurs near each of the corners of the opening. A moment-shear interaction curve was identified from which the capacity of a particular load case was obtained. The bearing capacity of these beams, which were provided with web stiffeners, is dependent on the resistance of both the web and stiffener. The capacity of stiffened web in bearing was evaluated using the theory given in Section 3.5.3. The results of the above analysis are tabulated in Table 4.3 and plotted in Figure 4.13.

Table 4.3 Results obtained from the theoretical analysis of samples of corrosion damaged beams

Beam No.	Thickness loss / mm	Ultimate load / kN				
		Moment	Lateral torsional buckling	Shear		Bearing
				Varying web thickness	Web hole	
As-new	0.00	672.2	523.9*	667.1		857.1
Beam 1	3.94	404.7	212.1*	233.4	317.6	667.7
Beam 2	3.65	424.7	240.5*	348.9		716.7
Beam 3	4.51	377.9	170.5*	212.7	294.6	655.7
Beam 4	2.63	471.7	340.4*	462.6		742.8

* = Critical failure load.

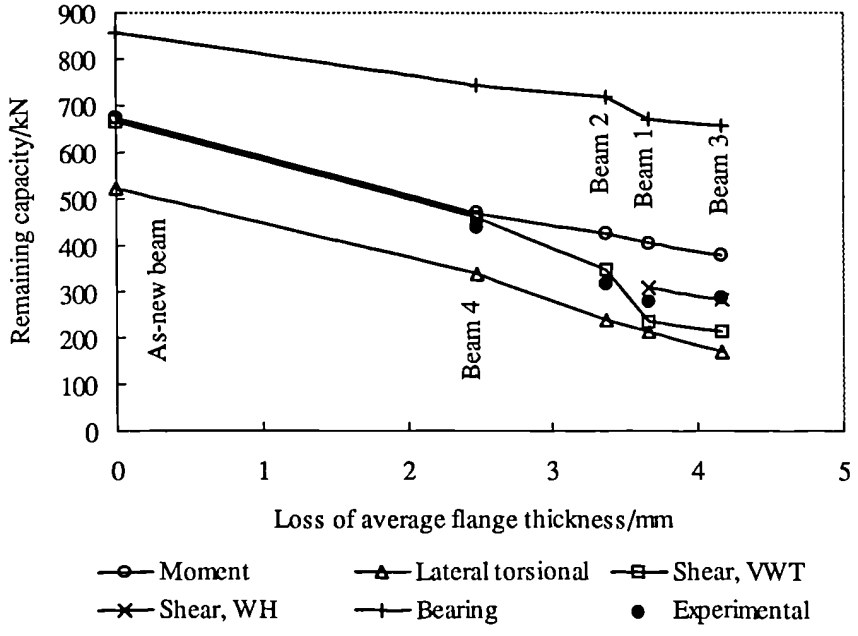

Figure 4.13 Remaining capacities of the four samples of corrosion damaged beams and an as-new beam

When beams have a cut-out at the top flange (coped beams), lateral torsional buckling governs failure of the member throughout its service life as can be seen from Figure 4.13. This was also evident from the buckled shape of the sample beams, which were tested in the laboratory (see Figure 4.10). The effect of cut-out in the top flange is more significant in short span beams than in long span beams [Cheng et al 1988a].

The predicted failure loads of Beams 1 and 3 using the proposed method of assessment for sections that have holes in the web [Wang et al 1975] are slightly greater than the load test results. It may not be possible to compare these loads with the load test results, as the sample beams including Beams 1 and 3 tested in the laboratory failed in lateral torsional buckling mainly due to the cut-out in the top flange. One of the limitations in the proposed method of assessment [Redwood et al 1987, and Wang et al 1975] is that the method considered the location of holes with reference to the web height only. The location of the hole with reference to its longitudinal length (length of stiffened web panel) can become an important factor if the hole is within the tension field area.

4.4.2 Confirmation of the method of assessment proposed for coped beams

In order to investigate the applicability of the proposed method of assessment [Cheng et al 1988a] for coped beams, the lateral torsional buckling capacities of the four samples of corrosion damaged beams were evaluated using the theory given in Section 3.4.1 for ordinary (uncoped) beams. These results were then compared with the results from the proposed method and experimental failure loads. When using the theory for ordinary beams, the effect of cope was taken into account as far as possible by using the following assumptions for end conditions:

1. Torsional restraint at the uncoped end but not at the coped end,
2. Compression flange was laterally restrained at the uncoped end but not at the coped end,
3. Only compression flange is free to rotate on plan at the uncoped end but both flanges are free to rotate on plan at the coped end, and
4. The load was destabilising in the tests.

The effective length of the beam was calculated based on these assumptions. Results from the two methods and the experimental failure loads are given in Table 4.4 and shown in Figure 4.14. The assumptions made for the end conditions may be a critical factor in assessing the lateral torsional buckling capacity of a beam. A sensitivity analysis was carried out assuming different end conditions, i.e. different effective lengths, to see how they affect the outcome of the assessment based on the theory for ordinary beams and the proposed method of Cheng et al. Beam 2 was used for this purpose. The result of the analysis is given in Table 4.5.

Table 4.4 Failure loads obtained using the theory for ordinary beams, the proposed method (Cheng et al) and from the load test

Beam No.	Lateral torsional buckling capacity / kN		Experimental failure load / kN
	Ordinary beam theory	Cheng et al	
As-new	620.3	523.9	
Beam 1	404.7	212.1	277.0
Beam 2	426.1	240.5	318.0
Beam 3	376.6	170.5	287.0
Beam 4	476.1	340.4	440.0

Table 4.5 Sensitivity analysis of end conditions for Beam 2

Effective length, L_E / mm	Lateral torsional buckling capacity / kN	
	Ordinary beam theory	Cheng et al
2066.0	407.1	236.9
1874.0	426.1	240.5
1336.8	476.3	248.5

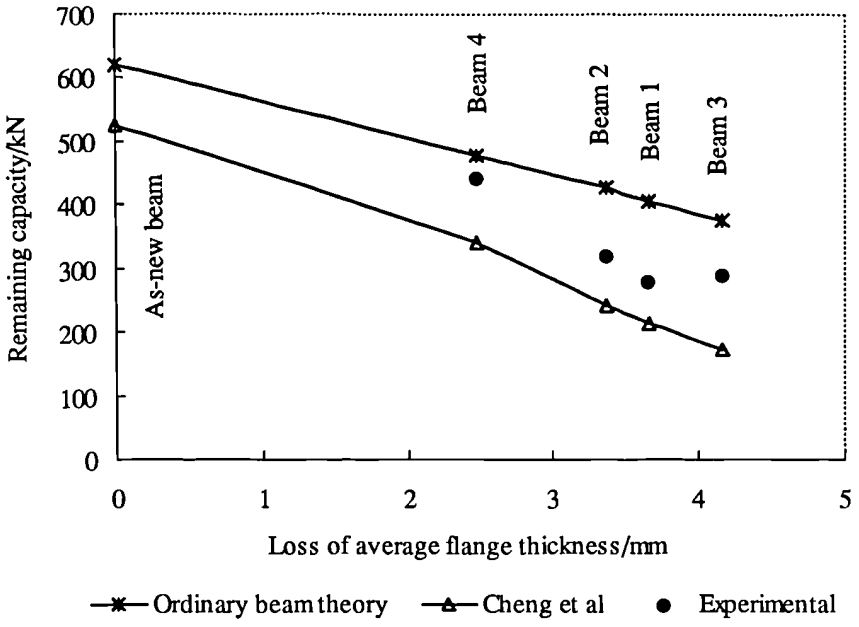

Figure 4.14 Comparison of the results obtained using the theory for ordinary beams and Cheng et al with experimental failure loads from load test

It is evident from Figure 4.14 that whilst the theory for ordinary beams over-estimates the remaining lateral torsional buckling capacity of the beams, which are coped at one end of the top flange, the proposed method of Cheng et al [1988a] gives conservative estimates of the ultimate failure loads. It was found that the capacity evaluation using the proposed method is not very sensitive to the assumptions made on the end conditions for the I-section (uncoped section) of coped beams. In the case of the theory for ordinary beams, the estimates are sensitive to these assumptions as can be seen from Table 4.5. All of these findings indicate that the method based on the theory for ordinary beams may not be suitable for evaluating the remaining lateral torsional buckling capacity of coped beams.

4.4.3 Confirmation of the method of assessment proposed for beams with web holes

It was observed during the load test of Beam 3 that a crack developed at a corner of a big hole in the web when the load was 215 kN. This crack propagated until the ultimate

failure of the beam occurred at 287 kN. This so-called 'Vierendeel' deformation occurs at openings placed at any height within the web under all combinations of moment and shearing force [Redwood et al 1987]. Therefore it is crucial that the effects of holes in the web (if there are any) must be taken into account when evaluating the capacity of corrosion damaged steel beams.

The shear capacity of a beam that has a hole may depend on the location and size of the hole. An analysis was carried out using Beam 3 to study how the strength of a beam is affected by the location and size of the hole. The shear capacity was calculated by (a) changing the location and keeping the size of the hole unchanged, and (b) changing the size of the hole and keeping the location unchanged. The results of the analysis are given in Table 4.6 and 4.7.

Table 4.6 Effect of hole location on the shear capacity

Hole location, d_b / mm	Shear capacity / kN
15	294.6
75	224.7
125	194.9
175	186.2
235	197.4

Note:

Size of the hole

$2a_H = 374$ mm

$d_H = 40$ mm

where

$2a_H$ and d_H are the hole width and depth, and

d_b is the height between the inside edge of the bottom flange and the nearest hole edge.

Table 4.7 Effect of hole size on the shear capacity

Hole width, $2a_H$ / mm	Hole depth, d_H / mm	Shear capacity / kN
374	40	294.6
400	50	286.7
425	60	278.7
450	70	270.3
475	80	261.4

Note:

Hole location

d_b = 15 mm

The results from the analysis of effect of location on the shear capacity (see Table 4.6) show that the location is an important factor on the shear capacity of a beam that has a hole. The shear capacity is significantly reduced when the hole is located in the middle part of the web. It should be noted that the holes in the web created by corrosion are normally located in the lower part of the web (see Figure 4.5). The size of the hole also has an effect on the shear capacity but not to the extent of the effect of the location as it can be seen from Table 4.7. The shear capacity is slightly reduced when the hole size becomes large. It should be noted that the effect of hole size was analysed for a hole that is located in the lower part of the web near the bottom flange.

4.5 Summary and conclusions

The analysis of corrosion effects on the carrying capacity of corrosion damaged beams showed that while loss of thickness of a section due to corrosion generally reduces the capacity of a loaded beam, it can also change the mode of failure from one mechanism to another depending on the relative thickness loss in the various parts. In addition to these, loss of thickness may also change the class of an element from one to another (e.g. plastic to semi-compact).

Lateral torsional buckling, local buckling of flanges and shear failure of web were the critical failure mechanisms of corrosion damaged beams, which were provided with load carrying stiffeners. For such beams bearing failure mechanism was found to be less significant. For corrosion damaged coped beams, which have cut-outs in the top flange, the lateral torsional buckling mode was found to be the critical failure mechanism.

The existence of holes in a member created by corrosion is likely to reduce the capacity significantly, although this will depend on the size and location of the holes. It was found that the shear capacity is greatly influenced by the location of the hole. The location where holes are normally created by corrosion is the lower part of the web near the bottom flange. It was found that if the hole is located in the lower part of the web, the reduction in shear capacity is small compared to other locations. The load test results show that even the most severely corrosion damaged beams, with holes in the web and flanges, possessed more than 50% of their calculated as-new strength.

The assessment methods proposed in Chapter 3 for coped beams and beams with web holes can be used for the assessment of such beams as they were found to give reasonably good results. The comparison of the failure loads in the tests with the analysis showed that, although the proposed method for the assessment of coped beams is conservative, the prediction is closer to the experimental failure loads. The theory given in Section 3.4.1 for ordinary beams may not be suitable for evaluating the lateral torsional buckling capacity of coped beams as it was found to over-estimate the capacity of such beams.

It was shown in the analysis of corrosion effects (see Figure 4.3) that a relationship can be established between the remaining capacities and the loss of thickness. For a given loss of thickness of that beam, these curves can be used to estimate the remaining capacity. This approach can form the basis for establishing a quantitative relationship between visual assessment of corrosion defects and the corresponding remaining capacity.

Chapter 5

Development of assessment methods for estimating the remaining capacity of corrosion damaged I-beams

5.1 Introduction

Current practice in the management of inspection and repair of exposed structural steelwork in the petro-chemical industry has been described by Gallon [1993]. Regular inspection of steel structures is usually based on visual examination and classification into condition categories, which identify the need for appropriate action. The most severe visual category refers to the presence of serious structural defects and the consequent need for full structural assessment and repair.

Gallon [1993] found that the current inspection and assessment methods, while being safe, were significantly conservative in some instances. This may lead to plant closures with consequent financial penalty when the corrosion damaged structures may be able to carry the required loads. On the other hand the over estimation of the remaining capacity may lead to structural failures, which can be catastrophic depending on the chemicals involved in the production. These factors indicate that there is an urgent need for a more realistic assessment method for quantifying visual inspection so that the capacity of corrosion damaged steel structures may be assessed more reliably.

The overall aim of this chapter is to develop assessment methods that can be used to make reliable estimates of the remaining capacity of corrosion damaged beams using thickness loss information provided by visual inspection.

The specific objectives of this chapter are:

1. To develop assessment methods that give the quantitative relationships between the magnitude of corrosion defects and the corresponding reduction in capacity of steel beams of all manufactured sizes in the UK.
2. To develop these methods for various failure modes.
3. To derive lower bound solutions to estimate the remaining capacity.
4. To compare experimental failure loads of samples of corrosion damaged beams with the estimates from these assessment methods.

5.2 Development of minimum curves

In the previous chapter, we have seen that it is possible to establish a relationship between the remaining capacities of various failure modes and the loss of thickness for a particular member. It was also said that this approach can form the basis for establishing a quantitative relationship between the magnitude of corrosion defects and the corresponding remaining capacity. The two corrosion decay models, namely uniform thickness loss and variable thickness loss models developed in Chapter 4, will be used separately for the development of assessment methods. It should be noted that the variable thickness loss model closely matches the pattern of samples of corrosion damaged steel beams (see Figure 4.5 and Table 4.1).

In this chapter, analytical relations will be obtained between percentage remaining capacity and percentage thickness loss of corrosion damaged I-beams. It will be seen that a few approximations will be required in order to derive these analytical relations. Therefore, this method will be called the Simple Assessment Method.

For a particular failure mode of a beam, if the percentage remaining capacity is plotted against the percentage loss of thickness, we will obtain a curve that gives the relationship between them. If this is repeated for all the available I-sections, we will obtain a family of curves from which we should be able to identify the curve that has the lowest value of percentage remaining capacity. This curve can be taken as the "minimum curve" for that

particular failure mode and can be used to estimate the percentage remaining capacity of any corrosion damaged beam regarding that particular failure mode. The estimates will be conservative for some sections since we consider the worst case to be the minimum curve. It will be seen later in this chapter that in many cases the variation in the percentage remaining capacity curves of all the I-sections is minimal. To obtain a minimum curve in this manner no approximations will be required (i.e. exact section sizes and properties will be used in the analysis). Therefore, this method will be called the Accurate Assessment Method.

The above approach involves analysing all the I-sections (71 sections) manufactured in the UK. This will require a considerable amount of man hours and computer time to identify the section that gives the minimum curve. The above problem was minimised by using the following procedure that involves only about 25 sections. Firstly, a family of sections (i.e. sections, which have the same serial size) was analysed to observe their behaviour regarding a particular failure mode and to identify the section that gives the minimum curve for the family. Considering the above observation, the sections with similar properties from each of the families were analysed to identify the section that gives the minimum curve for all the sections. For simplicity, the results of the analysis are given in this chapter for only a few sections including the sections that have the maximum and minimum percentage remaining capacity. The sections are numbered according to their position in the section table (e.g. UB1, UB2, etc.).

5.3 Corrosion decay models

For the development of assessment methods, the two corrosion decay models that were developed in Chapter 4 will be used. The two models are described in the following sections.

5.3.1 Uniform thickness loss model sections

The corrosion decay model developed for the uniform thickness loss model sections is as follows (see Section 4.2.1):

Thickness of the top flange $= T_N(1 - \xi)$

Thickness of the bottom flange $= T_N(1 - \xi)$

Average thickness of the flanges, $T_C = T_N(1 - \xi)$ (5.1a)

Thickness of the web, $t_C = t_N(1 - \xi)$ (5.1b)

where

$\xi = \xi_F = \xi_W$,

$\xi_F = \%LFT/100$,

$\xi_W = \%LWT/100$,

%LFT is the percentage loss of flange thickness, and

%LWT is the percentage loss of web thickness.

5.3.2 Varying thickness loss model sections

The corrosion decay model developed for the varying thickness loss model sections is as follows (see Section 4.2.1):

Thickness of the top flange $= T_N(1 - 0.7\xi)$ (5.2a)

Thickness of the bottom flange $= T_N(1 - 1.3\xi)$ (5.2b)

Average thickness of the flanges, $T_C = T_N(1 - \xi)$ (5.2c)

Thickness of the upper part of the web $(0.75h_w) = t_N(1 - 0.25\xi)$ (5.2d)

Thickness of the lower part of the web $(0.25h_w) = t_N(1 - 1.25\xi)$ (5.2e)

Average thickness of the web, $t_C = t_N(1 - 0.5\xi)$ (5.2f)

where $\xi = \xi_F = 2\xi_W$.

In this case, the average thickness is used to calculate the percentage loss of both flanges and web thickness.

5.4 Assessment methods for Moment Capacity

The loss of thickness in the flanges and web due to corrosion, results in reduction in the moment capacity. Besides this, we have seen in Section 4.2.3.1 that the loss of thickness may change the class of an element (plastic, compact, semi-compact or slender) from one to another. For example, an element that is plastic in its as-new condition may become semi-compact due to corrosion during its service life and local buckling may prevent the development of full plastic moment in such cases. Therefore, minimum curves will be developed for various possible cases by considering the above facts. The effect of shear force on the moment capacity will also be taken into account. The theory given in Section 3.2 was used for the evaluation of remaining moment capacity of corrosion damaged beams.

5.4.1 Simple assessment method

5.4.1.1 Moment capacity with low shear load

The effect of shear force (F_V) is to reduce the plastic moment capacity but the reduction for an I-section is small for $F_V < 0.6P_V$, where P_V is the shear capacity [Morris and Randall 1979]. For low shear load ($F_V < 0.6P_V$) the moment capacity, M_c, is as follows:

For plastic and compact sections,

$M_{cC} = p_y S_C$ but $< 1.2p_y Z_C$ for corrosion damaged sections (5.3a)

$M_{cN} = p_y S_N$ but $< 1.2p_y Z_N$ for as-new section sections (5.3b)

For semi-compact sections

$M_{cC} = p_y Z_C$ for corrosion damaged sections (5.4a)

$M_{cN} = p_y Z_N$ for as-new section sections (5.4b)

For slender sections

$M_{cC} = p_y Z_C$ for corrosion damaged sections (5.5a)

$M_{cN} = p_y Z_N$ for as-new section sections (5.5b)

where

p_y is the design strength (reduced for slender sections - see cl 3.6 of BS 5950 [1985]),

S is the plastic modulus of the section about the relevant axis, and

Z is the elastic modulus of the section about the relevant axis.

The percentage remaining moment capacity (%RMC) of a corrosion damaged section is the ratio of the capacity of the corrosion damaged section (M_{cC}) to the capacity of the as-new section (M_{cN}). It can be expressed as:

$$\%RMC = 100\,(M_{cC}/M_{cN}) \tag{5.6}$$

For corrosion damaged beams of the same section size, the overall dimensions B, D, and h_w can be considered as constant throughout their service life, although there will be a small reduction due to corrosion. Therefore, the plastic modulus of I-sections with equal flanges about its major axis may be given by:

$$S_{xC} = BT_C(D-T_C) + t_C\frac{h_w^2}{4} \quad \text{for corrosion damaged sections} \tag{5.7a}$$

$$S_{xN} = BT_N(D-T_N) + t_N\frac{h_w^2}{4} \quad \text{for as-new sections} \tag{5.7b}$$

A) Uniform thickness loss model sections

Substituting for T_C and t_C (Equations 5.1a and 5.1b) into Equation 5.7a, gives the plastic modulus of corrosion damaged I-sections as:

$$\begin{aligned} S_{xC} &= BT_N D(1-\xi) - BT_N^2(1-\xi)^2 + t_N\frac{h_w^2}{4}(1-\xi) \\ &= \left(BT_N(D-T_N) + t_N\frac{h_w^2}{4}\right) - \xi\left(BT_N(D-2T_N) + t_N\frac{h_w^2}{4}\right) - BT_N^2\xi^2 \end{aligned} \tag{5.8}$$

The first bracketed term of Equation 5.8 is the plastic modulus of as-new sections given by Equation 5.7b. Now, using the following approximation,

$$BT_N(D-2T_N) + t_N\frac{h_w^2}{4} \approx S_{xN} \tag{5.9}$$

and neglecting the ξ^2 term, the plastic modulus of corrosion damaged sections, S_{xC}, is obtained as:

$$S_{xC} \approx S_{xN} - \xi S_{xN} \tag{5.10}$$

B) Varying thickness loss model sections

Substituting for T_C and t_C (Equations 5.2c and 5.2f) into Equation 5.7a, gives the plastic modulus of corrosion damaged I-sections as:

$$S_{xC} = BT_N D(1-\xi) - BT_N^2(1-\xi)^2 + t_N\frac{h_w^2}{4}\left(1-\frac{\xi}{2}\right) \tag{5.11}$$

$$= \left(BT_N(D-T_N)+t_N\frac{h_w^2}{4}\right) - \xi\left(BT_N(D-2T_N)+t_N\frac{h_w^2}{8}\right) - BT_N^2\xi^2$$

$$= \left(BT_N(D-T_N)+t_N\frac{h_w^2}{4}\right) - \xi\left(BT_N(D-2T_N)+t_N\frac{h_w^2}{4}\right) + \xi t_N\frac{h_w^2}{8} - BT_N^2\xi^2$$

If Equations 5.7b and Equation 5.9 are substituted into Equation 5.11 and the ξ^2 term is neglected, the following relation is obtained for the plastic modulus of corrosion damaged sections,

$$S_{xC} \approx S_{xN} - \xi\left(S_{xN} - t_N\frac{h_w^2}{8}\right) \tag{5.12}$$

where the term, $t_N h_w^2/8$, of Equation 5.12 is the plastic modulus of the half of the shear area.

5.4.1.1.1 Class of section unchanged by corrosion

Although corrosion reduces the thickness of the compression flange of a section, some sections that are plastic, compact or semi-compact in their as-new condition may remain the same for part or all of their service life.

A) Plastic and compact sections

For a given design strength, the factor that governs the plastic moment of resistance of a section is the plastic modulus of that section about its relevant axis. The plastic modulus of I-sections about their major axis may be written as:

$$S_x \approx BT^2(x-1) + t\frac{h_w^2}{4} \qquad (5.13)$$

where x is the torsional index $\approx D/T$. The reason for giving this relation (Equation 5.13) will be realised later in this section.

The %RMC of plastic and compact sections may be written in terms of plastic section modulus of the corrosion damaged (S_{xC}) and as-new (S_{xN}) sections as described below. Substituting Equations 5.3a and 5.3b into Equation 5.6 gives the %RMC as:

$$\%RMC = 100\left(\frac{S_{xC}}{S_{xN}}\right) \qquad (5.14)$$

For uniform thickness loss model sections, if Equations 5.10 and 5.14 are combined, then the following expression is obtained for the %RMC (Equation 5.14) of plastic and compact corrosion damaged sections,

$$\%RMC = 100\,(1-\xi) \qquad (5.15)$$

For varying thickness loss model sections, substituting Equation 5.12 into Equation 5.14 gives the %RMC (Equation 5.14) of plastic and compact corrosion damaged sections as:

$$\%RMC = 100\left[1 - \xi\,(1-\omega)\right] \tag{5.16}$$

$$\text{where, } \omega = \frac{t_N h_w^2/8}{S_{xN}} \tag{5.17}$$

For minimum of %RMC (Equation 5.16), ω must be minimum. It was found by analysing the sections that the minimum of ω can be obtained for the section that has the minimum values of torsional index, x, and D/B ratio. The section that has the above properties was found to be UB60 (254×146 UB 43) and the minimum value of ω was obtained as 0.09. Substituting the above minimum value of ω into Equation 5.16 gives the minimum of %RMC of plastic and compact sections as:

$$\text{Min}(\%RMC) = 100\,(1 - 0.91\xi) \tag{5.18}$$

Therefore, for the case of low shear load, the %RMC curves of sections that are plastic or compact in their as-new condition and remain the same for part or all of their service life will be straight lines with a slope of approximately -1.0 for uniform thickness loss model sections, and -0.91 for varying thickness loss model sections. These curves (Equations 5.15 and 5.18) may be used as the minimum curves for estimating the %RMC of any sections that are plastic or compact in both their as-new and corrosion damaged conditions.

B) Semi-compact sections

For semi-compact sections, the elastic modulus of the sections about the relevant axis is used for the moment capacity. The elastic modulus, Z_x, may be expressed in terms of the plastic modulus, S_x, and the shape factor, SF, as follows:

$$Z_x = S_x/SF \tag{5.19}$$

For corrosion damaged I-sections, the shape factor 'SF' may be assumed as constant for all of their service life. If Equation 5.19 is substituted into Equations 5.4a and 5.4b, the following relations are obtained for the moment capacity of semi-compact sections,

$M_{cC} = p_y S_{xC} / SF$ for corrosion damaged sections (5.20a)

$M_{cN} = p_y S_{xN} / SF$ for as-new section sections (5.20b)

Substituting Equations 5.20a and 5.20b into Equation 5.6 gives the %RMC of corrosion damaged semi-compact sections as:

$$\%RMC = 100\left(\frac{S_{xC}}{S_{xN}}\right) \tag{5.21}$$

Equation 5.21 is identical to Equation 5.14. Therefore, Equations 5.15 and 5.18 may still be used as the minimum curves to estimate the %RMC of semi-compact sections which remain in this class even in their corroded states.

5.4.1.1.2 Class of section changed by corrosion

A) Plastic or compact to semi-compact

Consider a section that is plastic or compact in its as-new condition and becomes semi-compact due to corrosion. When the section is plastic or compact, Equations 5.15 and 5.18 may be used as the minimum curves for the %RMC. When the section becomes semi-compact, using Equations 5.3b and 5.20a together with Equation 5.6, the %RMC may be given by the following expression:

$$\%RMC = \frac{1}{SF}\left[100\left(\frac{S_{xC}}{S_{xN}}\right)\right] \tag{5.22}$$

The minimum of the term within the square brackets was obtained in the previous section and is given by Equations 5.15 and 5.18. Therefore, using Equations 5.15 and 5.18, and making a substitution for 'SF', which is approximately 1.15 for I-sections, the minimum of %RMC (Equation 5.22) may be given by:

$\text{Min}(\%RMC) = 87\,(1 - \xi)$ for uniform thickness loss model (5.23)

$$\text{Min}(\%RMC) = 87\,(1 - 0.91\xi) \quad \text{for varying thickness loss model} \qquad (5.24)$$

Therefore, when a section that is plastic or compact in its as-new condition becomes semi-compact during its service life, Equations 5.23 and 5.24 may be used for estimating the %RMC. These curves will have a new %RMC intercept of 87.0% and a slope of approximately -0.87 for uniform thickness loss model sections, and -0.79 for varying thickness loss model sections.

B) Semi-compact to slender

Consider a section that is semi-compact in its as-new condition and becomes slender due to corrosion. If it remains semi-compact during the early stages of corrosion, Equations 5.15 and 5.18 may be used as the minimum curves to estimate the %RMC as before.

However, if the outstanding flange becomes too thin, as corrosion develops, then there is a risk of failure by local buckling of the flange in compression. The buckling stress may be evaluated by a method proposed by Trahair [1977]. The simplest practical way of including this analysis in the assessment of remaining moment capacity is to use a stress reduction factor (SRF) following the procedure given in BS 5950 [1985].

For example, for welded I-sections, the 'SRF' is defined as (see Table 8 of BS 5950):

$$SRF = \frac{10}{(b/T\varepsilon) - 3} \qquad (5.25)$$

Substituting the stress reduction factor, SRF, into Equation 5.5a gives the following expression for the moment capacity of corrosion damaged slender sections,

$$M_{cc} = (SRF_C)p_yZ_C \qquad (5.26)$$

Using Equations 5.4b and 5.26 together with Equations 5.6 and 5.19, the %RMC of corrosion damaged slender sections that were originally semi-compact is obtained as:

$$\%RMC = (SRF_C)\left[100\left(\frac{S_{xC}}{S_{xN}}\right)\right] \qquad (5.27)$$

As mentioned earlier, the minimum of the term within the square brackets was obtained in the previous section and is given by Equations 5.15 and 5.18. Now, the stress reduction factor, SRF_C, is not a constant and it is a function b/T and ε. Therefore in order to obtain the minimum of %RMC given by Equation 5.27, it is necessary to obtain the minimum of SRF_C. Let us first consider the case of uniform thickness loss model sections using a corrosion damaged welded section.

Combining Equations 5.1a and 5.25 gives,

$$SRF_C = \frac{10}{\frac{b}{T_N(1-\xi)}\sqrt{\frac{p_y}{275}} - 3} \qquad (5.28)$$

The minimum value of SRF_C can be obtained when the values of b/T_N and p_y are maximum. The possible maximum values of b/T_N and p_y are as follows:

$Max(b/T_N) = 8.81$ for section UB48 (356×171 UB 45), and
$Max(p_y) = 450.0\ N/mm^2$

Substituting the above values into Equation 5.28 gives the minimum of 'SRF_C' as:

$$Min(SRF_C) = \frac{1-\xi}{0.827+0.3\xi} \qquad (5.29)$$

Now, using Equations 5.15 and 5.29, the minimum of %RMC (Equation 5.27) of welded slender sections that were originally semi-compact may be given by:

$$Min(\%RMC) = 100\frac{(1-\xi)^2}{0.827+0.3\xi} \qquad (5.30)$$

Similarly, for corrosion damaged rolled slender sections that were semi-compact in their as-new condition, the minimum of %RMC may be given by:

$$\text{Min}(\%\text{RMC}) = 100\frac{(1-\xi)^2}{0.66+0.36\xi} \tag{5.31}$$

If the denominators of Equations 5.30 and 5.31 are compared, then it is clear that,

$$(0.827 + 0.3\xi) > (0.66 + 0.36\xi)$$

Hence, for uniform thickness loss model sections, Equation 5.30, which was obtained for the welded sections, may be used as the minimum curve to estimate the %RMC of any corrosion damaged slender sections that were originally semi-compact in their as new condition.

Now, let us consider the case of varying thickness loss model sections. Substituting Equation 5.2a into Equation 5.25 gives the SRF_C of a welded section as:

$$SRF_C = \frac{10}{\frac{b}{T_N(1-0.7\xi)}\sqrt{\frac{P_y}{275}}-3} \tag{5.32}$$

Using the similar approach used in the case of uniform thickness loss model sections, the minimum of 'SRF_C' is obtained as:

$$\text{Min}(SRF_C) = \frac{1-0.7\xi}{0.827+0.21\xi} \tag{5.33}$$

Now, using Equations 5.18 and 5.33, the minimum of %RMC (Equation 5.27) of welded slender sections that were originally semi-compact may be given by:

$$\text{Min}(\%\text{RMC}) = 100\frac{(1-0.7\xi)(1-0.91\xi)}{0.827+0.21\xi} \tag{5.34}$$

For rolled sections, the minimum of %RMC may be given by:

$$\text{Min}(\%\text{RMC}) = 100\frac{(1-0.7\xi)(1-0.91\xi)}{0.66+0.255\xi} \qquad (5.35)$$

It is clear from the comparison of the denominators of Equations 5.34 and 5.35 that,

$$(0.827 + 0.21\xi) > (0.66 + 0.255\xi)$$

For varying thickness loss model sections, when sections that are semi-compact in their as-new condition become slender due to corrosion, Equation 5.34 that was obtained for the welded sections may be used as the minimum curve for estimating the %RMC.

5.4.1.2 Moment capacity with high shear load

If a shear force is applied to an I-section, most of the shear force is resisted by the web. In general the effect of a shear force is to reduce the plastic moment capacity. A theory that describes the effect of shear force on the plastic moment capacity is given by Horne [1971]. For the assessment of remaining moment capacity, the effect of shear force may be analysed by following the procedure given in BS 5950 [1985]. For high shear load, i.e. where $F_V > 0.6P_V$, the moment capacity, M_c, should be taken as follows:

For plastic and compact sections,

$$M_{cC} = p_y(S_C - \rho_1 S_{vC}) \quad \text{but} \quad \leq 1.2p_yZ_C \quad \text{for corrosion damaged sections} \qquad (5.36a)$$

$$M_{cN} = p_y(S_N - \rho_1 S_{vN}) \quad \text{but} \quad \leq 1.2p_yZ_N \quad \text{for as-new sections} \qquad (5.36b)$$

where $\rho_1 = [2.5F_v/P_v] - 1.5$

and S_v is taken as the plastic modulus of the shear area (A_v) for sections with equal flanges and the plastic modulus of the gross section less the plastic modulus of that part of the section remaining after deduction of the shear area for sections with unequal flanges.

The moment capacities of semi-compact and slender sections are given by Equations 5.4 and 5.5 as in the case of low shear load.

As before, the overall dimensions B, D, and h_w of corrosion damaged beams of the same section size can be assumed as constant throughout their service life. For sections with equal flanges (I-sections), subtracting the term $\rho_l S_v$ from Equations 5.7a and 5.7b gives the reduced plastic modulus, $(S - \rho_l S_v)$, of the sections as:

$$S_{xC} - \rho_l S_{vC} = BT_C(D - T_C) + t_C \frac{h_w^2}{4}(1-\rho_l) \quad \text{for corroded sections} \qquad (5.37a)$$

$$S_{xN} - \rho_l S_{vN} = BT_N(D - T_N) + t_N \frac{h_w^2}{4}(1-\rho_l) \quad \text{for as-new sections} \qquad (5.37b)$$

A) Uniform thickness loss model sections

If Equations 5.1a and 5.1b are substituted into Equation 5.37a, the following expression is obtained for the reduced plastic modulus of corrosion damaged sections,

$$S_{xC} - \rho_l S_{vC} = BT_N D(1-\xi) - BT_N^2(1-\xi)^2 + t_N \frac{h_w^2}{4}(1-\xi)(1-\rho_l)$$

$$= \left(BT_N(D-T_N) + t_N \frac{h_w^2}{4}(1-\rho_l)\right) - \xi\left(BT_N(D-2T_N) + t_N \frac{h_w^2}{4}(1-\rho_l)\right) - BT_N^2\xi^2 \qquad (5.38)$$

The first bracketed term of Equation 5.38 is the reduced plastic modulus of as-new sections given by Equation 5.37b. Now, using the following approximation,

$$BT_N(D-2T_N) + t_N \frac{h_w^2}{4}(1-\rho_l) \approx S_{xN} - \rho_l S_{vN} \qquad (5.39)$$

and neglecting the ξ^2 term, the reduced plastic modulus of corrosion damaged sections, $(S_{xC} - \rho_l S_{vC})$, may be given by:

$$S_{xC} - \rho_l S_{vC} \approx (S_{xN} - \rho_l S_{vN}) - \xi\,(S_{xN} - \rho_l S_{vN}) \qquad (5.40)$$

B) Variable thickness loss model sections

Substituting for T_C and t_C (Equations 5.2c and 5.2f) into Equation 5.37a gives the reduced plastic modulus of corrosion damaged I-sections about the major axis as:

$$S_{xC} - \rho_1 S_{vC} = BT_N D(1-\xi) - BT_N^2(1-\xi)^2 + t_N \frac{h_w^2}{4}\left(1-\frac{\xi}{2}\right)(1-\rho_1)$$

$$= \left(BT_N(D-T_N)+t_N\frac{h_w^2}{4}(1-\rho_1)\right) - \xi\left(BT_N(D-2T_N)+t_N\frac{h_w^2}{8}(1-\rho_1)\right) - BT_N^2\xi^2$$

$$= \left(BT_N(D-T_N)+t_N\frac{h_w^2}{4}(1-\rho_1)\right) - \xi\left(BT_N(D-2T_N)+t_N\frac{h_w^2}{4}(1-\rho_1)\right) +$$

$$\xi t_N \frac{h_w^2}{8}(1-\rho_1) - BT_N^2\xi^2 \qquad (5.41)$$

Now, using Equations 5.37b and 5.39, and neglecting the ξ^2 term, the reduced plastic modulus of corrosion damaged sections, $(S_{xC} - \rho_1 S_{vC})$, may be written as:

$$S_{xC} - \rho_1 S_{vC} \approx (S_{xN} - \rho_1 S_{vN}) - \xi\left((S_{xN} - \rho_1 S_{vN}) - t_N\frac{h_w^2}{8}(1-\rho_1)\right) \qquad (5.42)$$

In the case of maximum high shear load, $\rho_1 = 1$. Therefore, for maximum high shear load cases, Equation 5.42 reduces to,

$$S_{xC} - S_{vC} \approx (S_{xN} - S_{vN}) - \xi\,(S_{xN} - S_{vN}) \qquad (5.43)$$

5.4.1.2.1 Class of section unchanged by corrosion

A) Plastic and compact sections

Consider a section that is plastic or compact in both its as-new and corrosion damaged conditions. For a given p_y, the factor that governs the plastic moment of resistance of a plastic or compact section is the reduced plastic modulus of that section about its relevant axis. Now using Equations 5.36a and 5.36b together with Equation 5.6, the

%RMC of plastic and compact sections may be given in terms of the reduced plastic modulus of the sections as:

$$\%RMC = 100\left[\frac{S_{xC} - \rho_l S_{vC}}{S_{xN} - \rho_l S_{vN}}\right] \qquad (5.44)$$

For uniform thickness loss model sections, substituting Equation 5.40 into Equation 5.44 gives the %RMC of corrosion damaged plastic and compact sections as:

$$\%RMC = 100\,(1 - \xi) \qquad (5.45)$$

For maximum high shear load cases, i.e. $\rho_l = 1$, if Equation 5.43 is combined with Equation 5.44, then the relation which can be obtained for the %RMC of varying thickness loss model plastic and compact sections is identical to Equation 5.45.

The %RMC given by Equation 5.45 is identical to Equation 5.15. We have only one equation for the %RMC of both uniform and varying thickness loss model sections since the capacity of these sections are based on the plastic modulus of the flanges alone for maximum high shear loads. The magnitude of average percentage flange thickness loss is the same for both thickness loss models. Therefore, for both uniform and varying thickness loss model sections, Equation 5.15 may be used as the minimum curve for estimating the %RMC of sections that are plastic or compact in their both as-new and corrosion damaged conditions.

B) Semi-compact sections

For high shear load cases, the moment capacity of semi-compact sections whose class is unaffected by the loss of material due to corrosion is identical to that of the case with low shear load. Therefore, as in the case of semi-compact sections with low shear load (Section 5.4.1.1.1B), Equations 5.15 and 5.18 may be used as the minimum curves for estimating the %RMC (percentage remaining moment capacity) of such sections.

5.4.1.2.2 Class of section changed by corrosion

A) Plastic or compact to semi-compact

Consider a section that is plastic or compact in its as-new condition and becomes semi-compact due to corrosion. When the section is plastic or compact, Equation 5.15 may be used to estimate the %RMC as suggested before. When it becomes semi-compact, using Equations 5.20a and 5.36b, the following relation is obtained for the %RMC,

$$\%RMC = \frac{1}{SF}\left[100\frac{S_{xC}}{S_{xN} - \rho_1 S_{vN}}\right] \tag{5.46}$$

As before, the shape factor 'SF' of the sections may be assumed as constant for all of their service life. Now, for the minimum of %RMC given by Equation 5.46, the value of the term $(S_{xN} - \rho_1 S_{vN})$ should be maximum. This maximum value can be obtained for the minimum value of S_{vN}. The plastic modulus of the shear area, S_{vN}, is given by:

$$S_{vN} = t_N h_w^2/4 \tag{5.47}$$

If we divide both sides of Equation 5.47 by $2S_{xN}$, we will get,

$$\frac{S_{vN}}{2S_{xN}} = t_N \frac{h_w^2}{8}\Big/S_{xN} \tag{5.48}$$

The right hand side term of Equation 5.48 was defined earlier by Equation 5.17 as ω and the minimum value of ω was obtained as 0.09. Hence, the minimum of $(S_{vN}/2S_{xN})$ may be given by:

$$\text{Min}\left(\frac{S_{vN}}{2S_{xN}}\right) = 0.09 \tag{5.49}$$

i.e. $\text{Min}(S_{vN}) = 0.18S_{xN}$

Now, for maximum high shear load cases ($\rho_1 = 1$), the maximum value of ($S_{xN} - \rho_1 S_{vN}$) is obtained as:

$$\text{Max}(S_{xN} - \rho_1 S_{vN}) = 0.82 S_{xN} \tag{5.50}$$

If Equation 5.50 and SF = 1.15 for I-sections are substituted into Equation 5.46, the following relation is obtained for the minimum of %RMC given by Equation 5.46,

$$\text{Min}(\%\text{RMC}) = 106 \left(\frac{S_{xC}}{S_{xN}} \right) \tag{5.51}$$

Hence, for maximum high shear load ($F_V = P_V$) cases, using Equations 5.15 and 5.18, the minimum of %RMC of corrosion damaged semi-compact sections that were originally plastic or compact may be given as:

$$\text{Min}(\%\text{RMC}) = 106 (1 - \xi) \quad \text{for uniform thickness loss model} \tag{5.52}$$

$$\text{Min}(\%\text{RMC}) = 106 (1 - 0.91\xi) \quad \text{for varying thickness loss model} \tag{5.53}$$

Therefore, when sections become semi-compact, the %RMC is given by Equations 5.52 and 5.53, which have a new %RMC intercept of 106.0% and a slope of approximately -1.06 for uniform thickness loss model sections, and -0.97 for varying thickness loss model sections. The increased new %RMC intercept of 106.0% and the slopes indicate that the Min(%RMC) curves will be raised above the minimum curve for the plastic and compact sections (Equation 5.15). Therefore, when the class of corrosion damaged sections change from plastic or compact to semi-compact, Equation 5.15 may still be used as the minimum curve to estimate the %RMC of such sections.

B) Semi-compact to slender

For sections that are semi-compact in their as-new condition and become slender due to corrosion with high shear load, the moment capacity is identical to that of the case with low shear load. Therefore, as in the case of sections with low shear load, when the

sections are semi-compact, Equations 5.15 and 5.18 may be used as the minimum curves for the %RMC. When the sections become slender, Equations 5.30 and 5.34 may be used as the minimum curves for estimating the %RMC of corrosion damaged sections.

5.4.2 Accurate assessment method

5.4.2.1 Moment capacity with low shear load

A family of sections with varying thickness loss was analysed first to study the behaviour of the %RMC of corrosion damaged beams. The results of the analysis together with the detail of the family of sections are given in Figure 5.1.

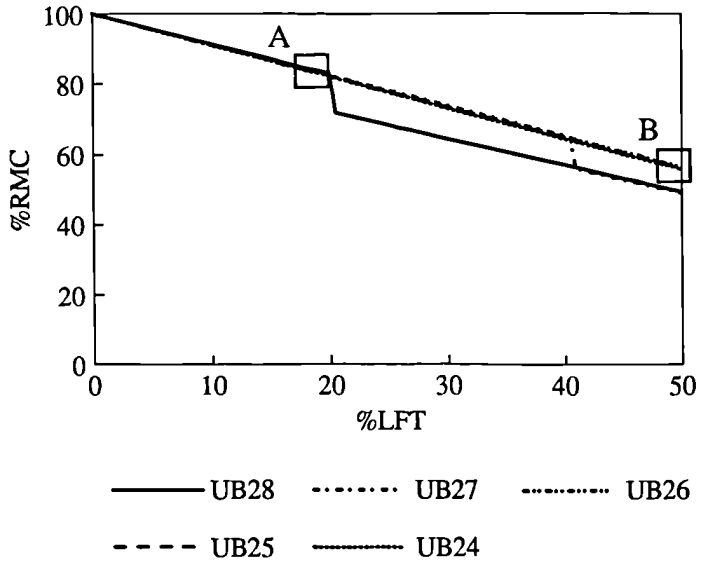

No.	Section	x	b/T
UB24	533×210 UB 122	27.6	4.97
UB25	533×210 UB 109	30.9	5.60
UB26	533×210 UB 101	33.1	6.04
UB27	533×210 UB 92	36.4	6.71
UB28	533×210 UB 82	41.6	7.91

where

x = Torsional index

LFT = Loss of flange thickness

RMC = Remaining moment capacity

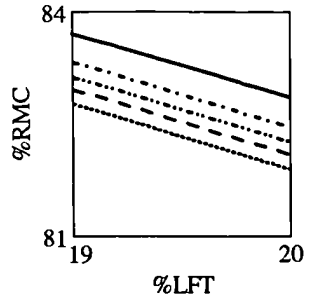

Expanded view of A

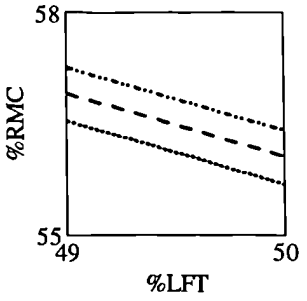

Expanded view of B

Figure 5.1 Behaviour of %RMC of a family of sections with low shear load

Figure 5.1 shows that, when the class of corrosion damaged sections remains as the same as their class in their as-new condition (for flange thickness loss of 0-20%), the section with the lowest value of torsional index, x, gives the minimum curve for that family. For sections, which change from one class to another during its service life (e.g. UB28), the section with the highest value of b/T gives the minimum curve.

5.4.2.1.1 Class of section unchanged by corrosion

Based on the above information, sections that have the lowest value of x from each of the families were analysed to obtain a minimum curve for the %RMC of plastic, compact or semi-compact sections whose class is unchanged by corrosion. The results for five beams, which are plastic or compact and remain in this class even during their corroded states, together with the detail of the sections are given in Figure 5.2.

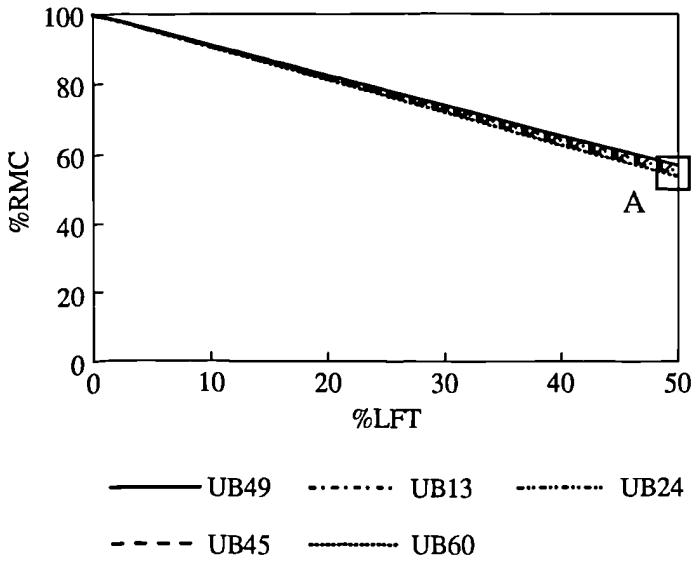

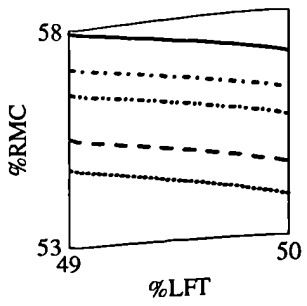

Expanded view of A

No.	Section	x
UB49	356x127 UB 39	35.3
UB13	686x254 UB 170	31.8
UB24	533x210 UB 122	27.6
UB45	356x171 UB 67	24.4
UB60	254x146 UB 43	21.1

Figure 5.2 Behaviour of %RMC of sections with the least value of x from five families

It is evident from Figure 5.2 that the section with the lowest value of torsional index, x, (UB60) gives the minimum curve for whole range of sections that are plastic or compact in both their as-new and corrosion damaged conditions. The above result was also obtained for sections that are semi-compact in their as-new condition and remain in the same class even after damaged by corrosion.

5.4.2.1.2 Class of section changed by corrosion

A) Plastic or compact to Semi-compact

Considering the information obtained from the behaviour of a family of sections, sections with the highest value of b/T from each of the families were analysed to obtain a minimum curve for the %RMC of sections that are plastic or compact in their as-new condition and become semi-compact due to corrosion. The design strength, p_y, was chosen such that the class of these sections changes from plastic or compact to semi-compact. The results for five beams and the sections' detail are given in Figure 5.3.

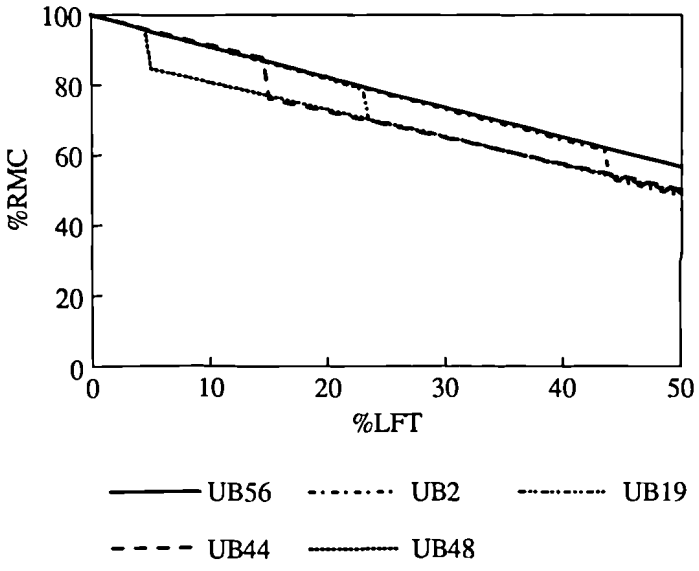

No.	Section	b/T
UB56	305×127 UB 37	5.77
UB2	914×419 UB 343	6.54
UB19	610×305 UB 149	7.74
UB44	406×140 UB 39	8.24
UB48	356×171 UB 45	8.81

Figure 5.3 Behaviour of %RMC of sections with the highest value of b/T from five families with $p_y = 300.0\ N/mm^2$

It can be seen from Figure 5.3 that the section with the highest value of b/T (UB48) gives a part of the minimum curve for the %RMC of sections that are plastic or compact

in their as-new condition and become semi-compact due to corrosion during their service life. This part of the minimum curve should be used for the %RMC when sections become semi-compact. The minimum curve obtained for the %RMC in the previous case (Section 5.4.2.1.1) should be used when sections are plastic or compact.

B) Semi-compact to Slender

Sections with the highest value of b/T from each of the families were analysed again to obtain a minimum curve for the %RMC of sections that are semi-compact in their as-new condition and become slender during their service life. In this case the design strength was chosen such that the class of the sections changes from semi-compact to slender. The results for four beams and the detail of the sections are given in Figure 5.4.

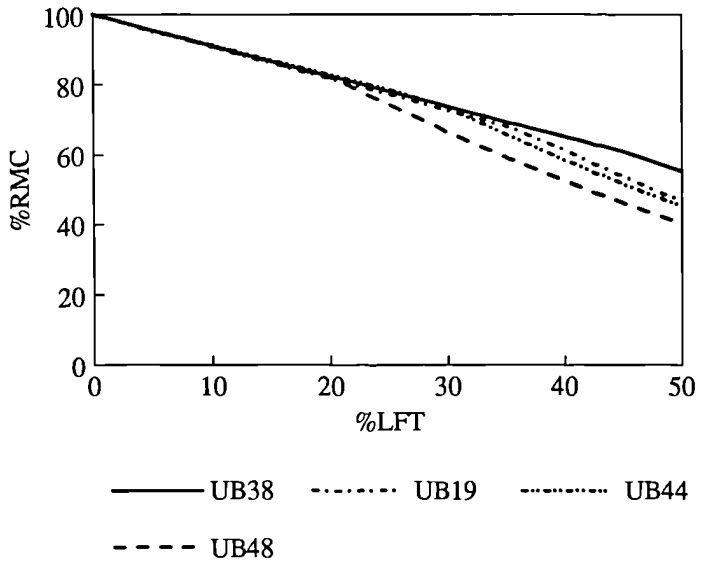

No.	Section	b/T
UB38	457×152 UB 52	6.99
UB19	610×305 UB 149	7.74
UB44	406×140 UB 39	8.24
UB48	356×171 UB 45	8.81

Figure 5.4 Behaviour of %RMC of sections with the highest value of b/T from four families with $p_y = 450.0\ N/mm^2$

It was found that the design strength of the material affects the %RMC of sections that are semi-compact in their as-new condition and become slender due to corrosion. It was also found that, for a section, the maximum value of design strength gives the minimum of %RMC. Figure 5.4 shows that the section with the highest value of b/T (UB48) gives the minimum curve for the %RMC of whole range of sections that are semi-compact in their as-new condition and become slender due to corrosion.

5.4.2.2 Moment capacity with high shear load

In the case of high shear load, only the moment capacities of plastic and compact sections differ from that of the case with low shear load. Therefore only the cases that involve plastic and compact sections will be analysed to obtain a minimum curve. A family of sections was analysed first to study the behaviour of %RMC. The results together with the detail of the family of sections are given in Figure 5.5.

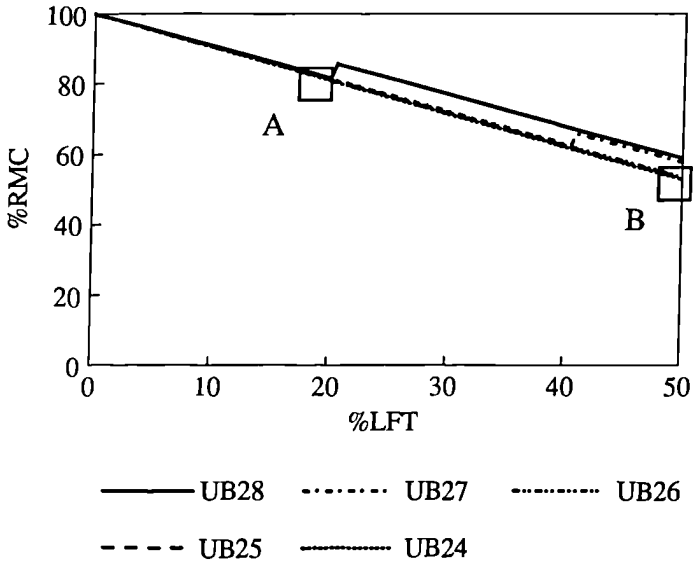

No.	Section	x	b/T
UB24	533x210 UB 122	27.6	4.97
UB25	533x210 UB 109	30.9	5.60
UB26	533x210 UB 101	33.1	6.04
UB27	533x210 UB 92	36.4	6.71
UB28	533x210 UB 82	41.6	7.91

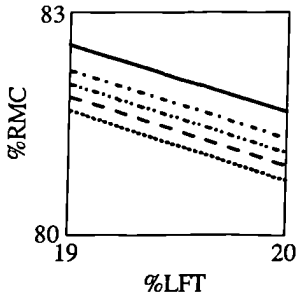

Expanded view of A

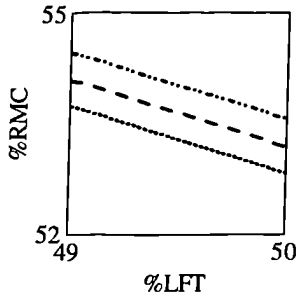

Expanded view of B

Figure 5.5 Behaviour of %RMC of a family of sections with high shear load

Figure 5.5 shows that, for sections that are plastic or compact in their as-new condition and remain the same for part or all of their service life (for flange thickness loss of 0-20%) and for sections that become semi-compact during their service life (e.g. UB28), the section with the lowest value of x gives the minimum curve for that family.

Considering the above observation, the sections with the lowest value of x from each of the families were analysed to obtain a minimum curve for the %RMC of (a) plastic and compact sections whose class is unaffected by the corrosion loss of material, and (b) sections that change from plastic or compact to semi-compact during their service life. The results for five beams together with the detail of the sections are given in Figure 5.6.

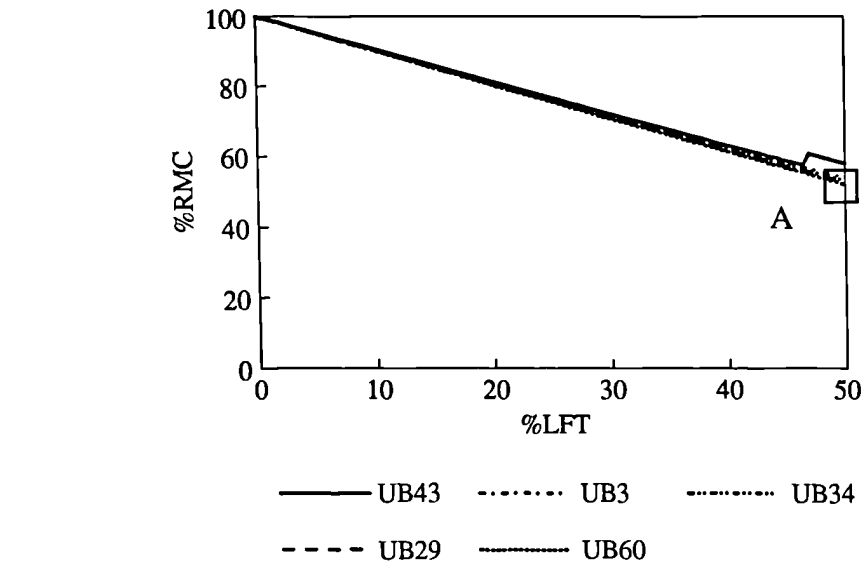

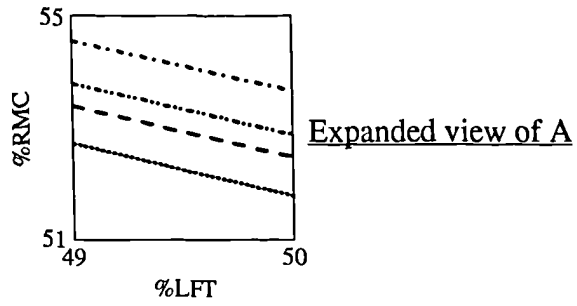

No.	Section	x
UB43	406x140 UB 46	38.8
UB3	914x305 UB 289	31.9
UB34	457x152 UB 82	27.3
UB29	457x191 UB 98	25.8
UB60	254x146 UB 43	21.1

Figure 5.6 Behaviour of %RMC of sections with the lowest value of x from five families

Figure 5.6 shows that, for the case of high shear load, the section with the lowest value of x (UB60) gives a single minimum curve for the %RMC of plastic and compact sections which remain in the same class even in their corroded states, and sections that are plastic or compact in their as-new condition and become semi-compact. This is because a reduced plastic moment of resistance was used for plastic and compact sections with high shear load. This causes a sudden rise in the %RMC curves when sections change from plastic or compact to semi-compact as shown in Figure 5.5.

5.4.3 Minimum curves

It was shown by the accurate assessment method that, it is possible to obtain minimum curves that can be used to estimate the %RMC of corrosion damaged beams with considerable accuracy. By taking into account the effect of corrosion on the moment capacity and the class of a section, three minimum curves were obtained using the results in Figures 5.2, 5.3, 5.4 and 5.6, and are given in Figure 5.7 for the cases of:

1. Sections that are plastic, compact or semi-compact in both their as-new and corrosion damaged conditions with any shear load.
2. Sections that are plastic or compact in their as-new condition and become semi-compact due to corrosion with low shear load.
3. Sections that are plastic or compact in their as-new condition and become semi-compact due to corrosion with high shear load.
4. Sections that are semi-compact in their as-new condition and become slender due to corrosion with any shear load.

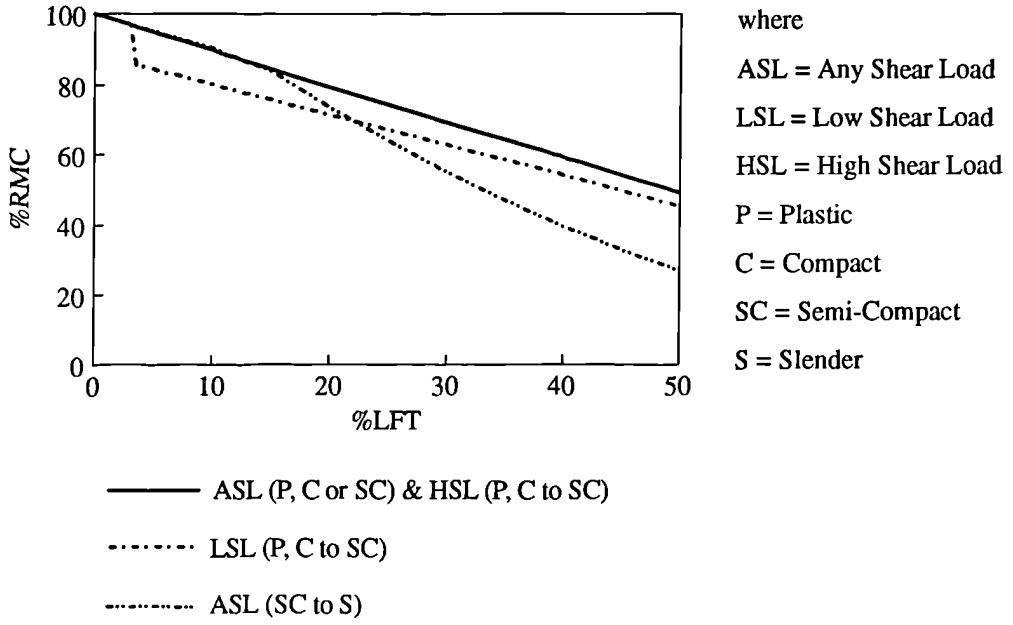

Figure 5.7a Minimum curves to estimate the %RMC of corrosion damaged beams with uniform thickness loss

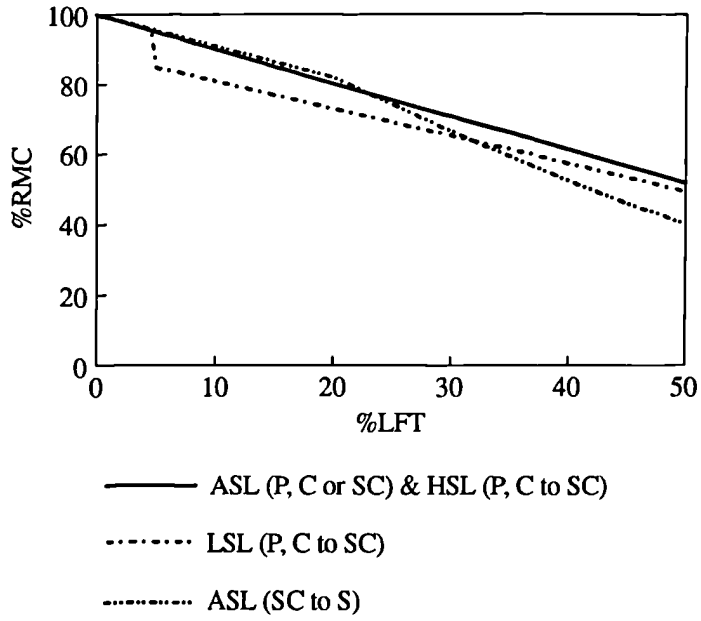

Figure 5.7b Minimum curves to estimate the %RMC of corrosion damaged beams with varying thickness loss

These minimum curves may be used with the information on the loss of thickness of the sections to estimate the percentage remaining moment capacity of corrosion damaged sections. For sections that change from one class to another, the minimum curves may be used in the following manner:

1. For sections with low shear loads, and that change from plastic or compact to semi-compact due to corrosion, the minimum curve 'ASL (P, C or SC)' may be used when sections are plastic or compact, and the minimum curve 'LSL (P, C to SC)' may be used when sections become semi-compact.
2. For sections with any shear loads, and that change from semi-compact to slender due to corrosion, the minimum curve 'ASL (P, C or SC)' may be used when sections are semi-compact, and the minimum curve 'ASL (SC to S)' may be used when sections become slender.

5.5 Assessment methods for Shear Capacity

Corrosion in the web and flanges leads to reduction in shear capacity. In addition, the class of a section may be changed from one to another as was discussed in Section 4.2.3.3. This may change the failure mode of the web from plastic yielding to shear buckling. If webs of corrosion damaged beams vary in thickness significantly, the shear capacity should be calculated from first principles assuming elastic behaviour. In sections where the variation in the web thickness due to corrosion is small, average web thickness may be used for evaluating the shear capacity. The theory given in Section 3.3 was used for the evaluation of remaining shear capacity of corrosion damaged beams.

The shear stresses in many structural steel members are transmitted by unstiffened webs, for which the aspect ratio, a_S/d, can be taken as large or infinity. For such cases, it was shown in Section 3.3.1 that:

if	$\lambda_w = 0.8$	then	$d/t = 62.3\varepsilon$
and if	$\lambda_w = 1.25$	then	$d/t = 97.3\varepsilon$

Taking into account that corrosion may change the class of a section, three categories of sections in terms of d/t ratio are considered for the development of assessment methods for the remaining shear capacity. The three categories are given below:

1. Category 1

   $d/t \leq 63\varepsilon$ and $q_{cr} = 0.6p_{yw}$

2. Category 2

   $63\varepsilon < d/t < 98\varepsilon$ and $q_{cr} = 0.6p_{yw}[1 - 0.8(\lambda_w - 0.8)]$

3. Category 3

   $d/t \geq 98\varepsilon$ and $q_{cr} = q_e$

The aim now is to obtain minimum curves to estimate the percentage remaining shear capacity (%RSC) of corrosion damaged beams. These minimum curves can be obtained by identifying the worst cases.

5.5.1 Shear capacity with tension field action

The shear strength of a web taking account of tension field action [Porter et al 1975] was given in Chapter 3. It is evident from Equations 3.20 and 3.22 (i.e. equations for the shear capacity of a web using tension field action) that the aspect ratio, a_S/d, is one of the major factors that governs the basic web capacity and tension field strength. In order to obtain minimum curves, the worst possible case can be taken as when no stiffener is provided. Therefore, when a_S/d becomes large or infinity, Equation 3.20 (i.e. equation for basic web capacity using tension field strength) reduces to:

$$q_b = q_{cr}$$

where q_{cr} is the shear capacity without tension field action.

The equations for the contribution of flanges (Equations 3.23a and 3.23b) show that when a_S/d becomes large or infinity, the contribution also becomes negligible. Therefore, it is not necessary to consider the case of shear capacity with tension field action to obtain minimum curves for the remaining shear capacity of corrosion damaged I-beams. Only the case of shear capacity without tension field action will be considered.

5.5.2 Simple assessment method for uniform thickness loss model sections

5.5.2.1 Category of section unchanged by corrosion

A) Category 1: $d/t \leq 63\varepsilon$

Although corrosion reduces the thickness of a web, some sections that have the lowest value of d/t in their as-new condition and hence Category 1 may remain in the same category even after damaged by corrosion. For Category 1 sections, the shear capacity, P_v, is given by:

$$P_{vC} = 0.6p_yA_{vC} \quad \text{for corrosion damaged sections} \quad (5.54a)$$

$$P_{vN} = 0.6p_yA_{vN} \quad \text{for as-new sections} \quad (5.54b)$$

where A_v is the shear area taken as follows:

$A_v = Dt$ for rolled I-sections, and

$A_v = dt$ for welded I-sections.

The percentage remaining shear capacity (%RSC) of any corrosion damaged beam, which is the ratio of the capacity of the corrosion damaged beam (P_{vC}) to the capacity of the as-new beam (P_{vN}), may be expressed as:

$$\%RSC = 100\,(P_{vC}/P_{vN}) \tag{5.55}$$

For a corrosion damaged I-beam, the magnitudes of depths, D, and d, can be taken as constant throughout its service life. Substituting Equations 5.54a and 5.54b into Equation 5.55 gives the following relation for the %RSC,

$$\%RSC = 100\,(t_C/t_N) \tag{5.56}$$

where

t_N is the web thickness of the beam in its as-new condition and

t_C is the web thickness of the corrosion damaged beam.

It should be noted that the design strength of the material has no effect on the %RSC of Category 1 sections as can be seen from Equation 5.56. The equation for the %RSC (Equation 5.56) may be written as follows:

$$\%RSC = 100\left(1 - \frac{t_N - t_C}{t_N}\right)$$

$$\therefore \quad \%RSC = 100\,(1 - \xi_W) \tag{5.57}$$

where

$\xi_W = \%LWT/100$, and

%LWT is the percentage loss of web thickness.

The %RSC (Equation 5.56) is a function of ξ_w alone. Therefore, Equation 5.56 may be used as the minimum curve for estimating the %RSC of any corrosion damaged sections that are Category 1 in both their as-new and corrosion damaged conditions. The estimates from the above equation will be almost exact for all the available I-sections.

B) Category 2: $63\varepsilon < d/t < 98\varepsilon$

Although corrosion reduces the thickness of a web, some sections that fall into Category 2 in their as new-condition may remain the same for part or all of their service life. For such sections, the shear capacity, P_v, is given by:

$$P_{vC} = 0.6 p_{yw} \phi_C A_{vC} \quad \text{for corrosion damaged sections} \qquad (5.58a)$$

$$P_{vN} = 0.6 p_{yw} \phi_N A_{vN} \quad \text{for as-new sections} \qquad (5.58b)$$

where

$$\phi = [1 - 0.8(\lambda_w - 0.8)] \qquad (5.59)$$

and A_v is as described in Section 5.5.2.1.A.

If it is assumed that the depths, D, and d, of corrosion damaged sections remain constant throughout their service life, and Equations 5.58a and 5.58b are combined with Equation 5.55, then the %RSC of Category 2 sections is obtained as:

$$\%RSC = 100\left(\frac{\phi_C}{\phi_N}\right)\left(\frac{t_C}{t_N}\right) \qquad (5.60)$$

Alternatively, using Equation 5.57, the above equation can be modified to give,

$$\%RSC = 100\left(\frac{\phi_C}{\phi_N}\right)(1 - \xi_W) \qquad (5.61)$$

In this case, the %RSC depends on both ξ_w and the ratio ϕ_C/ϕ_N. In order to obtain the minimum of %RSC given by Equation 5.61, the minimum of the ratio ϕ_C/ϕ_N must be obtained. Using Equation 5.59, the ratio ϕ_C/ϕ_N may be written as:

$$\frac{\phi_C}{\phi_N} = \frac{1-0.8(\lambda_{wC}-0.8)}{1-0.8(\lambda_{wN}-0.8)} \qquad (5.62)$$

where λ_w is the web slenderness factor and is given by (see Section 3.3.1):

$$\lambda_w = \frac{(0.6p_y)^{1/2}}{995.0}\frac{d}{t} \qquad (5.63a)$$

Assuming that d is constant, substituting Equation 5.1b into Equation 5.63a gives,

$$\lambda_{wC} = \frac{(0.6p_y)^{1/2}}{995.0}\frac{d}{t_N(1-\xi_w)} = \frac{\lambda_{wN}}{1-\xi_w} \qquad (5.63b)$$

Now, substituting Equation 5.63b into Equation 5.62, gives the following expression for the ratio ϕ_C/ϕ_N,

$$\frac{\phi_C}{\phi_N} = \frac{\frac{2.05}{\lambda_{wN}} - \frac{1}{1-\xi_w}}{\frac{2.05}{\lambda_{wN}} - 1} \qquad (5.64)$$

Equation 5.64 shows that, for a given value of ξ, when the value of λ_{wN} increases, the value of ϕ_C/ϕ_N decreases. Hence, for the minimum value of ϕ_C/ϕ_N, λ_{wN} must be maximum which can be obtained for the maximum values of p_y and d/t_N (see Equation 5.63a). The possible maximum values of p_y and d/t_N of Category 2 sections are:

$\text{Max}(p_y) = 450\ \text{N/mm}^2$ and
$\text{Max}(d/t_N) = 57.1$ for section UB44 (406×140 UB 39)

If the above maximum values are substituted into Equation 5.63a, then the possible maximum value of λ_{wN} is obtained as:

$$\text{Max}(\lambda_{wN}) = 0.943 \qquad (5.65)$$

Combining 5.64 and 5.65 gives the minimum of ϕ_C/ϕ_N as:

$$\text{Min}\left(\frac{\phi_C}{\phi_N}\right) = 1.85 - \frac{0.85}{1-\xi_W} \qquad (5.66)$$

Now, if Equations 5.61 and 5.66 are combined, the following relation is obtained for the minimum of %RSC of Category 2 sections,

$$\text{Min}(\%RSC) = 100\,(1 - 1.85\xi_W) \qquad (5.67)$$

Therefore, Equation 5.67 may be used as the minimum curve to estimate the %RSC of any corrosion damaged sections that are Category 2 in their as-new condition and remain in this category even in their corroded states. The estimates will be conservative for some sections since Equation 5.67 was derived for the worst combinations of p_y and d/t.

C) Category 3: $d/t \geq 98\varepsilon$

Plate girders that have the highest value of d/t may fall into Category 3 in their as-new condition. For Category 3 beams, the shear buckling capacity, P_v, is given by:

$P_{vC} = q_{eC}A_{vC}$ for corrosion damaged sections (5.68a)

$P_{vN} = q_{eN}A_{vN}$ for as-new sections (5.68b)

where q_e is the shear buckling stress given by Equation 3.12 and $A_v = dt$.

Substituting $a_S/d = \infty$ (for minimum q_e) into Equation 3.12b gives the shear buckling stress of Category 3 sections as:

$$q_e = \left(\frac{995.0}{d}\right)^2 t^2 \qquad (5.69)$$

Assuming that the beam depth, d, remains constant for all of its service life, combining Equations 5.68a and 5.68b with Equation 5.55 gives the %RSC of Category 3 beams as:

$$\%RSC = 100\left(\frac{t_C}{t_N}\right)^3 \tag{5.70}$$

The above equation for the %RSC may also be written as:

$$\%RSC = 100\left(1-\xi_W\right)^3 \tag{5.71}$$

The %RSC of Category 3 sections is a function of ξ_W alone. Therefore, Equation 5.71 may be used as the minimum curve for estimating the %RSC of any corrosion damaged sections that are Category 3 in both their as-new and corrosion damaged conditions. The above equation will give almost exact estimates of the %RSC for all the sections.

5.5.2.2 Category of section changed by corrosion

A) Category 1 to Category 2 to Category 3

Some sections that are Category 1 in their as-new condition may become Category 2 and then Category 3 during their service life due to loss of thickness in the web. When sections are Category 1, Equation 5.57 may be used as the minimum curve for estimating the %RSC as suggested before.

Let us first consider the case in which the sections become Category 2 due to corrosion. When they become Category 2, using Equations 5.54b and 5.58a together with Equation 5.55, the %RSC may be given by:

$$\%RSC = 100\,\phi_C(1-\xi_W) \tag{5.72}$$

where

$$\phi_C = 1 - 0.8(\lambda_{wC} - 0.8) \tag{5.73}$$

For obtaining the minimum of %RSC given by Equation 5.72, the minimum of ϕ_C must be obtained. Combining Equations 5.63b and 5.73 gives,

$$\phi_C = 1.64 - \frac{0.8\lambda_{wN}}{1-\xi_w} \quad (5.74)$$

For a given ξ_w, the minimum value of ϕ_C can be obtained for the maximum value of λ_{wN}. As in the previous section, the maximum value of λ_{wN} is obtained for the maximum values of p_y and d/t_N. The possible maximum values of p_y and d/t_N for sections that are Category 1 in their as-new condition are as follows:

$\text{Max}(p_y) = 334\ \text{N/mm}^2$ and
$\text{Max}(d/t_N) = 57.1$ for section UB44

Note: If $p_y > 334\ \text{N/mm}^2$, the section, UB44, is Category 2 in its as new condition.

Using the above values, the possible maximum value of λ_{wN} is obtained as:

$$\text{Max}(\lambda_{wN}) = 0.81 \quad (5.75)$$

Substituting Equation 5.75 into Equation 5.74 gives the minimum of ϕ_C as:

$$\text{Min}(\phi_C) = 1.64 - \frac{0.64}{1-\xi_w} \quad (5.76)$$

Now, if Equations 5.72 and 5.76 are combined, then the following relation is obtained for the minimum of %RSC of Category 2 sections that were originally Category 1 in their as-new condition,

$$\text{Min}(\%\text{RSC}) = 100\,(1 - 1.64\xi_w) \quad (5.77)$$

Therefore, when a corrosion damaged section that is Category 1 in its as-new condition becomes Category 2, Equation 5.77 may be used for estimating the %RSC. This equation will give conservative estimates for some sections since it was derived for the worst combinations of p_y and d/t ratio.

Now, let us consider the case in which the sections become Category 3 due to corrosion. When they become Category 3, using Equations 5.54b and 5.68a together with Equation 5.55, the %RSC may be given as:

$$\%RSC = \frac{100}{\lambda_{wN}^2}(1-\xi_w)^3 \qquad (5.78)$$

For the minimum of %RSC given by Equation 5.78, the value of λ_{wN}^2 must be maximum. The maximum value of λ_{wN} was obtained as 0.81 (see Equation 5.75), which gives the maximum value of λ_{wN}^2 as 0.66.

If the maximum value of λ_{wN}^2 is substituted into Equation 5.78, the minimum of %RSC of Category 3 sections which were Category 1 in their as-new condition is obtained as:

$$\text{Min}(\%RSC) = 152\,(1-\xi_w)^3 \qquad (5.79)$$

Therefore, when a corrosion damaged section that is Category 1 in its as-new condition becomes Category 3, Equation 5.79 may be used as the minimum curve for estimating the %RSC. As Equation 5.79 was derived for the worst combinations of p_y and d/t, the estimates will be conservative for some sections.

B) Category 2 to Category 3

Some sections that are Category 2 in their as-new condition may become Category 3 due to loss of thickness in the web. When corrosion damaged sections are Category 2, Equation 5.67 may be used as the minimum curve for estimating the %RSC as before.

When they become Category 3, substituting Equations 5.58b and 5.68a into Equation 5.55, gives the %RSC as:

$$\%RSC = \frac{100}{\lambda_{wN}^2 \phi_N}(1-\xi_w)^3 \qquad (5.80)$$

where the term $\lambda_{wN}^2 \phi_N$ may be given by:

$$\lambda_{wN}^2 \phi_N = \lambda_{wN}^2 (1.64 - 0.8\lambda_{wN}) \quad (5.81)$$

In order to obtain the minimum of %RSC given by Equation 5.80, the maximum value of $\lambda_{wN}^2 \phi_N$ must be obtained. Equation 5.81 shows that when the value of λ_{wN} increases, the value of $\lambda_{wN}^2 \phi_N$ also increases. Therefore for the maximum value of $\lambda_{wN}^2 \phi_N$, λ_{wN} must be maximum. For sections that are Category 2 in their as-new condition, the maximum value of λ_{wN} was obtained as 0.943 (see Equation 5.65). Using the above value, the maximum value of $\lambda_{wN}^2 \phi_N$ is obtained as:

$$\text{Max}(\lambda_{wN}^2 \phi_N) = 0.79 \quad (5.82)$$

Now, substituting Equation 5.82 into Equation 5.80 gives the minimum of %RSC of Category 3 sections that were originally Category 2 in their as new condition as:

$$\text{Min}(\%\text{RSC}) = 127 \left(1 - \xi_W\right)^3 \quad (5.83)$$

Therefore, when a corrosion damaged section that is Category 2 in its as-new condition becomes Category 3, Equation 5.83 can be used as the minimum curve for estimating the %RSC. The estimates will be conservative for some sections as Equation 5.83 was obtained for the worst possible case.

5.5.3 Accurate assessment method

5.5.3.1 Effect of design strength on %RSC

It was found that the %RSC of a Category 1 section does not depend on the design strength of the material (see Section 5.5.2.1.A). When d/t exceeds 63ε, i.e. Category 2 and 3 sections, the design strength has an effect on the %RSC (see Section 5.5.2.2). In order to verify the effect of design strength on the %RSC of corrosion damaged beams

when $d/t > 63\varepsilon$, a universal beam, UB16, with varying thickness loss was analysed. The beam was assigned four values of design strength (from 245.0 to 450.0 N/mm^2). The length of the beam was taken as $L_E/D = 30$. The results of the analysis and the detail of the section are given in Figure 5.8.

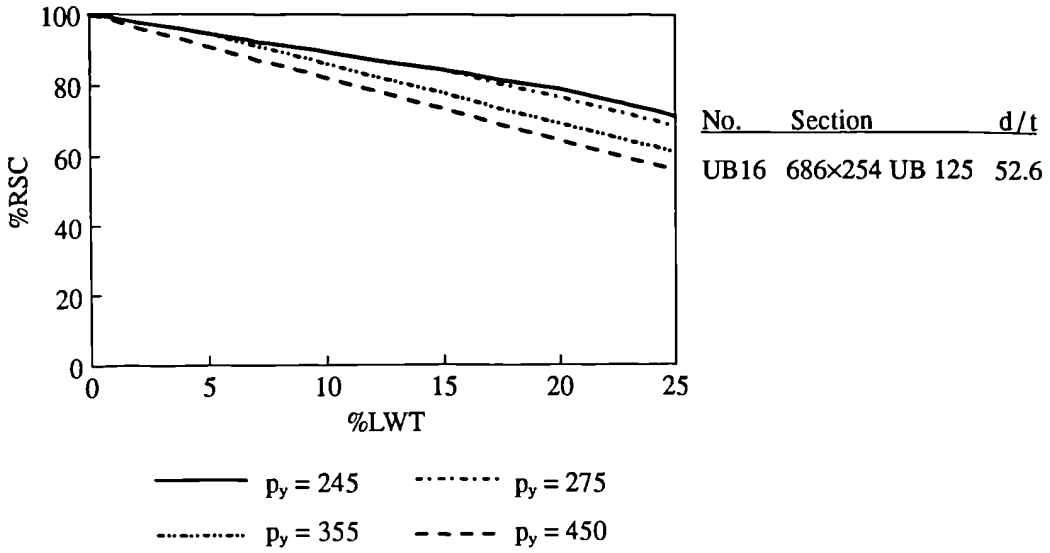

Figure 5.8 Effect of design strength on the %RSC of a corrosion damaged I-beam

It can be seen from Figure 5.8 that the effect of design strength on the %RSC of a corrosion damaged beam, when $d/t > 63\varepsilon$, is quite considerable. When the design strength increases, the %RSC of the section decreases. The highest value of the design strength gives the lowest %RSC of the section.

5.5.3.2 %RSC with tension field action

An I-section, UB44, with varying thickness loss was analysed to compare the %RSC of corrosion damaged beams taking account of tension field action and without tension field action. In both cases two stiffener spacings ($a_S = L$ and $a_S = L/10$) were used. Since the method that involves taking account of tension field action is applicable to sections with $d/t > 63\varepsilon$, the design strength was chosen such that the section is Category 2 in its as-new condition. The results are given in Figure 5.9.

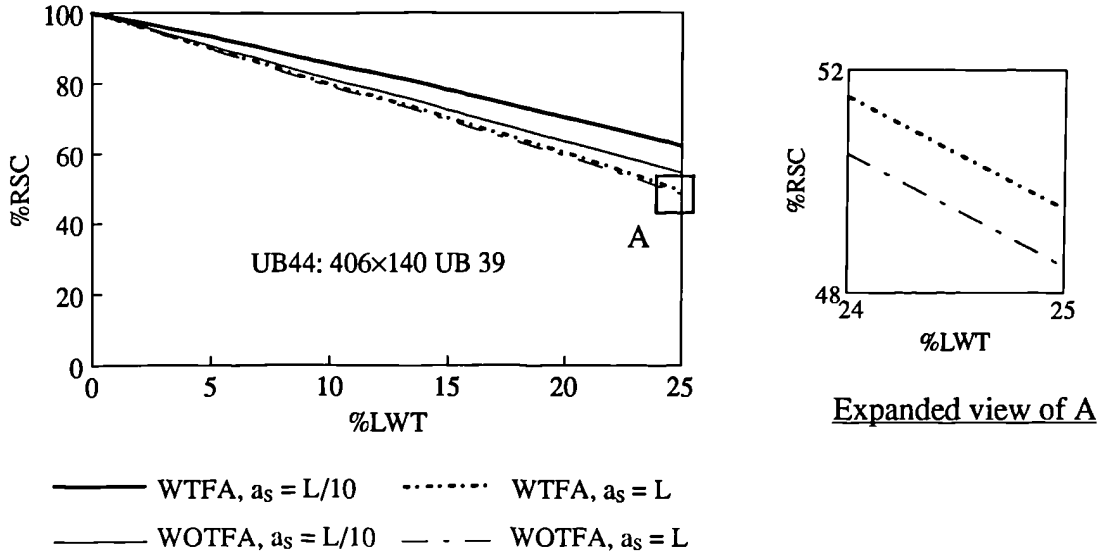

where WTFA = With Tension Field Action, and WOTFA = Without Tension Field Action

Figure 5.9 Comparison of the %RSC of a corrosion damaged I-beam with and without tension field action

It is evident from Figure 5.9 that when the stiffener spacing is large, the variation between the %RSC with and without using tension field action is quite small. When the stiffener spacing is small, the variation becomes large. However, in both cases, the lowest %RSC is obtained without using tension field action. Therefore, when obtaining minimum curves for the assessment of remaining shear capacity, it is not necessary to consider tension field action.

5.5.3.3 %RSC of uniform thickness loss model sections

A) Behaviour of %RSC of a family of sections

A family of sections was analysed first to study the behaviour of %RSC of corrosion damaged beams that are (a) Category 1 in their as-new condition and remain in this category throughout or for part of their service life, and (b) Category 1 in their as-new condition and become Category 2 due to corrosion during their service life. The family and the design strength were chosen such that the sections change category from Category 1 to Category 2. The results and the detail of the family of sections are given in Figure 5.10.

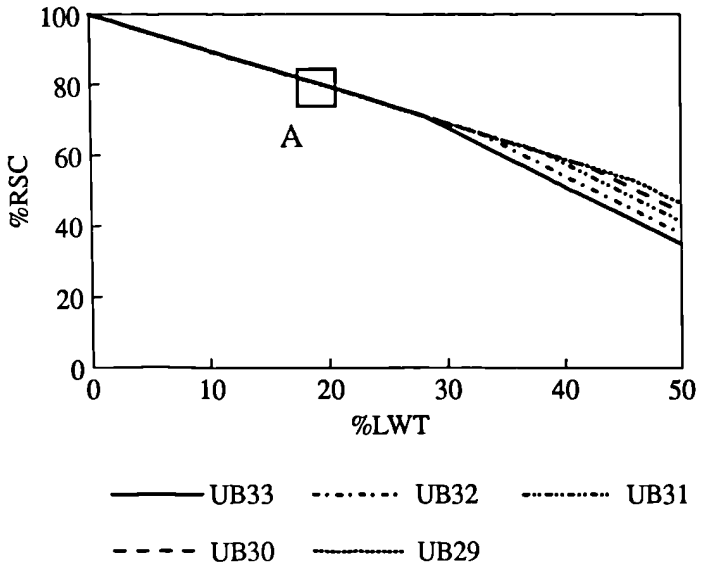

For uniform thickness loss model sections,

$\xi = \xi_F = \xi_W$

where

ξ_F = %LFT / 100,

ξ_W = %LWT / 100,

LFT = Loss of Flange Thickness, and

LWT = Loss of Web Thickness.

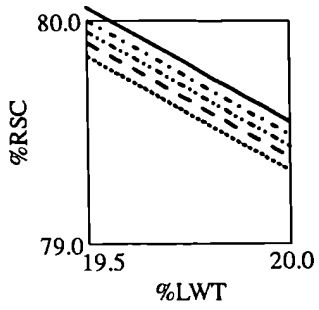

Expanded view of A

No.	Section	d/t
UB29	457×191 UB 98	35.8
UB30	457×191 UB 89	38.5
UB31	457×191 UB 82	41.2
UB32	457×191 UB 74	44.8
UB33	457×191 UB 67	48.0

Figure 5.10 Behaviour of %RSC of a family of sections with uniform thickness loss

Figure 5.10 shows (for web thickness loss of 0-20%) that the %RSC curves of Category 1 sections, whose category is unchanged by the loss of material due to corrosion, are straight lines with a slope of approximately -1.0 as predicted earlier. The section with the lowest value of d/t (UB29) gives the minimum curve for the %RSC of the family of sections when they remain as Category 1. The variation in the %RSC within the family is negligible (less than 1.0% when the web thickness loss is 20%).

When the category of a section changes from Category 1 to Category 2 (e.g. UB32), the rate of reduction in the %RSC increases, i.e. the slope is increased. The section with the highest value of d/t (UB33) gives the minimum curve for the family when the category of sections becomes Category 2. The section with the highest value of d/t was also found to give minimum curves for families of sections that are (a) Category 1 in their as-new condition and become Category 2 and then Category 3, (b) Category 2 in their as-

new condition and remain in the same category even after corrosion, and (c) Category 2 in their as-new condition and become Category 3 during their service life.

B) Category 1

Based on the above observations, all the sections with the lowest value of d/t ratio from each of the families were analysed to obtain a minimum curve for the %RSC of whole range of sections that are Category 1 in both their as-new and corrosion damaged conditions. The results for five beams together with the detail of the sections are given in Figure 5.11.

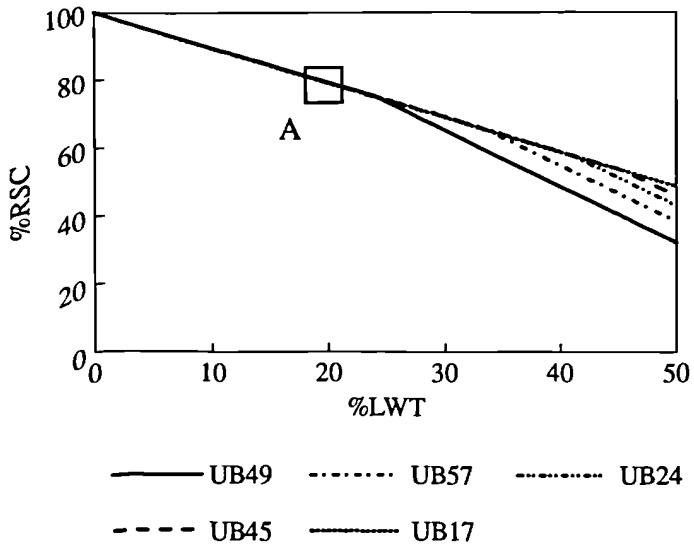

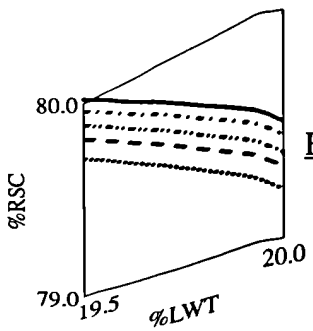

Expanded view of A

No.	Section	d/t
UB49	356x127 UB 39	47.9
UB57	305x102 UB 33	41.8
UB24	533x210 UB 122	37.2
UB45	356x171 UB 67	34.3
UB17	610x305 UB 238	28.9

Figure 5.11 Behaviour of %RSC of Category 1 sections from five families

It is evident from Figure 5.11 (for web thickness loss of 0-20%) that the section with the lowest value of d/t ratio (UB17) gives the minimum curve for the %RSC of whole range

of Category 1 sections which remain in this category even after damaged by corrosion. As predicted earlier, the minimum curve is a straight line with a slope of approximately -1.0. The variation in the %RSC of beams that have the maximum and minimum values of d/t ratio is negligible (less than 0.5% when the percentage loss of web thickness is 20.0%).

C) Category 1 to Category 2 and then to Category 3

Sections that have the highest value of d/t from each of the families were analysed to obtain a minimum curve for the %RSC of sections that are Category 1 in their as-new condition and become Category 2 and then Category 3 due to corrosion during their service life. The design strength of the sections was chosen such that the design strength is maximum to give the minimum of %RSC (see Section 5.5.3.1) and the sections are Category 1 in their as-new condition. The results for five beams together with the detail of the sections are given in Figure 5.12.

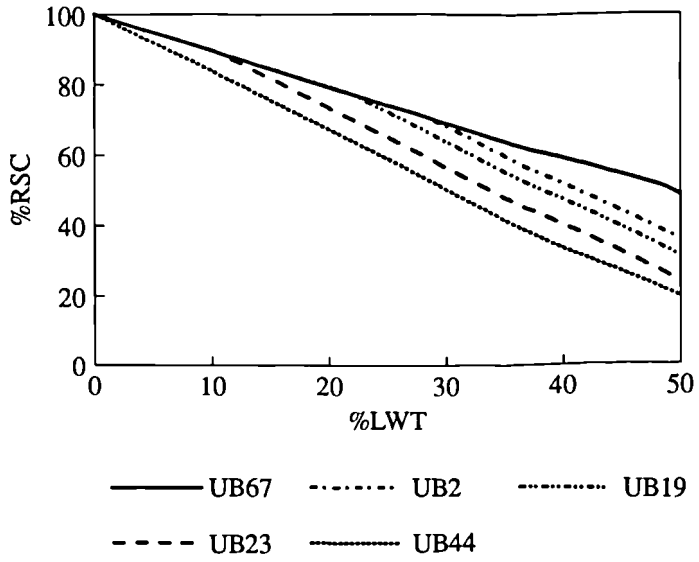

No.	Section	d/t
UB67	203×133 UB 25	29.7
UB2	914×419 UB 343	41.2
UB19	610×305 UB 149	45.1
UB23	610×229 UB 101	51.6
UB44	406×140 UB 39	57.1

Figure 5.12 Behaviour of %RSC of sections that change from Category 1 to Category 3 from five families ($p_y = 334\ N/mm^2$)

It can be seen from Figure 5.12 that the section with the highest value of d/t (UB44) gives the minimum curve for whole range of sections that are Category 1 in their as-new condition and become Category 2 and then Category 3 during their service life. The

variation in the %RSC of beams with the maximum and minimum values of d/t is quite considerable (more than 20.0% when the thickness loss is 50.0%). It should be noted that the above minimum curve will give very conservative estimates for some sections.

D) Category 2 to Category 3

Sections that have the highest value of d/t from each of the families were analysed to obtain a minimum curve for the %RSC of sections that are Category 2 in their as-new condition and become Category 3 during their service life. The design strength of the sections was chosen such that the sections are Category 2 in their as-new condition and it is maximum to give the minimum value of %RSC (see Section 5.5.3.1). The results for five beams together with the detail of the sections are given in Figure 5.13.

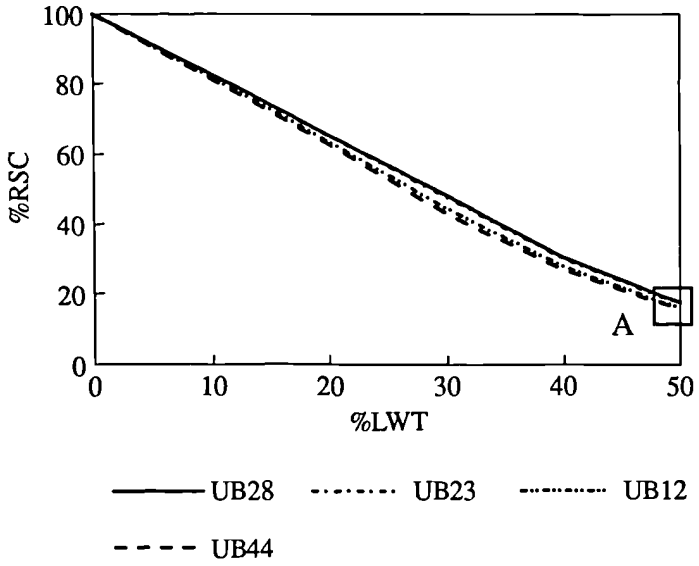

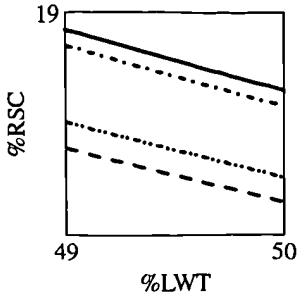

Expanded view of A

No.	Section	d/t
UB28	533x210 UB 82	49.6
UB23	610x229 UB 101	51.6
UB12	762x267 UB 147	53.2
UB44	406x140 UB 39	57.1

Figure 5.13 Behaviour of %RSC of sections that change from Category 2 to Category 3 from five families ($p_y = 450\ N/mm^2$)

It can be seen from Figure 5.13 that when sections become Category 3 the %RSC curves become polynomial as predicted earlier. The figure also shows that the section with the highest value of d/t (UB44) gives the minimum curve for the %RSC of corrosion damaged Category 3 sections which were originally Category 2 in their as-new condition. The variation in the %RSC of beams that have the maximum and minimum of d/t is quite small (less than 3.0% when the web thickness loss is 50.0%).

5.5.3.4 %RSC of varying thickness loss model sections

A) Category 1

The family of sections that was used in Section 5.5.3.3(A) was analysed again to study the behaviour of %RSC of corrosion damaged beams with varying web thickness loss. The results and the detail of the family of sections are given in Figure 5.14.

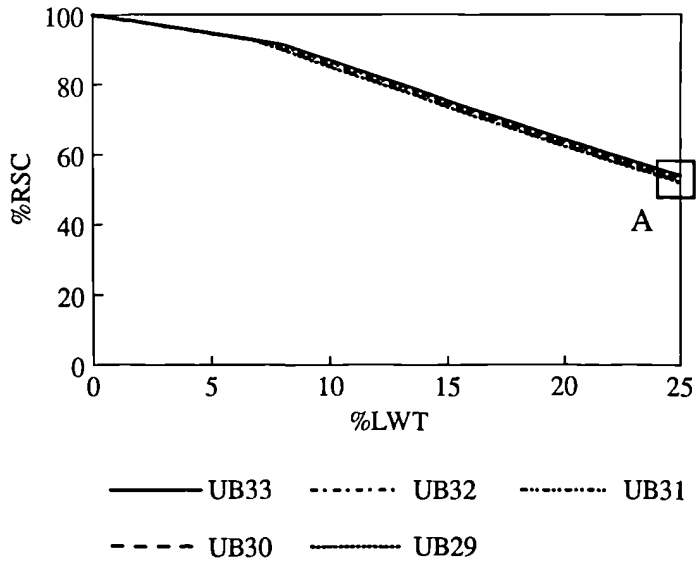

For varying thickness loss model sections,

$\xi = \xi_F = 2\xi_W$

where

ξ_F = %LFT / 100,

ξ_W = %LWT / 100,

LFT = Loss of Flange Thickness, and

LWT = Loss of Web Thickness.

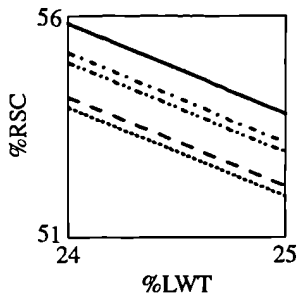

Expanded view of A

No.	Section	d/t
UB29	457×191 UB 98	35.8
UB30	457×191 UB 89	38.5
UB31	457×191 UB 82	41.2
UB32	457×191 UB 74	44.8
UB33	457×191 UB 67	48.0

Figure 5.14 Behaviour of %RSC of a family of sections with varying thickness loss

It is evident from Figure 5.14 that when using varying web thickness the rate of reduction in the %RSC is quite considerable. The section with the lowest value of d/t (UB29) gives the minimum curve for the family. The variation in the %RSC of beams within the family is quite small (less than 3.0% when the thickness loss is 25.0%).

Using the above information, the sections with the lowest value of d/t from each of the families were analysed to obtain a minimum curve for the %RSC of Category 1 sections, whose category is unaffected by the loss of material in the web due to corrosion. The results and the detail of the sections are given in Figure 5.15.

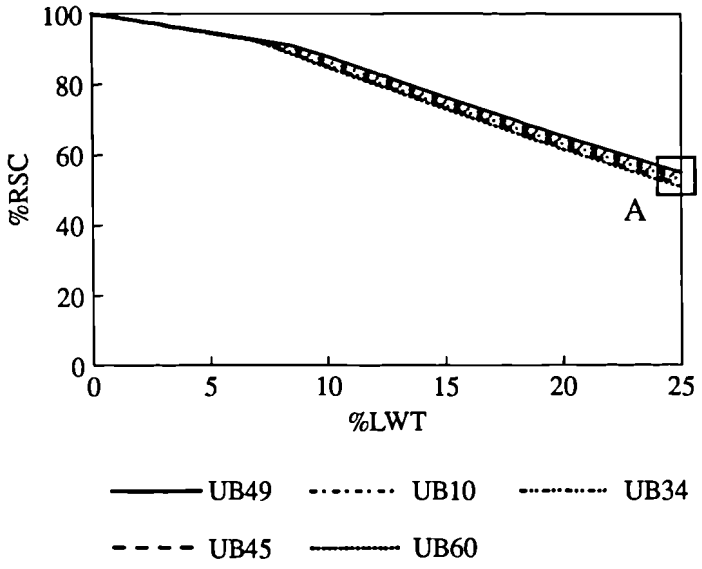

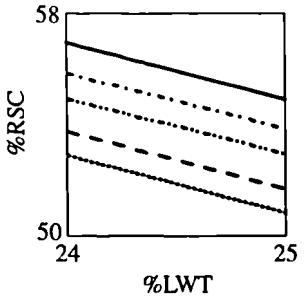

Expanded view of A

No.	Section	d/t
UB49	356×127 UB 39	47.9
UB10	762×267 UB 197	44.0
UB34	457×152 UB 82	38.0
UB45	356×171 UB 67	34.3
UB60	254×146 UB 43	30.0

Figure 5.15 Behaviour of %RSC of Category 1 sections from five families

It can be seen from Figure 5.15 that the section UB60 with a d/t ratio of 30.0 gives the minimum curve for the %RSC of sections that are Category 1 in their as-new condition and remain so even in their corroded states. It should be noted that the d/t ratio of 30.0

is very close to the lowest d/t ratio of 28.9. The rate of reduction in the %RSC is quite considerable. The variation in the %RSC of beams that have the maximum and minimum values of d/t is small (less than 6.0% when the thickness loss is 25.0%).

B) Categories 2 and 3

A family of sections with varying thickness loss was analysed to study the behaviour of %RSC of corrosion damaged beams with $d/t > 63\varepsilon$. The family and the design strength of the sections were chosen such that all the sections are Category 2 in their as-new condition. The results and the detail of the family of sections are given in Figure 5.16.

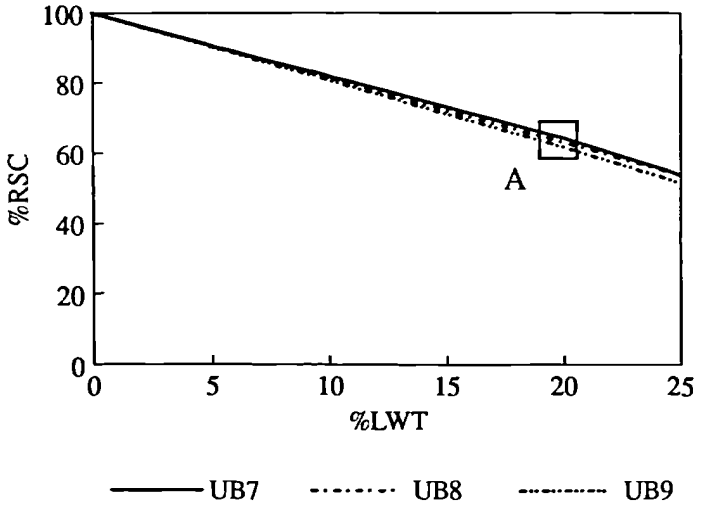

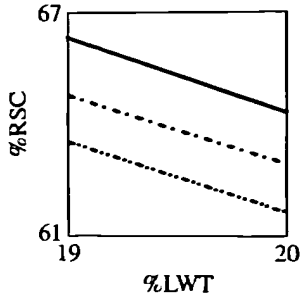

Expanded view of A

No.	Section	d/t
UB7	838x292 UB 226	47.3
UB8	838x292 UB 194	51.8
UB9	838x292 UB 176	54.4

Figure 5.16 Behaviour of %RSC of a family of sections with $d/t > 63\varepsilon$

The section with the highest value of d/t gives the minimum curve for the %RSC of the family of sections with $d/t > 63\varepsilon$ as is evident from Figure 5.16. When using varying web thickness, the rate of reduction in the %RSC is quite considerable.

Using the above information, the sections with the highest value of d/t from each of the families were analysed to obtain a minimum curve for the %RSC of sections that are Category 2 in their as-new condition and remain in this category for all of their service life, and that become Category 3 during their service life. The results and the detail of the sections are given in Figure 5.17 for four beams.

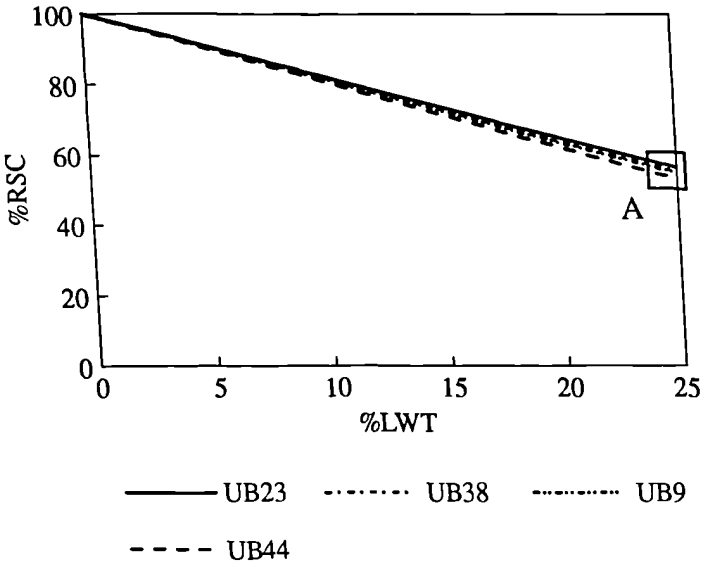

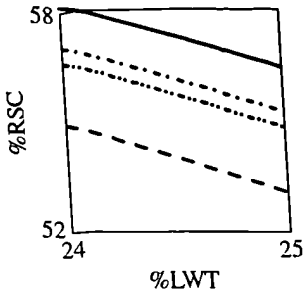

Expanded view of A

No.	Section	d/t
UB23	610×229 UB 101	51.6
UB38	457×152 UB 52	53.6
UB9	838×292 UB 176	54.4
UB44	406×140 UB 39	57.1

Figure 5.17 Behaviour of %RSC of sections from five families with $d/t > 63\varepsilon$

Figure 5.17 shows that the section with the highest value of d/t gives the minimum curve for (a) whole range of sections that are Category 2 in their as-new condition and remain in the same category even after damaged by corrosion, and (b) sections that become Category 3 due to corrosion during their service life. The variation in the %RSC of sections that have the maximum and minimum values of d/t is small (less than 4.0% when the loss of web thickness is 25.0%).

5.5.4 Minimum curves

5.5.4.1 Uniform thickness loss model sections

It was found that the section with the lowest value of d/t (UB17) gives the minimum curve for the %RSC of sections that are Category 1 in both their as-new and corrosion damaged conditions, regardless of their design strength. For a given design strength, the section with the highest value of d/t (UB44) gives the minimum curve for sections that are Category 1 in their as-new condition and become Category 2 and then Category 3, and that are Category 2 in their as-new condition and become Category 3 due to corrosion. The design strength of material was found to influence the %RSC of Category 2 and Category 3 sections. Based on the above findings, minimum curves were obtained and are given in Figure 5.18a for the following cases:

A. Category 1 sections whose category is unaffected by corrosion: (C1),
B. Sections that are Category 1 in their as-new condition and become Category 2 and then Category 3 due to corrosion and $p_y = 245$: (C1 to C3, $p_y = 245$),
C. Sections that are Category 1 in their as-new condition and become Category 2 and then Category 3 during their service life and $p_y \leq 335$: (C1 to C3, $p_y < 335$), and
D. Sections that are Category 2 in both their as-new and corrosion damaged conditions, and that change from Category 2 to Category 3 and $p_y \leq 450$: (C2 to C3, $p_y < 450$).

5.4.4.2 Varying thickness loss model sections

It was shown that the section UB60, which has a d/t value of 30.0, gives the minimum curve for the %RSC of sections that are Category 1 in their as-new condition and remain so for part or all of their service life. The section with the highest value d/t (UB44) gives the minimum curve for the %RSC of sections that are Category 2 in both their as-new and corrosion damaged conditions, and that are Category 2 in their as-new condition and become Category 3 during their service life. It was found that the second minimum curve may be used for the %RSC of sections that change from Category 1 to Category 2 due to corrosion. Using the above findings, minimum curves were obtained and are given in Figure 5.18b for the following cases:

A. Category 1 sections whose category is unaffected by corrosion: (C1), and

B. Sections that are Category 1 in their as-new condition and become Category 2 due to corrosion, Sections that are Category 2 in their as-new condition and remain in this category even after corrosion, and Sections that are Category 2 in their as-new condition and become Category 3 during their service life: (C1 to C2 & C2 to C3).

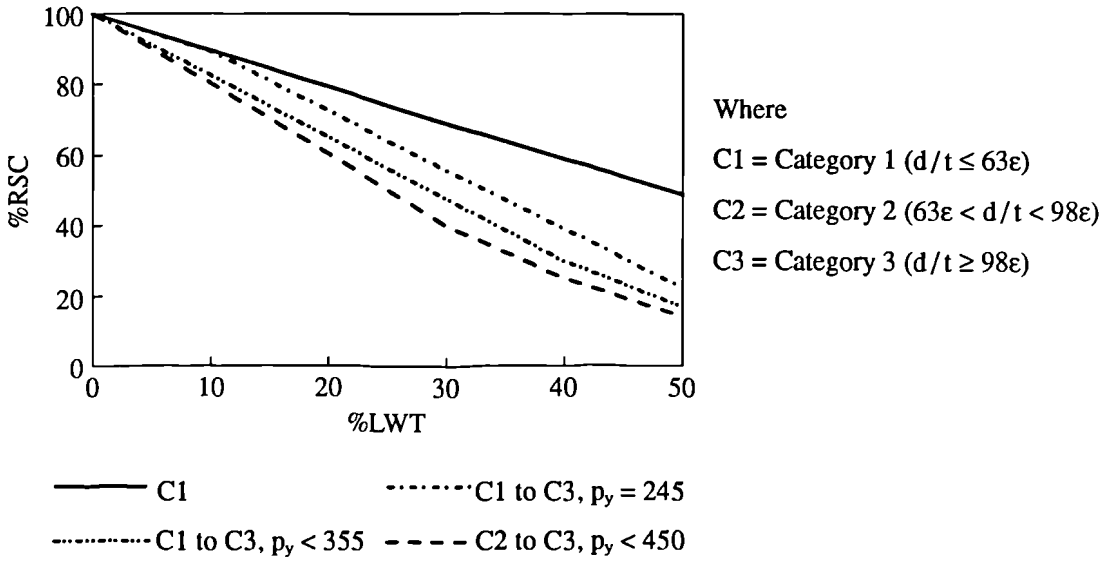

Figure 5.18a Minimum curves for estimating the %RSC of corrosion damaged beams with uniform thickness loss

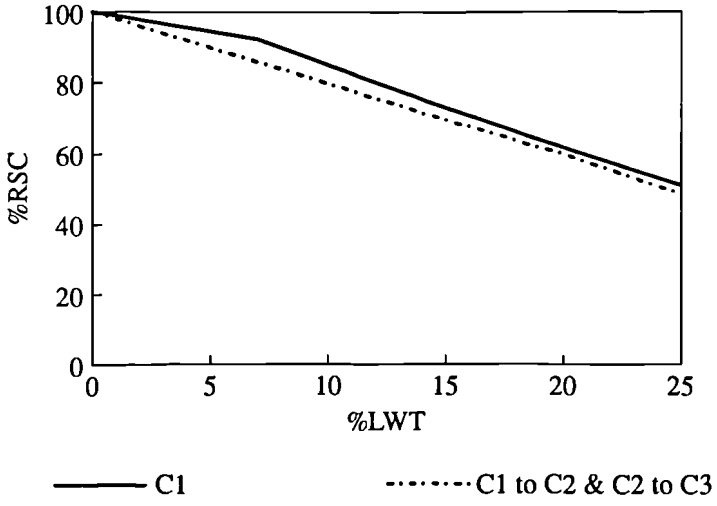

Figure 5.18b Minimum curves for estimating the %RSC of corrosion damaged beams with varying thickness loss

5.6 Assessment methods for Lateral Torsional Buckling Capacity

Loss of thickness in the flanges and web leads to reduction in section properties of steel beams which in turn leads to reduction in lateral torsional buckling capacity. Lateral torsional buckling is a critical failure mode mainly for long span beams that are laterally unrestrained, and short span beams that are laterally unrestrained and coped in the flanges. Several geometric parameters, such as the beam length, end conditions, plastic modulus, lateral stiffness, torsional properties, and the warping resistance of the section influence the lateral torsional buckling capacity of beams. In this work, the theory given in Section 3.4 was used for the evaluation of remaining lateral torsional buckling capacity of corrosion damaged ordinary and coped beams.

5.6.1 Bending strength of a beam

A simplified equation for the bending strength, p_b, of a beam was derived by the writer to verify the influence of some of these factors on the lateral torsional buckling capacity. The equation was derived in terms of the equivalent slenderness factor, λ_{LT}, and material properties, p_y and E, using Equation 3.50, and making a few approximations. The expression is given below:

$$\frac{M_b}{S_x} = p_b \approx \frac{1.022\pi^2 E\left(\lambda_{LT}^2 + \frac{0.007\pi^2 E}{p_y}\lambda_{LT} + \frac{\pi^2 E}{p_y}\left(1-0.0028\left(\frac{\pi^2 E}{p_y}\right)^{1/2}\right)\right)}{\left(\left(\lambda_{LT}^2 + \frac{0.007\pi^2 E}{p_y}\lambda_{LT} + \frac{\pi^2 E}{p_y}\left(1-0.0028\left(\frac{\pi^2 E}{p_y}\right)^{1/2}\right)\right)^2 - \frac{\pi^2 E}{p_y}\lambda_{LT}^2\right)} \quad (5.84)$$

where

$$\lambda_{LT} = nuv\left(\frac{L_E}{r_y}\right) \quad \text{and} \quad (5.85)$$

$$v \text{ is the slenderness factor } = \left(1+\frac{1}{20}\left(\frac{L_E}{r_y x}\right)^2\right)^{-1/4} \quad (5.86)$$

Note: Validity of Equation 5.84

To check the validity of the simplified Equation 5.84, it was evaluated for various values of λ_{LT} and compared with data in Table 11 of BS 5950 [1985]. It was found that Equation 5.84 differs from BS 5950 by only -5.0% to +6.5%. The comparison is shown graphically in Figure 5.19 for two values of design strength (275 and 355 N/mm^2).

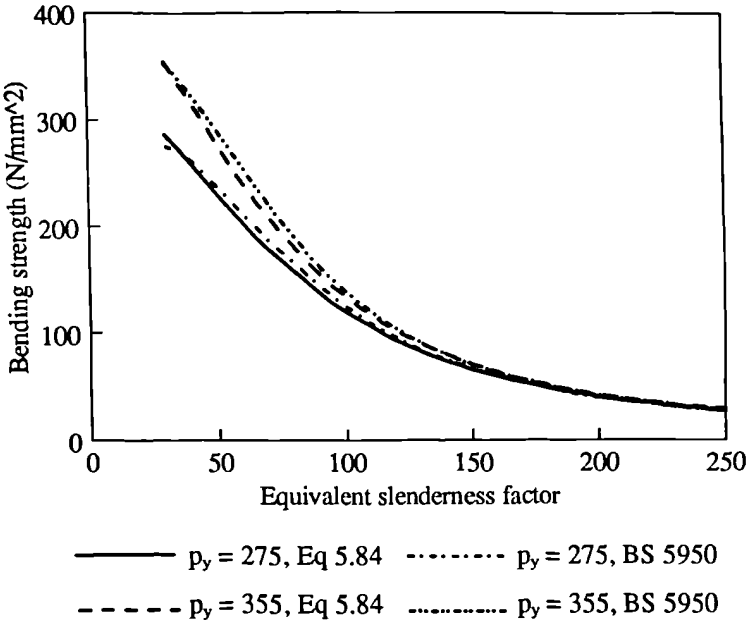

Figure 5.19 Validity of Equation 5.84

5.6.1.1 Critical effective length for maximum bending strength

One of the important factors that governs the lateral torsional buckling capacity of a beam is the effective length of the beam. Therefore this must be taken into account when developing minimum curves for the assessment of remaining lateral torsional buckling capacity. A critical effective length ($L_{E(Crit)}$) for maximum bending strength can be found for any beam at which the bending strength is equal to the design strength, by equating the equivalent slenderness to the limiting equivalent slenderness, λ_{LO}. Using Equations 3.52 and 5.85, a simplified relation is obtained for the critical effective length as:

$$L_{E(Crit)} = 0.408\left(\frac{\pi^2 E}{p_y}\right)^{1/2}\left(\frac{r_y}{u}\right) \qquad (5.87)$$

The above equation may be written in another form as:

$$\frac{L_{E(Crit)}u}{r_y} = 0.408\left(\frac{\pi^2 E}{p_y}\right)^{1/2} = k_1 \text{ (constant for a given } p_y) \qquad (5.88)$$

It follows from Equation 5.88 that,

$$\lambda = \frac{L_{E(Crit)}}{r_y} = \frac{k_1}{u} \qquad (5.89)$$

Using Equations 5.89 and 5.86 together with Equation 5.85, the following expression is obtained for the equivalent slenderness factor,

$$\lambda_{LT} = nk_1\left(1+\frac{1}{20}\left(\frac{k_1}{ux}\right)^2\right)^{1/4} \qquad (5.90)$$

where k_1 is a constant and given by Equation 5.88.

Using Equation 5.90, it can be said that the factors that influence the equivalent slenderness in this case are the torsional index, x, and the buckling parameter, u. Equation 5.84 shows that for a given p_y, the equivalent slenderness is the critical factor that governs the bending strength, p_b, of beams. In summary, x and u are the critical factors that govern the bending strength of beams with critical effective length, $L_{E(Crit)}$, and constant design strength, p_y.

5.6.1.2 Slenderness, λ, is constant

Let us consider a case where the slenderness, λ, and the design strength of the beams are constant.

$$\lambda = \frac{L_E}{r_y} = k_2 \text{ (constant)} \qquad (5.91)$$

Combining Equations 5.91 and 5.86 together with Equation 5.85 gives,

$$\lambda_{LT} = nuk_2\left(1+\frac{1}{20}\left(\frac{k_2}{x}\right)^2\right)^{-1/4} \qquad (5.92)$$

where k_2 is a constant and given by Equation 5.91.

Therefore, for beams which have constant slenderness, λ, and design strength, using Equations 5.92 and 5.84 it can be said that the torsional index, x, and the buckling parameter, u, are the critical factors that govern the bending strength of such beams. It should be noted that the critical parameters are identical to the ones that govern the bending strength of beams with critical effective length.

5.6.1.3 Ratio L_E/D is constant

$$\frac{L_E}{D} = k_3 \quad \text{(constant)} \qquad (5.93)$$

Equation 5.85 can be modified using the following approximations,

$x \approx D/T$ and

$B \approx 4.4r_y$

whence,

$$\lambda_{LT} \approx nu\frac{4.4k_3}{(B/D)}\left(1+\frac{1}{20}\left(\frac{4.4k_3}{2(b/T)}\right)^2\right)^{-1/4} \qquad (5.94)$$

where k_3 is a constant and given by Equation 5.93.

Using Equations 5.94 and 5.84, it can be said that the buckling parameter, u, and the ratios of (b/T) and (B/D) are the critical factors that govern the bending strength of beams with constant (L_E/D) and p_y.

5.6.2 Effect of design strength on the percentage remaining lateral torsional buckling capacity

The simplified equation obtained for the bending strength of a beam (Equation 5.84) shows that the design strength is an important factor on the lateral torsional buckling capacity of a beam. In order to verify the effect of design strength on the percentage remaining lateral torsional buckling capacity (%RLTBC) of corrosion damaged beams, a universal beam, UB60, with varying thickness loss was analysed. The beam was assigned four values of design strength (from 245.0 to 450.0 N/mm^2). The length and the restraint conditions were assumed to be the same in all the cases. The results of the analysis are given in Figure 5.20.

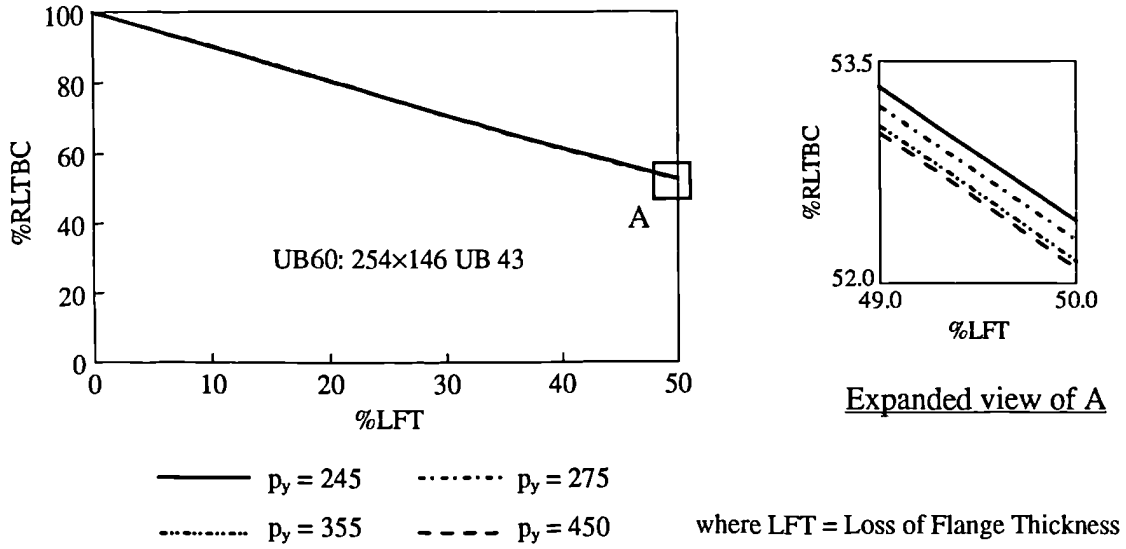

Figure 5.20 Effect of design strength on the %RLTBC of a corrosion damaged beam

It is evident from Figure 5.20 that the variation in the %RLTBC curves for different values of design strength is negligible (less than 0.5% when the flange thickness loss is 50%). When the above analysis was carried out using various span beams, it was found that the above is true for beams of any span. Therefore, the effect of design strength on the %RLTBC need not be considered when developing minimum curves for the %RLTBC of corrosion damaged beams. Any value for the design strength may be used for developing minimum curves.

5.6.3 Short span beams with critical effective length

A family of sections with varying thickness loss was analysed first to study the behaviour of %RLTBC of corrosion damaged short span beams. The effective length of the beams was taken as the critical effective length. The %RLTBC was calculated based on the buckling resistance moment (M_b) of the beams. The detail of the family of sections and the results of the analysis are given in Figure 5.21.

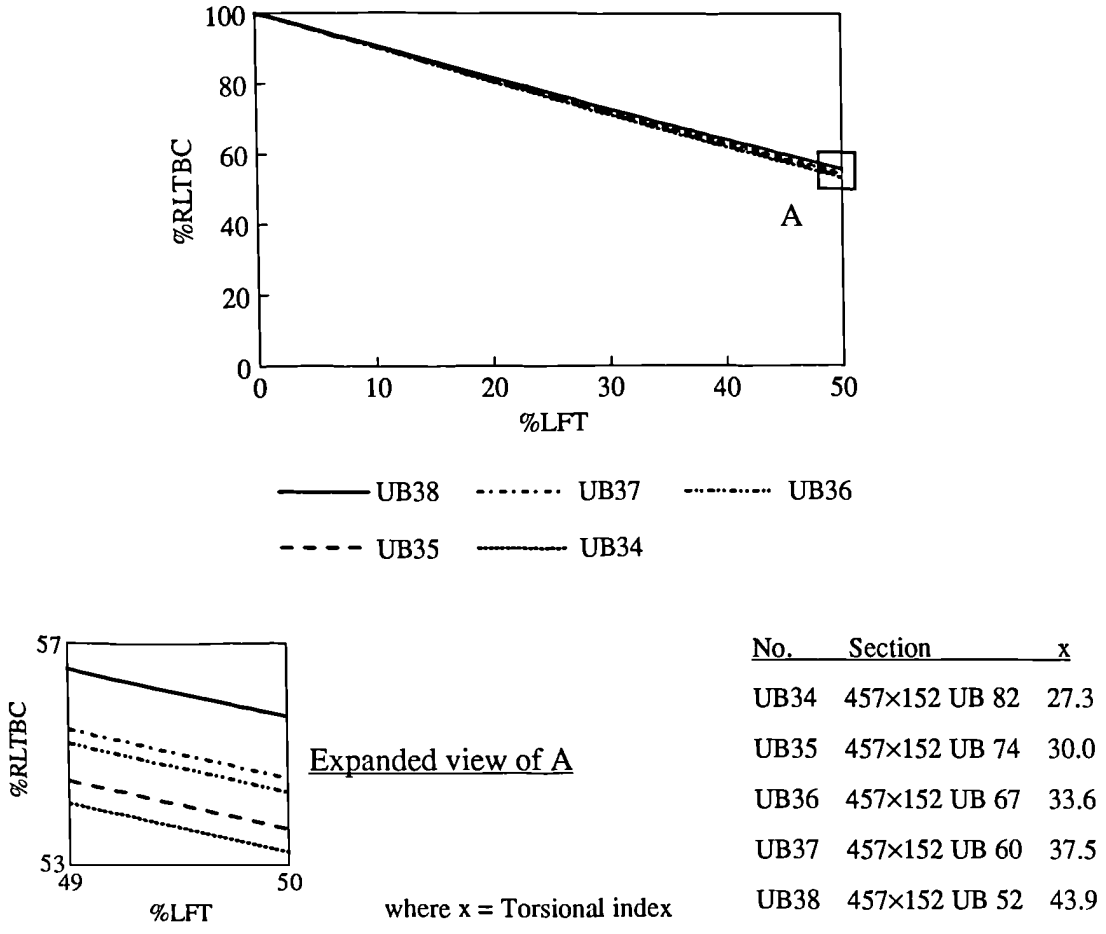

No.	Section	x
UB34	457×152 UB 82	27.3
UB35	457×152 UB 74	30.0
UB36	457×152 UB 67	33.6
UB37	457×152 UB 60	37.5
UB38	457×152 UB 52	43.9

Figure 5.21 Behaviour of %RLTBC of a family of short span beams

Figure 5.21 shows that, for a family of sections with critical effective length, the beam with the lowest value of torsional index, x, (UB34) gives the minimum curve for the family. The %RLTBC curves of these beams are straight lines. For beams with critical effective length, the bending strength is equal to the design strength of the sections and this corresponds to the case of plastic moment capacity of the beams.

Using the above information, all the beams with the lowest value of x from each of the families were analysed to obtain a minimum curve for the %RLTBC of short span beams with critical effective length. The results for five beams and the detail of the sections are given in Figure 5.22.

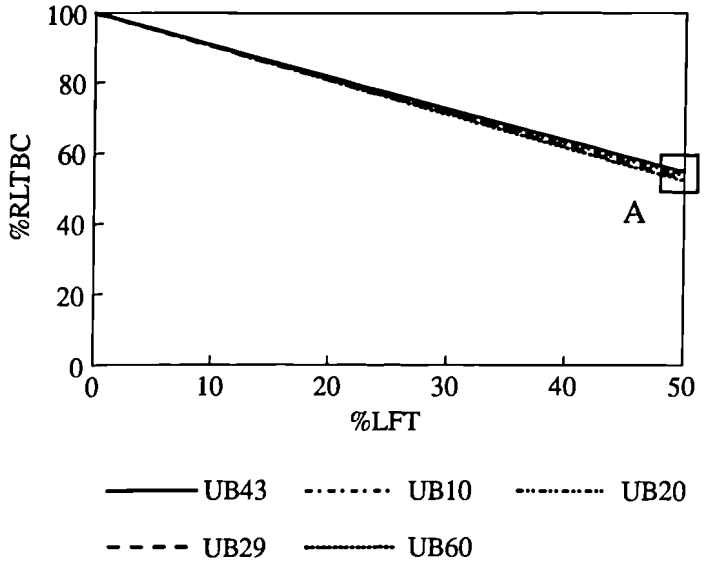

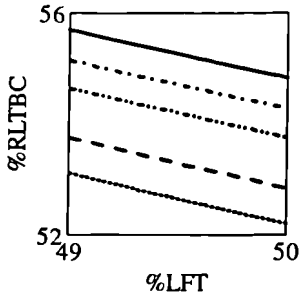

Expanded view of A

No.	Section	x
UB43	406×140 UB 46	38.8
UB10	762×267 UB 197	33.2
UB20	610×229 UB 140	30.5
UB29	457×191 UB 98	25.8
UB60	254×146 UB 43	21.1

Figure 5.22 Behaviour of %RLTBC of short span beams from five families

It can be seen from Figure 5.22 that the beam that has the lowest value of torsional index (UB60) gives the minimum curve for the %RLTBC of whole range of beams with critical effective length. The variation in the %RLTBC curves of beams with the maximum and minimum value of x is quite small (less than 3% when the thickness loss is 50%). The above minimum curve, which is a straight line with a slope of approximately -0.94, is quite similar to the minimum curve obtained for the moment capacity of plastic and compact sections with varying thickness loss (Equation 5.18).

5.6.4 Long span beams

In order to obtain minimum curves for the %RLTBC of long span beams, it is necessary to define the span that is long and widely used. Two sets of long spans in terms of the slenderness of beams (λ) and the ratio of L_E/D are considered for the development of minimum curves for the %RLTBC. However, the results of the analysis are presented in this work for the case of long span beams with $L_E/D = 30$. A family of sections with varying thickness loss was analysed first to study the behaviour of %RLTBC of long span beams with $L_E/D = 30$. The detail of the family of sections and the results are given in Figure 5.23.

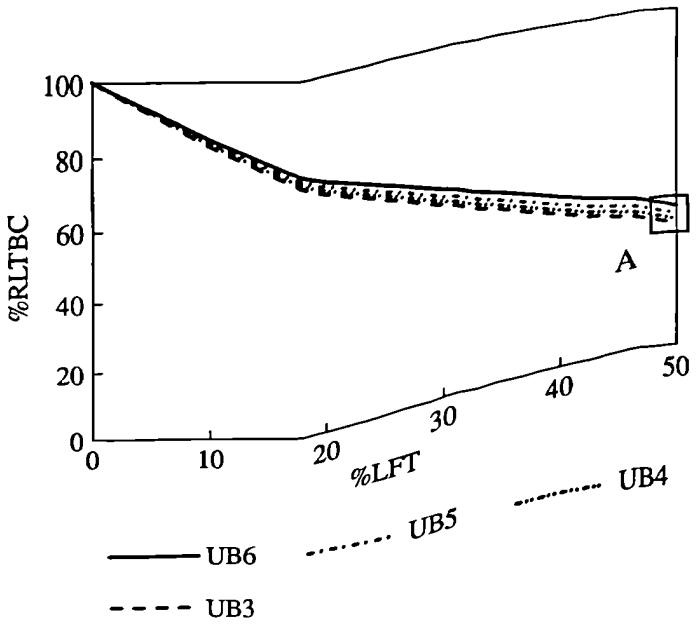

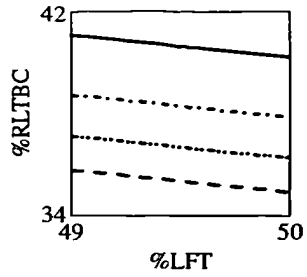

Expanded view of A

No.	Section	b/T
UB3	914x305 UB 289	4.81
UB4	914x305 UB 253	5.47
UB5	914x305 UB 224	6.36
UB6	914x305 UB 201	7.51

Figure 5.23 Behaviour of %RLTBC of a family of long span beams with $L_E/D = 30$

It is evident from Figure 5.23 that the rate of reduction in the %RLTBC of long span beams increases with decreasing b/T ratio. The beam with the lowest value of b/T (UB3) gives the minimum curve for the family. The variation in the %RLTBC curves is small (less than 7% when the thickness loss is 50%). Based on the above findings, all the sections that have the lowest value of b/T from each of the families were analysed to obtain a minimum curve for the %RLTBC of long span beams with $L_E/D = 30$. The results for five beams and the detail of the sections are given in Figure 5.24.

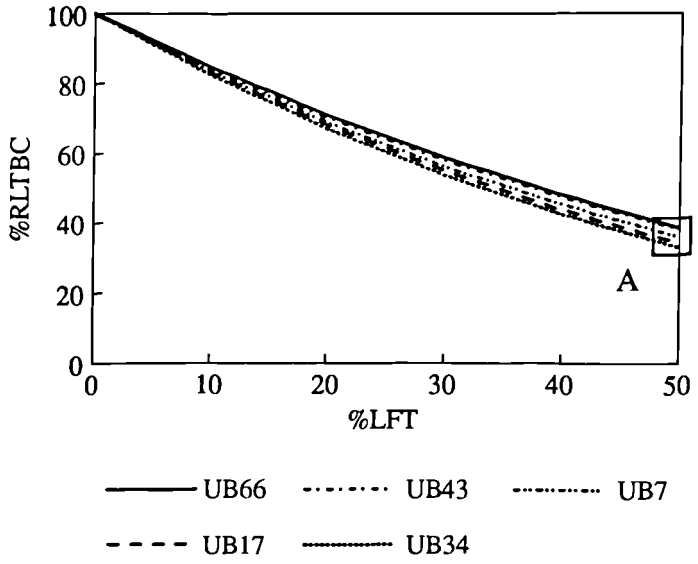

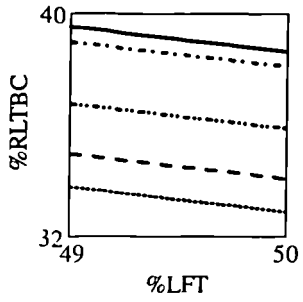

Expanded view of A

No.	Section	b/T
UB66	203×133 UB 30	6.97
UB43	406×140 UB 46	6.36
UB7	838×292 UB 226	5.48
UB17	610×305 UB 238	4.96
UB34	457×152 UB 82	4.06

Figure 5.24 Behaviour of %RLTBC of long span beams from five families

It is evident from Figure 5.24 that the beam that has the lowest value of b/T ratio (UB34) gives the minimum curve for the %RLTBC of whole range of long span beams with $L_E/D = 30$. It can also be seen that the variation in the percentage remaining capacities of beams with maximum and minimum values of b/T ratio is small (less than 7% when the thickness loss is 50%).

5.6.5 Coped beams

It was found in Chapter 4 that lateral torsional buckling was the critical failure mode for the samples of corrosion damaged beams tested in the laboratory. These beams, which were coped at one end of the top flange, were laterally unrestrained during the test. Therefore the effect of copes on the %RLTBC of corrosion damaged beams should be analysed in detail. As can be seen from Equations 3.55 and 3.56, the cope length (L_C) and cope depth (d_C) are important factors on the lateral torsional buckling capacity of coped beams. In this work, the analysis was carried out with $L_C = 0.75B$ and $d_C = 0.1D$ for all the beams as these dimensions would cover most cases of copes in practice [Cheng et al 1988a].

5.6.5.1 Effect of copes on the %RLTBC of corrosion damaged beams

The effect of copes in the top flange on the %RLTBC of corrosion damaged beams was analysed by using three beams of the same section size (UB20) and with same span lengths ($L_{E(Crit)}$). One beam is ordinary (UNCOPED) and the other two beams are coped at one end (COPED 1) and both ends (COPED 2) of the top flange. The results are given in Figure 5.25. It was assumed that all the beams are laterally unrestrained.

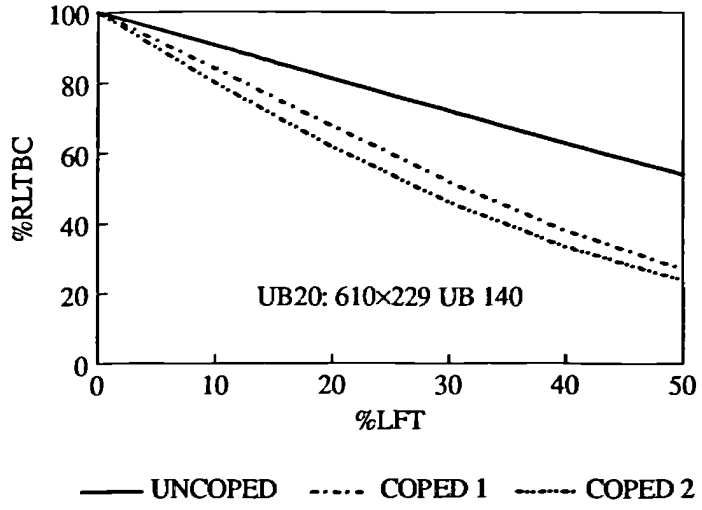

Figure 5.25 Effect of copes in the top flange on the %RLTBC

The copes in the top flange have a very significant effect on the %RLTBC of corrosion damaged beams as can be seen from Figure 5.25. The figure shows that the variation in the percentage remaining capacities between the ordinary and coped beams is quite considerable (more than 30% for thickness loss of 50%). This indicates that the minimum curves to be obtained for the %RLTBC of ordinary beams may not be valid for the coped beams.

5.6.5.2 Effect of span length on the %RLTBC of top flange coped beams

The effect of span length on the %RLTBC of coped beams was analysed by using two different span lengths; one is short span with $L_{E(Crit)}$ and the other is long span with $L_E/D = 30$. In each case, three beams of the same section size (UB20) were used. One is an ordinary beam, i.e. uncoped beam, and the other two are coped at one end and both ends of the top flange. The results are given in Figure 5.26.

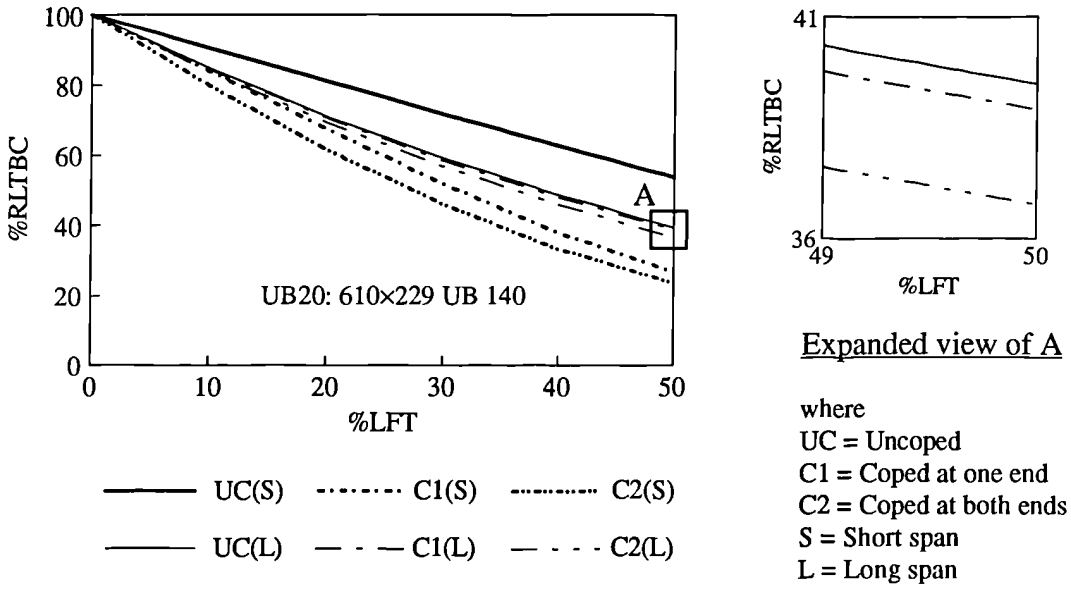

Figure 5.26 Effect of span length on the %RLTBC of corrosion damaged coped beams

The comparison of the %RLTBC curves of long span ordinary and coped beams shows (Figure 5.26) that the cope has very little effect on the long span coped beams (both coped at one end and both ends). The long span coped beams behave like ordinary beams and the buckling capacity is mainly controlled by the uncoped section (I-section)

although the cope does decrease the capacity (see Figure 5.26). Therefore the long span top flange coped beams can be treated as ordinary beams and the minimum curve to be obtained for the %RLTBC of long span ordinary beams may be used for such beams.

In the case of short span top flange coped beams the effect is very significant as can be seen from Figure 5.26. The buckling capacity of short span top flange coped beams is mainly controlled by the coped (Tee) section since the full section remains relatively straight in the buckled position and severe cross-section distortion occurs in the coped region. This is evident from the buckled shape of the samples of corrosion damaged beams tested in the laboratory (see Figure 4.10).

5.6.5.3 Short span coped beams with critical effective length

Two families of beams with varying thickness loss were analysed separately to study the behaviour of the %RLTBC of corrosion damaged beams that are coped at one end and both ends of the top flange. The effective length of the beams was taken as the critical effective length. The details of the two families of beams and the results are given in Figures 5.27a and 5.27b.

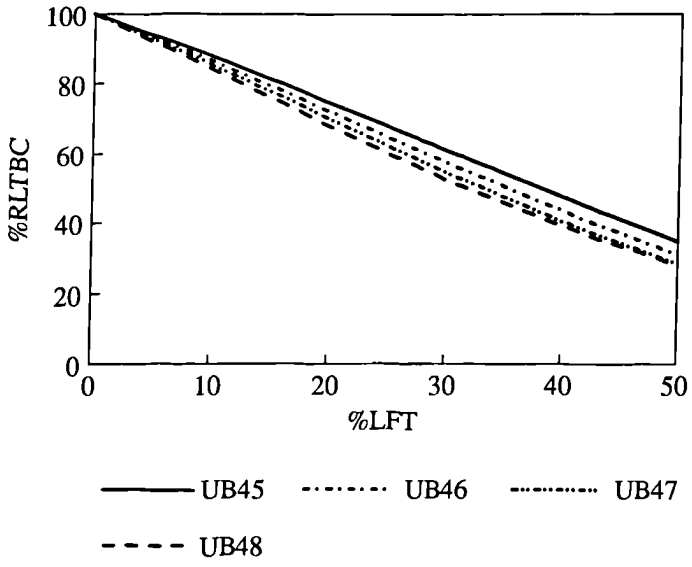

No.	Section	d/t
UB45	356x171 UB 67	34.3
UB46	356x171 UB 57	39.0
UB47	356x171 UB 51	42.8
UB48	356x171 UB 45	45.3

Figure 5.27a Behaviour of %RLTBC of a family of short span beams coped at one end of the top flange

It can be seen from Figure 5.27a that the rate of reduction in the percentage remaining capacities of beams that are coped at one end of the top flange with critical effective length increases with increasing d/t ratio. The coped beam that has the highest value of d/t ratio (UB48) gives the minimum curve for that family.

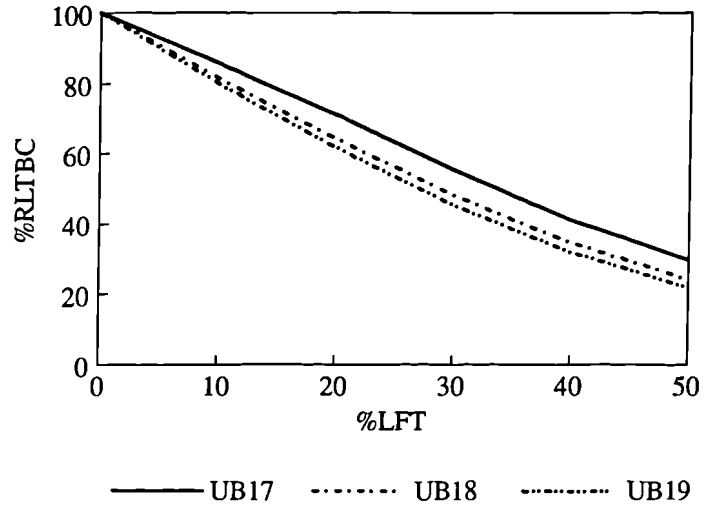

No.	Section	B/D
UB17	610×305 UB 238	0.492
UB18	610×305 UB 179	0.497
UB19	610×305 UB 149	0.500

Figure 5.27b Behaviour of %RLTBC of a family of short span beams coped at both ends of the top flange

It is evident from Figure 5.27b that the rate of reduction in the percentage remaining capacities of beams that are coped at both ends of the top flange with $L_{E(Crit)}$ increases with increasing B/D ratio. The beam that has the highest value of B/D ratio gives the minimum curve for the %RLTBC of the family of beams.

Based on the above information, all the sections that have the highest value of d/t from each of the families were analysed to obtain a minimum curve for whole range of beams that are coped at one end of the top flange. The results for five beams and the detail of the sections are given in Figure 5.28a.

For beams that are coped at both ends of the top flange, all the sections that have the highest value of B/D ratio from each of the families were analysed to obtain a minimum curve for the %RLTBC. The results for five beams and the detail of the sections are given in Figure 5.28b.

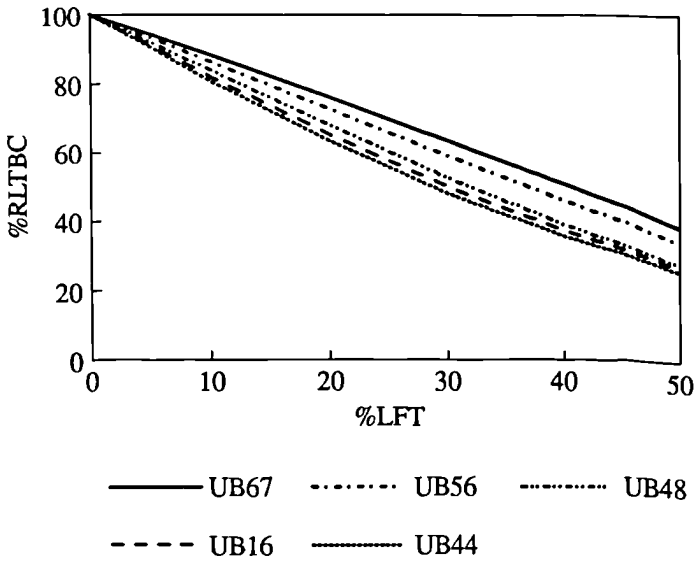

No.	Section	d/t
UB67	203x103 UB 30	29.7
UB56	305x127 UB 37	36.7
UB48	356x171 UB 45	45.3
UB16	686x254 UB 125	52.6
UB44	406x140 UB 39	57.1

Figure 5.28a Behaviour of %RLTBC of beams coped at one end from five families

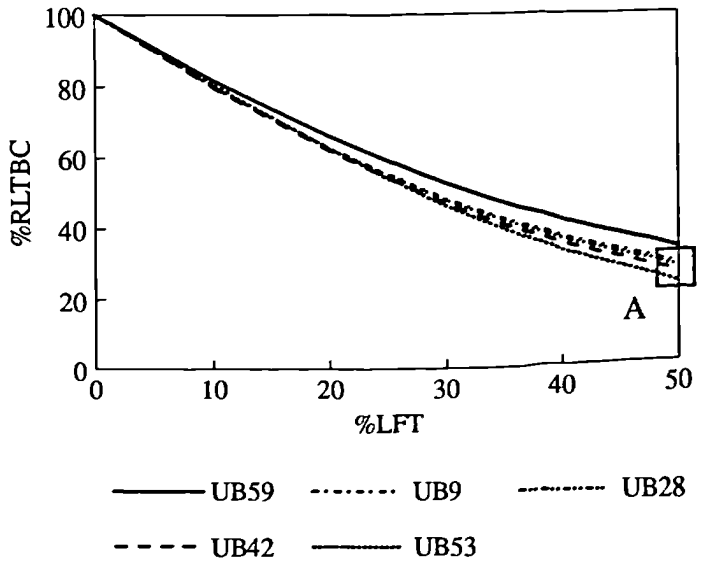

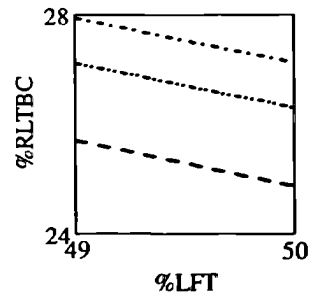

Expanded view of A

No.	Section	B/D
UB59	305x102 UB 25	0.333
UB9	838x292 UB 176	0.349
UB28	533x210 UB 82	0.395
UB42	406x178 UB 54	0.441
UB53	305x165 UB 40	0.544

Figure 5.28b Behaviour of %RLTBC of beams coped at both ends from five families

It can be seen from Figure 5.28a that the section that has the highest value of d/t ratio (UB44) gives the minimum curve for the %RLTBC of short span beams that are coped at one end of the top flange with $L_{E(Crit)}$. It is evident from Figure 5.28b that the section with the highest value of B/D ratio (UB53) gives the minimum curve for the %RLTBC of short span beams that are coped at both ends of the top flange with $L_{E(Crit)}$.

5.6.6 Minimum curves

As the effective length is the major factor that governs the bending strength of ordinary beams, minimum curves were developed for the %RLTBC of ordinary beams in terms of their length. For coped beams, minimum curves were obtained in terms of number of copes in the top flange. Using the results obtained in the accurate assessment method minimum curves were obtained and are given in Figure 5.29 for the following cases:

1. Short span beams with $L_{E(Crit)}$: ($L_{E(Crit)}$),
2. Long span beams with $L_E/r_y = 200$: ($L_E/r_y = 200$),
3. Long span beams with $L_E/D = 30$: ($L_E/D = 30$),
4. Short span beams coped at one end of the top flange with $L_{E(Crit)}$: (COPE 1), and
5. Short span beams coped at both ends of the top flange with $L_{E(Crit)}$: (COPE 2).

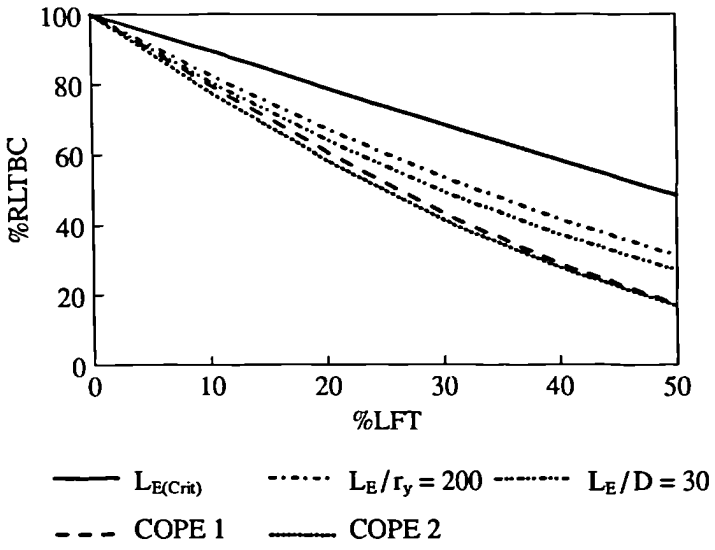

Figure 5.29a Minimum curves for estimating the %RLTBC of corrosion damaged beams with uniform thickness loss

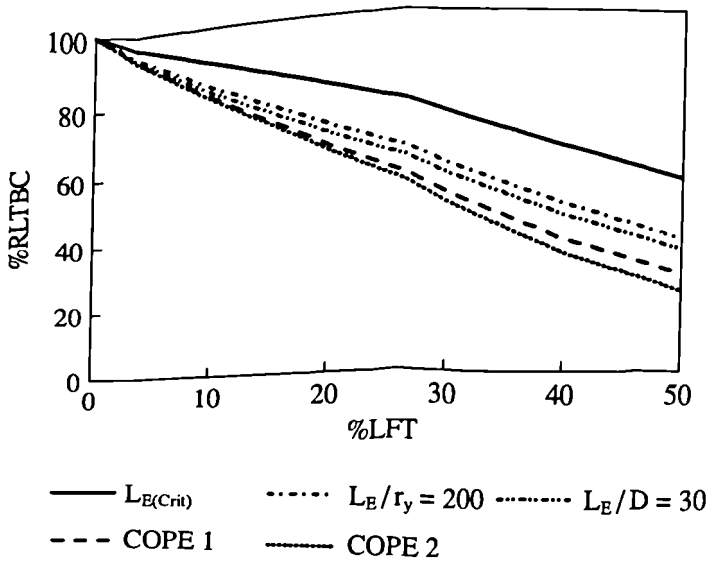

Figure 5.29b Minimum curves for estimating the %RLTBC of corrosion damaged beams with varying thickness loss

The minimum curves obtained for the short and long span beams may be used to estimate the %RLTBC of intermediate span beams by using interpolation. The minimum curve 'COPE 2' may be used as the minimum curve for the %RLTBC of both beams coped at one end and both ends of the top flange, as the two minimum curves obtained for coped beams are very close. For the long span coped beams the minimum curve obtained for the long span ordinary beams, '$L_E/D = 30$', may be used since they behave like long span ordinary beams (see Section 5.6.5.2).

The variation in the minimum curves for the %RLTBC of long span ordinary beams and the short span coped beams is about 12% when the loss of thickness in the flanges is 50% (see Figure 5.29). Therefore, for intermediate span top flange coped beams, the minimum curve 'COPE 2' may be used to obtain conservative estimates of the remaining capacity. If accurate assessment is required, then the minimum curves obtained for the short span coped beams and long span ordinary beams may be used to estimate the %RLTBC by using interpolation.

5.7 Assessment methods for Web Bearing and Buckling Capacities

5.7.1 Web bearing capacity

5.7.1.1 Simple assessment method

The web bearing strength, P_{wbg}, of a section can be evaluated using the theory given in Section 3.5.1, in which the web bearing strength is given as follows:

$$P_{wbg} = (b_1 + n_2)tp_{yw} \quad (5.95)$$

where

b_1 is the stiff bearing length, and

n_2 can be taken as follows (see Section 3.5.1):

$n_2 = 2\times2.5(T + r)$ for forces applied through a flange by loads or reactions in the length between the ends, and

$n_2 = 2.5(T + r)$ for forces applied through a flange by loads or reactions at the ends.

Equation 5.95 may be written as:

$$P_{wbg} = [b_1 + 2.5c(T + r)]tp_{yw} \quad (5.96)$$

where

$c = 2$ for forces applied through a flange by loads or reactions in the length between the ends, and

$c = 1$ for forces applied through a flange by loads or reactions at the ends.

The percentage remaining web bearing capacity (%RWBC) of a corrosion damaged section is the ratio of the capacity of the corrosion damaged section (WBC_C) to the capacity of the section in its as-new condition (WBC_N). It can be expressed as:

$$\%RWBC = 100\ (WBC_C / WBC_N) \quad (5.97)$$

Using Equation 5.96, the %RWBC is obtained as:

$$\%\text{RWBC} = 100\frac{t_C}{t_N}\frac{[b_1+2.5c(T_C+r)]}{[b_1+2.5c(T_N+r)]} \tag{5.98}$$

The root radius, r, may be taken as constant throughout the service life of a beam. Equation 5.98 shows that the design strength has no effect on the %RWBC. In order to obtain a minimum for the %RWBC, it is necessary to identify the worst possible case, which can be taken as when $b_1 = 0$, i.e. stiff bearing plates are not provided. Substituting $b_1 = 0$ into Equation 5.98 gives the %RWBC as:

$$\%\text{RWBC} = 100\frac{t_C}{t_N}\left(\frac{T_C+r}{T_N+r}\right) \tag{5.99}$$

For uniform thickness loss model sections in which $\xi_W = \xi_F = \xi$ where ξ = %LFT / 100, if Equations 5.1a and 5.1b (for T_C and t_C) are combined with Equation 5.99, the following relation is obtained for the %RWBC as:

$$\%\text{RWBC} = 100\,(1-\xi)\frac{(1-\xi)+(r/T_N)}{1+(r/T_N)} \tag{5.100}$$

Equation 5.100 shows that when (r/T_N) decreases, the %RWBC also decreases. Hence, the minimum of %RWBC can be obtained when the value of (r/T_N) is minimum. By analysing the available I-sections, the minimum of (r/T_N) was obtained as 0.5 for section UB29 (457×191 UB 98). Now, substituting the minimum of (r/T_N) into Equation 5.100 gives the minimum of %RWBC of uniform thickness loss model sections as:

$$\text{Min}(\%\text{RWBC}) = 100\,(1-\xi)\left(1-\frac{2}{3}\xi\right) \tag{5.101}$$

For varying thickness loss model sections in which $\xi_W = \xi_F/2 = \xi/2$, combining Equations 5.2c, 5.2f (for T_C and t_C) and 5.99 together with the minimum value of (r/T_N) gives the minimum of %RWBC as:

$$\text{Min}(\%\text{RWBC}) = 100\left(1-\xi_w\right)\left(1-\frac{4}{3}\xi_w\right) \qquad (5.102)$$

Therefore, Equations 5.101 and 5.102 may be used as the minimum curves for estimating the percentage remaining web bearing capacity of corrosion damaged beams that are not provided with web bearing stiffeners.

5.7.1.2 Accurate assessment method

A family of sections with varying thickness loss was analysed to study the behaviour of %RWBC of corrosion damaged sections that are not provided with web bearing stiffeners. The results and the detail of the family of sections are given in Figure 5.30.

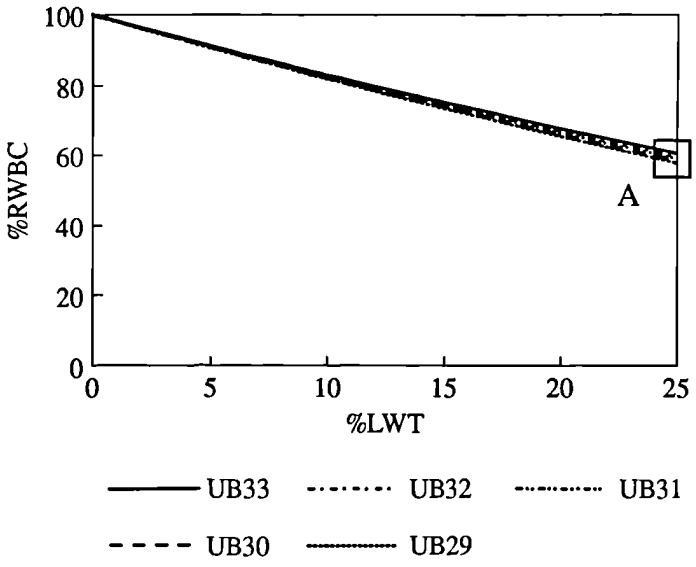

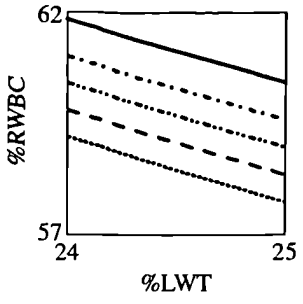

Expanded view of A

where

LWT = Loss of Web Thickness

No.	Section	d/t
UB29	457×191 UB 98	35.8
UB30	457×191 UB 89	38.5
UB31	457×191 UB 82	41.2
UB32	457×191 UB 74	44.8
UB33	457×191 UB 67	48.0

Figure 5.30 Behaviour of %RWBC of a family of sections

It can be seen from Figure 5.30 that the section with the lowest value of d/t (UB29) gives the minimum curve for the %RWBC of the family of sections. Based on the above observation, sections that have the lowest value of d/t from each of the families were analysed to obtain a minimum curve for the %RWBC. The results for five beams and the detail of the sections are given in Figure 5.31.

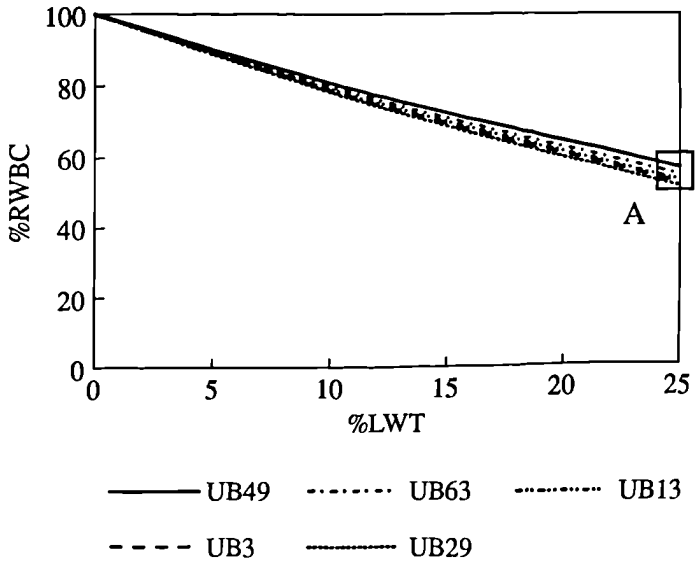

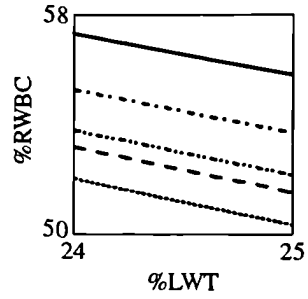

Expanded view of A

No.	Section	d/t
UB49	356×127 UB 39	47.9
UB63	254×102 UB 28	35.2
UB13	686×254 UB 170	42.4
UB3	914×305 UB 289	42.1
UB29	457×191 UB 98	35.8

Figure 5.31 Behaviour of %RWBC of sections from five families

It is evident from Figure 5.31 that the section that has the lowest value of d/t ratio (UB29) gives the minimum curve for the %RWBC of the whole range of corrosion damaged beams that are not provided with web bearing stiffeners. The variation in the percentage remaining capacities between the maximum and minimum values of d/t ratio is small (less than 7% for web thickness loss of 25%).

5.7.2 Buckling resistance of webs

The buckling resistance of webs that are not provided with load carrying web stiffeners can be evaluated using the theory given in Section 3.5.2. A simplified equation for the compressive strength, p_c, of unstiffened webs was derived by the writer to verify the effect of slenderness on the compressive strength. The equation was derived in terms of the web slenderness, λ, and the limiting slenderness, λ_o, using Equations 3.62 to 3.66 and making a few approximations. The expression is given below:

$$p_c \approx \frac{1.07\pi^2 E\left[\lambda^2 + 0.1375\lambda_0^2\lambda + (25 - 0.1375\lambda_0)\lambda_0^2\right]}{\left[\left(\lambda^2 + 0.1375\lambda_0^2\lambda + (25 - 0.1375\lambda_0)\lambda_0^2\right)^2 - 25\lambda_0^2\lambda^2\right]} \qquad (5.103)$$

where

$$\lambda_0 = 0.2\left(\frac{\pi^2 E}{p_y}\right)^{1/2}$$

The compressive strength of webs depends on the slenderness of the unstiffened web and the limiting slenderness, which in turn depends on the design strength of the web material (see Section 3.5.2). For a given design strength, the slenderness of the unstiffened web, λ, which is equal to $2.5d/t$, is the major factor that governs the compressive strength of unstiffened webs.

5.7.2.1 Accurate assessment method

As it was not possible to derive simple analytical relations using simple assessment method for the percentage remaining buckling resistance of webs (%RBRW) of corrosion damaged beams, the minimum curves were obtained using accurate assessment method as described in this section. A family of sections with varying thickness loss was analysed first to study the behaviour of %RBRW of corrosion damaged beams that are not provided with load carrying web stiffeners. The results of the analysis and the detail of the family of sections are given in Figure 5.32.

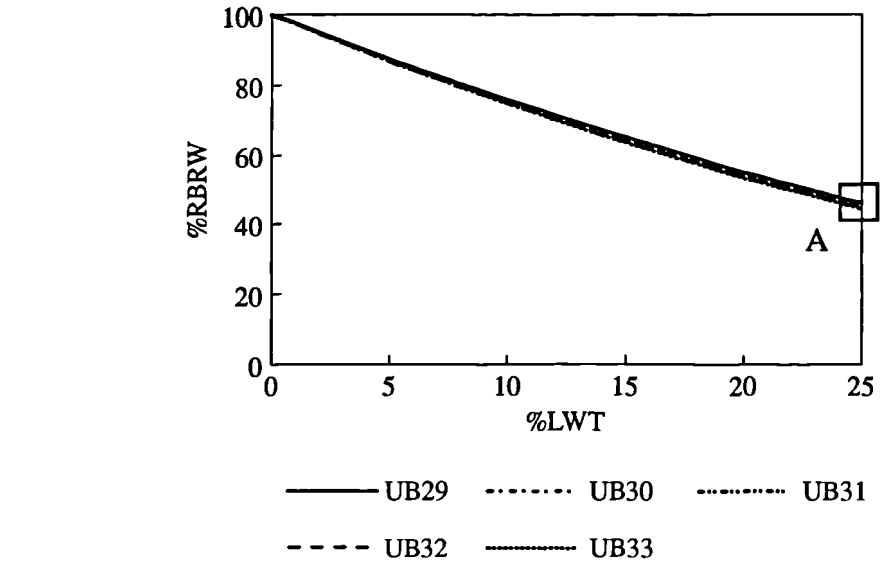

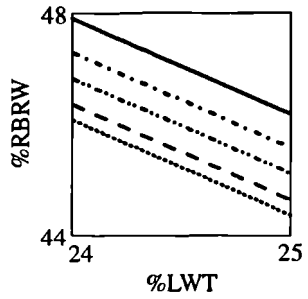

Expanded view of A

No.	Section	d/t
UB29	457×191 UB 98	35.8
UB30	457×191 UB 89	38.5
UB31	457×191 UB 82	41.2
UB32	457×191 UB 74	44.8
UB33	457×191 UB 67	48.0

Figure 5.32 Behaviour of %RBRW of a family of sections

It can be seen from Figure 5.32 that the section with the highest value of d/t ratio gives the minimum curve for the family with regard to the buckling resistance of webs. Based on the above information, sections that have the highest value of d/t from each of the families were analysed to obtain a minimum curve for the %RBRW. The results of the analysis for five sections and the detail of the sections are given in Figure 5.33.

It is evident from Figure 5.33 that, for the whole range of corrosion damaged beams that are not provided with load carrying web stiffeners, the section that has the highest value of d/t ratio (UB44) gives the minimum curve for the %RBRW. The variation in the %RBRW curves of maximum and minimum values of d/t ratio is very small (less than 6% for web thickness loss of 25%).

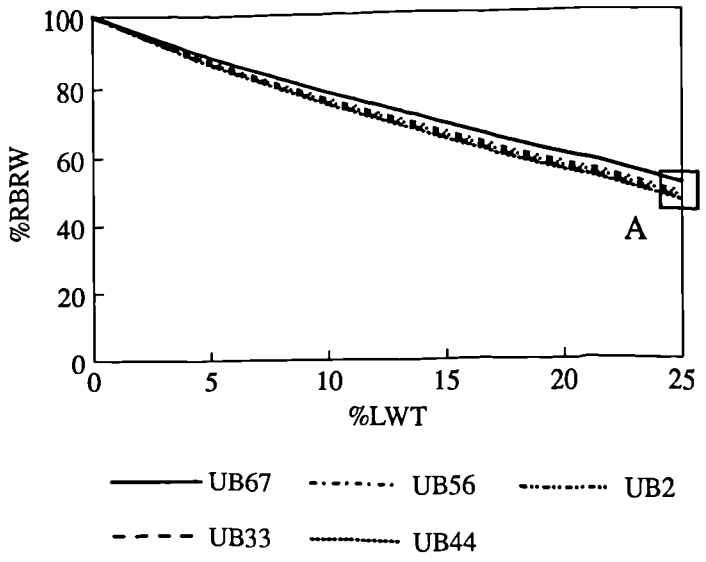

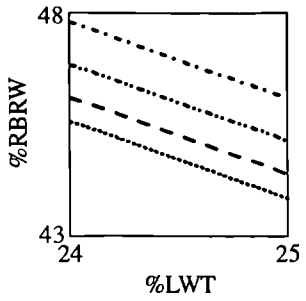

Expanded view of A

No.	Section	d/t
UB67	203×133 UB 25	29.7
UB56	305×127 UB 37	36.7
UB2	914×419 UB 343	41.2
UB33	457×191 UB 67	48.0
UB44	406×140 UB 39	57.1

Figure 5.33 Behaviour of %RBRW of sections from five families

5.7.3 Minimum curves

It was found in the analysis that the section with the lowest value of d/t (UB29) gives the minimum curve for the %RWBC of corrosion damaged sections that are not provided with web bearing stiffeners. It was also found that the section with the highest value of d/t (UB44) gives the minimum curve for the %RBRW of corrosion damaged sections that are not provided with load carrying web stiffeners. Using these results two minimum curves were obtained and are given in Figure 5.34 for the following cases:

A. Web bearing capacity and
B. Buckling resistance of webs.

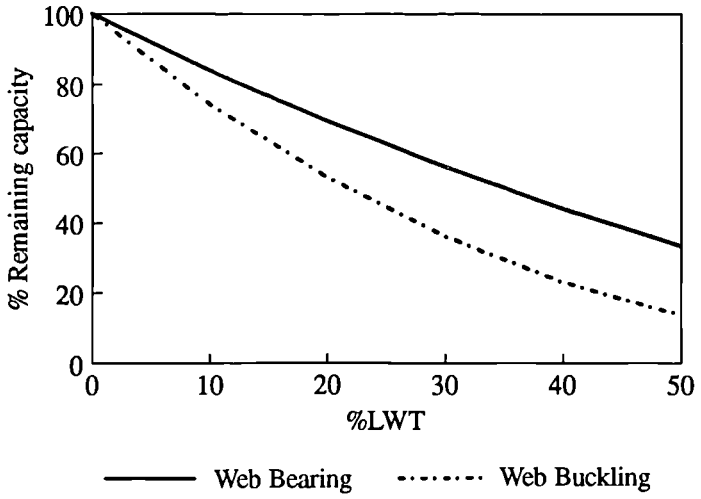

Figure 5.34a Minimum curves for estimating the %RWBC and %RBRW of corrosion damaged beams with uniform thickness loss

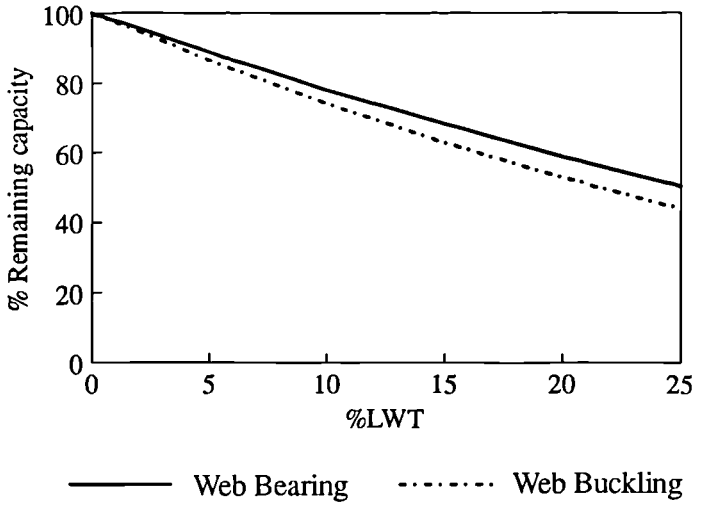

Figure 5.34b Minimum curves for estimating the %RWBC and %RBRW of corrosion damaged beams with varying thickness loss

The rate of reduction of web bearing and buckling strengths of corrosion damaged beams that are not provided with web bearing or load carrying stiffeners is quite considerable. It was found in Section 4.4.1 that, for corrosion damaged beams that are provided with web bearing or load carrying stiffeners, web bearing and buckling failure modes are less significant. Therefore, if a member is to be exposed to a corrosive environment, then provision of stiffeners will increase the web bearing and buckling capacities significantly.

5.8 Comparison of the solutions obtained by the simple and accurate assessment methods

As a result of our search for assessment methods to estimate the percentage remaining capacity of corrosion damaged I-beams some analytical relations were derived by the simple assessment method for the assessment of remaining moment, shear and web bearing capacities. In addition, minimum curves were obtained by the accurate assessment method by analysing families of I-sections over a range of spans and displaying the results graphically. It should be noted that it was not possible to obtain simple equations analytically for the assessment of remaining lateral torsional buckling capacity and buckling resistance of webs. The equations obtained by the simple assessment method for various cases were used to plot the relationship between the minimum percentage remaining capacity and the percentage loss of thickness of corrosion damaged I-beams. These graphs were then compared with the minimum curves that were obtained using the accurate assessment method. The comparisons of the two solutions for various failure modes are given in Figures 5.35, 5.36, and 5.37.

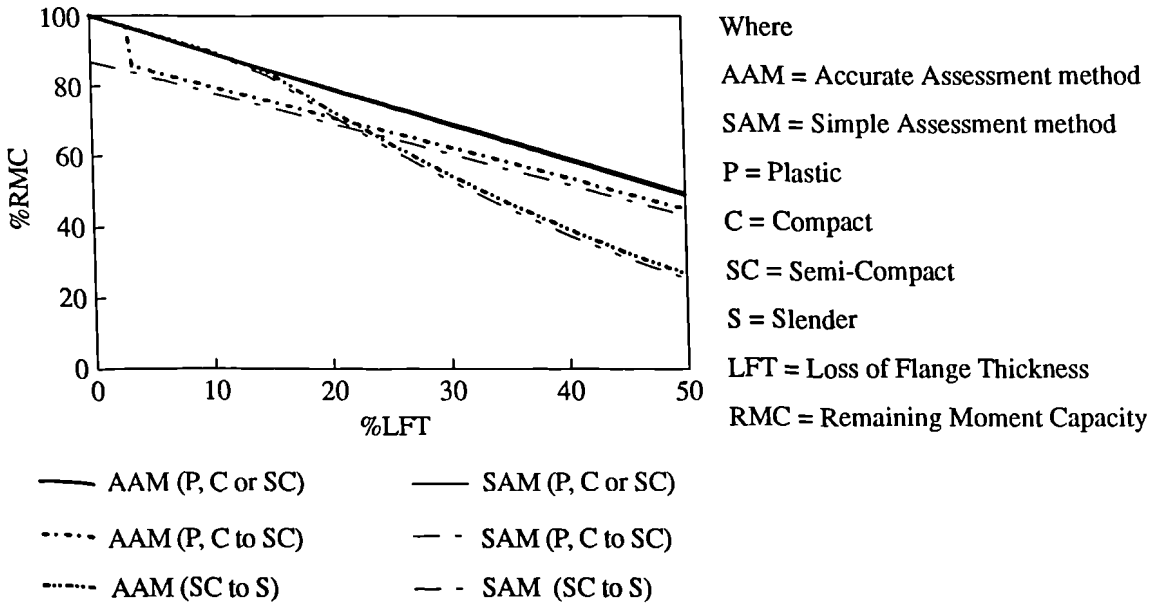

Figure 5.35a Comparison of the minimum curves obtained by the simple and accurate assessment methods for the percentage remaining moment capacity of corrosion damaged I-beams with uniform thickness loss

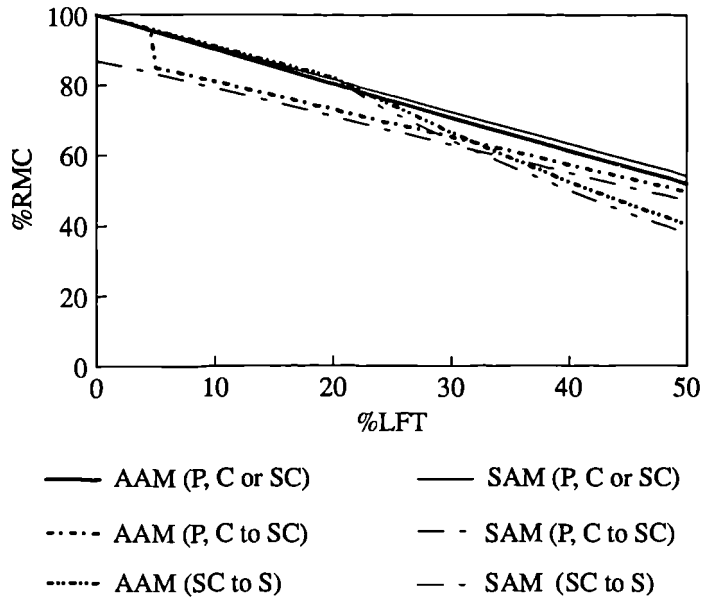

Figure 5.35b Comparison of the minimum curves obtained by the simple and accurate assessment methods for the percentage remaining moment capacity of corrosion damaged I-beams with varying thickness loss

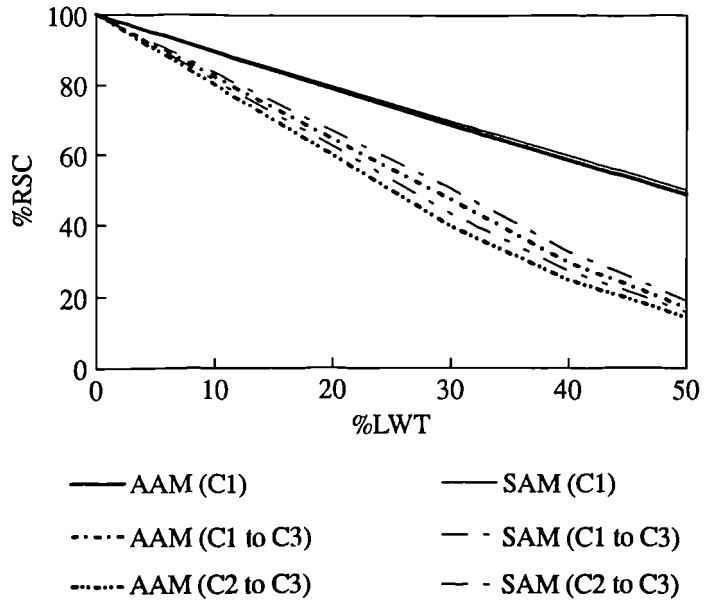

Where

C1 = Category 1 ($d/t \leq 63\varepsilon$)

C2 = Category 2 ($63\varepsilon < d/t < 98\varepsilon$)

C3 = Category 3 ($d/t \geq 98\varepsilon$)

LWT = Loss of Web Thickness

RSC = Remaining Shear Capacity

Figure 5.36 Comparison of the minimum curves obtained by the simple and accurate assessment methods for the percentage remaining shear capacity of corrosion damaged I-beams with uniform thickness loss

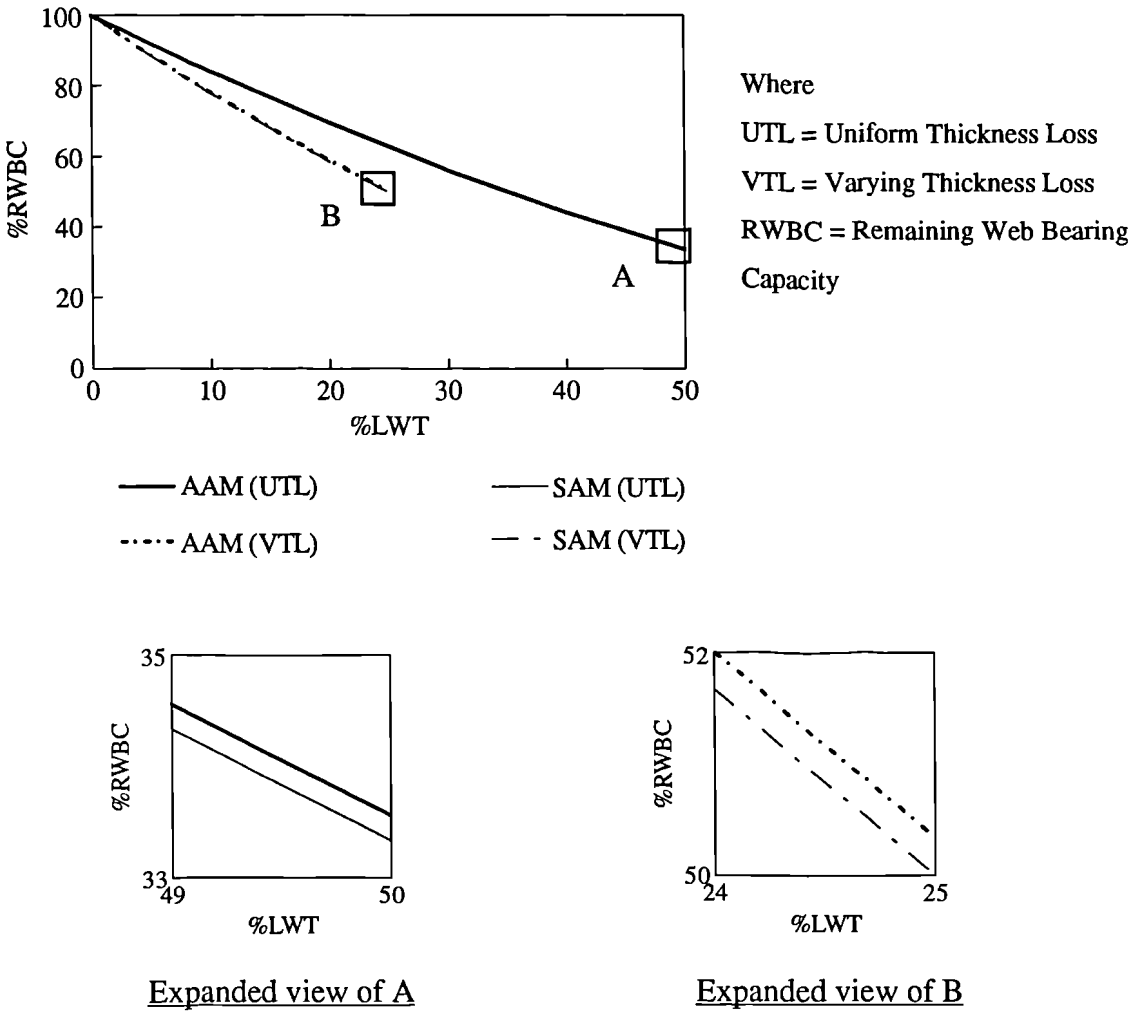

Figure 5.37 Comparison of the minimum curves obtained by the simple and accurate assessment methods for the percentage remaining web bearing capacity of corrosion damaged I-beams with uniform and varying thickness losses

The minimum curves obtained for assessing the remaining capacity of corrosion damaged beams by the simple and accurate assessment methods are in good agreement with each other as can be seen from Figures 5.35, 5.36, and 5.37. There is a small variation between the two assessment methods developed for moment and shear capacities. This is because a few approximations had to be made to derive equations by the simple assessment method (see Sections 5.4.1 and 5.5.2). The comparison of the two solutions indicates that either of the two methods may be used to obtain minimum curves. The comparison also shows that reliable estimates of remaining capacities can be made using the equations of the simple assessment method, which are easy to use in practice.

5.9 Assessment of remaining capacity using minimum curves

It was shown that it is possible to develop minimum curves that can be used to predict the percentage remaining capacity of corrosion damaged beams. These curves were developed for moment, shear, lateral torsional buckling, and web bearing and buckling failure modes of I-beams. The critical failure mode (failure load) of a corrosion damaged beam can be identified by comparing the remaining capacities of the relevant failure modes. These capacities can be obtained using the percentage remaining capacities and the as-new capacities. The way, in which the assessment can be done, is illustrated by the following example using the corrosion damaged sample Beam 3 (see Section 4.4.1).

The beam, which has a cut-out or cope at one end of the top flange, has the following corrosion pattern which is similar to the varying thickness loss model. The measured percentage losses of flange and web thickness are 40.8% and 20.0% respectively. The class of the compression flange of the section was plastic in its as-new condition and was semi-compact at the time of the removal from the plant. The ratio of d/t remained less than 63ε throughout its service life. The web bearing and buckling failure modes can be ignored for the assessment because the beam was provided with a load carrying web stiffener. Using this information, and Figures 5.7b, 5.18b, and 5.29b, the critical failure load was obtained as shown in Table 5.1.

Table 5.1 Remaining capacity assessment using minimum curves

Failure mode	As-new strength / kN (Using the theories given in Chapter 3)	Remaining capacity (RC)	
		%RC	RC / kN
Moment capacity	672.7	55.4	372.7
Shear capacity	667.1	62.0	413.6
Lateral torsional buckling capacity	523.9	33.0	172.9*

* - critical failure load

The above critical load obtained using the minimum curves is in good agreement with the load obtained for the same beam in the theoretical analysis in Section 4.4.1, which is 170.5 kN. It can be seen from Table 5.1 that the critical failure mode of the beam is lateral torsional buckling, which, in this case, has the lowest percentage remaining capacity compared other failure modes. This is not necessarily true always. It is possible that the failure mode, which has the lowest percentage remaining capacity, may not be the critical failure mode of a beam. This is because the magnitudes of various failure mode capacities in as-new condition are not the same.

It should be noted that the as-new strength of a beam in various failure modes is required in order to use this approach. Therefore the above approach may be used where the information on the as-new capacities of relevant failure modes is available and where more accurate assessment is needed. This information may not be readily available in practice and one may have to resort to detailed analysis to get this information. In such cases it may not be possible to make a rapid estimate of the remaining capacity.

The example shows that it may not be necessary to use all the relevant minimum curves to assess the remaining capacity except for the failure mode that gives the lowest value. In the example, the minimum curve for lateral torsional buckling capacity of short span top flange coped beams would have been sufficient to assess the remaining capacity of the beam. This shows that it is possible to derive a single curve for a particular type of beam. This curve will give a lower bound estimate of the percentage remaining capacity. The actual remaining capacity can then be evaluated using the above information together with the design loads. Such curves can be used to obtain a rapid remaining capacity assessment following visual inspection.

5.10 Conservative lower bound solutions

It was noted in the previous section that conservative estimates can be made using single lower bound minimum curves that can be obtained for various types of beams. These curves can be obtained by joining the most bottom parts of the minimum curves that are relevant to a particular type of beam (e.g. short span coped beams) or by selecting the

minimum curve that gives the lowest percentage remaining capacity. This single minimum curve can then be used to predict the percentage remaining capacity of similar types of beams. Five types of beams were identified to obtain conservative lower bound solutions. Using the above approach, lower bound minimum curves were obtained for uniform and varying thickness loss models and are given in Figures 5.38, 5.39, 5.40, and 5.41 for the following types of beams:

1. Type 1

   Any span beams, which are laterally restrained and provided with web stiffeners.
2. Type 2

   Short span beams with critical effective length, $L_{E(Crit)}$, which are laterally unrestrained and provided with web stiffeners.
3. Type 3

   Long span beams with $L_E / D = 30$, which are laterally unrestrained and provided with web stiffeners.
4. Type 4

   Short span top flange coped beams with $L_{E(Crit)}$, which are laterally unrestrained and provided with web stiffeners.
5. Type 5

   Any span beams, which are not provided with load carrying or web bearing stiffeners.

The minimum curves given in Figures 5.38, 5.39, 5.40, and 5.41 may be used to assess the percentage remaining capacity of corrosion damaged beams as explained in Tables 5.2, 5.3, 5.4, and 5.5. The tables give the condition of a section and the corresponding minimum curve that may be used to estimate the percentage remaining capacity of both uniform and varying thickness loss model beams. The equations of the lower bound minimum curves are also given in the tables to make the assessment simple.

The minimum curves, which are given Figures 5.38, 5.39, 5.40, and 5.41, are labelled as MC1a, MC1b, MC2a, etc., where MC = Minimum Curve, and the descriptions of these minimum curves are given in Tables 5.2, 5.3, 5.4, and 5.5.

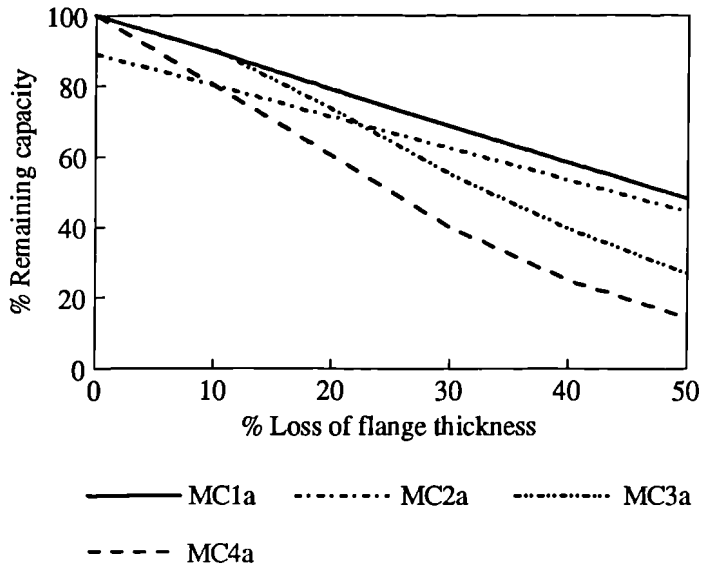

Figure 5.38a Lower bound minimum curves for the assessment of percentage remaining capacity of Type 1 and 2 beams with uniform thickness loss

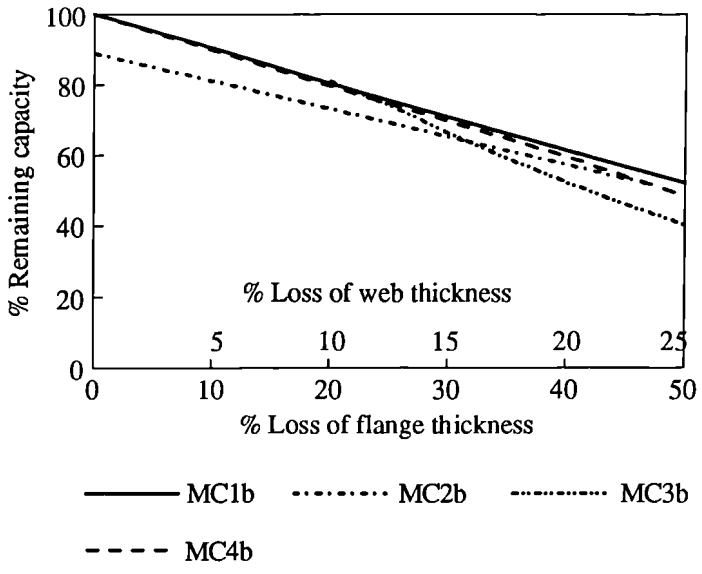

Figure 5.38b Lower bound minimum curves for the assessment of percentage remaining capacity of Type 1 and 2 beams with varying thickness loss

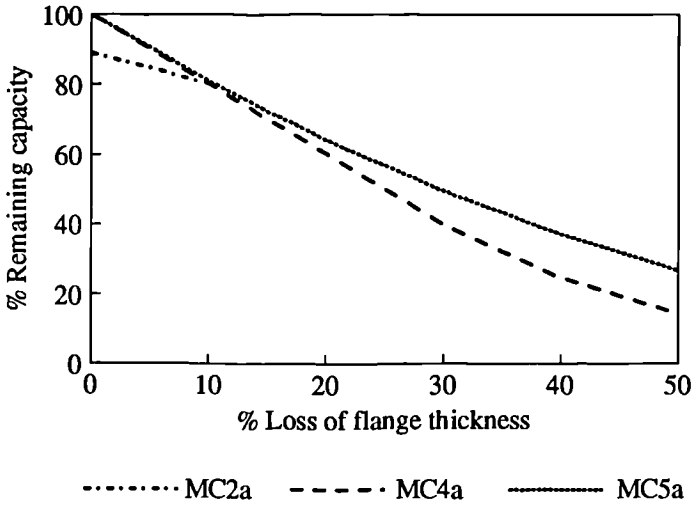

Figure 5.39a Lower bound minimum curves for the assessment of percentage remaining capacity of Type 3 beams with uniform thickness loss

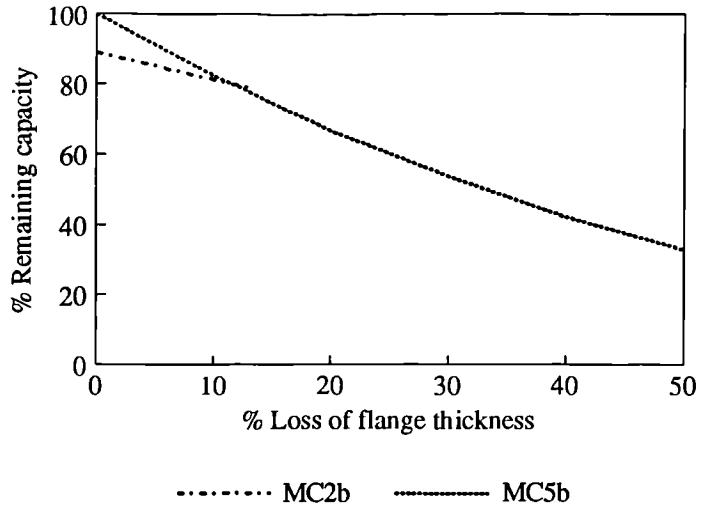

Figure 5.39b Lower bound minimum curves for the assessment of percentage remaining capacity of Type 3 beams with varying thickness loss

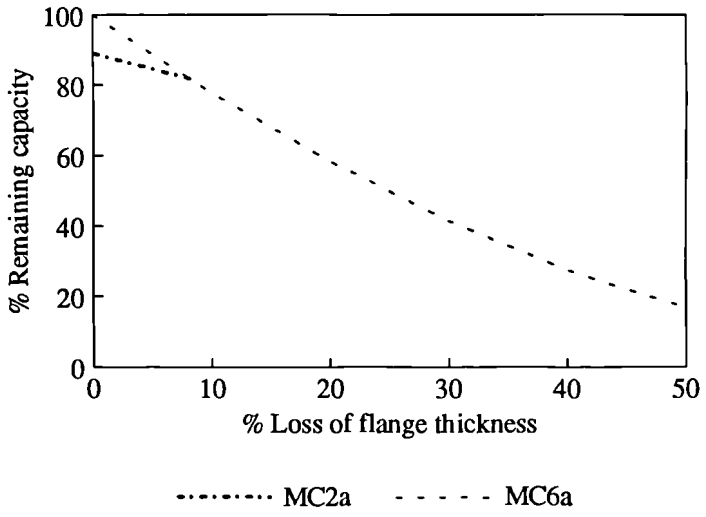

Figure 5.40a Lower bound minimum curves for the assessment of percentage remaining capacity of Type 4 beams with uniform thickness loss

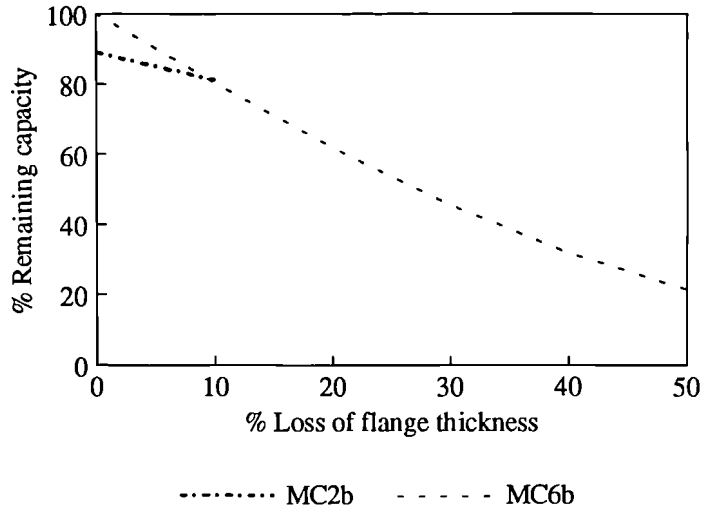

Figure 5.40b Lower bound minimum curves for the assessment of percentage remaining capacity of Type 4 beams with varying thickness loss

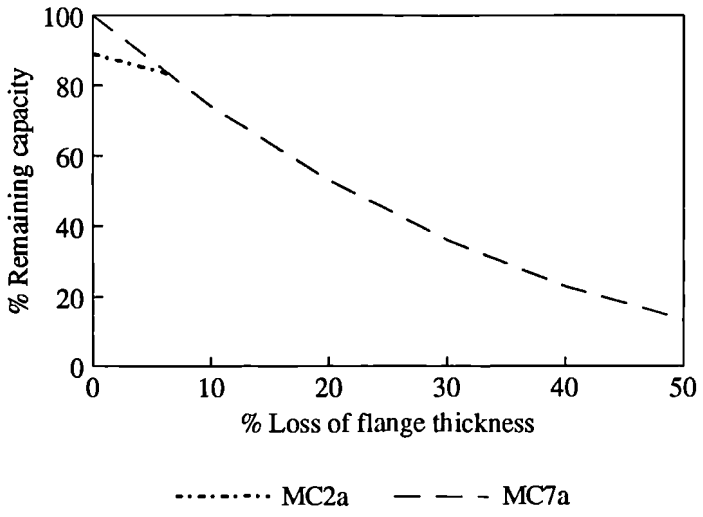

Figure 5.41a Lower bound minimum curves for the assessment of percentage remaining capacity of Type 5 beams with uniform thickness loss

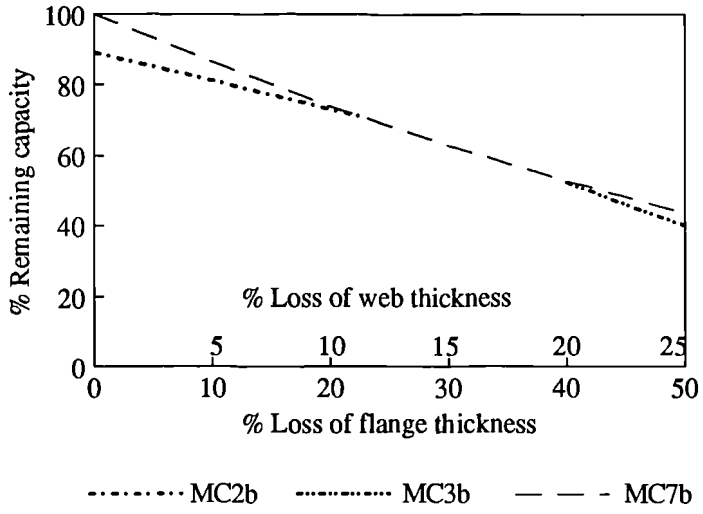

Figure 5.41b Lower bound minimum curves for the assessment of percentage remaining capacity of Type 5 beams with varying thickness loss

Table 5.2 Assessment of Type 1 and 2 beams

Element	Class of section		Minimum curve (MC)	
	As-new state	**Corroded state**	**UTL**	**VTL**
1 Compression flange	Plastic, compact or Semi-compact	Same as as-new	MC1a: $100 - 104\xi$	MC1b: $100 - 96\xi$
Web	$d/t < 63\varepsilon$	Same as as-new		
2 Compression flange	Plastic or Compact	Semi-compact	MC2a: $89 - 89\xi$	MC2b: $89 - 79\xi$
Web	$d/t < 63\varepsilon$	Same as as-new		
3 Compression flange	Semi-compact	Slender	MC3a: $120 - 259\xi + 150\xi^2$	MC3b: $120 - 207\xi + 94\xi^2$
Web	$d/t < 63\varepsilon$	Same as as-new		
4 Compression flange	Plastic, Compact or Semi-compact	Same as as-new	MC4a: $100 - 227\xi + 106\xi^2$	MC4b: $100 - 100\xi_w$
Web	$d/t <$ or $> 63\varepsilon$	$d/t > 63\varepsilon$		
5 Compression flange	Plastic or Compact	Semi-compact	MC2a and MC4a	MC2b
Web	$d/t <$ or $> 63\varepsilon$	$d/t > 63\varepsilon$		
6 Compression flange	Semi-compact	Slender	MC4a	MC3b
Web	$d/t <$ or $> 63\varepsilon$	$d/t > 63\varepsilon$		

Table 5.3 Assessment of Type 3 beams

Element	Class of section		Minimum curve (MC)	
	As-new state	**Corroded state**	**UTL**	**VTL**
1 Compression flange	Plastic, compact or Semi-compact	Same as as-new	MC5a: $100 - 202\xi + 112\xi^2$	MC5b: $100 - 186\xi + 105\xi^2$
Web	$d/t < 63\varepsilon$	Same as as-new		
2 Compression flange	Plastic or Compact	Semi-compact	MC2a and MC5a	MC2b and MC5b
Web	$d/t < 63\varepsilon$	Same as as-new		
3 Compression flange	Semi-compact	Slender	MC5a	MC5b
Web	$d/t < 63\varepsilon$	Same as as-new		
4 Compression flange	Plastic, Compact or Semi-compact	Same as as-new	MC4a	MC5b
Web	$d/t <$ or $> 63\varepsilon$	$d/t > 63\varepsilon$		
5 Compression flange	Plastic or Compact	Semi-compact	MC2a and MC4a	MC2b and MC5b
Web	$d/t <$ or $> 63\varepsilon$	$d/t > 63\varepsilon$		
6 Compression flange	Semi-compact	Slender	MC4a	MC5b
Web	$d/t <$ or $> 63\varepsilon$	$d/t > 63\varepsilon$		

Table 5.4 Assessment of Type 4 beams

Element	Class of section		Minimum curve (MC)	
	As-new state	**Corroded state**	**UTL**	**VTL**
1 Compression flange	Plastic, Compact or Semi-compact	Same as as-new	MC6a: $100 - 238\xi + 142\xi^2$	MC6b: $100 - 214\xi + 113\xi^2$
Web	Any	Any		
2 Compression flange	Plastic or Compact	Semi-compact	MC2a and MC6a	MC2b and MC6b
Web	Any	Any		
3 Compression flange	Semi-compact	Slender	MC6a	MC6b
Web	Any	Any		

Table 5.5 Assessment of Type 5 beams

Element	Class of section		Minimum curve (MC)	
	As-new state	**Corroded state**	**UTL**	**VTL**
1 Compression flange	Plastic, Compact or Semi-compact	Same as as-new	MC7a: $100 - 275\xi + 205\xi^2$	MC7b: $100 - 141\xi_w + 57\xi_w^2$
Web	Any	Any		
2 Compression flange	Plastic or Compact	Semi-compact	MC2a and MC7a	MC2b and MC7b
Web	Any	Any		
3 Compression flange	Semi-compact	Slender	MC7a	MC7b
Web	Any	Any		

where

UTL = Uniform Thickness Loss model,

VTL = Varying Thickness Loss model,

ξ = %LFT/100

ξ_w = %LWT/100

where

%LFT is the percentage loss of flange thickness, and

%LWT is the percentage loss of web thickness.

Note:

$\xi_w = \xi$ for uniform thickness loss model

$\xi_w = \xi/2$ for varying thickness loss model

5.11 Comparison of the experimental failure loads of samples of corrosion damaged beams with the proposed assessment method

An attempt was made to compare the suggested minimum curves for the short span top flange coped beams (Type 4 beams) with the failure loads of four samples of corrosion damaged beams. These beams, which were severely corrosion damaged and coped at one end of the top flange, were obtained from a chemical plant. The four beams were tested individually for their ultimate failure loads in the laboratory (see Section 4.3). The comparison of the experimental failure loads with the suggested minimum curves (MC2b and MC6b) is given in Figure 5.42.

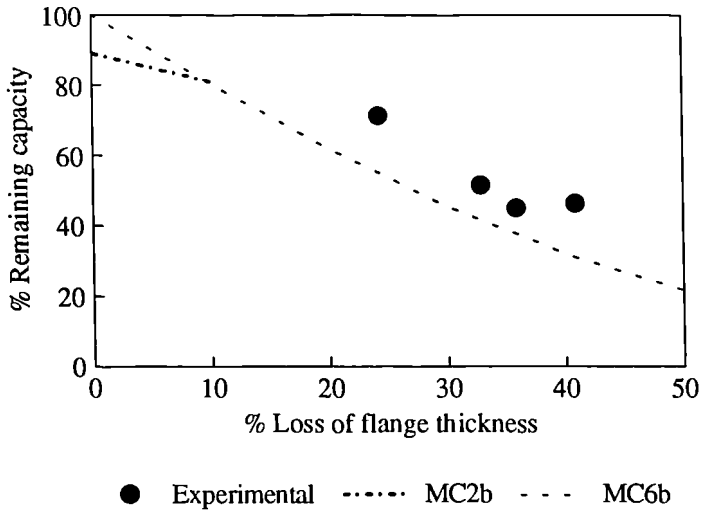

Figure 5.42 Comparison of the experimental failure loads of sample beams with the proposed minimum curves for the short span top flange coped beams (Type 4 beams)

Figure 5.42 suggests that it is possible to estimate the remaining capacity of corrosion damaged beams using the minimum curves obtained by the assessment methods. The estimates will be conservative for some sections, since some of the minimum curves were obtained for the worst cases. It should be noted that in order to calculate the experimental percentage remaining capacities of the samples of corrosion damaged beams the experimental capacity of the as-new beam was required. Since such a beam was not tested in the laboratory, its capacity was obtained as described below. It was found that the critical failure mode of the samples of corrosion damaged beams is lateral

torsional buckling (Section 4.4.1). The comparison of the experimental failure loads of the beams and the ultimate loads obtained theoretically for the lateral torsional buckling failure mode (see Figure 4.13) showed that the experimental loads are approximately 100 kN greater than the theoretical loads. Therefore the ultimate lateral torsional buckling failure load obtained theoretically for the as-new beam (524 kN) was increased by 100 kN to obtain the as-new capacity of the beam. This increased load (624 kN) was then used to calculate the experimental percentage remaining capacities of the sample beams.

5.12 Summary and conclusions

For the assessment of the remaining capacity of corrosion damaged I-beams, two methods have been proposed in this chapter, namely the simple and accurate assessment methods. They were developed for various failure modes of I-beams of all manufactured sizes in the UK. In addition, lower bound estimates of the remaining capacity have also been proposed. These methods give the quantitative relationship between the magnitude of structural defects (loss of thickness) and the corresponding remaining capacity (expressed as percentage of the as-new strength) of corrosion damaged beams. These methods require only the information regarding thickness loss of the appropriate elements (e.g. web thickness loss for shear capacity, flange thickness loss for moment capacity, etc.) and the capacity of the beam in its as-new condition, to assess the remaining capacity of a corrosion damaged beam.

These methods will give almost exact estimates of the remaining capacity of corrosion damaged beams for most cases including shear capacity of Category 1 sections, moment capacity of plastic, compact and semi-compact sections, and lateral torsional buckling capacity of short span beams with critical effective length, $L_{E(crit)}$. In other cases (e.g. shear capacity of Category 2 sections, lateral torsional buckling capacity of long span beams and coped beams), the remaining capacity estimates using these methods will be conservative for some sections, as the worst possible conditions and sections were used to obtain minimum curves for such cases. The accurate assessment method analysis showed that in many cases the variation in the percentage remaining capacity curves, of all the available I-sections for a particular failure mode, is very small. Typically the difference is less than 10% when the thickness loss is 50%.

The comparison of the simple and accurate assessment methods showed that both methods yield nearly the same remaining capacity estimates for various cases. This indicates that any one of the methods may be used to obtain minimum curves, which may be used to estimate the remaining capacity. These assessment methods, which give considerably reliable estimates of the remaining capacity of corrosion damaged I-beams, are easy to use without the need for any lengthy calculations. In particular, the equations obtained in the simple assessment method will be more effective in assessing the capacity of corrosion damaged I-beams. They readily give the estimates of percentage remaining capacity if the thickness losses of the elements are known.

The proposed lower bound solution has an advantage over the other two assessment methods. This approach does not involve various failure modes of an I-beam. These solutions, which were derived from the failure mode that gives the lowest percentage remaining capacity, may be used with the design loads to evaluate the remaining capacity and compare immediately with the service loads. They are easy to use and give rapid estimates of the remaining capacity of corrosion damaged beams.

The comparison of the experimental failure loads of samples of corrosion damaged beams with the proposed minimum curves for the short span top flange coped beams showed that the proposed method gives slightly conservative estimates for the remaining capacity of these beams. This shows that these assessment methods may be used for the realistic appraisal of the remaining capacity of corrosion damaged I-beams.

It is believed that these methods will be beneficial in terms of cost and safety. The realistic appraisal of the capacity of corrosion damaged beams using these methods will avoid plant closures when the capacity of steel works may be adequate. In addition, these methods may be used to identify the weaker members whose capacities are closer to the service loads. These assessment methods will help the practising engineer to make a fast and reliable decision regarding the future of a corrosion damaged I-beam. Using these methods it is also possible to improve the condition categories [ICI Engineering 1990a] presently used in chemical industry and which is presented in the next Chapter.

Chapter 6

Improvement of visual assessment condition categories

6.1 Introduction

Currently, steel structures in the chemical industry are assessed initially by visual inspection. Members with severe corrosion damage (significant loss of section, holes in members, etc.) are then subjected to further investigation, repair, replacement or removal [ICI Engineering 1990a]. There have been cases where a plant or process has been closed down following visual inspection, with consequent financial penalty, when subsequently it was found that the damaged structure was able to carry the service loads.

Many structural members are normally subjected to service loads well below their ultimate capacities. These members may have considerable reserves of strength even in their corroded states. It was found from the experimental study of samples of corrosion damaged beams that even the most severely damaged beam possessed nearly 50% of its calculated as-new strength. For some types and conditions of beam, it was estimated, using the assessment methods developed in Chapter 5, that if the loss of flange thickness is about 15% then the remaining capacity is about 85% of the as-new condition (capacity loss is almost linearly proportional to the thickness loss). These factors indicate that it may be possible to quantify the current visual assessment procedures and hence avoid premature closure of plants. It is proposed that the minimum curves developed in the previous chapter be used as the basis for achieving this objective.

The main aim of this chapter is to introduce improved condition categories for the assessment of corrosion damaged steel beams using the knowledge gained from the experimental study and the minimum curve assessment method.

The specific objectives of this chapter are:

1. To review the current visual assessment procedure of ICI engineering.
2. To introduce improved condition categories for the assessment of corrosion damaged steel beams.

6.2 Review of the current visual assessment procedure of ICI Engineering

Recently, a formal procedure for inspection of deteriorated steel and concrete structures was introduced throughout the UK by ICI Engineering [1990a]. The inspection procedure is shown in Figure 6.1 in a flow chart form. The procedure defines several important requirements relating to the design, modification, inspection and maintenance of such structures with the prime aim of ensuring safe operation. One of the requirements is filing data on each structure including design calculations, drawings, and inspection history. Condition categories were specified for different levels of deterioration for both steel and concrete structures. This approach ensured consistency and provided a means of identifying commonly recurring problems [Gallon 1993].

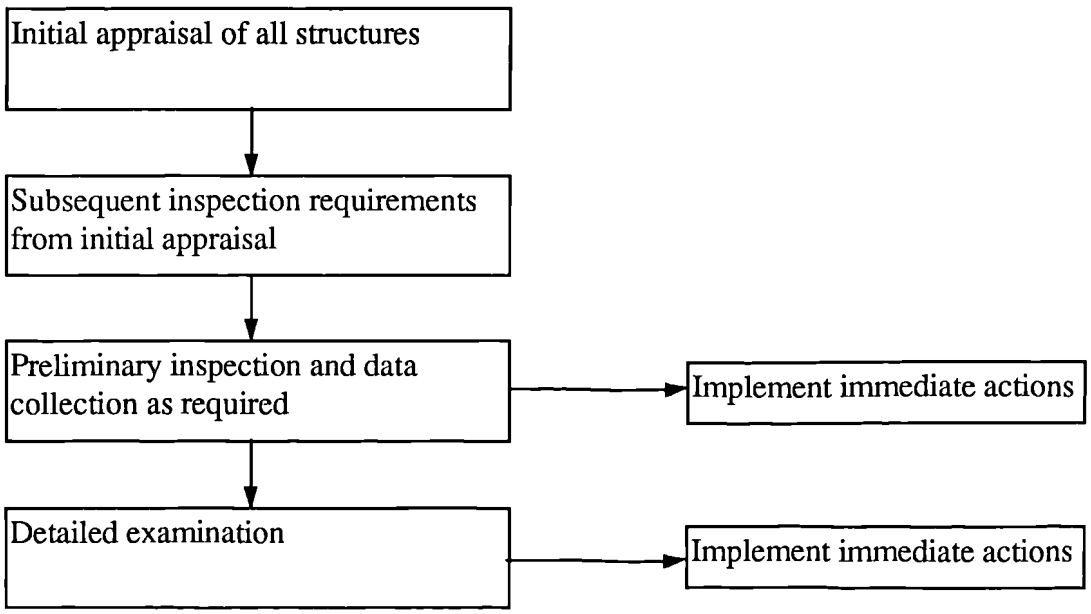

Figure 6.1 Inspection procedure (adapted from ICI Engineering 1990a)

The inspection methods adopted are primarily visual although thickness measurements using callipers are taken where more detail is required. Limited use of ultrasonics has been made because of its inability to penetrate thick protective coatings and corrosion products. However, there have been some recent developments in ultrasonics which overcome this problem [Cygnus Instruments Ltd 1995]. Structural design checks are carried out to appropriate codes and standards using re-assessed section properties based on measured section sizes and simple analytical models.

6.2.1 Condition categories

In the current visual assessment procedure of ICI Engineering [1990a], the preliminary inspection, which is basically a visual assessment, requires structural elements to be described using the defined condition categories, for which subsequent actions are prescribed. The description of these four condition categories for steel structures, and their associated actions are as follows:

1. Condition Category, V1
   Paint system intact with no signs of corrosion, sub-surface defects or previous repairs. This category is likely to apply only to recently installed steelwork or to internal steelwork in a dry environment.

2. Condition Category, V2
   Paint system intact but signs of surface pitting or loss of section on steel surface underneath. In this case, loss of section may have occurred, although now protected by an adequate paint system. Members that have obvious significant loss such as holed or noticeably thin sections will fall into category V4. However, it is possible that section loss greater than 15% may not be reported as corrosion category V4, unless a comprehensive programme of thickness measurement is undertaken.

3. Condition Category, V3
   Paint system breaking down or some areas unpainted, (loose scale to measurable pits likely on steel surface), structurally insignificant loss of section. If the section

loss is estimated as up to 15% of the gross section area and provided that the section loss is evenly distributed then it is taken as structurally insignificant loss of section. Members in category V3 may be stressed above their permissible working stress. Steelwork reported in this category will require thorough cleaning down or shot-blasting followed by repainting to an ICI Engineering Specification.

4. Condition Category, V4
   Significant loss of section, holing of members, member distorted, member missing or connection deficient. Significant loss of section is section loss estimated as greater than 15% of the gross section. Members in this category will require further investigation, repair, replacement or removal. Significant loss of section may not necessarily be structurally detrimental, since the member may only be lightly loaded or redundant altogether.

where 'V' prefix is to indicate that the classification has been made on the basis of a visual appraisal and no thickness measurements are involved. The 15% thickness loss is based on visual assessment.

These procedures, if properly carried out, provide invaluable assurance that structures for production plant are safe. However, it is possible that these assessments may be either conservative or even the opposite.

6.2.2 Disadvantages of current condition categories

The condition category V3 refers to members with loss of section estimated visually to be less than about 15%. The only subsequent action required in the case of category V3 is to arrest deterioration (thorough cleaning down or shot-blasting followed by repainting). However, using the minimum curves given in Section 5.10, the remaining capacity estimates for various types and conditions of beam when the loss of section is about 15% were found to vary between 67% and 85% of the as-new strength of the beams. In the worst case if there may be lateral torsional buckling, there is a possible capacity reduction of up to 33%, which can be significant in some cases, when the

section loss is about 15%. Some of the beams that come under this category may be weaker and the subsequent action prescribed for this category may not be appropriate for such beams. They may require other courses of action that should be relevant to the strength of these beams.

The category V4 refers to members with significant loss of section (loss of greater than 15% of the section area) and holing of member. Members reported in this category require further investigation, repair, replacement or removal. The holing of a member reduces the capacity significantly (see Chapter 4). However, overall section loss may not necessarily lead to significant reduction in capacity. When the loss of section is about 15%, the capacity loss was found to be only 15% for some types and conditions of beam. In practice, some members may be redundant or only lightly loaded and for such members even a significant loss of section may not lead to failure. Classification of such members into category V4 may cause false alarm and lead to unnecessary actions to be taken. The appropriate course of action for such beams may be the one that is prescribed for category V3 members.

Therefore, it would be most helpful if these condition categories could be related quantitatively to the remaining capacity of the members, instead of loss of section. If the condition categories are based on the remaining capacity, then the visual assessment procedure may help to avoid further investigation into the strength of corrosion damaged members and enable a reliable decision about their future.

6.3 Introduction of improved condition categories

In the previous chapter, a more precise method of assessment of remaining capacity of corrosion damaged steel beams has been proposed. In order to estimate the percentage remaining capacity of any corrosion damaged I-beam of all the manufactured sizes in the UK, minimum curves were developed that can be used in conjunction with the information on the thickness loss of the elements of the beams. They were developed for various failure modes of various types of I-beam. It was found that these minimum curves give almost exact estimates of the remaining capacity in some cases.

Using the assessment methods developed in Chapter 5 it may be possible to introduce improved condition categories based on the remaining capacity for the assessment of corrosion damaged steel beams. Following a visual assessment of the section loss of a beam, it is now possible, using the minimum curves, to relate this to the remaining capacity of the beam, which may be compared immediately with the service load. The remaining capacity may be readily obtained using the proposed equations for the minimum curves (Section 5.10). Therefore, corrosion damaged steel beams can be specified into different categories based on their remaining capacity. These categories may be called the Strength Categories as they are based on their remaining strength.

The review of the current visual assessment procedure shows that the condition categories V1 and V2 with minimal deterioration do not require any immediate action to be taken. Therefore, there is no need to improve these two categories as they are structurally sound. The condition categories V3 and V4 may be improved for the reasons given in the previous section. The proposed improved categories with an additional category, which are based on the capacity loss as well as the condition of beams, are as follows:

1. Strength Category, S1
   Similar to condition category V1.

2. Strength Category, S2
   Similar to condition category V2.

3. Strength Category, S3
   Structurally insignificant loss of capacity. Structurally insignificant loss of capacity may be taken as if the capacity loss is estimated to be up to 20% of the as-new strength. The condition of the members is similar to that of condition category V3, i.e. paint system breaking down or some areas unpainted but loss of section estimated visually to be less than 15%. However, for the above condition of members, if the capacity loss is estimated to be greater than 20% of the as-new strength, then they will fall into strength category S4. The subsequent action

required for this category is similar to the one prescribed for condition category V3, i.e. thorough cleaning down or shot-blasting followed by repainting.

4. Strength Category, S4

   Significant loss of capacity. Significant loss of capacity may be taken as if the capacity loss is estimated to be greater than 20% of the as-new strength. The condition of the members is taken as same as that of condition category V4 but members with holes, distorted members and damaged connections are excluded. The remaining capacity of these members may be compared immediately with the service loads. Depending on the outcome of the comparison, appropriate action may be taken. Members in this category may require repair, replacement or removal. It should be noted that further investigation may not be necessary, as the category is based on the remaining capacity. If the capacity loss is less than 20% of the as-new strength for members with above conditions, they will fall into strength category S3.

5. Strength Category, S5

   Holing of members, member distorted, or connection deficient. Members in this category will require further investigation, repair, replacement or removal.

where 'S' prefix is to indicate that the classification has been made mainly on the basis of the remaining strength.

The advantage of using these strength categories is that they enable reliable decisions to be taken about the subsequent course of action for a deteriorated member. If the deterioration is only an overall section loss, then these categories may not require further investigation as the strength of the members has already been established.

6.4 Summary and conclusions

The existing formal procedure for inspection of structural steelwork in the petro-chemical industry has been reviewed in this chapter. The review has helped us to identify

the disadvantages associated with the condition categories used in the current visual assessment procedure. It was found that the current form of classification of steel beams, which is based only on the condition of beams, may lead to inappropriate actions to be taken causing loss of production or even structural failures. The discussion on the disadvantages of the current condition categories clearly showed the necessity to improve these categories especially the condition categories V3 and V4 to ensure safe operation.

Using the knowledge obtained from the assessment methods developed in Chapter 5 improved condition categories called the Strength Categories have been proposed in this chapter. The classification of deteriorated steel beams into these categories is now based on both the capacity loss and the condition of the beams. This form of classification will allow the practising engineer to make a realistic appropriate course of action concerning the future of a deteriorated member. These strength categories may not require detailed investigation about the strength of a deteriorated member since the classification was already based on the remaining capacity of the member. It is believed that the use of these strength categories will avoid plant closures when the steelwork may be able carry the required service loads and avoid structural failures when service loads exceed the capacity of steelwork.

Chapter 7

Structural reliability

7.1 Introduction

Engineering decisions concerning the performance of existing structures must be made in the presence of uncertainties. These uncertainties arise from inherent randomness in the external loads on the structures and their capacity to withstand those external loads, imperfect modelling, insufficient data, and lack of experience. The remaining capacity of corrosion damaged steel structures is a good example of different aspects of uncertainty including: unknown or partially known extent of damage; variability in loading; uncertain reserve of structural capacity depending on mode of failure. While many of the factors that determine the performance of existing structures are uncertain, they nonetheless exhibit statistical regularity. Probability and statistics provide a framework for dealing with such uncertainties.

The theory of structural reliability has been developed to provide an appropriate method of analysis of structural safety. One of the main purposes of the reliability theory is to find the probability of safety, or the reliability function of a structure in a prescribed load environment during its service life. Since Freudenthal [1956] first introduced the concept of the probability of failure, the area of Probabilistic Risk Assessment has attracted the attention of many researchers and structural engineers (e.g. Cornell, Ditlevsen, Moses, Rackwitz, Hasofer, Melchers, Thoft-Christensen, Blockley). A great number of methods have been developed since then to evaluate structural reliability.

The main aim of this chapter is to review the current available methods for reliability of structural components and systems, and to introduce Interval Probability Theory for the reliability of structural systems. In particular it is intended to explore the usefulness of

modern reliability analysis when applied to the difficult decisions that have to be made regarding corrosion damaged steelwork.

The specific objectives of this chapter are:

1. To review the structural reliability theory.
2. To review the methods for component reliability.
3. To review the current methods for system reliability and their applications to steelwork.
4. To introduce Interval Probability Theory for system reliability.

7.2 Reliability of structures

The term structural reliability should be considered as having two meanings - a general one and a mathematical one.

1. In the most general sense, the reliability of a structure is its ability to fulfil its design purpose for some specified time.
2. In a narrow sense, it is the probability that a structure will not attain each specified limit state (ultimate or serviceability) during a specified reference period.

Because the majority of structural loads vary with time in an uncertain manner, the probability that any selected load intensity will be exceeded in a fixed interval of time is a function of the length of that interval (and possibly the time at which it begins). Hence, in general, the structural reliability is dependent on time of exposure to the loading environment. It is also affected if the material properties change with time. Only for the rare cases, when loads and strength are constant, can the reference period be ignored. In such cases, the loads are applied once and the structure either does or does not fail.

Structural reliability analysis is concerned with the calculation and prediction of the probability of failure for structures at any stage during their service life. The probability of failure of a structure is the probability that the resistance of the structure, R, will be

exceeded by the extreme load effect, S, during the reference period. The numerical value of the probability of failure is dependent on upon two radically different types of uncertainty - firstly, the physical variability of the extreme load effect and secondly, lack of knowledge about the true value of the resistance.

7.3 Basic variables and types of uncertainties

7.3.1 Basic variables

For the purpose of quantifying uncertainties in the field of structural engineering and for subsequent reliability analysis it is necessary to define a set of basic variables. These are defined as the set of quantities governing the static and dynamic response of the structure. Basic variables are quantities such as mechanical properties of materials, dimensions, unit weights, environmental loads, etc. They are basic in the sense that they are the most fundamental quantities normally recognised and used by the designers and analysts in structural calculations. Ideally basic variables should be chosen such that they are statistically independent quantities.

7.3.2 Types of uncertainties

For the purposes of structural reliability analysis it is necessary to distinguish between at least three types of uncertainties namely physical uncertainty, statistical uncertainty and model uncertainty.

7.3.2.1 Physical uncertainty

Whether or not a structure or structural element fails when loaded depends partly on the actual values of the relevant material properties that govern its strength. The reliability analysts therefore must be concerned with the nature of the actual variability of physical quantities such as loads, material properties and dimensions. Physical uncertainty can be reduced but not eliminated with greater availability of data, or greater effort in quality control. It is a fundamental property of the basic variables [Melchers 1987].

7.3.2.2 Statistical uncertainty

This is concerned with variations between the parameter values of a number of samples. For example, a hundred tests on the yield strength of coupons of nominally identical steel will show evidence of scatter. However, statistical properties such as mean and standard deviation will show stationary qualities. Statistical estimators such as the sample mean and higher moments can be determined from available data and then used to suggest an appropriate probability density function and associated parameters. For a given set of data, the distribution parameters may themselves be considered to be random variables, the uncertainty in which is dependent on the amount of sample data or in general, on the amount of data and any prior knowledge. This uncertainty is termed statistical uncertainty and arises solely as a result of lack of information.

7.3.2.3 Model uncertainty

This occurs as a result of simplifying assumptions in the analytical process, unknown boundary conditions and as a result of the unknown effects of other variables and their interactions that are not included in the mathematical model. In its simplest form, model uncertainty concerns the uncertainty of physical models, such as limit state equations. In many components and structures, model uncertainties have a large effect on structural reliability and should not be neglected.

7.4 Reliability of structural components

7.4.1 Limit state function

Structural reliability analysis begins with the formulation of a limit state function in terms of a number of basic random variables [Thoft-Christensen and Baker 1982]. The limit state function represents the performance of a structure or an element. The basic structural reliability problem considers only one load effect S resisted by one resistance R. Each of S and R are random variables and are described by known probability density functions (PDF) $f_S(\,)$ and $f_R(\,)$. In general, the limit state function is defined as follows:

$$M = R - S \tag{7.1}$$

where M is the 'safety margin' sometimes referred to as the 'failure indicator'. The limit state function represents the boundary beyond which the structure will no longer function. In terms of the safety margin, M, it is the point where the load effect, S, is greater than or equal to the resistance, R. A graphical representation of the random load effect and resistance is shown in Figure 7.1. It should be noted that, in reliability theory, different symbols are used for a random variable and its values. For example, 'S' is used for the random variable load effect and 's' is used for its values.

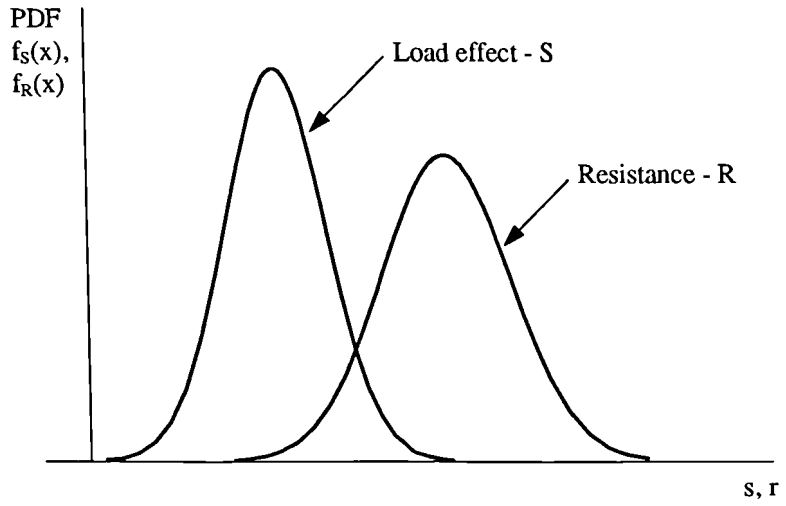

Figure 7.1 Load and Resistance distributions

The structural element will be considered to have failed if the resistance R is less than the load effect S (i.e. $M \leq 0$). If R and S are statistically independent then the probability of failure, P_f, of the structural element can be determined by the following equation [Freudenthal et al 1966]:

$$P_f = P(R-S \leq 0) = \int_{-\infty}^{+\infty} F_R(x) f_S(x) dx \tag{7.2}$$

where $F_R(x)$ is the cumulative probability distribution function (CDF) of R, defined as $F_R(x) = P(R < x)$, or the probability that the actual resistance R of the member is less

than some value x. The term $f_S(x)$ is the PDF of S, which represents the probability that the load effect S acting in the member has a value between x and $(x + \Delta x)$ in the limit as Δx approaches zero. By considering all possible values of x, i.e. by taking the integral over all x, the probability of failure is obtained.

It should be noted that R and S must necessarily have the same dimensions (e.g. loads and load carrying capacity). This integral is also known as a "convolution integral". For the general case, closed form solutions do not exist for the convolution integral (Equation 7.2). There are, however, a number of distributions for which it is possible to integrate the convolution integral. Two such distributions are given below.

1) If R and S are independent normally distributed variables, P_f may be given by [Melchers 1987]:

$$P_f = P(M \leq 0) \quad \text{where,} \quad M = R - S \tag{7.3a}$$

$$P_f = P(R - S \leq 0) \tag{7.3b}$$

The mean, μ_M, and the variance, Var[M], of the safety margin, M, can be expressed as:

$$\mu_M = E[M] = \mu_R - \mu_S \quad \text{and} \tag{7.4}$$

$$\text{Var}[M] = \sigma_M^2 = \sigma_R^2 + \sigma_S^2 \tag{7.5}$$

Since R and S are normal variables, M, which is a linear function of R and S, is also normally distributed. Equation 7.3a then becomes (see Appendix A),

$$P_f = \Phi\left(\frac{0 - \mu_M}{\sigma_M}\right) \tag{7.6}$$

which gives the probability of failure as,

$$P_f = \Phi\left(-\frac{\mu_R - \mu_S}{\sqrt{\sigma_R^2 + \sigma_S^2}}\right) \tag{7.7}$$

Where Φ is the standard normal distribution function, which is given by:

$$\Phi_X(x) = \int_{-\infty}^{x} \frac{1}{\sqrt{2\pi}} \exp\left(-\frac{t^2}{2}\right) dt \qquad (7.8)$$

μ_R and μ_S are the means of R and S, and

σ_R and σ_S are the standard deviations of R and S respectively.

The term within the brackets of Equation 7.6 is defined as the reliability index, β, [Cornell 1969] and is given by:

$$\beta = \frac{\mu_M}{\sigma_M} = \frac{\mu_R - \mu_S}{\sqrt{\sigma_R^2 + \sigma_S^2}} \qquad (7.9)$$

A graphical interpretation of the reliability index is shown in Figure 7.2. The reliability index, β, is equal to the ratio μ_M / σ_M or the number of standard deviations by which μ_M exceeds zero. The reliability index, β, is widely used as a measure of safety or measure of reliability of a structure.

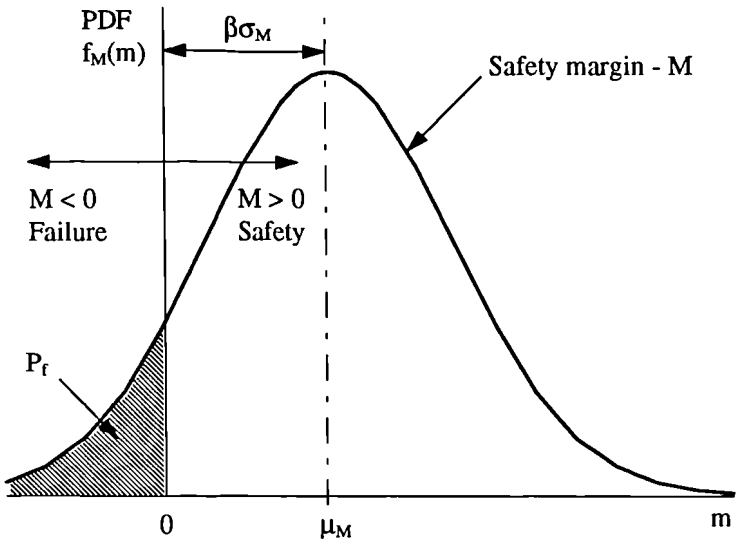

Figure 7.2 Distribution of the safety margin, M, and illustration of the reliability index, β

2) If R and S are independent and log-normally distributed variables, P_f may be given by:

$$P_f = P(M' \leq 1) \qquad \text{where,} \qquad M' = R/S \tag{7.10}$$

Taking logarithms to the base 'e' and putting $M = \ln M'$ gives,

$$M = \ln R - \ln S = A - B \tag{7.11a}$$

where $A = \ln R$ and $B = \ln S$

Failure occurs when $M' \leq 1$ or when $M \leq 0$. If R and S are log-normally distributed, then A and B are normally distributed, so that M is also normally distributed. Thus,

$$P_f = P(M \leq 0) \tag{7.11b}$$

$$\mu_M = E[M] = \mu_A - \mu_B = \mu_{\ln R} - \mu_{\ln S} \tag{7.12}$$

$$\sigma_M^2 = Var[M] = \sigma_A^2 + \sigma_B^2 = \sigma_{\ln R}^2 + \sigma_{\ln S}^2 \tag{7.13}$$

$$P_f = \Phi\left(-\frac{\mu_A - \mu_B}{\sqrt{\sigma_A^2 + \sigma_B^2}}\right) = \Phi\left(-\frac{\mu_{\ln R} - \mu_{\ln S}}{\sqrt{\sigma_{\ln R}^2 + \sigma_{\ln S}^2}}\right) \tag{7.14}$$

The properties of the log-normal distribution are such that if Y is log-normally distributed and $X = \ln Y$, then

$$\sigma_X^2 = \ln\left[V_Y^2 + 1\right] \tag{7.15a}$$

$$\tilde{m}_Y = \mu_Y \exp\left(-\sigma_X^2/2\right) \tag{7.15b}$$

$$\mu_X = \ln\left(\tilde{m}_Y\right) \tag{7.15c}$$

where $\tilde{m}_Y$ is the median of Y and V_Y is the coefficient of variation of Y.

For many problems the simple formulations are not entirely adequate, since it may not be possible to reduce the structural reliability problem to a simple R versus S formulation

with R and S independent random variables. In general, R is a function of material properties and element or structural dimensions, while S is a function of applied loads, material densities and perhaps dimensions of the structure. Also R and S may not be independent, such as when the same dimensions affect both R and S. In this case it is not valid to use the convolution integral (Equation 7.2). It is also not valid when there is more than one applied stress resultant acting at a section, or more than one factor contributing to the resistance of the structure.

In such cases, the best solution to the problem is to express each limit state equation or failure function in terms of the set of n basic variables, $\overline{X}$, where $\overline{X} = X_i = X_1, X_2, ..., X_n$, which affect the structural performance, such that

$$M = G(X_1,X_2,...,X_n) \leq 0 \tag{7.16}$$

corresponds to failure. In general the function (Equation 7.16) can take any form provided that $M \leq 0$ corresponds to a failure state and $M > 0$ to a safe state. The equation, $G(X_1,X_2,...,X_n) = 0$, defines an $(n - 1)$-dimensional hyper-surface in the n-dimensional basic variable space. This surface is commonly referred to as the 'failure surface' or 'failure boundary' for the limit state under consideration. The failure boundary divides all possible combinations of the variables, $\overline{X}$, which cause failure from all possible combinations which do not cause failure.

The probability of failure is equivalent to the integration of the joint distributions over the failure region and is given by:

$$\begin{aligned} P_f = P(M \leq 0) &= \int ... \int f_{X_1,X_2,...,X_n}(x_1,x_2,...,x_n)dx_1dx_2...dx_n \\ &= \int ... \int f_{\overline{X}}(\overline{x})dx_1dx_2...dx_n \end{aligned} \tag{7.17}$$

where $f_{X_1,X_2,...,X_n}(x_1,x_2,...,x_n)$, or $f_{\overline{X}}(\overline{x})$, is the joint probability density function for the n basic variables $\overline{X}$.

The multi-variant integration of the joint probability density function is very difficult and time consuming because firstly the integration is numerically complex and secondly there is almost never sufficient data to define the joint probability density function for the n basic variables [Shinozuka 1983]. Analytical solutions for this formulation (Equation 7.17) do not exist for the majority of practical problems. These difficulties can be overcome in practice by using approximate methods, which were developed to determine the probability of failure, such as First Order Second Moment method (FOSM). The only other possibility is to use Monte Carlo simulation.

7.4.2 First Order Second Moment (FOSM) method

The difficulties in evaluating the probability of failure for general reliability problems motivated the development of the FOSM method. The following procedure was suggested by Melchers [1987].

A linear limit state function, $G(\overline{X})$, of the n basic random variables, $X_1,X_2,...,X_n$, may be expressed as follows:

$$M = G(\overline{X}) = a_0 + a_1X_1 + a_2X_2 + ... + a_nX_n \tag{7.18}$$

If the variables, $X_1,X_2,...,X_n$, are normally distributed random variables then the function, $G(\overline{X})$, is also normally distributed, and the mean, μ_M, and variance, σ_M^2, are given by:

$$\mu_M = a_0 + a_1 \mu_{X_1} + a_2 \mu_{X_2} + ... + a_n \mu_{X_n} \tag{7.19}$$

$$\sigma_M^2 = a_1^2 \sigma_{X_1}^2 + ... + a_n^2 \sigma_{X_n}^2 + \sum_{i=1}^{n} \sum_{j=1, j\neq i}^{n} \gamma_{X_iX_j} a_i a_j . \sigma_{X_i} \sigma_{X_j} \tag{7.20}$$

where the last term of Equation 7.20 accounts for correlation between any pair of basic variables and $\gamma_{X_iX_j}$ is a correlation coefficient which is given by:

$$\gamma_{X_iX_j} = \frac{E[(X_i - \mu_{X_i})(X_j - \mu_{X_j})]}{\sigma_{X_i} \sigma_{X_j}} \tag{7.21}$$

The reliability index β is defined by [Cornell 1969]:

$$\beta = \frac{\mu_M}{\sigma_M} \tag{7.22}$$

In general, it is not possible to evaluate the probability of failure given by Equation 7.17 directly from the reliability index, β, defined by equation 7.22. This is because, in some cases, it may not be possible to calculate the mean and standard deviation of the safety margin M and hence the reliability index, β. However, if the limit state function is linear and the basic random variables are normally distributed, then the following functional relationship may be obtained:

$$P_f = \Phi(-\beta) \tag{7.23}$$

If the limit state function, $G(\overline{X})$, is non-linear in the n basic random variables, $\overline{X}$, then the function will not be normally distributed even if all variables are normally distributed [Melchers 1987]. In this case, the actual non-linear function may be approximated by a linear function by the first order Taylor series expansion in order to obtain approximate values for the mean and standard deviation of the safety margin M (hence the term 'First Order' in FOSM).

Second moment means that each random variable is represented only by its first two moments, i.e. by its mean and standard deviation (or variance). Equation 7.9 shows that the reliability index, β, depends only on the means and standard deviations of the random variables rather than on their complete distributions (hence the term 'Second Moment' in FOSM). The second moment properties of random variables provide the most basic descriptions of the uncertainty represented in full by their probability distributions.

Let the limit state function, $G(\overline{X})$, be non-linear in the basic random variables $\overline{X} = X_1,X_2,...,X_n$,

$$M = G(\overline{X}) = G(X_1,X_2,...,X_n) \tag{7.24}$$

The first order Taylor series expansion keeping only the linear terms of Equation 7.24 around the means of the random variables, μ_{Xi}, i.e. around $X_i = \mu_{Xi}$, can be expressed as follows:

$$M = G(\overline{X}) \approx G(\mu_{X_1}, \mu_{X_2}, \ldots, \mu_{X_n}) + \sum_{i=1}^{n} \frac{\partial G}{\partial X_i}(X_i - \mu_{X_i}) \tag{7.25}$$

Using Equation 7.25, approximate values of the mean and standard deviation of M were determined by [Melchers 1987]:

$$\mu_M \approx G(\mu_{X_1}, \mu_{X_2}, \ldots, \mu_{X_n}) \tag{7.26}$$

$$\sigma_M^2 = \sum_{i=1}^{n} \sum_{j=1}^{n} \frac{\partial G}{\partial X_i} \frac{\partial G}{\partial X_j} \gamma_{X_i X_j} \sigma_{X_i} \sigma_{X_j} \tag{7.27}$$

When the variables are not normally distributed or the limit state function is non-linear, the probability of failure given by Equation 7.23 does not hold exactly. The probability of failure obtained by this formula is called the nominal value of the probability of failure [Blockley 1980]. It is obvious that the reliability index, $\beta = \mu_M / \sigma_M$, depends on the point, X_i, around which the limit state function $G(\overline{X})$ was expanded. The reliability index will also change when different but equivalent non-linear limit state functions are used [Thoft-Christensen and Baker 1982].

The determination of the reliability index based on Equation 7.22 can be inaccurate. Errors may arise because of possible non-linearities in the limit state function and because the basic variables may be correlated or non-normal. A more consistent definition of the reliability index has been developed by Hasofer and Lind [1974] based on the transformation of the variables to an independent standard normal space. The reliability index found using this method is failure function invariant because all equivalent failure functions result in the same failure boundary [Thoft-Christensen and Baker 1982].

7.4.3 Monte Carlo simulation

7.4.3.1 Direct sampling (crude Monte Carlo) method

The evaluation of the probability of failure given by Equation 7.17 requires that the joint PDF, $f_{\overline{X}}(\overline{x})$, be integrated over the failure region of x in which $G(\overline{X}) \leq 0$. If $G(\overline{X})$ can be expressed as a sum of normal variables or as a product of log-normal variables, the multi-dimensional integration can be reduced to a one-dimensional integration (e.g. Equations 7.3 and 7.10). If the variables are not normally distributed or $G(\overline{X})$ is non-linear, the integration of Equation 7.17 is difficult and usually cannot be performed in closed form. One solution to the above problem is a Monte Carlo simulation.

A Monte Carlo simulation is a numerical experiment [Rubenstein 1981]. This method involves sampling at random to simulate artificially a large number of experiments and to observe the result. The usefulness of this method is commonly recognised in solving integrals, integral and differential equations [Schueller and Stix 1986].

Consider a limit state function $G(\overline{X})$ of n basic random variables $X_1,X_2,...,X_n$, which are independent with known distribution functions,

$$M = G(\overline{X}) = G(X_1,X_2,...,X_n) \tag{7.28}$$

The mathematical expected value (mean) of M is determined by:

$$E[M] = J = \int_{-\infty}^{\infty} \int_{-\infty}^{\infty} G(\overline{x}) f_{\overline{X}}(\overline{x}) dx_1 dx_2 ... dx_n \tag{7.29}$$

The Monte Carlo approach is to use appropriate random number generators [Rubenstein 1981] to generate independent sample values x_i for each of the basic variables X_i and to determine the corresponding value of the safety margin M using the following equation,

$$m = G(x_1,x_2,...,x_n) \tag{7.30}$$

If the above corresponding value m of the safety margin M is less than or equal to zero, then the structural element has failed. This experiment is repeated many times, each time with randomly chosen sample values x_i to simulate the probability distribution for M by progressively building up a larger sample.

Let $\overline{x}_j = (x_{1j},x_{2j},...,x_{nj})$ represent an outcome from one simulation out of N trials and let $m_j = G(\overline{x}_j)$. Repeating the experiment N times, the expected value (mean) of the safety margin M may be estimated as:

$$J_1 \approx \frac{1}{N}\sum_{j=1}^{N} G(\overline{x}_j) \tag{7.31}$$

The expected value of the estimated mean J_1 may be expressed as:

$$E[J_1] = E\left[\frac{1}{N}\sum_{j=1}^{N} G(\overline{x}_j)\right] = \frac{1}{N} N\, E[M] = E[M] = J \tag{7.32}$$

so that the estimated mean J_1 is an unbiased estimator of J [Melchers 1987]. The sample variance is given by:

$$\sigma^2_{J_1} = \sum_{j=1}^{N} \frac{1}{N^2} Var[G(\overline{x}_j)] = \frac{1}{N^2} N\, Var[M] = \frac{1}{N}\sigma^2_M \tag{7.33}$$

Now, the probability of failure given by Equation 7.17 may be written in a special form. To do this, define an indicator function as:

$$I_f(\overline{x}) = \begin{cases} 1 & \text{if } G(\overline{X}) \le 0 \\ 0 & \text{if } G(\overline{X}) > 0 \end{cases} \tag{7.34}$$

The probability of failure given by Equation 7.17 can then be expressed as:

$$P_f = P(M \le 0) = \int_{-\infty}^{\infty} \cdots \int_{-\infty}^{\infty} I_f(\overline{x}) f_{\overline{X}}(\overline{x}) dx_1 dx_2 ... dx_n \tag{7.35}$$

If Equations 7.29 and 7.35 are compared then it is clear that Equation 7.35 represents the expected value of $I_f(\overline{x})$. Therefore, the probability of failure may be given as:

$$P_f = P(M \leq 0) = E[I_f(\overline{x})] \tag{7.36}$$

Thus to compute the probability of failure by Monte Carlo simulation (using Equations 7.31 and 7.36),

$$P_f \approx \frac{1}{N}\sum_{j=1}^{N} I_f(\overline{x}_j) = \frac{k}{N} \tag{7.37}$$

where k is the number of trials in which the structural element has failed, i.e. $G(\overline{X}) \leq 0$, and N is the total number of Monte Carlo trials.

Clearly, the accuracy of the probability of failure found using this method depends on the number of trials conducted. In general, the exact probability distribution for M will not be of any form, although it may be governed by the form of the probability distribution of the most dominant basic variable. The most serious deficiency of the above method is that it is time consuming. This is particularly so when the probabilities of failure are low, since the vast majority of the samples fall in the safe region in this case.

7.4.3.2 Importance sampling

Equation 7.33 shows that the standard deviation of J_1 and hence of the Monte Carlo estimate (Equation 7.37) varies directly with the standard deviation of M and inversely with $N^{1/2}$. There are two ways to increase the accuracy of Monte Carlo estimate: (a) increase N, and (b) reduce the standard deviation of M [Melchers 1987]. Increasing N may become very costly in analysing the safety of complex systems in which the desired probabilities of failure are small. Variance reduction techniques aim at reducing the standard deviation for samples of a finite size by either modifying the random sampling process or utilising prior knowledge in formulating the problem to be solved. One way to gain this prior knowledge is through a direct crude Monte Carlo simulation. Results

from this simulation can then be used to define variance reduction techniques that will refine and improve the efficiency of a second simulation [Rubenstein 1981]. Therefore the more that is known about the problem, the more effective the variance reduction techniques that can be employed.

One of the variance reduction techniques is importance sampling which has been used successfully in structural reliability analysis [Schueller and Stix 1986]. The basic idea of this technique consists of concentrating the distribution of the sample points in the parts of the region that are of most "importance" instead of spreading them out evenly [Rubenstein 1981]. Hence, an appropriate important sampling PDF, $h_v(\bar{x})$, is chosen instead of the original PDF, $f_{\bar{X}}(\bar{x})$, in order to reduce the standard deviation of J_1.

Let us consider the probability of failure given by Equations 7.17 and 7.37. The probability of failure given by Equation 7.17 may be written as:

$$P_f = \int_{-\infty}^{\infty} \cdots \int_{-\infty}^{\infty} \frac{I_f(\bar{x}) f_{\bar{X}}(\bar{x})}{h_v(\bar{x})} h_v(\bar{x}) dx_1 dx_2 \cdots dx_n = E\left[\frac{I_f(\bar{x}) f_{\bar{X}}(\bar{x})}{h_v(\bar{x})}\right] \tag{7.38}$$

The probability of failure estimate given by Equation 7.37 becomes,

$$P_f \approx \frac{1}{N} \sum_{j=1}^{N} \frac{I_f(\bar{x}_j) f_{\bar{X}_j}(\bar{x}_j)}{h_v(\bar{x}_j)} \tag{7.39}$$

The standard deviation of J_1 can be shown to become negligibly small for a given N, if the PDF $h_v(\bar{x})$ is chosen as [Rubenstein 1981]:

$$h_v(\bar{x}) = \frac{I_f(\bar{x}) f_{\bar{X}}(\bar{x})}{P_f} \tag{7.40}$$

The function $h_v(\bar{x})$ is known as the importance sampling function. It is evident from Equation 7.40 that the probability of failure to be determined is needed for choosing the function $h_v(\bar{x})$ and this is not very helpful. However, it is clear that, even if the probability of failure is only approximately evaluated, the variance of J_1 can be reduced.

For the importance sampling function, $h_v(\overline{x})$, Schueller and Stix [1986] suggested the use of a normal probability density function with the mean at the design point and the covariance matrix being identical to the covariance matrix of the original random variables, X_i. The design point, which is the shortest distance from the origin to the failure boundary (see Figure 7.3), defined by $G(\overline{X}) = 0$, may be calculated using optimisation procedures generally available for solving non-linear constrained programming problems [Bourgund and Bucher 1986]. The above suggested distribution function for $h_v(\overline{x})$ will give greater sampling density in the neighbourhood of the region where it is of most importance.

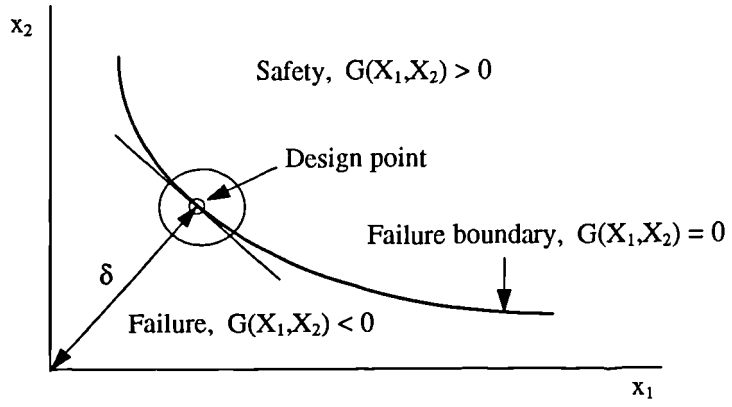

Figure 7.3 Design point for a two dimensional case

The effectiveness of the method depends on how good an important sampling function can be selected [Ellingwood 1992]. The advantages of importance sampling technique are that all calculations can be performed in the original X space, regardless of the type of the random variable, and it has considerable potential to reduce the number of samples and hence the required computing time [Melchers 1987].

In the next chapter, for the computation of probability of failure of components, a software package called ISPUD (**I**mportance **S**ampling **P**rocedure **U**sing **D**esign points) written by Bourgund and Bucher [1986] will be used. This package is a multi-purpose program for general reliability analysis and computes the probability of failure using

importance sampling technique in connection with an optimisation procedure for the calculation of the design point.

7.5 Reliability of structural systems

The reliability of a real structure is usually much more difficult to evaluate than the reliability of a single structural member with a single failure mode. In most structures several elements or members contribute to their performance. In addition, even in simple structures composed of just one element, various limit states such as moment, shear, buckling, axial stress, deflection, etc., may all need to be considered. Such a composition is referred to as a "structural system". The reliability of a structural system will be a function of the reliability of its members for the following reasons:

1. Load effects on different members are obtained from one or more common loads.
2. Loads and resistance may not be independent.
3. Correlation of member strength properties may exist between different locations in the structure.
4. Construction practices may influence member strength for a group of members.
5. The configuration of the structure and the possible existence of limit states for the structure as a whole (e.g. overall deflection, foundation settlement, etc.).

The reliability assessment of structural systems, therefore, will involve considering multiple correlated or uncorrelated limits states.

The mechanical properties of the structural elements are of great importance in the structural reliability analysis. Two abstract models of perfectly brittle and perfectly ductile are widely assumed [Thoft-Christensen and Baker 1982]. A structural element is called perfectly brittle, if it becomes ineffective after failure, i.e. if it loses its load carrying capacity completely (see Figure 7.4a). If an element maintains its load level after failure then it is called perfectly ductile. A typical example of perfectly ductile behaviour is shown in Figure 7.4b.

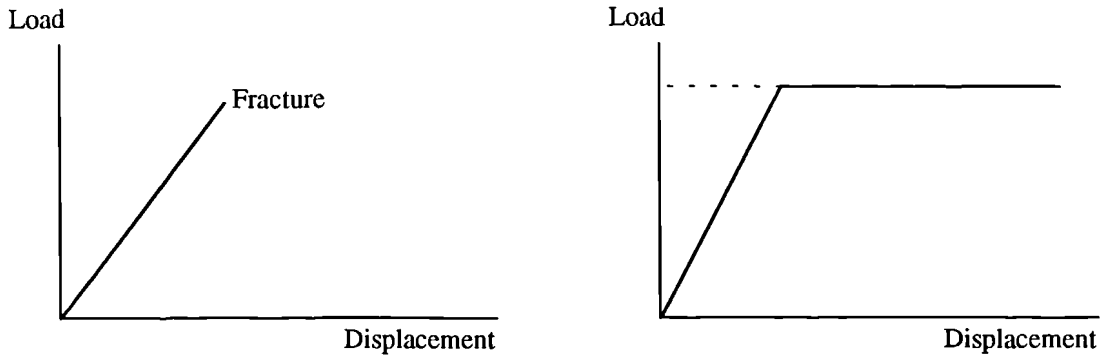

(a) Perfectly brittle behaviour (b) Perfectly ductile behaviour

Figure 7.4 Structural element behaviours

There are two fundamental types of systems, namely series systems and parallel systems [Ditlevsen and Bjerager1986]. A system of single elements is a series system if it is in a state of failure whenever any one of its elements fails. Such a system is also called weakest-link system. A typical example of a series system is a statically determinate structure as shown in Figure 7.5a. Failure of a single member in a structural system will not always result in failure of the total system as in the case of statically indeterminate structures. Failure of such structures will always require that more than one element fails and such a set of elements is called a parallel system. A parallel system with perfectly ductile elements is shown Figure 7.5b.

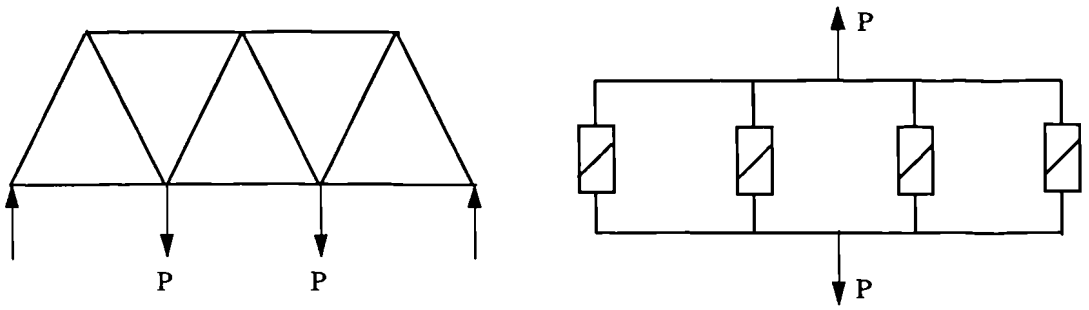

(a) Series system (b) Parallel system

Figure 7.5 Fundamental types of systems

It should be noted that for a series system the distinction between brittle and ductile elements is irrelevant because the total system fails as soon as one element fails whether it is brittle or ductile. However, the behaviour of parallel system depends to a higher degree on whether the elements are perfectly ductile or perfectly brittle because a system with all of its elements in parallel will only fail when all the elements in that system fail.

The calculation of overall system reliability (or probability of failure) is very difficult. The difficulty is caused by identifying which elements will fail, and in what sequence. The problem is further complicated by possible correlation between separate elements.

7.5.1 Failure modes approach

One approach that can be used for the reliability analysis of structural systems is the failure modes approach. This approach is based on the identification of all possible failure modes for the structural system. For example, four possible failure modes of a beam are given in Figure 7.6 (in this case, the beam can be considered as a system). Since the failure of any one mode implies the failure of the beam, the overall failure of the beam is the union of all four failure modes.

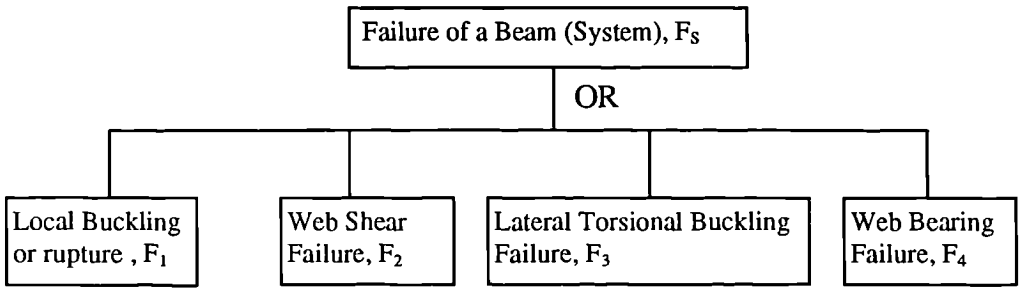

Figure 7.6 Possible failure modes of a beam

The overall probability of failure of the beam may be given by:

$$P_f = P(F_S) = P(F_1 \cup F_2 \cup F_3 \cup F_4) \qquad (7.41)$$

A real complex structure is generally neither series nor parallel. The structure will be described by a number of failure modes. Each failure mode is modelled by a parallel system and these parallel systems are then combined as a series system [Melchers 1987].

In general, if there are m failure modes, F_i, then:

$$P_f = P(F_S) = P(F_1 \cup F_2 \cup ... \cup F_m) \tag{7.42}$$

For each failure mode, a sufficient number of members must fail, thus,

$$P(F_i) = P(F_{i1} \cap F_{i2} \cap ... \cap F_{in}) \tag{7.43}$$

where F_{ij} is the event of failure of the member j in the failure mode i.

A very special case is that if F_{i1}, F_{i2},..., F_{in} are independent, then

$$P(F_i) = P(F_{i1})P(F_{i2}) ... P(F_{in}) \tag{7.44}$$

and if F_1, F_2,..., F_m are also independent, then

$$P_f = P(F_S) = 1 - \prod [1 - P(F_i)] \tag{7.45}$$

where, i = 1, 2, ..., m

However, in practical problems, the above case is very rare. Most probably the member failure events and the failure modes are dependent. Under these circumstances, the exact determination of the probability of failure of structural systems is not possible. A numerical calculation is often rather time consuming. Therefore upper and lower bounds for the exact probability of failure have been proposed [Cornell 1967]. Two bounds, proposed by Cornell [1967] and Ditlevsen [1979b], are widely used. The practical value of such bounds depends on how narrow they are.

7.5.2 Cornell's bounds

Simple upper and lower bounds for the probability of failure can be derived for a series system. If the failure modes are independent, then the probability of failure of a structural system is given by Equation 7.45.

$$P_f = P(F_S) = 1 - \prod [1 - P(F_i)]$$

where $P(F_i)$ is the probability of failure of the failure mode i as before.

If $P(F_i) << 1$, then Equation 7.45 may be approximated by the following equation as [Freudenthal et al 1966]:

$$P_f = P(F_S) \approx \sum_{i=1}^{m} P(F_i) \qquad (7.46)$$

In the case where all failure modes are fully dependent, the weakest failure mode will always be weakest, irrespective of the random nature of the strength [Melchers 1987]. Hence,

$$P_f = P(F_S) = \text{Max } [P(F_i)] \qquad (7.47)$$

Using Equations 7.45 or 7.46 and 7.47, the following bounds for the probability of failure of any structural system of the series type when the failure modes are neither completely independent nor fully dependent can be obtained [Cornell 1967]:

$$\text{Max } [P(F_i)] \leq P(F_S) \leq 1 - \prod [1 - P(F_i)] \qquad (7.48)$$

For many practical structural systems the Cornell's bounds are too wide to be meaningful [Grimmelt and Schueller 1982]. The bounds are too wide because they were obtained for the extreme cases of perfect dependence and independence.

7.5.3 Ditlevsen's narrow bounds

Consider a structural system of the series type that may fail in m different failure modes. The probability of failure of such system can be given by Equation 7.42.

$$P_f = P(F_S) = P(F_1 \cup F_2 \cup ... \cup F_m)$$

The above expression may be written as:

$$\begin{aligned} P(F_S) &= P(F_1) \\ &\quad + P(F_2) - P(F_1 \cap F_2) \\ &\quad + P(F_3) - P(F_1 \cap F_3) - P(F_2 \cap F_3) + P(F_1 \cap F_2 \cap F_3) \\ &\quad + P(F_4) - .... \\ &= \sum_{i=1}^{m} P(F_i) - \sum\sum_{i<j}^{m} P(F_i \cap F_j) + \sum\sum\sum_{i<j<k}^{m} P(F_i \cap F_j \cap F_k) - ..... \end{aligned} \quad (7.49)$$

It is clear from Equation 7.49 that an upper bound for the $P(F_S)$ can be obtained, if only the first order terms, i.e. $P(F_i)$, are considered because of the alternating signs as the order of the term increases. If only the first and second order terms, i.e. $P(F_i)$ and $P(F_i \cap F_j)$, are considered then a lower bound will be obtained.

It should also be clear that consideration of an additional failure mode cannot reduce the probability of failure, so that each complete line in Equation 7.49 makes a non-negative contribution to $P(F_S)$. Noting that $P(F_i \cap F_j) \geq P(F_i \cap F_j \cap F_k)$,..., a lower bound for $P(F_S)$ can be obtained by considering only the first and second order terms, provided that each makes a non-negative contribution [Ditlevsen 1979b] and be given as:

$$P(F_S) \geq P(F_i) + \sum_{i=2}^{m} \text{Max}\left[\left(P(F_i) - \sum_{j=1}^{i-1} P(F_i \cap F_j)\right), 0\right] \quad (7.50)$$

An upper bound may be obtained by simplifying each line in Equation 7.49. Let us consider line 3 of Equation 7.49.

$$U_3 = P(F_3) - P(F_1 \cap F_3) - P(F_2 \cap F_3) + P(F_1 \cap F_2 \cap F_3)$$
$$= P(F_3) - P((F_1 \cap F_3) \cup (F_2 \cap F_3)) \quad (7.51)$$

For any pair of events A and B it is well known that $P(A \cup B) \geq \text{Max}\,[P(A), P(B)]$. Hence,

$$P((F_1 \cap F_3) \cup (F_2 \cap F_3)) \geq \text{Max}\,[P(F_1 \cap F_3), P(F_2 \cap F_3)] \quad (7.52)$$

If Equation 7.52 is substituted in to Equation 7.51, the right hand side of Equation 7.51 will be increased. Therefore,

$$U_3 \leq P(F_3) - \text{Max}\,[P(F_1 \cap F_3), P(F_2 \cap F_3)] \quad (7.53)$$

Since line 3 was a typical example, an upper bound for $P(F_S)$ can be given by [Ditlevsen 1979b]:

$$P(F_S) \leq \sum_{i=1}^{m} P(F_i) - \sum_{i=2,i<j}^{m} \text{Max}\,[P(F_i \cap F_j)] \quad (7.54)$$

The ordering of the failure modes may influence the right hand side of Equations 7.50 and 7.54 [Ditlevsen 1979b]. A useful rule of thumb is to order the failure modes in the order of decreasing importance. Following the same idea of Ditlevsen [1979b], if the higher order terms of Equation 7.49 are considered, even narrower bounds than those of Ditlevsen can be obtained. However, the calculation of higher order intersections needs more information and is much more difficult.

7.6 Interval Probability Theory for system reliability

Recently a method for the computation of the reliability of structural systems based on Interval Probability Theory (IPT) was proposed by Cui and Blockley [1991]. It was suggested that IPT is relatively simple and robust theory for practical computation. This method involves computing the reliabilities of each individual failure mode using Monte

Carlo simulation or FOSM method and then computing the reliability of the system in terms of the reliabilities of each individual failure mode using IPT.

7.6.1 Review of probability theory

A complete set of all possible outcomes of any random phenomenon is called its sample space, Ω, and each individual outcome is a sample point. An event A is any subset of the sample space ($A \subset \Omega$). An event A has occurred if the outcome of the random phenomenon has sample points that are members of A. If it contains no sample points it is called an impossible event. A certain event contains all the sample points in the sample space, i.e. a certain event is equal to the sample space itself. The Kolmogarov axioms of probability theory are important and are given below:

$0 \leq P(A) \leq 1$

$P(\Omega) = 1$ and

$P(A) + P(-A) = 1$

where P(A) is the probability of the event A.

If A and B are mutually exclusive events (i.e. $P(A \cap B) = 0$), then

$P(A \cup B) = P(A) + P(B)$

7.6.2 Degree of dependence

In classical probability theory, the use of the independence assumption is often required. Zadeh (1986) argued that very often the relations among proposition or event sets are dependent in nature. A new parameter, ρ, called degree of dependence was defined by Cui and Blockley [1990] in order to describe the dependence relation between events. This parameter allows a wider interpretation of the range of possible assumptions about dependence and explains that different models of dependence can be used in probability theory.

For any events A and B with probabilities P(A) and P(B), the union is given by:

$$P(A \cup B) = P(A) + P(B) - P(A \cap B) \tag{7.55}$$

Now it is clear that,

$$\text{Max}\,[0, P(A) + P(B) - 1] \leq P(A \cap B) \leq \text{Min}\,[P(A), P(B)] \quad \text{and} \tag{7.56}$$

$$\text{Max}\,[P(A), P(B)] \leq P(A \cup B) \leq \text{Min}\,[1, P(A) + P(B)] \tag{7.57}$$

The degree of dependence, ρ_{AB}, between events A and B was defined as [Cui and Blockley 1990]:

$$\rho_{AB} = \frac{P(A \cap B)}{\text{Min}\,[P(A),\ P(B)]} \tag{7.58}$$

Thus

$\rho_{AB} = 0$ indicates that A and B are mutually exclusive,

$\rho_{AB} = 1$ indicates that A and B are maximally dependent (i.e. $A \subset B$ or $B \subset A$), and

$0 < \rho_{AB} < 1$ indicates that A and B are neither minimally nor maximally dependent.

These can be shown in Venn diagram as in Figure 7.7.

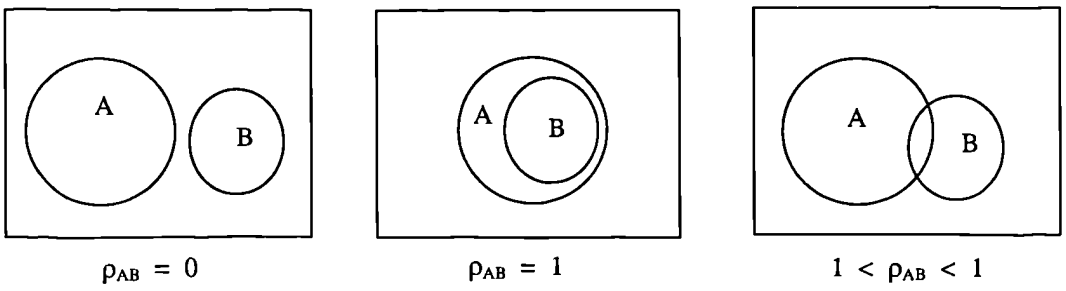

Figure 7.7 Venn Diagram representation of degree of dependence

The intersection and union between events A and B can be expressed as a function of degree of dependence, ρ_{AB}, as:

$$P(A \cap B) = \rho_{AB} \text{ Min } [P(A), P(B)] \quad \text{and} \tag{7.59}$$

$$P(A \cup B) = P(A) + P(B) - \rho_{AB} \text{ Min } [P(A), P(B)] \tag{7.60}$$

Thus the parameter ρ models the dependency relation between A and B, knowing ρ is equivalent to knowing $P(A \cap B)$. Special cases of degree of dependence which have been proposed by Cui and Blockley [1991] are as follows:

a) Mutually exclusive, $\rho_{AB} = 0$

Therefore,

$$P(A \cap B) = 0 \quad \text{and} \tag{7.61a}$$

$$P(A \cup B) = P(A) + P(B) \tag{7.61b}$$

b) Independence, $\rho_{AB} = \text{Max } [P(A), P(B)]$

Therefore

$$P(A \cap B) = P(A).P(B) \quad \text{and} \tag{7.62a}$$

$$P(A \cup B) = P(A) + P(B) - P(A).P(B) \tag{7.62b}$$

c) Maximum dependence, $\rho_{AB} = 1$

Therefore

$$P(A \cap B) = \text{Min } [P(A), P(B)] \quad \text{and} \tag{7.63a}$$

$$P(A \cup B) = \text{Max } [P(A), P(B)] \tag{7.63b}$$

d) Minimum dependence, $\rho_{AB} = \dfrac{\text{Max } [0,\ P(A) + P(B) - 1]}{\text{Min } [P(A),\ P(B)]}$

Therefore

$$P(A \cap B) = \text{Max } [0, P(A) + P(B) - 1] \quad \text{and} \tag{7.64a}$$

$$P(A \cup B) = \text{Min } [P(A) + P(B), 1] \tag{7.64b}$$

The minimum and maximum dependence models produce the upper and lower bounds for the union. This contrasts with the assumption made by Cornell [1967] that the independence and maximum dependence give the upper and lower bounds for the union. Cornell's assumption will exclude any possible values lying in the range from minimum dependence to independence.

In reliability analysis, the dependence between random variables and between event sets (e.g. failure modes) are often described using only the correlation matrix. Cui and Blockley [1991] suggested that the dependence between random variables is different from the dependence between event sets. The former can be described by the probability density function (PDF) or all of the moments. The intersection of event sets is a formal measure of the dependence of event sets. They argued that the correlation, which only represents one of the moments, is not sufficient for describing the dependence between two event sets.

The degree of dependence can be regarded as a measure of the weighted overlapping between two event sets. Since there is a one to one correspondence between the size of the intersection and the degree of dependence, the later is a sufficient measure for the dependence between two event sets. The independence of event sets is also different from the independence of random variables. The independence of two random variables is defined only on the relation between their joint PDF and their marginal PDFs, i.e. $f_{XY}(x, y) = f_X(x)f_Y(y)$. Thus, the dependence between random variables can be described by all of the moments or the PDF, while the dependence between event sets can be described by the degree of dependence. In reliability analysis, this distinction is important since the failure modes are different event sets [Cui and Blockley 1991].

7.6.3 Interval Probability Theory

In classical probability theory, the single number representation of probability has the capacity to deal with fuzzy events [Cui 1989], but it is too precise to capture all of the uncertainty. Very often the truth of the single number is in question. For example, the proposition "Joe's height is 1.73m" may be wrong, but if we say that "Joe is tall" or

"Joe's height is between 1.70m and 1.75m", we may be right. In classical probability theory, precision and truthfulness are in conflict in the sense that the more precise the definition of a concept (proposition, event), the higher the information content will be but less likely it is to be true. The interval representation of probability allows a compromise between these two requirements and contains classical probability as a special case [Cui and Blockley 1991, and Baldwin 1987].

The interval probability theory is intended for use in problems involving sparse data and incomplete and possibly inconsistent knowledge. An interval number is used to represent the probability measure in order to capture, in relatively simple manner, features of fuzziness and incompleteness [Cui and Blockley 1990].

In interval probability theory, an interval variable is used to represent probability measure, so that

$$P(A) = [S_n(A), S_p(A)] \tag{7.65}$$

where $S_n(A)$ is the lower bound and $S_p(A)$ is the upper bound of the probability P(A). The negation is:

$$P(-A) = [1 - S_p(A), 1 - S_n(A)] \tag{7.66}$$

If we interpret probability as a measure of belief, then $S_n(A)$ represents the extent to which it is certainly believed that A is true, $S_n(-A) = 1 - S_p(A)$ represents the extent to which it is certainly believed that A is false and the value $(S_p(A) - S_n(A))$ represents the extent of the uncertainty of belief of whether A is true or false.

The three cases of [0, 0], [1, 1] and [0, 1] therefore represent the cases of 'certainly false', certainly true' and 'do not know' or 'unknown'. Thus interval probability theory is an open world model since any constraints on the value P(A) from evidence in favour of A are quite separate from those constraints from evidence against A [Cui and Blockley 1990].

The Vertex Method [Dong and Shah 1987] was used by Cui and Blockley [1990] to find the bounds for the union and intersection of A and B. In the general case, assuming that,

$\rho_{AB} = [\rho_l, \rho_u]$,
$P(A) = [S_n(A), S_p(A)]$, and
$P(B) = [S_n(B), S_p(B)]$,

the bounds for the union and intersection of A and B are given by:

$$S_n(A \cap B) = \rho_l \text{ Min } [S_n(A), S_n(B)] \quad (7.67a)$$

$$S_p(A \cap B) = \rho_u \text{ Min } [S_p(A), S_p(B)] \quad (7.67b)$$

$$S_n(A \cup B) = S_n(A) + S_n(B) - \rho_u \text{ Min } [S_n(A), S_n(B)] \quad (7.67c)$$

$$S_p(A \cup B) = S_p(A) + S_p(B) - \rho_l \text{ Min } [S_p(A), S_p(B)] \quad (7.67d)$$

The bounds for the union and intersection of A and B given above can be extended to different models of dependence.

a) Mutually exclusive, $\rho_{AB} = [0, 0]$

Therefore

$$P(A \cap B) = 0 \quad (7.68a)$$

$$S_n(A \cup B) = S_n(A) + S_n(B) \quad (7.68b)$$

$$S_p(A \cup B) = S_p(A) + S_p(B) \quad (7.68c)$$

b) Independence, $\rho_{AB} = \{\text{Max } [S_n(A), S_n(B)], \text{Max } [S_p(A), S_p(B)]\}$

Therefore

$$S_n(A \cap B) = S_n(A).S_n(B) \quad (7.69a)$$

$$S_p(A \cap B) = S_p(A).S_p(B) \quad (7.69b)$$

$$S_n(A \cup B) = \text{Min } \{1, S_n(A) + S_n(B) - \text{Max } [S_p(A), S_p(B)].\text{Min } [S_n(A), S_n(B)]\} \quad (7.69c)$$

$$S_p(A \cup B) = \text{Min}\,\{1, S_p(A) + S_p(B) - \text{Max}\,[S_n(A), S_n(B)].\text{Min}\,[S_p(A), S_p(B)]\} \quad (7.69d)$$

c) Maximum dependence, $\rho_{AB} = [1, 1]$

Therefore

$$S_n(A \cap B) = \text{Min}\,[S_n(A), S_n(B)] \quad (7.70a)$$

$$S_p(A \cap B) = \text{Min}\,[S_p(A), S_p(B)] \quad (7.70b)$$

$$S_n(A \cup B) = \text{Max}\,[S_n(A), S_n(B)] \quad (7.70c)$$

$$S_p(A \cup B) = \text{Max}\,[S_p(A), S_p(B)] \quad (7.70d)$$

d) Minimum dependence, $\rho_{AB} = \dfrac{\text{Max}\,[0,\ P(A)+P(B)-1]}{\text{Min}\,[P(A),\ P(B)]}$

$$\rho_l = \frac{\text{Max}\,[0,\ S_n(A)+S_n(B)-1]}{\text{Min}\,[S_n(A),\ S_n(B)]}$$

$$\rho_u = \frac{\text{Max}\,[0,\ S_p(A)+S_p(B)-1]}{\text{Min}\,[S_p(A),\ S_p(B)]}$$

Therefore

$$S_n(A \cap B) = \text{Max}\,[0, S_n(A) + S_n(B) - 1] \quad (7.71a)$$

$$S_p(A \cap B) = \text{Max}\,[0, S_p(A) + S_p(B) - 1] \quad (7.71b)$$

$$S_n(A \cup B) = \text{Min}\,\{1, S_n(A) + S_n(B) - \rho_u\,\text{Min}\,[S_n(A), S_n(B)]\} \quad (7.71c)$$

$$S_p(A \cup B) = \text{Min}\,\{1, S_p(A) + S_p(B) - \rho_l\,\text{Min}\,[S_p(A), S_p(B)]\} \quad (7.71d)$$

e) Unknown dependence

Cui and Blockley [1991] introduced this model as an additional case using $\rho_{AB} = (\rho_l, 1)$.

where

$$\rho_l = \frac{\text{Max}\,[0,\ S_n(A)+S_n(B)-1]}{\text{Min}\,[S_n(A),\ S_n(B)]}$$

Therefore

$$S_n(A \cap B) = \text{Max}\,[0, S_n(A) + S_n(B) - 1] \quad (7.72a)$$

$$S_p(A \cap B) = \text{Min}\,[S_p(A), S_p(B)] \quad (7.72b)$$

$$S_n(A \cup B) = \text{Max}\,[S_n(A), S_n(B)] \quad (7.72c)$$

$$S_p(A \cup B) = \text{Min}\,\{1, S_p(A)+S_p(B) - \rho_I\,\text{Min}\,[S_p(A), S_p(B)]\} \quad (7.72d)$$

7.6.4 Application of interval probability theory to the assessment of corrosion damaged steel structural systems

The degree of uncertainty involved in thickness measurements or visual assessment of thickness loss of corroded elements is quite high. Generally, thickness of corroded elements varies from one location of the element to another. The variation depends on the degree of corrosion. For severely corroded elements, the variation will be very high. For the purpose of reliability analysis, it is common to represent the uncertainty using a suitable distribution function. The interval probability theory, in which an interval number is used to represent the probability of failure, allows the variation to be represented by an interval number (for example, thickness of a corroded web may be given as between t_a and t_b). The probability of failure may then be given as an interval number $[P_{fb}, P_{fa}]$ by calculating the probability of failure for each t_a and t_b assuming that they are deterministic values. This allows us to include the uncertainty involved in thickness measurements of corroded elements in a relatively simple manner.

Cui and Blockley [1991] have shown, using several numerical examples, that if the degree of dependence is reasonably judged the bounds obtained using interval probability theory are satisfactory compared to that of Ditlevsen's or Cornell's bounds and are obtained relatively easily. They have also shown, using an example, that it is possible to derive even narrower bounds than Ditlevsen's bounds based on the same amount of information (pairwise dependence). In obtaining Cornell's bounds, it is assumed that independence and maximum dependence give the upper and lower bounds for the probability of failure, neglecting possible values from minimum dependence to independence. However, if the probabilities are small, the practical effect of this omission is negligible.

It is now possible to use different models of dependence in system reliability because of the introduction of the degree of dependence parameter. This is unique to interval probability theory. If it is difficult to estimate the degree of dependence, the unknown dependence model may be used to calculate the system probability of failure. The accuracy of the results using interval probability theory depends on how good the estimation of the degree of dependence is. The most important aspect of interval probability theory is that the computation of system probability of failure is easy and can be carried out using a pocket calculator or a spreadsheet without the need for a sophisticated software package. By taking into account the above factors, it was decided to use interval probability theory for system reliability in this work.

7.6.5 Application of interval probability theory to system reliability

Let us consider a series type structural system with two failure modes (F_1 and F_2). The probability of failure of the system is the union of the probabilities of failure of each failure mode. Using Equation 7.60, this may be given by:

$$P(F) = P(F_1 \cup F_2) = P(F_1) + P(F_2) - \rho_{F_1F_2} \text{ Min } [P(F_1), P(F_2)]$$

Therefore in order to assess P(F), it is necessary to assess $\rho_{F_1F_2}$ as an interval number and then Equation 7.67 can be used. For a general case in which m failure modes are involved, the above equation can be extended as:

$$\begin{aligned} P(F) &= P(F_1 \cup F_2 \cup \ldots \cup F_m) \\ &= P(F_1 \cup F_2 \cup \ldots \cup F_{m\,1}) + P(F_m) - \rho_{F_1F_2 \ldots Fm} \text{ Min } [P(F_1 \cup F_2 \cup \ldots \cup F_{m-1}), P(F_m)] \end{aligned} \tag{7.73}$$

Thus, to use interval probability theory to calculate the probability of failure of a system with m failure modes, it is necessary to assess (m – 1) dependence parameters $\rho_{F_1F_2}$, $\rho_{F_1F_2F_3}$, ..., $\rho_{F_1F_2 \ldots Fm}$. The need for these (m – 1) assessments can be compared with the

suggestion by Ditlevsen for [m(m – 1)/2] pairwise assessments of $P(F_i \cap F_j)$. Both methods require difficult judgements to be made and the judgements of higher order dependence $\rho_{F_1F_2 \ldots Fm}$ are more difficult than judgements of pairwise dependence $\rho_{F_iF_2}$.

A strategy for the use of interval probability theory for reliability analysis was suggested by Cui and Blockley [1991]. Firstly, the unknown dependence model is used to calculate the bounds for the probability of failure. If the bounds are too wide for the problem to be solved, then each of the failure modes is examined in turn and an estimate is made for the degree of dependence, where possible. The difficulty in assessing higher order dependencies can be avoided by a hierarchical method that was introduced by Cui and Blockley [1991]. By considering the hierarchical structure of failure modes into sub-systems, the problem may be substantially eased. For example, six failure modes of a beam are organised in this way as shown in Figure 7.8.

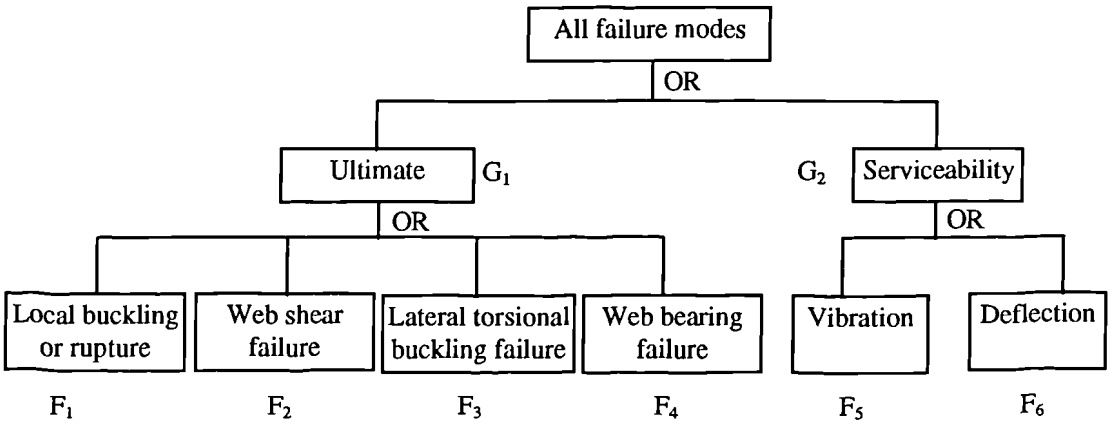

Figure 7.8 A hierarchical structure of failure modes of a beam

Figure 7.8 suggests that the failure modes can be divided into two separate groups G_1 (F_1, F_2, F_3 and F_4) and G_2 (F_5 and F_6), and the assessment of dependence can be done in the following way; firstly $\rho_{F_1F_2}$, $\rho_{F_1F_2F_3}$, $\rho_{F_1F_2F_3F_4}$ followed by $\rho_{F_5F_6}$ and finally $\rho_{G_1G_2}$. In this way, the probability of system failure may be estimated separately for ultimate and serviceability limit states, which are then combined to give an estimate for the total probability of failure of the beam. It will be seen in the next chapter that the number of dependency assessments may be reduced by ignoring the less critical failure modes. For

the example given in Figure 7.8, if load carrying web stiffeners are provided then the web bearing failure mode may not be critical for the performance of the beam and in such cases, the web bearing failure mode may be ignored.

As mentioned earlier, the degree of dependence is a measure of the weighted overlapping between two event sets. Its value can therefore be estimated from the size of the intersection of the limit state functions. If one of the limit state functions is included in the other, then that is maximum dependence. If two limit state functions have no common area, then it is mutually exclusive. For the partially inclusive cases, the value has to be estimated by an interval number.

7.7 Summary and conclusions

The remaining capacity assessment of corrosion damaged steel structures involves considerable degree of uncertainty. The main cause for the high uncertainty is that the prediction or assessment of corrosion damage is very difficult and it itself involves high degree of uncertainty. Modern reliability theory provides a framework for analysing such uncertainties. In this chapter, the structural reliability theory has been discussed. The calculation methods for the probability of failure (or reliability index) of components and structural systems have also been discussed.

The calculation methods for the probability of failure of components can be divided into three categories. They are direct integration, first order second moment (FOSM) and simulation methods. The direct integration method is very difficult and time consuming. For many practical problems, analytical solutions do not exist for the formulation. FOSM method became popular because it is relatively simple and was enhanced by the contribution of Hasofer and Lind [1974] by defining the invariant reliability index. Monte Carlo methods have also attracted interest. This is partly due to the development of variance reduction techniques such as importance sampling.

The exact calculation of probability of failure of structural systems is very difficult and may be impossible. Therefore most of the attention has been focused on the estimation

of the bounds for the probability of failure. In this chapter, Cornell' bounds and Ditlevsen's bounds have been presented. Cornell's bounds were obtained using only the first order terms while Ditlevsen's bounds were obtained using first and second order terms. Therefore, to obtain Cornell's bounds, no information is required regarding dependence between failure modes. To obtain Ditlevsen's bounds, information is required regarding all the pairwise dependencies. Ditlevsen's bounds may depend on the order in which the various failure modes are labelled. Ditlevsen's bounds are narrower than Cornell's bounds.

In system reliability analysis, the most difficult problem is the assessment of dependence. A parameter called degree of dependence, which can be regarded as a measure of the weighted overlapping between two event sets, was defined by Cui and Blockley [1990]. The dependence parameter allows an easy and practically useful way of exploring different dependence assumptions when the exact nature of the dependency relation is not known. By introducing this parameter, Cui and Blockley proposed a relatively new theory, interval probability theory, which has been presented in this chapter, to calculate the probability of failure of structural systems.

The computation of system probability of failure using interval probability theory is relatively simple. If the degree of dependence is reasonably estimated, the results obtained using interval probability theory are as good as Ditlevsen's or Cornell's bounds [Cui and Blockley 1991]. The interval representation of probability of failure in interval probability theory allows one to capture the uncertainty involved in thickness measurements of corroded elements in a relatively simple manner by using an interval number for the corroded thickness.

By considering the above factors it was concluded that interval probability theory may be a better choice for the reliability assessment of corrosion damaged steel structures. A method for the calculation of the bounds for the probability of failure of structural system based on the use of interval probability theory has been given. The application of this method to a practical problem will be illustrated in the next chapter by calculating the system probability of failure of samples of corrosion damaged beams.

Chapter 8

Reliability of corrosion damaged steel structures

8.1 Introduction

Steel structures are subjected to corrosion due to environmental exposure. As a consequence, the carrying capacity and hence the level of safety of these structures diminishes with time due to accumulation of corrosion damage (e.g. section loss). The level of uncertainty about the structural performance increases due to inherent randomness in the deterioration process. The rate of corrosion is often non-uniform and difficult to predict.

The loads imposed on structures and the resistance of the structures are random variables. These parameters (load and resistance) are themselves functions of several basic random variables such as material properties, section dimensions, etc. Since the applied load and resistance are random, along with the rate and location of corrosion, it is convenient to quantify the reduction in safety of corrosion damaged steel structures in terms of reliability. Reliability analysis provides a framework for incorporating the uncertainty in both load and resistance.

Methods are available to assess the reliability (or the probability of failure) of structural elements and systems (Chapter 7). Since it is difficult to calculate the exact probability of failure of structural systems, methods have been developed to calculate approximate bounds for the probability of failure. In particular, interval probability theory was developed by Cui and Blockley [1991] for calculating the probability of failure of structural systems (Section 7.6).

The main aims of this chapter are to present a method for the reliability assessment of corrosion damaged steel members and to illustrate the application of interval probability theory for the reliability assessment of corrosion damaged steelwork structures.

The specific objectives are:

1. To present a method for the reliability assessment of corrosion damaged steel members (or single failure mode).
2. To examine the effects of corrosion damage on the reliability of steel beams.
3. To illustrate the application of interval probability theory to calculate system probability of failure using samples of corrosion damaged beams.

8.2 Load and load effect modelling

The loads which may act on a structure can be broadly divided into two groups: those due to natural phenomena such as wind, wave, snow and earthquake loading; and those due to man-imposed effects such as dead loads and live loads. The magnitude of most loads vary with time and location. In addition, dynamic effects may occur as a result of load-structure interaction. Because of these possibilities, the modelling of load processes may be quite difficult. Perfect models are not possible owing to insufficient data, imperfect understanding and the necessity to predict future loading. Appropriate models are therefore sought, particularly since loading is usually the most uncertain factor in reliability analysis.

8.2.1 Permanent loads

Permanent loads are those that do not vary significantly throughout the life of the structure (e.g. loads due to the weights of the construction materials), even though their actual value may be uncertain. Dead loads are typically of this type. They result from the self weight of the materials used in construction and from permanent installations. The self weight of the structure is generally not treated as a basic variable, as it is a function of two other types of more fundamental quantities: dimensions; and densities.

The statistical distribution functions of dead loads are commonly assumed to be normal, typically with a mean equal to the nominal load and a coefficient of variation of 0.05 - 0.1. However, there is limited evidence that dead loads are underestimated [Ellingwood et al 1980] and a mean somewhat greater (say 5%) than the nominal may be appropriate.

8.2.2 Variable loads and imposed deformations

Many common loads come within this category (e.g. wind loads, wave loads, and superimposed floor loads). For loads of this type that vary with time throughout the life of the structure, it is necessary to know the distribution of the maximum load likely to occur in a specified time interval. Wind loading can be derived from statistical data for wind speeds. In principle, the correct probabilistic model for instantaneous wind speed at a point is therefore a normal process [Davenport 1961]. In practice, departures from the idealised mode have been noted [e.g. Melbourne 1977].

8.3 Resistance modelling

In order to describe adequately the uncertainties associated with the resistance properties of structural elements, information about the following is required:

1. Statistical properties for material strength and stiffness,
2. Statistical properties for dimensions,
3. Rules for the combination of various properties, and
4. Influence of time (e.g. strength changes, deterioration mechanisms such as corrosion, fatigue and weathering)

8.3.1 Steel material properties

The material properties that are of most importance for steel are yield strength and modulus of elasticity. Considerable quantities of data are available for the strength of steel. The strength of most ductile materials including steel is well represented by the log-normal distribution as shown in Figure 8.1. This distribution function also satisfies the practical requirement that the frequency of negative values should be zero. For the

case of brittle fracture of steel, there are good theoretical reasons for fitting the data to a Weibull distribution [CIRIA 1977].

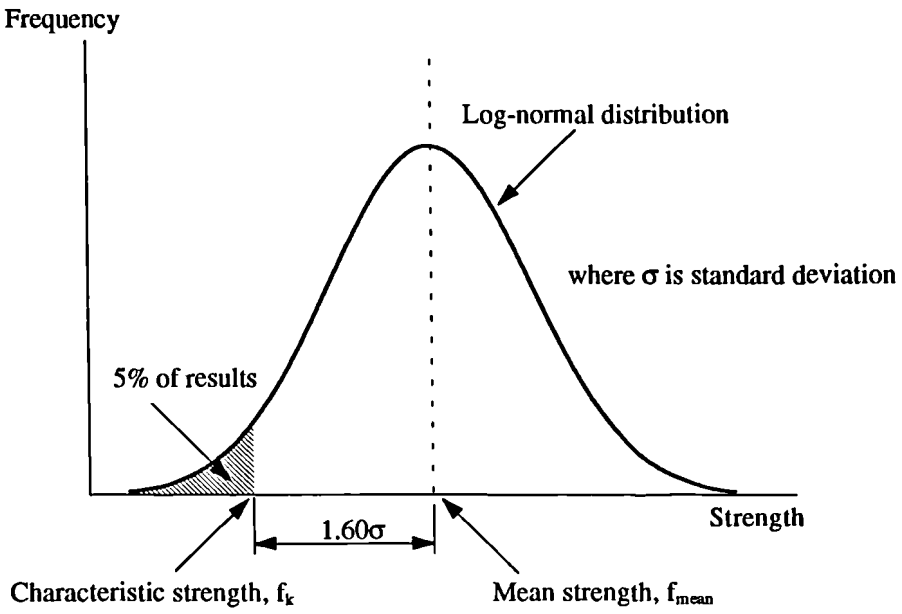

Figure 8.1 Variation in material properties

The characteristic value of material strength is usually defined as 95% confidence level (see Figure 8.1). Normally, it will be found that the actual characteristic strength exceeds the specified strength (i.e. specified minimum strength or specified characteristic strength) by a considerable margin. For the purpose of reliability analysis it should be assumed that 95% confidence level actually corresponds with the specified strength as this is deemed to be the lowest acceptable level of quality [CIRIA 1977].

The characteristic strength is calculated from the following equation [CIRIA 1977],

$$f_k = f_{mean} - 1.60\sigma$$

Typical British mill test data given by Baker [1969] for both steel plates and structural sections to BS 15 and BS 968 are given in Table 8.1. A summary of American mill test data for the elastic modulus, E, Poisson's ratio, υ, and shear modulus, G, are given in Table 8.2. These data cover a period of more than twenty years.

Table 8.1 British yield stress, p_y, data [Baker 1969]

Type of steel	Plate thickness (mm)	Mean mill p_y / specified p_y	Estimated Mean p_y / specified p_y	Coefficient of variation
Structural carbon steel plates	10-13	1.15	1.04	0.09
	37-50	1.03	0.92	0.12
High strength steel plates	10-13	1.11	1.03	0.08
	37-50	1.06	0.98	0.06
Structural carbon steel webs	10-13	1.20	1.09	0.05
	16-20	1.19	1.10	0.12
High strength steel webs	6-10	1.19	1.11	0.06
	37-50	1.06	0.98	0.05

Table 8.2 Elastic modulus of structural steel data [Galambos and Ravindra 1978]

Property	Mean / specified	Coefficient of variation	Number of tests	Type of test
E	1.01	0.010	7	Tension coupon
E	1.02	0.014	56	Tension coupon
E	1.02	0.01	67	Tension coupon
E	1.02	0.01	67	Compression coupon
E	1.03	0.038	50	Compression and tension coupon
υ	0.99	0.026	57	Tension coupon
υ	0.99	0.021	48	Compression coupon
G	1.08	0.042	5	Torsion coupon

8.3.2 Structural dimensions and geometry

Except for structures that are sensitive to geometrical imperfections (e.g. compression members and thin slabs), the variability of structural dimensions and geometry tends to be rather less important than variability in loading and strength parameters. This is generally because the coefficient of variation of the dimensions tends to be small - generally considerably less than 5%. The variation in the depth and width of hot rolled sections appears to be quite small, typically with a coefficient of variation of 0.2% [Melchers 1987]. There is slightly greater variation in the thickness of elements (e.g. flange thickness). These variables may be assumed to be distributed with mean values corresponding to the specified nominal dimensions. The variation in the thickness of elements influences the variation in section properties such as cross-sectional area, second moment of area, plastic and elastic modulus. For these properties an average coefficient of variation of 5% has been suggested [Ellingwood et al 1980]. Most dimensional variables can be adequately modelled by normal or log-normal distributions.

8.4 Corrosion decay model

The reliability assessment of corrosion damaged steel structures requires information concerning the loss of section at the time of the assessment. Thickness measurements of samples of corrosion damaged beams (see Appendix B) showed that there is a large variation in the measured thicknessess. Measurements were taken at various locations (more than hundred) to get an average value for the thickness of each element. It was also found that the variation in thickness measurements is directly related to the degree of corrosion, i.e. the variation increased as the degree of corrosion increased.

Visual assessment of thickness loss also involves a considerable degree of uncertainty. It is now possible to represent this variation by using an interval number for the thickness of corroded elements and to obtain an interval probability of failure as described in Section 7.6.3. Let us assume that the thickness of a corroded element of a beam (flange, web or stiffener) $\overline{T}_C$ can be expressed by:

$$\overline{T}_C = [\overline{T}_{Ca}, \overline{T}_{Cb}] \quad (8.1)$$

where $\overline{T}_{Ca}$ and $\overline{T}_{Cb}$ are the lower and upper bounds of the corroded thickness.

Assuming that $\overline{T}_{Ca}$ and $\overline{T}_{Cb}$ are deterministic values, the probability of failure of a specific failure mode can be calculated for each thickness. Let us say $\overline{T}_{Ca}$ and $\overline{T}_{Cb}$ give probabilities of failure of P_{fa} and P_{fb} respectively. Since $\overline{T}_{Ca} \leq \overline{T}_{Cb}$, it is clear that $P_{fb} \leq P_{fa}$. Therefore the corresponding interval probability of failure may be given by:

$$P_f = [P_{fb}, P_{fa}] \quad (8.2)$$

The interval probability theory makes it possible to represent the uncertainty associated with the thickness of corroded elements using an interval number as described above. The uncertainty may also be included in reliability analysis using existing methods, i.e. use of a distribution function for the variable thickness or thickness loss of corroded elements, as explained below.

Corrosion decay models have been developed in Chapter 4 using percentage thickness loss of elements. These models may be used for the reliability assessment of corrosion damaged steel beams. For varying thickness loss model beams, the thickness of a corroded element (flange, web or stiffener) may be expressed as a function of the as-new thickness and the percentage loss of thickness as follows (see Section 4.2.1):

$$\overline{T}_C = \overline{T}_N - c\xi\overline{T}_N \quad (8.3)$$

where

$\overline{T}_N$ is the as-new thickness of the element,

c is a constant, which has the following values:

- 0.7 for top flange,
- 1.3 for bottom flange,
- 0.25 for upper part of web ($0.75h_w$) and stiffeners,

1.25 for lower part of web ($0.25h_w$),

ξ = %LFT/100, and

%LFT is the percentage loss of flange thickness.

Although $\overline{T}_N$ is a random variable in principle, we have seen in the previous section that it can be assumed to be effectively a constant. Thickness loss ξ is considered as a random variable, which is assumed to be normally distributed. Since ξ is a normally distributed random variable, the thickness of a corroded element $\overline{T}_C$, which is a linear function of ξ, is also a normally distributed random variable.

The distribution parameters, mean and standard deviation, of $\overline{T}_C$ can be calculated using Equations 7.19 and 7.20 as:

$$\mu_{\overline{T}_c} = \overline{T}_N - c\overline{T}_N \mu_\xi \tag{8.4}$$

$$\sigma_{\overline{T}_c} = c\overline{T}_N \sigma_\xi \tag{8.5}$$

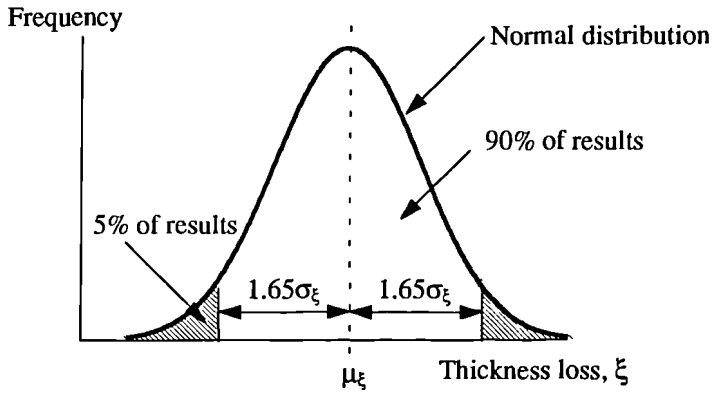

Figure 8.2 Variation in thickness loss assessment

In order to establish distribution parameters for the thickness of corroded elements, the distribution parameters of the variable thickness loss ξ are required. If the reliability assessment is going to be based on the visual assessment of thickness loss, then μ_ξ may be assumed as the average estimated thickness loss. The uncertainty involved in the assessment of percentage thickness loss mainly depends on the experience of the

inspector. If it is assumed that 90% of the assessment samples lie within an acceptable variation range (see Figure 8.2), then this variation in the assessment of thickness loss can be calculated using the following equation [Martin and Purkiss 1992],

$$\xi = \mu_\xi \pm 1.65\sigma_\xi \qquad (8.6)$$

Assuming that the visual assessment of thickness loss has a coefficient of variation, V, of 0.15 (where $V = \sigma_\xi/\mu_\xi$), the variations in the assessment of thickness loss were calculated for various values of μ_ξ using Equation 8.6 and are given in Table 8.3.

Table 8.3 Variation in thickness loss assessment

Mean, μ_ξ	Standard deviation, σ_ξ	Variation in assessment
0.1	0.015	$0.075 \leq \xi \leq 0.125$
0.2	0.03	$0.150 \leq \xi \leq 0.250$
0.3	0.045	$0.225 \leq \xi \leq 0.375$
0.4	0.06	$0.300 \leq \xi \leq 0.500$
0.5	0.075	$0.375 \leq \xi \leq 0.625$

It can be seen from Table 8.3 that the variation in the assessment of percentage thickness loss increases as the thickness loss increases (i.e. as the degree of corrosion increases). This reflects the earlier finding that the uncertainty in thickness measurements increases with the degree of corrosion. Therefore a constant value for the coefficient of variation may be used to include the uncertainty involved in the assessment of thickness loss. This value may be chosen according to the experience of the inspector. In this work, a coefficient of variation of 0.15 was used as assumed above.

Having established the distribution for the thickness of the corroded elements it is now possible to evaluate the structural behaviour. For the evaluation of structural behaviour of corrosion damaged steel beams regarding various failure modes, the assessment methods given in Chapter 3 can be used.

8.5 Effects of corrosion damage on the reliability of steel beams

8.5.1 Reliability assessment of corrosion damaged steel beams

The structural behaviour of steel beams subjected to bending has been discussed in Section 4.2.2. To examine the effects of corrosion damage on the reliability of steel beams, an analysis was carried out on two corrosion damage models. The I-beam used in Sections 4.3 and 4.4 (305×165 UB 40 kg) was used for this purpose. The two models are as follows:

1. I-beams with thickness loss corresponding to the four samples of corrosion damaged beams (see Section 4.3) and an as-new beam, and
2. Varying thickness loss model beams (see Section 4.2.1).

The specifications of the beams, which were coped in the top flange, are given in Section 4.4. It was assumed that the beams carry a dead load of 150 kN near the mid-span (see Figure 4.6). The bearing failure mode is not considered here for the reliability analysis because it was found in Section 4.4 that this failure mode was not critical at all. The software package ISPUD [1986] was used to calculate the probability of failure of each failure mode. The reliability package ISPUD computes the probability of failure using the important sampling technique. The basic variables involved in the analysis and their type and distribution parameters are tabulated in Table 8.4.

For the samples of corrosion damaged beams, the probabilities of failure were calculated using both an interval representation for the corroded thickness and a distribution function for the variable ξ. The probabilities of failure obtained for each failure mode of the sample beams are given in Table 8.5 and the reliability index, β, based on the use of the distribution function for ξ is plotted in Figure 8.3. The probabilities of failure of the varying thickness loss model beams were calculated using the distribution function for the variable ξ. The results for the varying thickness model beams are plotted in Figure 8.4 in the form of reliability index for each failure mode.

Table 8.4 Distribution type and parameters of the basic variables

Basic variable	Distribution type	Mean	Coefficient of variation	Standard deviation
Thickness loss, ξ	Normal		0.15	
Design strength	Log-normal	300 N/mm^2	0.09	27 N/mm^2
Elastic modulus	Log-normal	205 kN/mm^2	0.05	10.3 kN/mm^2
Shear modulus	Log-normal	79 kN/mm^2	0.05	3.95 kN/mm^2
Load	Normal	150 kN	0.07	10.5 kN
Modelling uncertainty	Normal	1.0	0.05 - 0.1	0.05 - 0.1

Table 8.5 Probabilities of failure of samples of corrosion damaged beams

Beam		As-new	Beam 1	Beam 2	Beam 3	Beam 4
% Thickness	Flange	0	36 (32-40)	33 (29-37)	41 (36-46)	24 (21-27)
loss	web	0	18	12	20	9
Moment	IPF	[3.500e-20, 3.500e-20]	[4.061e-11, 8.173e-10]	[1.249e-12, 1.077e-11]	[1.492e-10, 2.325e-8]	[1.600e-13, 8.433e-13]
	PFDF	3.500e-20	3.133e-10	4.443e-12	1.627e-9	3.984e-13
Lateral torsional	IPF	[1.392e-15, 1.392e-15]	[6.935e-5, 1.359e-1]	[6.901e-6, 1.143e-1]	[7.634e-3, 4.843e-1]	[2.669e-10, 1.636e-8]
	PFDF	1.392e-15	4.017e-2	1.755e-3	2.757e-1	2.700e-9
Shear	IPF	[1.199e-19, 1.199e-19]	[1.015e-3, 1.746e-1]	[9.595e-8, 2.508e-5]	[5.317e-3, 3.850e-1]	[1.545e-11, 3.127e-9]
	PFDF	1.199e-19	2.317e-2	2.547e-6	1.006e-1	2.102e-10

where

IPF = Interval probability of failure obtained using interval representation for the thickness of corroded elements (interval thickness loss is given in brackets), and

PFDF = Probability of failure obtained using a distribution function for the variable ξ.

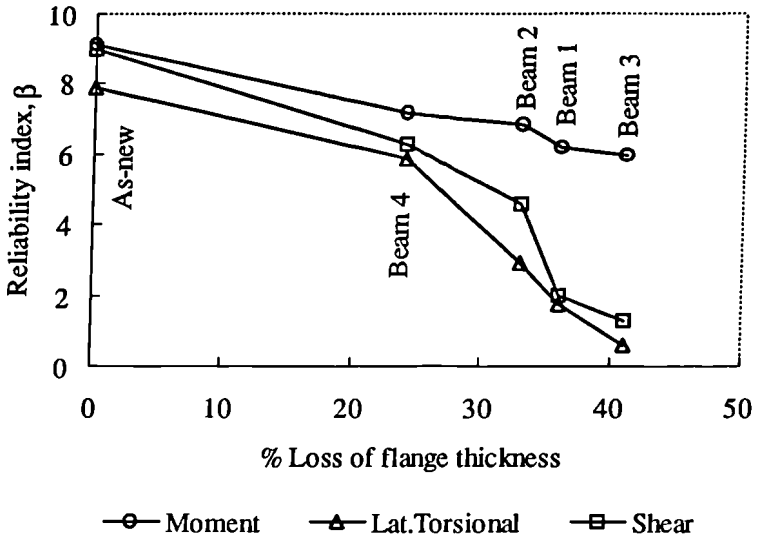

Figure 8.3 Reliability index of samples of corrosion damaged beams

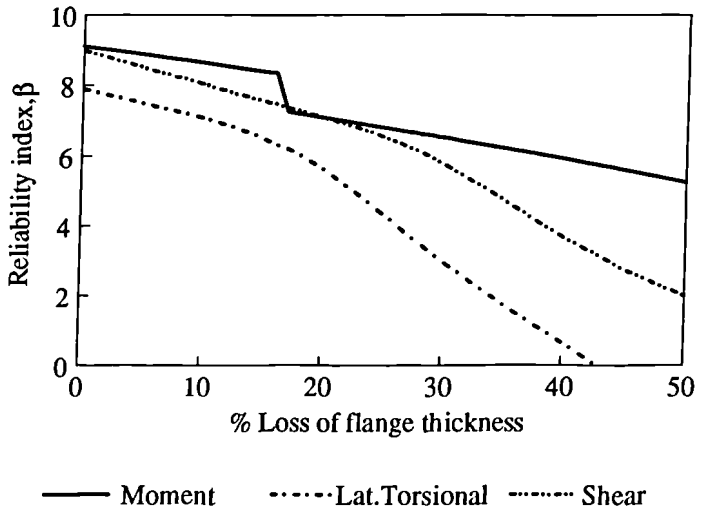

Figure 8.4 Reliability index of varying thickness loss model beams

8.5.2 Discussion

Although the probabilities of failure obtained using the distribution function for ξ (PFDF) are precise (see Table 8.5), the question is whether they are true. The degree of uncertainty associated with the thickness of corroded elements is considerable. Therefore, in reality, the probability of failure may be greater or less than the single value. The probabilities of failure obtained using interval representation for the corroded

thickness (IPF) provide bounds which reflect the high uncertainty associated with the thickness of corroded elements (see Table 8.5). The variation in the thickness measurements, which were taken for the samples of corrosion damaged beams, was found to be more than 1 mm for some elements.

It can be seen from Figures 8.3 and 8.4 that the rate of reduction in moment reliability is less significant for the beams considered in the analysis. For the case of varying thickness loss model beams, there is a sudden drop in the moment reliability at a certain stage of corrosion (approximately 17% of flange thickness loss). This sudden drop is caused when the class of section changes from one to another and reflects the change of analytical model. In this case, the class of section changed from compact to semi-compact when the average flange thickness loss was about 17%.

There is a severe reduction in the lateral torsional buckling reliability as more material is lost due to corrosion. The severe reduction in the reliability is partly due to the fact that the beams considered are short span coped beams. For these beams, the lateral torsional buckling capacity is mainly controlled by the coped (Tee) section. Thickness measurements of the sample beams (see Table 4.1) showed that there is significant thickness loss in the bottom flange, which is part of the coped section. For varying thickness loss model sections, it was assumed that the thickness loss in the bottom flange is nearly twice that of the top flange. Significant thickness loss in the bottom flange caused the lateral torsional buckling reliability to decline at a greater rate compared with other failure modes. The reliability of the varying thickness loss model beams becomes zero when the average flange thickness loss is about 43%.

The loss of material has more effect on the shear reliability than the moment reliability. The rate at which the shear reliability decreases is also quite considerable. When webs are subjected to shear forces the probability of buckling of the web increases as the thickness of the web decreases. The loss of material in the lower part of the web is very significant (approximately five times that of the upper part of the web). In addition, the initial thickness of the web is small compared with the flange thickness. These factors cause the considerable reduction in the shear reliability.

In the above analysis, the reliability index was plotted against percentage thickness loss of the section. This information is useful when considering the reliability of the structure over its service life. This may be done by relating the percentage thickness loss to the number of years of exposure using available information on rate of corrosion at a particular environment (or location).

8.6 System reliability using interval probability theory

8.6.1 Application of interval probability theory

The carrying capacity of a beam depends on all the possible failure modes as discussed in Section 4.2.2. Hence, all the possible failure modes must be taken into account when considering the failure of the beam. The moment, lateral torsional buckling and shear failure modes will be considered here when calculating the system probabilities of failure of the samples of corrosion damaged beams. The bearing failure mode is not considered as it was found to be insignificant for these beams.

Let us denote the probabilities of failure of the different failure modes of the beams as follows:

$P(F_1)$ = Probability of failure due to lack of moment capacity,
$P(F_2)$ = Probability of failure due to lateral torsional buckling,
$P(F_3)$ = Probability of failure due to lack of shear capacity, and
$P(F) \approx$ System probability of failure of the beam.

By applying interval probability theory (Equation 7.73), the system (total) probability of failure of a beam may be expressed by:

$$P(F) = P(F_1 \cup F_2 \cup F_3) = P(F_1 \cup F_2) + P(F_3) - \rho_{F_1F_2F_3} \text{Min}\,[P(F_1 \cup F_2), P(F_3)] \tag{8.7}$$

where

$$P(F_1 \cup F_2) = P(F_1) + P(F_2) - \rho_{F_1F_2} \text{Min}\,[P(F_1), P(F_2)] \tag{8.8}$$

Therefore, in order to assess the system probability of failure, it is necessary to estimate the degree of dependence parameters $\rho_{F_1F_2}$ and $\rho_{F_1F_2F_3}$ as an interval number and then use Equation 7.67.

Let us consider the case of Beam 1 of the samples of corrosion damaged beams. The probability of failure of each failure mode obtained using the distribution function for ξ will be used to compute the system probability of failure in this example. If we use an unknown dependence model [0, 1] to compute the system probability of failure according to the strategy suggested by Cui and Blockley [1991], then the result is,

$P(F) = [4.017e\text{-}2, 6.333e\text{-}2]$

These are the widest bounds since maximum and minimum dependence between failure modes were used to calculate the bounds for the probability of failure of the system. The bounds may be narrowed by using estimates for the degree of dependence which is better than unknown. The degree of dependence between failure modes may be estimated as described below.

Consider the moment and lateral torsional buckling failure modes of the beam. The moment capacity of the beam is a function of length, design strength and plastic or elastic modulus of the section. This may be expressed in a mathematical form as:

$$F_1 = f(p_y, L, S_x \text{ or } Z_x) = f(p_y, L, D, B, T, t) \quad (8.9)$$

Similarly, the lateral torsional buckling capacity may be expressed by:

$$F_2 = f(p_b, L, S_x) = f(p_y, E, G, L, D, B, T, t) \quad (8.10)$$

The basic variables associated with both failure modes may be represented in a Venn diagram as shown in Figure 8.5a. It can be seen that all the basic variables used to calculate the moment capacity are included in the set of basic variables that are used to calculate the lateral torsional buckling capacity. This suggests that there may be

maximum dependence between the two failure modes. For beams with critical effective length, the bending strength is equal to the design strength of the section, i.e. lateral torsional buckling capacity is equal to plastic moment capacity (see Section 5.5.3). Therefore moment capacity may be considered as a special case of lateral torsional buckling capacity. This supports the suggestion that there may be maximum dependence between them. Hence, the degree of dependence between moment and lateral torsional buckling failure modes is estimated as $\rho_{F_1F_2} = [1, 1]$, i.e. maximum dependence.

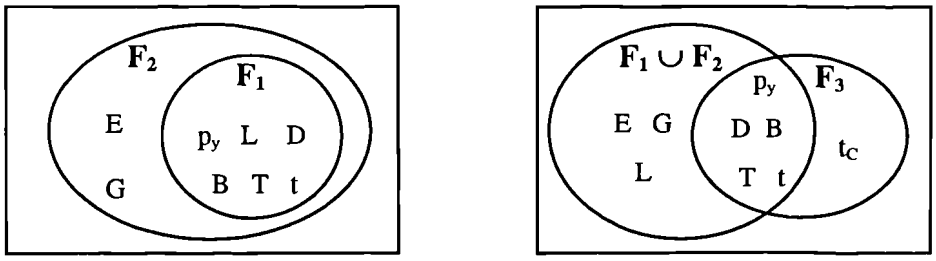

(a) F_1 and F_2 (b) $(F_1 \cup F_2)$ and F_3

Figure 8.5 Basic variables associated with the failure modes

Now, the degree of dependence between $(F_1 \cup F_2)$ and F_3 needs to be estimated. As before, the shear capacity of the varying thickness loss model sections may be expressed as follows (using Equation 3.25):

$$F_3 = f(p_y, D, B, T, t, t_C) \qquad (8.11)$$

It is evident from Figure 8.5b that nearly 55% of the basic variables are common to both sets of failure modes. While the shear capacity of a section mainly depends on the strength of the web, the lateral torsional buckling capacity depends on both the flanges and web. Taking into account these factors, the degree of dependence between $(F_1 \cup F_2)$ and F_3 is estimated as $\rho_{F_1F_2F_3} = [0.5, 0.6]$.

If the estimated values for the degree of dependence are used to calculate the system probability of failure, then the result is,

P(F) = [4.943e-2, 5.175e-2]

The above bounds for the system probability of failure are narrower than the bounds obtained using the unknown dependence model. However, the accuracy of the results depends on the degree of dependence estimation.

Using the above approach, the bounds for the system probabilities of failure of the samples of corrosion damaged beams together with an as-new beam were calculated and are given in Table 8.6. It can be seen from Table 8.6 that the bounds for the system probabilities of failure obtained using a distribution function for the thickness loss ξ (Using PFDF) is very narrow compared to that of using interval representation for the corroded thickness (Using IPF). Therefore, in the case of (Using PFDF), the system reliability indices were obtained as single numbers since these narrow bounds will give nearly the same values for the reliability indices. For the case of (Using IPF), the upper and lower bounds for the system reliability indices were obtained. The calculated system reliability indices of the beams are plotted in Figure 8.6.

Table 8.6 System probabilities of failure of samples of corrosion damaged beams using interval probability theory

Beam	Using IPF	Using PFDF
As-new	[1.392e-15, 1.392e-15]	[1.392e-15, 1.392e-15]
Beam 1	[1.043e-3, 2.425e-1]	[4.943e-2, 5.175e-2]
Beam 2	[6.939e-6, 1.144e-2]	[1.756e-3, 1.756e-3]
Beam 3	[9.760e-3, 6.768e-1]	[3.159e-1, 3.260e-1]
Beam 4	[2.731e-10, 1.793e-8]	[2.784e-9, 2.805e-9]

where

Using IPF = Using interval probabilities of failure of single failure modes which were obtained using interval representation for the corroded thickness of elements, and

Using PFDF = Using probabilities of failure of single failure modes which were obtained using a distribution function for the variable ξ.

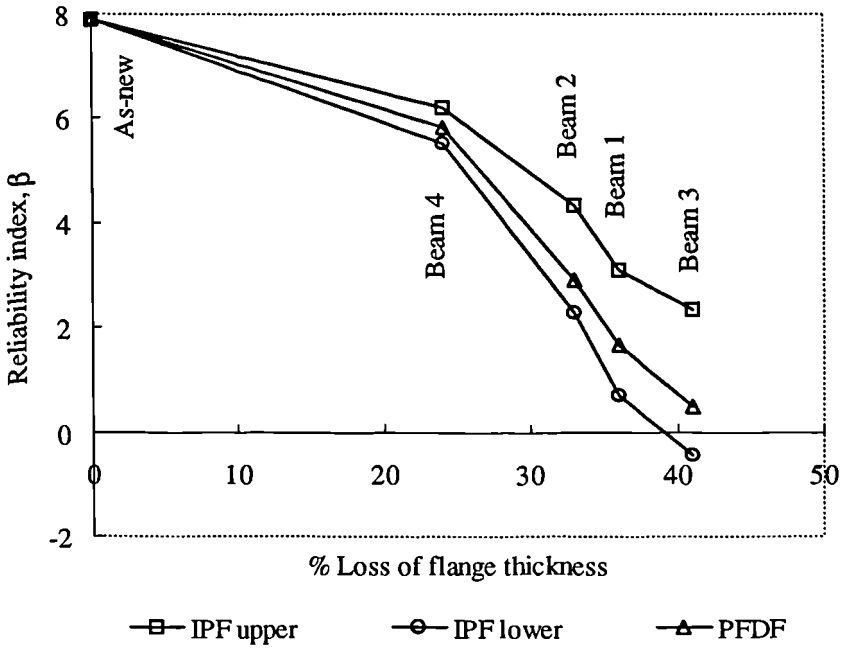

where

IPF upper and IPF lower are the upper and lower bounds of the reliability index obtained using interval representation for the corroded thickness of elements, and PFDF is the reliability index obtained using a distribution function for the variable ξ.

Figure 8.6 System reliability index of samples of corrosion damaged beams

8.6.2 Discussion

In using interval probability theory, the important parameter is the degree of dependence. The application of interval probability theory showed that narrower bounds for the system probability of failure can be obtained if the degree of dependence between two failure modes can be established. If the estimation of degree of dependence is not possible, the unknown dependence model may be used. The unknown dependence model gives the widest bounds for the system probability of failure.

The probabilities of failure of component failure modes were compared with the system probabilities of failure of the as-new beam and Beam 2 obtained using a distribution function for the thickness loss ξ (see Tables 8.5 and 8.6). This showed that the system probability of failure is almost equal to the probability of failure of the lateral torsional buckling failure mode. For these two beams, the effect of the other two failure modes is

negligible, i.e. the probabilities of failure are very much less. Similarly, the effect of the moment failure mode is negligible for all these beams. Therefore less critical failure modes may be ignored when considering system probability of failure. This will reduce the number of degree of dependencies to be estimated.

8.7 Summary and conclusions

The distributions of the basic random variables involved in the structural reliability analysis of steel structures have been discussed. Two methods have been proposed to calculate the component probability of failure of corrosion damaged steel members. While one method was based on the interval representation for the corroded thickness, the other was based on a probabilistic distribution for the percentage thickness loss. The reliability index and probabilities of failure of the samples of corrosion damaged beams and varying thickness loss model beams have been evaluated based on the proposed methods. Finally, interval probability theory was used to illustrate its application for calculating the system probability of failure using the samples of corrosion damaged beams.

Most structural dimensions of as-new members may be assumed to be distributed with mean values corresponding to the specified nominal dimensions with zero standard deviation. In the case of the thickness of corroded elements, there will be a large variation in the measurement of thickness. The variation in thickness measurements was found to be directly related to the degree of corrosion, i.e. the variation increases as the degree of corrosion increases. Visual assessment of thickness loss also involves a considerable degree of uncertainty.

The degree of uncertainty involved in the assessment of thickness loss may be included in the reliability analysis by using a constant value for the coefficient of variation of the random variable ξ (thickness loss). The component probability of failure obtained using the above, which is represented by a single number, is too precise numerically and unlikely to be true. It is now possible to represent the uncertainty associated with the thickness of corroded elements by using an interval number for the thickness because of

the introduction of interval probability theory. The corresponding probability of failure obtained as an interval number provides reasonable bounds which reflect the high uncertainty associated with the thickness of corroded elements. The interval representation of corroded thickness and hence the probability of failure gives a wider picture which is useful in decision making.

The reliability analysis of corrosion damaged beams showed that the lateral torsional buckling reliability of coped beams declines at a fast rate with the thickness loss. For the given load, the reliability of the corrosion damaged beam becomes zero when the thickness loss is about 43%. This significant reduction is caused partly by the coping of the beam. The next important mechanism is the shear failure mode. The shear reliability of the beams also decreases at a considerable rate. The severe loss of material in the lower part of the web causes this considerable reduction in the shear reliability. The moment reliability of the beams was found to be less critical. Generally, the loss of material in the compression flange of corrosion damaged beams is not very significant.

The application of interval probability theory for system reliability showed that the important part of the theory is the estimation of degree of dependence. Its value can be estimated from the size of intersection of the limit state functions [Cui and Blockley 1991]. The number of dependencies needed to be estimated can be reduced by ignoring the failure modes that are less critical to the system performance.

Chapter 9

Conclusions

9.1 The scope of the problem

The number of exposed steelwork structures used in various industries is steadily increasing as a result of new build and extension of life of older structures. About 25% of steel structures are more than 50 years old and corrosion damage is a significant problem. Current assessment methods of corrosion damaged steelwork involve visual inspection which is inaccurate and tends to be used very conservatively often resulting in plant closure which may not always be necessary. There is a need for more accurate assessment methods to provide a more reliable basis for making decisions affecting safety and costs.

9.2 Corrosion pattern in steel beams

The main critical factor of corrosion of steel is the local environment. Another important aspect is the occurrence of various forms of corrosion. The most common form is the general surface corrosion which causes the gradual thinning of members. Corrosion of steel occurs on the surface where water and contaminants can accumulate. Detailed measurements of corrosion penetration led to the following conclusions concerning the corrosion pattern of an I-beam:

1. The top surface of the bottom flange and the bottom part of the web ($0.25h_w$) are the places where the severest corrosion takes place.
2. Corrosion takes place on the top surface of the top flange but not to the extent of bottom flange.

3. Corrosion also takes place in the top part of the web ($0.75h_w$) but the loss is very much less compared to that of the bottom part of the web.
4. In the initial stages of corrosion, corrosion penetration may be taken as uniform everywhere.

The corrosion loss may be predicted by an exponential curve (Equation 2.6), but it will be very approximate when applied to a real situation, as the equation was obtained using experimental data from small test coupons. The rate and location of corrosion of steel are highly variable depending on the local environment.

The assessment of the remaining capacity of corrosion damaged steel structures requires only information on the thickness loss of the elements at the time of the assessment. Therefore the analysis of corrosion effects can be carried out using a percentage loss of thickness of elements.

9.3 Effect of corrosion damage of steel beams

The loss of thickness of a section generally causes the capacity of a loaded beam to be reduced. Depending on the relative thickness loss in the various parts, it can also change the failure mode of the beam from one mechanism to another. In addition, the class of an element may also be changed from one to another (e.g. plastic to semi-compact) due to a loss of thickness.

For corrosion damaged beams, which are laterally unrestrained and provided with load carrying web stiffeners, lateral torsional buckling, over-stress in bending, and shear failure of webs are the critical failure mechanisms. For such beams, the bearing failure mechanism is found to be less significant. For corrosion damaged coped beams, which have cut-outs in the top flange, the lateral torsional buckling mode is usually the critical failure mechanism.

The lower part of the web near the bottom flange, which is vulnerable to corrosion, may be subjected to a complete loss of material due to severe corrosion and consequent

holing of the element. The existence of holes in the web created by corrosion reduces the shear capacity of beams significantly. For the assessment of coped beams and beams with web holes, the assessment methods proposed in Chapter 3 can be used. These include a method for calculating the lateral torsional buckling capacity of coped beams.

9.4 Methods for assessing remaining capacity of corroded beams

For the remaining capacity assessment of corrosion damaged I-beams, two methods have been proposed. They are called the simple and accurate assessment methods. They were developed for various failure modes of I-beams of all manufactured sizes in the UK. In addition, lower bound estimates of the remaining capacity have also been proposed.

These methods provide a quantitative relationship between the magnitude of percentage loss of thickness and the corresponding remaining capacity expressed as percentage of as-new strength. The only information required are the thickness loss of the appropriate elements (e.g. web thickness loss for shear capacity) and the capacity of the beam in its as-new condition.

For some cases, these methods give almost exact estimates of the remaining capacity of corrosion damaged beams. In other cases, the remaining capacity estimates using these methods will be conservative but the variation in the percentage remaining capacity curves, of all the available I-sections for a particular failure mode, is very small. Typically the difference is less than 10% for a thickness loss of 50%.

Any one of the methods can be used to obtain minimum curves as both methods give nearly the same remaining capacity estimates for various cases. These assessment methods are easy to use without the need for any detailed calculations. In particular, the equations obtained in the simple assessment method will be more effective as they readily give the estimates for the capacity if the thickness losses of the elements are known.

The proposed lower bound estimate has an advantage over the other two methods as it does not involve consideration of various failure modes of an I-beam. These estimates

can be used with the design loads to evaluate the remaining capacity which may be compared immediately with the service loads. They are easy to use and give rapid estimates of the remaining capacity of corrosion damaged beams.

The remaining capacity of corrosion damaged I-beams can be assessed realistically using these assessment methods. The comparison of the experimental failure loads of samples of corrosion damaged beams with the corresponding minimum curve showed that the proposed methods give slightly conservative estimates for the remaining capacity.

These methods will be beneficial in terms of cost and safety. Fast and reliable decisions concerning the future of a corrosion damaged I-beam can be made using these methods. The proposed methods will help to avoid plant closures when the capacity of steel work may be adequate. In addition, they will help to identify the members whose capacities are nearing the service load levels.

9.5 Improvement of visual assessment procedures

In the current visual assessment procedure, the classification of steel beams, which is based only on the condition of the beams, may lead to inappropriate actions being taken causing loss of production or even structural failures.

Improved condition categories called the Strength Categories have been proposed using the knowledge gained from the proposed assessment methods. The classification of the beams is now based on both the capacity loss and the condition of the beams. These strength categories will not require detailed investigation concerning the strength of a deteriorated beam since the classification is based on the remaining capacity of the beam in percentage reduction terms.

9.6 Reliability theory

In structural reliability analysis, there are three well-known methods for the calculation of component reliability. These are direct integration, first order second moment (FOSM)

and simulation methods. The direct integration method cannot be used for many practical problems and it is very difficult and time consuming. FOSM method became popular because it is relatively simple, and its use was further enhanced by the introduction of the invariant reliability index (Hasofer and Lind's reliability index). Simulation methods became popular because of the development of variance reduction techniques such as importance sampling.

The structural reliability of a whole structural system is determined from the reliability of its members. The exact calculation of the reliability of structural systems is very difficult and may be impossible. Therefore methods were developed to estimate the upper and lower bounds for the system reliability.

Cornell's bounds, which were obtained using only the first order terms, do not require any information regarding dependence between failure modes. Ditlevsen's bounds, which were obtained using first and second order terms, require information regarding all the pairwise dependencies. Ditlevsen's bounds may depend on the order in which the various failure modes are labelled.

The most difficult problem in system reliability analysis is the assessment of dependence. A parameter called degree of dependence allows an easy and practically useful way of exploring different dependence assumptions when the exact nature of the dependency relation is not known. By introducing this parameter, Cui and Blockley [1991] proposed interval probability theory to calculate the probability of failure of structural systems. Cui and Blockley [1991] showed that the results obtained using interval probability theory are satisfactory compared to those of Ditlevsen and Cornell.

The interval probability theory is an effective method for the reliability assessment of corrosion damaged steel structures. The theory made it possible to include the uncertainty associated with the thickness of corroded elements using an interval number for the thickness. The computation of probability of failure of structural systems using this theory is relatively simple (can be carried out using a pocket calculator).

9.7 Reliability of corrosion damaged steel structures

There is a large variation in the measurement of thickness of corroded elements. The variation in thickness measurements is directly related to the degree of corrosion, i.e. the variation increases as the degree of corrosion increases. Visual assessment of thickness loss also involves a considerable degree of uncertainty.

A constant value for the coefficient of variation can be used to represent the uncertainty associated with the assessment of thickness loss (ξ) of corroded elements (0.15 was used in this work). Because of the introduction of interval probability theory, this uncertainty may also be represented by an interval number for the corroded thickness. The corresponding interval probability of failure is more likely to be true and it reflects the high uncertainty associated with the thickness of corroded elements.

There is rapid reduction in the reliability index for lateral torsional buckling of coped beams that are laterally unrestrained. This significant reduction is caused partly by the coping of the beam. The next important mechanism is the shear failure mode. The severe loss of material in the lower part of the web causes the shear reliability index to decrease at a considerable rate. The moment reliability of the beams was found to be less critical because the loss of material in the compression flanges is not very significant.

The important part of the interval probability theory is the estimation of degree of dependence. Its value can be estimated from the size of intersection of the limit state functions [Cui and Blockley 1991]. The unknown dependence model can be used in cases where it is hard to establish the degree of dependence between two failure modes (or members). The number of degree of dependencies to be estimated can be reduced by ignoring the failure modes (or members) that are less critical to the system performance.

In this work, attention was focused only on the system performance of corrosion damaged steel beams. The method is capable of considerable development and in particular to complete structures made up of several corroded members.

9.8 Conclusions

The varying thickness loss corrosion damage model, which was developed based on the detailed measurements of four samples of corrosion damaged beams, is very useful in analysing the effect of corrosion of steel beams. The corrosion of steel generally reduces the capacity of a beam and it can also change the failure mode of the beam and the class of an element.

The proposed assessment methods, which give the remaining capacity of any I-beam manufactured in the UK, can be used for the reliable assessment of corrosion damaged steel beams. The proposed Strength Categories, which are based on the capacity loss and the condition of the beams, will improve the current visual assessment procedures to a great extent. The assessment methods and the Strength Categories will help to make fast and reliable decisions regarding the future of corrosion damaged members and will avoid inappropriate actions being taken (e.g. premature plant closures). It is believed that these methods and the improvement to the visual assessment procedures will be beneficial in terms of cost and safety.

There is a considerable degree of uncertainty in the measurement of thickness of corroded elements and in the visual assessment of thickness loss. Structural reliability analysis can be used to incorporate this uncertainty and to quantify the reduction in safety of corrosion damaged steel structures. The cost involved in the inspection and maintenance of corrosion damaged steel structures may be reduced by formulating inspection and maintenance strategies based on reliability analysis.

REFERENCES

Alprecht P, and Naeemi A H [1984]

Performance of weathering steel in bridges. National co-operative highway research program: Report 272, Transportation Research Board, National Research Council, Washington, DC.

Al-Zaid R Z [1986]

Reliability of prestressed concrete girder bridges. Ph.D. Thesis, Department of Civil Engineering, University of Michigan.

Astill A W, Holmes M, and Martin L H [1980]

Web buckling of steel I-beams. CIRIA Technical Note 102.

Baker M J [1969]

Variations in the mechanical properties of structural steels. Symposium on Concepts of Safety of Structures and Methods of Design, IABSE, London, pp 165-174.

Baldwin J F [1987]

Evidential support logic programming. Fuzzy Sets and Systems, Volume 24, pp 1-26.

Bellenoit J R, Yen B T, and Fisher J W [1985]

Stresses in hanger plates of suspended bridge girders. Transportation Research Record, No. 950, Volume 2, pp 20-23.

Benjamin J R, and Cornell C A [1970]

Probability Statistics and Decision for Civil Engineers. McGraw-Hill, New York.

Blockley D I [1980]

The Nature of Structural Design and Safety. Ellis Horwood, Chichester, England.

Bourgund U, and Bucher C G [1986]

ISPUD - Importance Sampling Procedure Using Design Points - A user's manual. Report 8-86, Institute of Engineering Mechanics, University of Innsbruck.

Brockenbrough R L [1983]

Considerations in the design of bolted joints for weathering steel. AISC Engineering Journal, American Institute of Steel Construction, Volume 20, No.1, pp 40-45.

BS 5950 Structural use of steel work in building: Part 1 [1985]

Code of practice for design in simple and continuos construction, Hot rolled sections, British Standards Institution, London.

Cheng J J R, Yura J A, and Johnson C P [1988a]

Lateral buckling of coped steel beams. Journal of Structural Engineering, ASCE, Volume 114, No.1, pp 1-15.

Cheng J J R, and Yura J A [1988b]

Lateral buckling tests on coped steel beams. Journal of Structural Engineering, ASCE, Volume 114, No.1, pp 16-30.

CIRIA Report 63 [1977]

The Rationalisation of Safety and Serviceability Factors in Structural Codes. CIRIA, Proceedings of the seminar, London.

Cornell C A [1967]

Bounds on the reliability of structural systems. Journal of Structural Division, ASCE, Volume 93, No.ST1, pp 171-200.

Cornell C A [1969]

A probability based structural code. Journal of American Concrete Institute, Volume 66, No.12, pp 974-985.

Cornell C A [1970]

A first order reliability theory of structural design. Structural Reliability and Codified Design, SM study No.3, University of Waterloo, Ontario, Canada.

Cui W [1989]

Uncertainty analysis in structural safety assessment. Ph.D. Thesis, Department of Civil Engineering, University of Bristol.

Cui W, and Blockley D I [1990]

Interval probability theory for evidential support. International Journal of Intelligent Systems, Volume 5, pp 183-192.

Cui W, and Blockley D I [1991]

On the bounds for structural system reliability. Structural Safety, Volume 9, No.4, pp 247-259.

Cygnus Instruments Ltd [1995]

Ultrasonic NDT Equipment. Cygnus House, 30, Prince of Wales Road, Dorchester, Dorset, England.

Davenport A G [1961]

The application of statistical concepts to the wind loading of structures. Proceedings of the Institution of Civil Engineers, Volume 19, pp 449-472.

Ditlevsen O [1979a]

Generalised second moment reliability index. Journal of Structural Mechanics, ASCE, Volume 7, No.4, pp 435-451.

Ditlevsen O [1979b]

Narrow reliability bounds for structural systems. Journal of Structural Mechanics, ASCE, Volume 7, No.4, pp 453-472.

Ditlevsen O [1981]

Uncertainty Modelling with Applications to Multidimensional Civil Engineering Systems. McGraw-Hill Inc., USA.

Ditlevsen O, and Bjerager P [1986]

Methods of structural systems reliability. Structural Safety, Volume 3, pp 195-229.

Dong W, and Shah C H [1987]

Vertex method for computing functions of fuzzy variables. Fuzzy Sets and Systems, Volume 24, pp 65-78.

Du Plessis D P [1977]

Lateral-Torsional buckling of end-notched steel beams. International Colloquium on Stability of Structures under Static and Dynamic Loads, Structural Stability Research Council, ASCE, Washington DC, pp 563-572.

Ellingwood B R [1992]

Probabilistic risk assessment. Engineering Safety (Edited by Blockley D I), McGraw-Hill Book Company Europe, England, pp 89-116.

Ellingwood B R, Galambos T V, MacGregor J C, and Cornell C A [1980]

Development of a probability based load criteria for American national standard A58. NBS special publication No. 577, National Bureau of Standards, US Department of Commerce, Washington, DC.

Ellis O B, and La Que F L [1951]

Area effects in crevice corrosion. Corrosion, Volume 7, No. 11, pp 362-364.

Evans U R [1972]

Mechanism of atmospheric rusting. Corrosion Science, Volume 12, pp 227-246.

Eyre J R, and Nokhasteh M A [1992]

Strength assessment of corrosion damaged reinforced concrete slabs and beams. Proceedings of Institution of Civil Engineers, Structures and Buildings, Paper 9851.

Fisher J W [1984]

Fatigue and Fracture in Steel Bridges. Third edition, John Wiley and Sons.

Fontana M G [1986]

Corrosion Engineering. Third edition, McGraw-Hill Book Company, New York.

Freudenthal A M [1956]

Safety and probability of structural failure. Trans., ASCE, Volume 121, pp 1337-1397.

Freudenthal A M, Garrelts J, and Shinozuka M [1966]

The analysis of structural safety. Journal of Structural Division, ASCE, Volume 92, No.1, pp 267-325.

Galambos T V, and Ravindra M K [1978]

Properties of steel for use in LRFD. Journal of Structural Division, ASCE, Volume 104, No.ST9, pp 1459-1468.

Gallon M J [1993]

Managing structural corrosion in chemical plants. New Steel Construction.

Gallon M J, Sarveswaran V, and Smith J W [1995]

Structural assessment of corrosion damaged steel work. Extending the Life Span of Structures, IABSE Symposium, San Francisco, Volume 73/1, pp 699-704.

Grimmelt M J, and Schueller G I [1982]

Benchmark study on methods to determine collapse failure probabilities of redundant structures. Structural Safety, Volume 1, No.2, pp 93-106.

Gupta A K [1984]

Buckling of coped steel beams. Journal of Structural Engineering, ASCE, Volume 110, No.9, pp 1977-1987.

Gurney T R [1979]

Fatigue of Welded Structures. Second edition, Cambridge University Press, Cambridge, UK.

Guttman H, and Sereda P J [1968]

Measurement of atmospheric factors affecting the corrosion of metals. Metal Corrosion in the Atmosphere, American Society for Testing and Materials, No. STP 435, pp 326-359.

Haaijer G [1957]

Plate buckling in the strain-hardening range. Journal of the Engineering Mechanics Division, ASCE, Volume 83, No.EM 2, pp 1212-1247.

Hasofer A M, and Lind N C [1974]

An exact and invariant second-moment code format. Journal of the Engineering Mechanics Division, ASCE, Volume 100, No.EM 1, pp 111-121.

Hogan T J, and Thomas I R [1980]

Design of Tee section members to AS 1250. Steel Construction, Journal of Australian Institute of Steel Construction, Volume 14, No.2, pp 2-22.

Horne M R [1958]

The full plastic moments of sections subjected to shear force and axial loads. British Welding Journal, Volume 5, pp 170-178.

Horne M R [1971]

Plastic Theory of Structures. Thomas Nelson and Sons Ltd, England.

ICI Engineering [1990a]

Procedure for: Condition categories for inspection of plant structures and pipebridges. Standards & Technical Information Services, ICI Engineering, Cheshire, England.

ICI Engineering [1990b]

Procedure for: Requirements for inspection of plant structures and pipebridges. Standards and Technical Information Services, ICI Engineering, Cheshire, England.

Johnston B G [1976]

Guide to Stability Design Criteria for Metal Structures. Third edition, John Wiley and Sons.

Kayser J R [1988]

The effects of corrosion on the reliability of steel girder bridges. Ph.D. Thesis, Department of civil engineering, University of Michigan.

Kayser J R, Malinski T, and Nowak A S [1987]

Corrosion damage models for steel girder bridges. Effects of Damage and Redundancy on Structural Performance (Edited by Frangopol D M), ASCE.

Kayser J R, and Nowak A S [1987]

Evaluation of corroded steel bridges. Bridge and Transmission Line Structures, ASCE.

Kayser J R, and Nowak A S [1989a]

Capacity loss due to corrosion in steel girder bridges. Journal of Structural Engineering, ASCE, Volume 115, No.6, pp 1525-1537.

Kayser J R, and Nowak A S [1989b]

Reliability of corroded steel girder bridges. Structural Safety, Volume 6, No.1, pp 53-63.

Kilcullen M B, and McKenzie M [1979]

Weathering steels. Proceedings of Corrosion in Civil Engineering Conference, Institution of Civil Engineers, London, UK, pp 95-105.

Komp M E [1987]

Weathering steels: Atmospheric corrosion ratings of weathering steels - Calculation and Significance. Material Performance, Volume 26, No.7, pp 42-44.

La Que F L [1951]

Corrosion testing. Proceedings of the American Society for Testing and Materials, Volume 51, pp 495-582.

Lay M G [1965]

Flange local buckling in wide-flange shapes. Journal of the Structural Division, ASCE, Volume 91, No.ST6, pp 95-116.

Longbottom E, and Heyman J [1956]

Experimental verification of the strength of plate girders designed in accordance with the revised BS 153: Tests on full-size and on model plate girders. Proc. of the Institution of Civil Engineers, Volume 5, Part 3, pp 462-521.

Martin L H, and Purkiss J A [1992]

Structural Design of Steelwork to BS 5950. First edition, Edward Arnold, London.

Melbourne W H [1977]

Probability distributions associated with the wind loading of structures. Civil engineering transactions, Institution of Engineers, Australia, CE 19, No.1, pp 58-67.

Melchers R E [1987]

Structural Reliability Analysis and Prediction. Ellis Horwood Limited, Chichester, England.

Morris L J, and Randall A L [1979]
Plastic Design. Constrado.

Nethercot D A [1974]
Residual stresses and their influence upon the lateral buckling of rolled steel beams. Structural Engineer, Institution of Structural Engineers, Volume 52, No.3, pp 89-96.

Ostapenko A [1964]
Local buckling. Structural Steel Design, Edited by Tall L, Ronald Press, New York.

Porter D M, Rockey K C, and Evans H R [1975]
The collapse behaviour of plate girders loaded in shear. Structural Engineer, Institution of Structural Engineers, Volume 53, No.8, pp 313-325.

Ramachandra Murthy D S, Madhava Rao A G, and Santhakumar A R [1994]
Corrosion fatigue of stiffened offshore steel tubular joints. Journal of Structural Engineering, ASCE, Volume 120, No.7, pp 1991-2010.

Redwood R G [1972]
Tables for plastic design of beams with rectangular holes. Engineering Journal, American Institute of Steel Construction, Volume 9, No.1, pp 2-19.

Redwood R G [1983]
Design of I beams with web perforations. Beams and Beam Columns, Stability and Strength, (Edited by Narayanan R), Applied science publishers, London, pp 95-133.

Redwood R G, and Cho S H [1987]
Design tools for steel beams with web openings. Composite Steel Structures, Elsevier Applied Science Publications Ltd, London, pp 75-83.

Redwood R G, and Cho S H [1993]

Design of steel and composite beams with web openings. Journal of Constructional Steel Research, Elsevier Applied Science Publications Ltd.

Rockey K C, Valtinat G, and Tang K H [1981]

The design of transverse stiffeners on webs loaded in shear - an ultimate load approach. Proc. of the Institution of Civil Engineers, Volume 71, Part 2, pp 1069-1099.

Rubenstein R Y [1981]

Simulation and the Monte Carlo Method. John Wiley and Sons, New York.

Schueller G I, and Stix R [1986]

A critical appraisal of methods to determine failure probabilities. Structural Safety, Volume 4, No.4, pp 293-310.

Scully J C [1990]

The Fundamentals of Corrosion. Third edition, Pergamon Press, Oxford, England.

Shinozuka M [1983]

Basic analysis of structural safety. Journal of Structural Engineering, ASCE, Volume 109, N0.3, pp 721-740.

Smith J W [1993]

Mechanical properties of samples of structural steel affected severely by corrosion. Report No.UBCE/JWS/93/01, University of Bristol.

Smith J W, and Woodman N J [1992]

Structural effects of corrosion damage to a pipe bridge: A theoretical study. Report No.UBCE/JWS/92/02, University of Bristol.

Stowell E Z, Heimerl G J, Libove C, and Lundquist E E [1952]

Buckling stresses for flat plates and sections. Trans., ASCE, Volume 117, pp 545-578.

Thoft-Christenson P, and Baker M J [1982]

Structural Reliability Theory and its Applications. Springer-Verlag Berlin, Heidelberg.

Timoshenko S P, and Gere J M [1961]

Theory of Elastic Stability. McGraw-Hill Book Company.

Townsend H E and Zoccola J C [1982]

Eight year atmospheric corrosion performance of weathering steel in industrial, rural, and marine environments. Atmospheric Corrosion of Metals, American Society for Testing and Materials, No. STP 767, pp 45-59.

Trahair N S [1977]

The Behaviour and Design of Steel Structures. Chapman and Hall, London.

Wang T M, Snell R R, and Cooper P B [1975]

Strength of beams with eccentric reinforced holes. Journal of the Structural Division, ASCE, Volume 101, No.ST9, pp 1783-1800.

Zadeh L A [1986]

Is probability theory sufficient for dealing with uncertainty in artificial intelligence: a negative view. Uncertainty in Artificial Intelligence (Edited by Kanal L N, and Lemmer J F), Elsevier Science Publishers, pp 103-116.

Zuraski P [1986]

The remaining life in Deteriorated steel deck-girder highway bridges. Ph.D. Thesis, Department of Civil and Environmental Engineering, University of Wisconsin.

BIBLIOGRAPHY

The following list of references are not specifically referred in the thesis but were used for the research work carried out.

Ang A H-S, and Ma H-F [1981]

On the reliability of structural systems. Structural Safety and Reliability (Edited by Moan T, and Shinozuka M), Proc. of ICOSSAR'81, The third International Conference on Structural Safety and Reliability, Trondheim, Norway, pp 295-314.

Bartlett F M, and Sexsmith R G [1991]

Bayesian technique for evaluation of material strengths in existing structures. ACI Materials Journal, Volume 88, No.2, pp 164-169.

Blockley D I, and Ellison E G [1979]

A new technique for estimating system uncertainty in design. Proceedings of the Institution of Mechanical Engineers, Volume 193, No.5, London, pp 159-168.

Bucher C G [1988]

Adaptive sampling - An iterative fast Monte Carlo procedure. Structural Safety, Volume 5, pp 119-126.

Chan H Y, and Melchers R E [1995]

Time-Dependent resistance deterioration in probabilistic structural systems. Civil Engineering Systems, Volume 12, pp 115-132.

Chou K C, and Yuan J [1992]

Safety assessment of existing structures using a filtered fuzzy relation. Structural Safety, Volume 11, Nos.3 + 4, pp 173-189.

CIRIA/SCI [1987]

Design for openings in the webs of composite beams. CIRIA special publication 51; SCI publication 068, The Steel Construction Institute, Ascot, UK.

Comerford J B, and Blockley D I [1993]

Managing safety and hazard through dependability. Structural Safety, Volume 12, No.1, pp 21-33.

Dagher H J, and Kulendran S [1992]

Finite element modelling of corrosion damage in concrete. ACI Structural Journal, American Concrete Institute, Volume 89, No.6, pp 699-708.

Evans H R, and Narayanan R [1986]

Simplified procedures for the design of plate girders with web stiffeners or openings. Steel Structures: Recent research advances and their applications to design (Edited by Pavlovic M N), Elsevier Applied Science Publications Ltd, England, pp 299-316.

Frangopol D M, Barakat S, and Lin K-Y [1995]

Reliability-based design of deteriorating bridges under corrosion effects. Extending the Life Span of Structures, IABSE Symposium, San Francisco, Vol 73/2, pp 1271-1276.

Frangopol D M, and Curley J P [1987]

Effects of damage and redundancy on structural reliability. Journal of the Structural Engineering, ASCE, Volume 113, No.7, pp 1533-1549.

Frangopol D M, and Hendawi S [1994]

Incorporation of corrosion effects in reliability-based optimisation of composite hybrid plate girders. Structural Safety, Volume 16, Nos.1 + 2, pp 145-169.

Furuta H, Ohshima M, and Shiraishi N [1989]

Reliability analysis of damaged redundant structures. Recent studies on Structural Safety and Reliability, edited by Nakagawa T, Ishikawa H, and Tsurui A, Current Japanese Materials Research - Volume 5, The Society of Materials Science, Japan, pp 105-117.

Gorman M R, and Moses F [1981]

Partial factors for structural damage. Proceedings on Probabilistic Methods in Structural Engineering, ASCE, St.Louis, New York.

Grigoriu M [1982]

Methods for approximate reliability analysis. Structural Safety, Volume 1, No.2, pp 155-165.

Itagaki H [1989]

Bayesian reliability analysis for evaluating in-service inspection. Recent studies on Structural Safety and Reliability, edited by Nakagawa T, Ishikawa H, and Tsurui A, Current Japanese Materials Research - Volume 5, The Society of Materials Science, Japan, pp 167-189.

Kameda H, and Koike T [1975]

Reliability theory of deteriorating structures. Journal of the Structural Division, ASCE, Volume 101, No.ST1, pp 295-310.

Kussman R L, and Cooper P B [1976]

Design example for beams with web openings. Engineering Journal, American Institute of Steel Construction, Volume 13, No.2.

Lai K L, and Ayyub B M [1994]

Generalised uncertainty in structural reliability assessment. Civil Engineering Systems, Volume 2, pp 81-110.

Li C Q [1995]

A case study on the reliability analysis of deteriorating structures. Structures and Buildings, Proc. of the Institution of Civil Engineers, Volume 110, pp 269-277.

Liu S-C, and Yao T P [1978]

Structural identification concept. Journal of the Structural Division, ASCE, Volume 104, No.ST12, pp 1845-1858.

Melchers R E [1995]

Probabilistic modelling of sea water corrosion of steel structures. Proceedings, Application of Statistics and Probability, Lemaire, Favre and Mebbarki, Balkema, Rotterdam.

Murotsu Y, and Okada H [1989]

Recent developments in the identification of dominant failure modes and reliability assessment for large-scale frame structures. Recent studies on Structural Safety and Reliability, edited by Nakagawa T, Ishikawa H, and Tsurui A, Current Japanese Materials Research - Volume 5, The Society of Materials Science, Japan, pp 85-104.

Narayanan R [1983]

Ultimate shear capacity of plate girders with openings in the web. Plated Structures, Stability and Strength, (Edited by Narayanan R), Applied Science Publishers, London, pp 39-76.

Rackwitz R, and Fiessler B [1978]

Structural reliability under combined random load sequences. Computers and Structures, Volume 9, No.5, pp 489-494.

Rashedi R, and Moses F [1988]

Identification of failure modes in system reliability. Journal of Structural Engineering, ASCE, Volume 114, No.2, pp 292-313.

Ravindra M K, and Galambos T V [1978]

Load and resistance factor design for steel. Journal of the Structural Division, ASCE, Volume 104, No.ST9, pp 1337-1353.

Reid S G [1992]

Acceptable risk. Engineering Safety (Edited by Blockley D I), McGraw-Hill Book Company Europe, England, pp 138-166.

Rockey K C, Evans H R, and Porter D M [1978]

A design method for predicting the collapse behaviour of plate girders. Proc. of the Institution of Civil Engineers, Volume 65, Part 2, pp 85-112.

Rosenblueth E [1981]

Two point estimates in probabilities. Journal of Applied Mathematical Modelling, Volume 5, No 5, pp 329-335.

Schneider J [1996]

VaP - Variables Processor. A user's manual, Institute of Structural Engineering, Zurich.

Shiraishi N, and Cranston W B [1992]

Bridge safety. Engineering Safety (Edited by Blockley D I), McGraw-Hill Book Company Europe, England, pp 293-312.

Soltani M, and Corotis R B [1988]

Failure cost design of structural systems. Structural Safety, Volume 5, No.4, pp 239-252.

Sommer A M, Nowak A S, and Thoft-Christenson P [1993]

Probability based bridge inspection strategy. Journal of Structural Engineering, ASCE, Volume 119, No.12, pp 3520-3536.

Tabsh S W, and Nowak A S [1991]

Reliability of highway girder bridges. Journal of Structural Engineering, ASCE, Volume 117, N0.8, pp 2373-2388.

Tang J P, and Yao J T P [1987]

Evaluation of structural damage and redundancy. Effects of Damage and Redundancy on Structural Performance (Edited by Frangopol D M), ASCE.

Tantawi H M, Nowak A S, and Lind N C [1991]

Point distribution methods for bridge reliability analysis. Journal of Forensic Engineering, Volume 3, No.2/3, pp 137-145.

Tee A B, and Bowman M D [1991]

Bridge condition assessment using fuzzy weighted averages. Civil Engineering Systems, Volume 8, No.1, pp 49-58.

Vrouwenvelder T [1993]

Codes of practice for the assessment of existing structures. Remaining Structural Capacity, IABSE colloquium, Copenhagen, Report, Volume 67, pp 5-16.

Xin Wu, Blockley D I, and Woodman N J [1993]

Vulnerability of structural systems. Civil Engineering Systems, Volume 10, No. 4.

Yao J T P [1979]

Damage assessment and reliability evaluation of existing structures. Engineering Structures, Volume 1, pp 245-251.

Yao J T P [1980]

Damage assessment of existing structures. Journal of Engineering Mechanics Division, ASCE, Volume 106, No.EM4, pp 785-799.

Yao J T P [1981]

Safety and reliability of existing structures. Structural Safety and Reliability (Edited by Moan T, and Shinozuka M), Proceedings of ICOSSAR'81, The third International Conference on Structural Safety and Reliability, Trondheim, Norway, pp 283-294.

Yao J T P, and Natke H G [1994]

Damage detection and reliability evaluation of existing structures. Structural Safety, Volume 15, Nos.1+2, pp 3-16.

Yura J A, Galambos T V, and Ravindra M [1978]

The bending resistance of steel beams. Journal of the Structural Division, ASCE, Volume 104, No.ST9, pp 1355-1370.

Zadeh L A [1965]

Fuzzy sets. The journal of Information and Control, Volume 8, pp 338-353.

Zhou J H, and Nowak A S [1988]

Integration formulas for functions of random variables. Structural Safety, Volume 5, No.4, pp 267-284.

Zhou J H, and Nowak A S [1990]

Reliability analysis for bridge systems. Journal of Forensic Engineering, Volume 2, N0.4, pp 449-457.

Appendix A

Properties of normal probability distribution

The normal (or Gaussian) probability distribution is one of the most commonly used distributions. It is a two-parameter distribution, which is described by its probability density function as [Benjamin and Cornell 1970]:

$$f_X(x) = \frac{1}{\sqrt{2\pi}\,\sigma_x}\exp\left(-\frac{(x-\mu_x)^2}{2\sigma_x^2}\right) \qquad (A.1)$$

where μ_x and σ_x are the mean and standard deviation of the variable X respectively. The cumulative distribution function corresponding to Equation A.1 is given by:

$$P(X \le x) = F_X(x) = \int_{-\infty}^{x} \frac{1}{\sqrt{2\pi}\,\sigma_x}\exp\left(-\frac{(t-\mu_x)^2}{2\sigma_x^2}\right)dt \qquad (A.2)$$

The above integral cannot be evaluated in a closed form. By the substitution,

$$s = \frac{t-\mu_x}{\sigma_x}, \quad \text{and hence} \quad dt = \sigma_x ds \qquad (A.3)$$

Equation A.2 becomes,

$$F_X(x) = \int_{-\infty}^{\frac{x-\mu_x}{\sigma_x}} \frac{1}{\sqrt{2\pi}}\exp\left(-\frac{s^2}{2}\right)ds = \Phi_X\left(\frac{x-\mu_x}{\sigma_x}\right) \qquad (A.4)$$

where Φ_X is the standard normal distribution function (Figure A.1) defined by:

$$\Phi_X(x) = \int_{-\infty}^{x} \frac{1}{\sqrt{2\pi}} \exp\left(-\frac{t^2}{2}\right) dt \qquad (A.5)$$

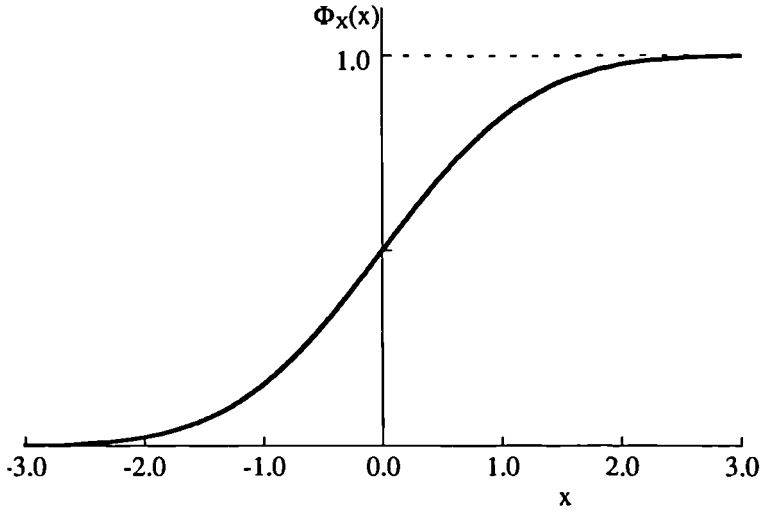

Figure A.1 Standard normal cumulative distribution function

The standard normal density function corresponding to Equation A.5 is (Figure A.2),

$$\varphi_X(x) = \frac{1}{\sqrt{2\pi}} \exp\left(-\frac{x^2}{2}\right) \qquad (A.6)$$

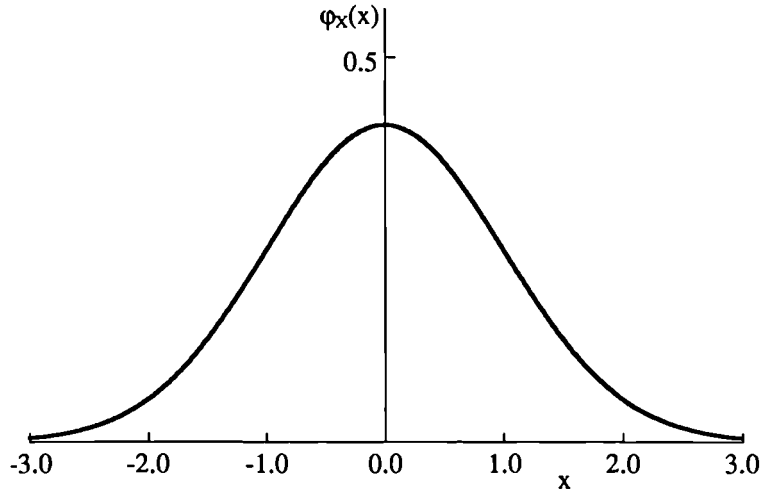

Figure A.2 Standard normal density function

The standard normal distribution is usually tabulated for both $\varphi_X(x)$ and $\Phi_X(x)$ (see Melchers [1987]).

Now, consider a case in which the probability of failure is given by:

$$P_f = P(M \leq 0) = F_M(0)$$

where M is a normally distributed variable.

Using Equation A.4, the probability of failure given by the above equation may be expressed by:

$$P_f = \Phi\left(\frac{0-\mu_M}{\sigma_M}\right) \tag{A.7}$$

where μ_M and σ_M are the mean and standard deviation of the variable M respectively.

The normal distribution has the following useful properties:

If $P_f = \Phi(-\beta)$, then

$$\beta = \Phi^{-1}(P_f) \tag{A.8}$$

$$\Phi(-\beta) = 1 - \Phi(\beta) \tag{A.9}$$

and, if $X = \sum_{i=1}^{m} X_i$ where X_i are independent normal variables, then

$$\mu_X = \sum_{i=1}^{m} \mu_{X_i} \tag{A.10}$$

$$\sigma_X^2 = \sum_{i=1}^{m} \sigma_{X_i}^2 \tag{A.11}$$

Appendix B

The variation in thickness measurements of corrosion damaged elements

In order to show the variation in the thickness measurements of corroded elements, thickness measurements taken at various locations of the web of the sample Beam 4 are given below. Thickness measurements were taken separately for the upper ($0.75h_w$) and lower parts ($0.25h_w$) of the web. The degree of corrosion was found to be quite severe in the lower part of the web compared with the upper part. The locations of measurement points were distributed uniformly over each area of the web.

B.1 Thickness of the upper part of the web ($0.75h_w$)

5.84	5.81	5.54	5.81	5.64	5.69	5.74	5.75	5.72	5.47
5.52	5.78	5.64	5.66	5.78	5.67	5.79	5.62	5.80	5.71
5.81	5.73	5.78	5.88	6.04	5.80	5.88	5.76	5.75	5.77
5.77	5.68	5.77	5.72	5.66	5.77	5.70	5.77	5.67	5.75

B.2 Thickness of the lower part of the web ($0.25h_w$)

3.77	4.51	2.93	3.28	1.82	1.71	2.74	2.92	2.27	4.38
4.79	2.96	2.85	1.65	3.87	2.97	2.80	3.05	4.75	5.42
3.50	4.80	2.32	2.82	4.52	3.18	4.14	5.71	5.82	5.64
5.77	4.79	5.69	5.74	4.90	5.44	3.60	3.71	2.53	4.57
2.13	3.86	2.94	4.13	2.55	1.54	4.76	2.04	0.94	3.02
4.90	3.54	2.72	4.61	4.17	4.33	4.90	5.71	4.99	4.73
5.60	5.29	5.66	4.74						